TECHNISCHE UNIVERSITÄT WIEN
Vienna | Austria

DISSERTATION

# Bewertung und Analyse der chemischen, physikalischen und tribologischen Merkmale von biobasierten Schmierstoffen und Kraftstoffen

ausgeführt zum Zwecke der Erlangung des akademischen Grades
Doktorin der technischen Wissenschaften
unter der Leitung von

Prof. Dr. Mag. **Martina Marchetti-Deschmann**
E164
Institut für Chemische Technologien und Analytik

eingereicht an der Technischen Universität Wien
Fakultät für Technische Chemie

von

Dipl.-Ing. **Jessica Pichler**
00475177

Wien, am 30. September 2024 _____

# Acknowledgement

Love goes out to ...

... my mom and Günther, for their unwavering support, their love, and their belief in me,
... my sisters, Vany, Anastasia, and Melissa,
... my dad and Brigitte,
... and the rest of my big, loving family!

... my friends and colleagues Stephi, Sophie, Emna, Manu, Daniel, Andre, Jasmin, and Rosi. And to Marcella for not only being an awesome supervisor but also for being a friend through all the ups and downs.

... Silvia and Rainer, for all the shared evenings and meals, and for the support through Corona times. Although the time all of us spent together could have been longer, it was precious, and I'll miss the shared laughs. And of course also to Jessi.

... Fenris, Phoenix, and Munin for hindering my writing process by stomping on the keyboard, demanding cuddles or attention, and drinking from my water glass, so I had some more breaks and exercise when getting a fresh one. Loki (♡) as the only important thing in your life was to give love (well, and to eat).

... Christoph, for being there all along by my side.

Lastly, I want to thank those who were part of my life journey but couldn't make it to the grand educational finale. I will always keep you in my heart.

# Kurzfassung

Diese Forschungsarbeit vereint zwei Hauptthemen: Kraft- und Schmierstoffe sowie Chemie und Technologie. Einerseits wird die Umweltauswirkung von Kraft- und Schmierstoffen diskutiert, die größtenteils aus fossilen Quellen stammen und durch ihre Verbrennung maßgeblich zum globalen atmosphärischen $CO_2$-Niveau beitragen. Andererseits liegt der Fokus auf der technischen Chemie, insbesondere auf den beträchtlichen $CO_2$-Emissionen der chemischen Industrie, darunter die Petrochemie, die einen wesentlichen Teil der chemischen Produktion ausmacht. $CO_2$ fungiert als das dominierende Treibhausgas und treibt den gegenwärtigen Klimawandel maßgeblich voran.

Als Reaktion auf den voranschreitenden anthropogenen Klimawandel strebt die Welt die Ziele für nachhaltige Entwicklung (Sustainable Development Goals, SDGs) und die Reduzierung des globalen Temperaturanstiegs gemäß dem Pariser Abkommen an, um eine gerechte und nachhaltige Zukunft zu gewährleisten. Dabei wird die Reduzierung von Treibhausgasen durch grundlegende Defossilisierung und Dekarbonisierung angestrebt. Verschiedene Ansätze zur Dekarbonisierung von Kraft- und Schmierstoffen werden untersucht, darunter die Verwendung alternativer Rohstoffe für mehr Nachhaltigkeit, die Einsparung von Ressourcen (Energie, Materialien) durch die Verringerung von Reibung und Verschleiß in tribologischen Kontaktzonen, die Ermittlung optimaler Leistungsbereiche und die Integration von Lebenszyklusanalysen zur genauen Bestimmung von Problemherden. Zusätzlich werden europäische Projekte im Detail untersucht, die sich auf die Substitution erdölbasierter Kraft- und Schmierstoffe konzentrieren, einschließlich Biomasse-zu-Kraftstoff, Abfall-zu-Treibstoff, $CO_2$-Abscheidung und -nutzung sowie Biomasse-Bilanzansätze, zusammen mit den dazugehörigen Technologien. Es werden tribologische Regimes und Tests zur Bewertung der Schmierstoffleistung erörtert, Empfehlungen vorgestellt und eine Auswahl umweltfreundlicher Schmierstoffadditiv-Alternativen präsentiert. Des Weiteren werden nachhaltige Alternativen für Schmierstoffgrundöle untersucht, inklusive vorhandener Informationen zur Toxizität und Tribologie. Diese Arbeit untersucht auch das Potenzial von Öl aus Kaffeesatz als biobasierte und aus Abfällen gewonnene Option für die Nutzung als Schmierstoff und zeigt im Zuge dessen vielversprechende Reibungs- und Verschleißeigenschaften auf.

Diese Studie untersucht die strukturellen Ähnlichkeiten und Unterschiede zwischen Dieselkraftstoff auf Erdölbasis und Biodiesel und legt dabei den Schwerpunkt auf die Parameter, die für die Bewertung gemäß gängiger Normungstests relevant sind. Sie analysiert die Differenzen in den physikalisch-chemischen Eigenschaften und ihre jeweiligen Auswirkungen auf Leistung und Umwelt, sowie die Vor- und Nachteile, die mit diesen Unterschieden einhergehen. Bei Biodiesel führen natürliche Spurenelemente zur Ausfällung von gesättigten Monoglyceriden über dem Trübungspunkt (Cloudpoint), was zu einer erhöhten Wahrscheinlichkeit von verstopften Kraftstofffiltern führt. Dies war der Ausgangspunkt für die Entwicklung einer verbesserten Methode, die Gaschromatographie mit Elektronenstoßionisations-Tandem-Massenspektrometrie kombiniert. Zuvor gab es keine geeignete Nachweismethode für handelsübliche Dieselmischungen mit einem Biodieselanteil von 7 %, insbesondere um die erforderliche niedrige Nachweisgrenze zu erreichen. Zusammenfassend liefert diese Arbeit ein umfassendes Verständnis der Herausforderungen und Möglichkeiten der Dekarbonisierung in den Bereichen Schmierstoffe und Kraftstoffe, sowie potenzielle Lösungsansätze für diese Probleme.

# Abstract

This thesis bridges two fields: fuels and lubricants and chemistry and technology. On the one hand, the environmental impact of fuels and lubricants is discussed, noting that the vast majority of them are based on fossil resources, contributing significantly to global atmospheric $CO_2$ levels through their combustion. On the other hand, as this thesis is written within the field of technical chemistry, attention is drawn to the chemical industry's substantial $CO_2$ emissions, particularly from petrochemicals, which constitute a significant portion of chemical production. $CO_2$ is the most dominant greenhouse gas and, thus, is driving today's climate change.

As countermeasures to the ongoing anthropogenic climate change, the world is speaking about the Sustainability Development Goals (SDGs) and a reduction of global temperature rise according to the Paris Agreement to provide an equitable and sustainable future. Furthermore, the reduction of greenhouse gases is pursued by fundamental defossilization and decarbonization. Different approaches for decarbonizing fuels and lubricants are explored, including the adoption of alternative materials for enhanced sustainability, resource conservation (energy, materials) through the reduction of friction and wear in tribological interfaces, identification of optimal performance ranges, and the integration of life-cycle assessments to pinpoint areas of concern accurately. Moreover, European projects focusing on replacing petroleum-based fuels and lubricants, including biomass-to-liquid, waste-to-fuel, carbon capture and utilization, and biomass-balance approaches, are examined in detail, along with their associated technologies. The discussion covers tribological regimes and tests designed to evaluate lubricant performance, presenting their recommendations, and a selection of environmentally friendly lubricant additive alternatives. Exploration includes sustainable alternatives for lubricant base oil, examining existing toxicity and tribological information. Additionally, the study investigates the potential of oil derived from spent coffee grounds as a bio-based and waste-derived option for lubrication, showing encouraging friction and wear characteristics.

This thesis delves into the comparative analysis of structural similarities and differences between petroleum-based diesel and biodiesel, with a particular focus on parameters required for evaluation according to prevailing standardization tests. It explores variations in their physicochemical properties and their respective impacts on performance and the environment, along with the advantages and drawbacks associated with these differences. As for biodiesel, natural trace elements cause precipitation of saturated monoglycerides above the cloud point, leading to an increased number of filter blocking incidents. This provided the starting point for an enhanced method development using gas chromatography coupled with electron ionization tandem mass spectrometry. Previously, there had been no detection technique accessible for commercially available diesel blends containing 7 % biodiesel, particularly for achieving the low limit of detection required. In conclusion, this thesis offers a comprehensive understanding of the obstacles and opportunities related to decarbonization in the domains of lubricants and fuels while also proposing potential solutions to address these challenges.

# Contents


**1 Introduction** **12**

1.1 Global trends in climate change . . . 12
1.2 Reaction and regulations to the climate change . . . 15
1.3 Aim of this work . . . 16
1.4 Fuels and lubricants . . . 16
1.4.1 Diesel . . . 22
1.4.2 Biodiesel . . . 24
1.4.3 Blends and applicability . . . 27
1.4.4 Tribology . . . 28
1.4.4.1 Tribology of different diesel blends . . . 28
1.4.5 Lubricants . . . 33
1.5 Carbon footprint . . . 36
1.5.1 Emission reduction – decarbonization . . . 36
1.5.2 Substitution projects . . . 39
1.5.3 The sustainability evaluation toolbox . . . 41
1.6 The road ahead . . . 43
1.7 Advanced structural elucidation for fuels and lubricants . . . 44
1.7.1 Gas chromatography coupled to mass spectrometry . . . 44
1.7.1.1 Gas chromatography . . . 44
1.7.1.2 Two-dimensional gas chromatography systems . . . 46
1.7.1.3 Electron ionization . . . 46
1.7.1.4 Quadrupole . . . 47
1.7.1.5 Triple Quad . . . 47
1.7.2 Electrospray ionization-high-resolution-mass spectrometry . . . 48
1.7.2.1 Electrospray ionization . . . 48
1.7.2.2 Linear ion trap . . . 49
1.7.2.3 Orbitrap mass analyzer . . . 49
1.7.2.4 Hybrid mass spectrometry . . . 49

**2 Publications** **51**

2.1 Publication I - A comprehensive review of sustainable approaches for synthetic lubricant components . . . 68
2.2 Publication II - Moving towards green lubrication: tribological behavior and chemical characterization of spent coffee grounds oil . . . 98
2.3 Publication III - Advanced Method for the Detection of Saturated Monoglycerides in Biodiesel using GC-EI-MS/MS . . . 116

# Acronyms


**AN** acid number . . . . . 36

**ATR** attenuated total reflection . . . . . 35

**C2C** cradle-to-cradle . . . . . 42

**CCU** carbon capture and utilization . . . . . 38

**CFPP** cold filter plugging point . . . . . 19

**CID** collision-induced dissociation . . . . . 50

**CN** cetane number . . . . . 17

**COP** Conference of the Parties . . . . . 15

**CP** cloud point . . . . . 19

**DSC** differential scanning calorimetry . . . . . 35

**EAL** environmentally acceptable lubricant . . . . . 51

**EC** European Commission . . . . . 43

**EFL** environmentally friendly lubricant . . . . . 28

**EI** electron ionization . . . . . 27

**ESI** electrospray ionization . . . . . 44

**ETD** electron-transfer dissociation . . . . . 50

**FAEE** fatty acid ethyl ester . . . . . 24

**FAME** fatty acid methyl ester . . . . . 17

**FID** flame ionization detector . . . . . 20

**FT** Fourier transform . . . . . 49

**FTIR** Fourier transform infrared spectroscopy . . . . . 35

**GC** gas chromatography . . . . . 20

**GHG** greenhouse gas . . . . . 13

**GWP** global warming potential . . . . . 14

**HCD** higher-energy collisional dissociation . . . . . 50

**HPLC** high-performance liquid chromatography . . . . . 20

**HR** high-resolution . . . . . 35
**ICP** inductively coupled plasma . . . . . 20
**ICR** ion cyclotron resonance . . . . . 49
**IV** iodine value . . . . . 36
**KOH** potassium hydroxide . . . . . 20
**LC** liquid chromatography . . . . . 47
**LCA** life cycle assessment . . . . . 28
**LCI** life cycle inventory . . . . . 41
**LCIA** life cycle impact assessment . . . . . 41
**MRM** multiple reaction monitoring . . . . . 48
**MS** mass spectrometry . . . . . 20
**OEF** organization environmental footprint . . . . . 43
**OES** optical emission spectroscopy . . . . . 20
**PAO** polyalphaolefin . . . . . 53
**PCF** product carbon footprint . . . . . 43
**PEF** product environmental footprint . . . . . 43
**PV** peroxide value . . . . . 36
**RFNBO** renewable fuels of non-biological origin . . . . . 23
**SCG** spent coffee grounds . . . . . 53
**SCGO** spent coffee grounds oil . . . . . 25
**SDGs** United Nations Sustainable Development Goals . . . . . 12
**SE** Soxhlet extraction . . . . . 53
**SIM** selected ion monitoring . . . . . 47
**SMG** saturated monoglyceride . . . . . 27
**SRM** selected reaction monitoring . . . . . 47
**SV** saponification value . . . . . 36
**TGA** thermogravimetric analysis . . . . . 35
**TIC** total ion current . . . . . 47
**ZDDP** zinc diorganodithiophosphate . . . . . 34

# Chapter 1

# Introduction

## 1.1 Global trends in climate change

Climate change is happening: glaciers are melting, sea levels are rising, temperatures are increasing, oceans are acidifying, biodiversity and harvest are threatened, clean water gets scarce, and extreme weather events grow and cause additional health risks [1].

As an answer to all these changes, the United Nations Sustainable Development Goals (SDGs) were created, providing a universal and comprehensive roadmap to guide countries and stakeholders in addressing the following interconnected 17 challenges (see Figure 1) and highlighting those mostly affected by petroleum and its derivatives (fuels, petrochemicals, etc.) [2]:

1. No poverty
2. Zero hunger
3. Good health and well-being: petroleum poses a risk to human health, e.g., through pollution of air, soil, or water; substitution with safer alternatives promotes SDG 3.
4. Quality education
5. Gender equality
6. Clean water and sanitation: Petroleum-derived products are known to be involved in the pollution of water sources. Sustainable alternatives support SDG 6 by reducing water pollution and promoting access to clean water [3].
7. Affordable and clean energy: Shifting the production of petroleum products toward bio-based or recycled materials can reduce the overall energy demand and promote cleaner energy sources. Biodiesel, for example, can be produced from renewable feedstocks, contributing to a more sustainable energy mix.
8. Decent work and economic growth: The development and production of alternatives to petroleum create new opportunities for research and the economy, serving as a foundation for new jobs.
9. Industry, innovation, and infrastructure: Substituting petrochemicals and fossil fuels with sustainable alternatives involves innovations in manufacturing processes and materials. Moreover, it encourages the growth of sustainable industries and contributes to developing resilient and sustainable infrastructure.
10. Reduced inequalities
11. Sustainable cities and communities

12. Responsible consumption and production: Shifting from traditional fossil-based products to more sustainable ones aligns with SDG 12. Sustainable alternatives often involve renewable resources and can contribute to more efficient and environmentally friendly production processes.

13. Climate action: Petroleum-derived products like fossil fuels are a significant source of greenhouse gas (GHG) emissions. A replacement with low-carbon or carbon-neutral alternatives helps mitigate climate change. Biodiesel, for instance, can reduce the carbon footprint of transportation and industrial activities, supporting efforts to achieve emission reduction targets [4].

14. Life below water: Contamination of water sources by, e.g., fossil fuels, through oil spills impairs the gas exchange at the water-atmosphere interface and leads to decreased oxygen levels in the water, threatening wildlife and aquatic plants. Reducing this pollution will help protect and preserve marine ecosystems and biodiversity [5].

15. Life on land: Terrestrial ecosystems are harmed by, e.g., diesel combustion. A replacement by greener alternatives can support a sustainable use of land and protect biodiversity. Without controversy in case of environmental emissions, such as micro drops or oil mist, hardly preventable during use, and especially spills of petroleum-based products come with a massive negative impact [5].

16. Peace, justice, and strong institutions

17. Partnership for the goals


**Figure 1:** The 17 United Nations Sustainable Development Goals [6].

The SDGs aim to create a more equitable, inclusive, and sustainable world by addressing complex issues and encouraging international collaboration. As can be seen above, petroleum-derived products have an impact on the majority of the SDGs.

In general, GHGs comprise carbon dioxide ($CO_2$), methane ($CH_4$), nitrous oxide ($N_2O$), fluorinated gases, ozone, and water vapor. Especially the burning of fossil fuels consistently accelerates the amount of $CO_2$ in the atmosphere, interfering with Earth's natural balance of atmospheric gases [7]. To compare the impact of the different GHGs, the global warming potential (GWP) was implemented. It defines the potential of gas to trap heat, slowing the transfer of energy to space and increasing climate change within one hundred years compared to $CO_2$. Therefore, the GWP of $CO_2$ is 1. $CH_4$ has a GWP 28 times that of $CO_2$, and $N_2O$ is even 265 times higher. Not only is the ability to absorb energy important, but also the lifetime of the gas in the atmosphere, which is thousands of years for $CO_2$. Figure 2 shows the human-provoked steeply rising $CO_2$ emissions since the mid-20$^{th}$ century and the simultaneous increase in atmospheric $CO_2$ [8, 9].

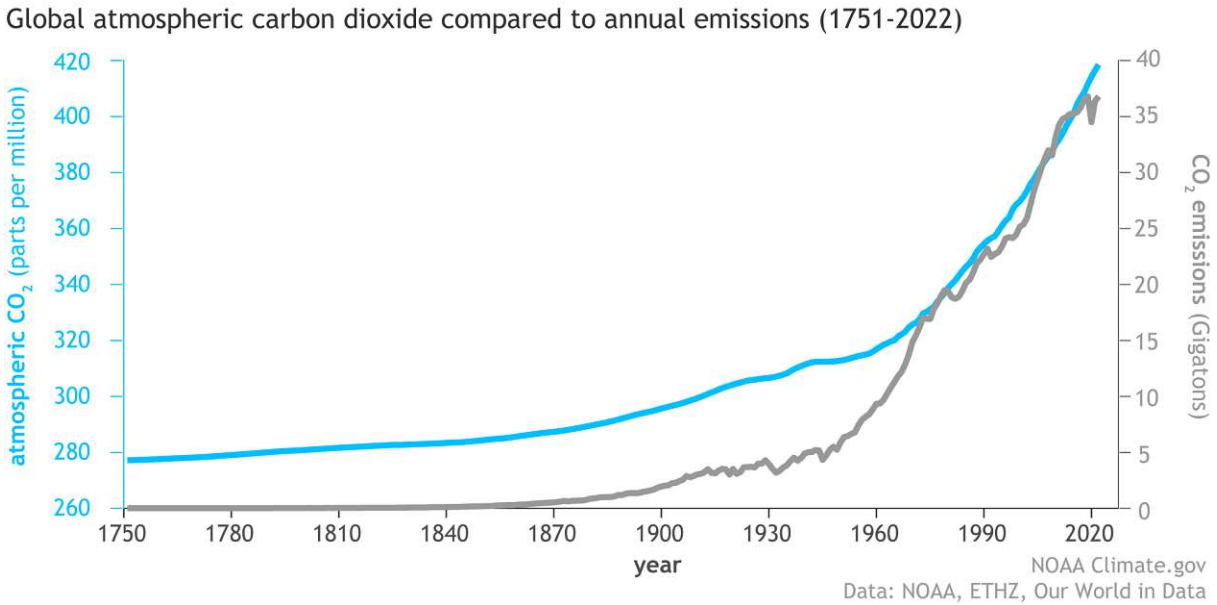


**Figure 2:** The amount of global $CO_2$ in the atmosphere (blue line) and human emissions (grey line) since the Industrial Revolution in 1750 [10].

The industrial sector makes up almost a third of all GHG emissions within the US [11]. The industries contributing the highest levels of emissions, coming from production and energy use, are the chemicals and petrol refining industries. The petrochemical industry has the most prominent impact within the chemical industry, which is still increasing as of 2022 [12]. To further empathize with the need for action following the SDGs, cleaner energy sources, more sustainable process designs, and alternative feedstocks will significantly impact this industry type.

## 1.2 Reaction and regulations to the climate change

The 26th UN Climate Change Conference of the Parties (COP) in Glasgow 2021 brought together over 100 international parties to address the next steps toward fighting climate change by reducing GHG emissions and achieving net-zero emissions by 2050, resulting in a carbon dioxide emission reduction by 45 %, launching a global methane reduction pledge to reduce methane emissions by at least 30 % until 2030, reverse deforestation and also firstly addressing the substitution of fossil fuel and phase-down of coal power as UN climate goals. All these changes are necessary to keep the global temperature rise below 2 °C (pre-industrial level) [13].

The temperature limit refers to the scenario set in the Paris Agreement 2015, a universal, legal framework to strengthen the global response to the threat of climate change. The goal is to keep the global temperature rise well below 2 °C (preferably below 1.5 °C; see Figure 3) compared to pre-industrial levels, not to exceed the point of no return for irreversible global warming effects [14, 15].

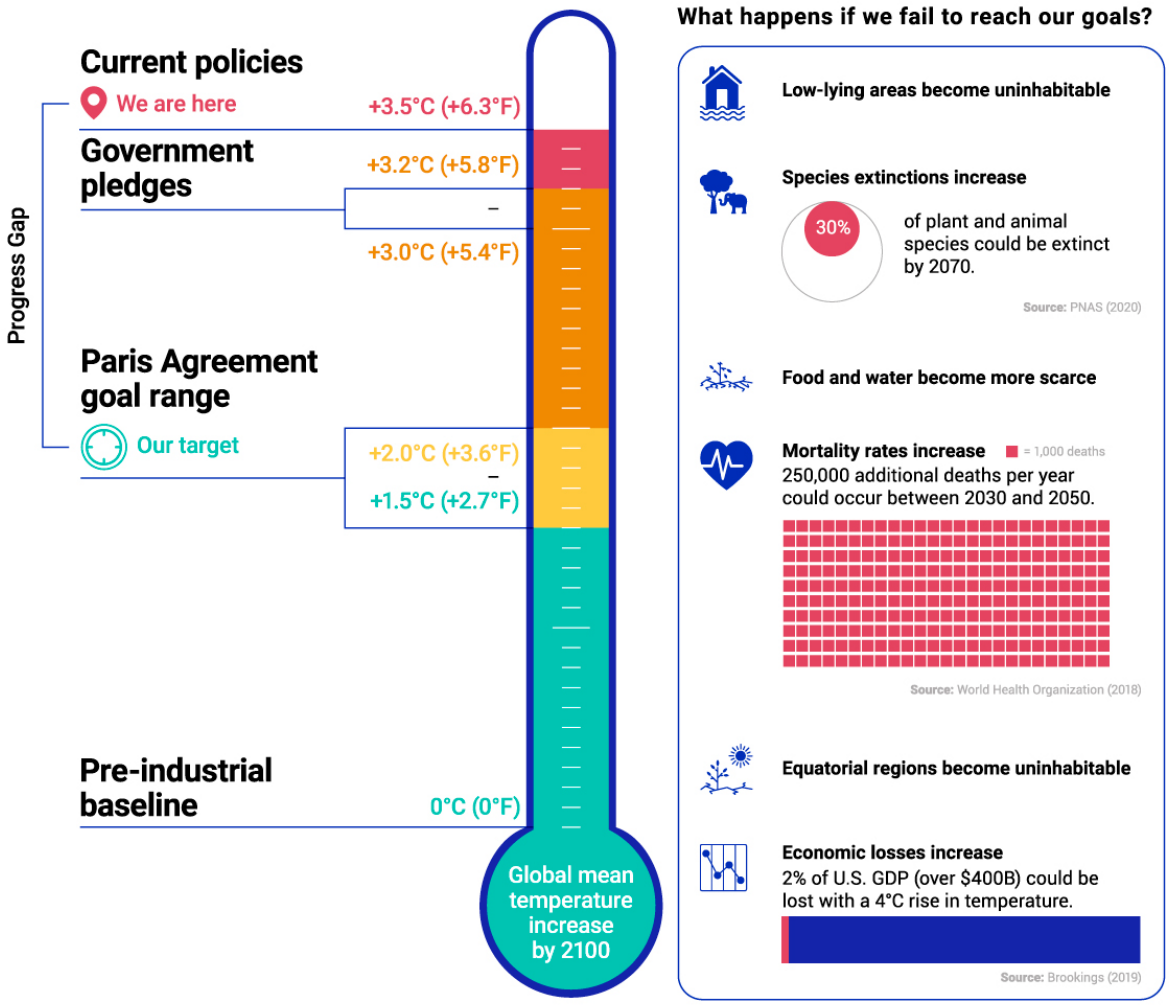


**Figure 3:** Temperature goals set within the Paris Agreement (2015) to limit global warming and their consequences when failed to meet [16].

At the COP28 in Dubai 2023, the Global Carbon Budget was presented, highlighting an increase in overall global fossil $CO_2$ emissions (see Figure 7 in Chapter *1.5.1 Emission reduction – decarbonization*). That indicates the bitter truth of an upward global temperature trend and denotes that much stricter policies are necessary to stop climate change [17].

## 1.3 Aim of this work

As stated above, the threat of climate change, driven by petroleum-based products, is a pressing reality. The increase in GHG emissions, air pollution, ecosystem collapse, and the decline in quality of life are already at alarming levels and continue to worsen.

Options to prevent further acceleration of climate change, focusing on the replacement of petroleum-based products with sustainable alternatives, are investigated within this work to aim at the preservation of finite resources, usage of cleaner forms of energy, independence and diversity of energy (local renewable energy industries instead of a few petroleum exporting countries and single companies).

Accordingly, diverse bio- or waste-derived lubricant components were investigated for their industrial capability to reduce or replace petroleum-derived components within the lubricant industry (see the first manuscript, Chapter *2.1 Publication I - A comprehensive review of sustainable approaches for synthetic lubricant components*).

Highlighting one of those bio-based and waste-derived components for its potential to replace petroleum-derived components in the lubricant industry is an oil extracted from spent coffee grounds, as those are a cheap and globally well-accessible resource (see the second manuscript, Chapter *2.2 Publication II - Moving towards green lubrication: tribological behavior and chemical characterization of spent coffee grounds oil*).

Moreover, directly replacing petroleum products with sustainable alternatives is often challenging and sometimes not entirely feasible. Bio-derived materials have certain drawbacks, including highly varying composition and rapid decomposition, which can be both an advantage and a disadvantage. For instance, Biodiesel has poorer cold flow properties compared to conventional diesel, primarily due to the presence of specific precipitates. Accurate detection and measurement of these precipitates in biodiesel blends are essential for improved quality control, which was part of the third manuscript (see Chapter *2.3 Publication III - Advanced Method for the Detection of Saturated Monoglycerides in Biodiesel using GC-EI-MS/MS*).

## 1.4 Fuels and lubricants

Fossil-derived fuels and lubricants still hold a considerable market share nowadays, but they are being replaced gradually by greener alternatives. A phase-out is pursued due to their enormous adverse effects harming human beings and the environment. However, changing to more sustainable systems is challenging due to global dependency on fossil products, and international consumption is still increasing as of 2023 despite all countermeasures [4].

In general, fuels like diesel are used in internal combustion engines. Diesel and biodiesel have distinct differences based on their origin, particularly in their composition and environmental impact. However, chemically and physically, they are similar enough (see Table 1.1) that biodiesel can be used for blending with diesel. To fulfill certain quality requirements, diesel fuel is regulated according to ASTM D975 [18] (USA) and EN 590 [19] (Europe) and biodiesel according to ASTM D6751 [20] (USA) and EN 14214 [21] (Europe).

| Symbolic structure | Name and formula |
|---|---|
| 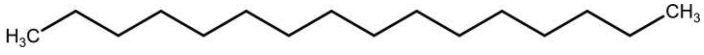 | **Diesel**<br>$CH_3$-$(CH_2)_n$-$CH_3$<br>n = 10 to 15 |
| 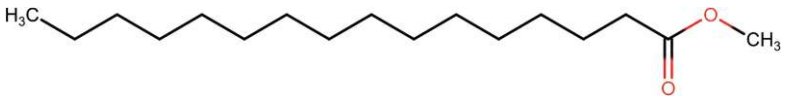 | **Biodiesel**<br>$CH_3$-$(CH_2)_n$-COO-$CH_3$<br>n = 12 to 22 |
| 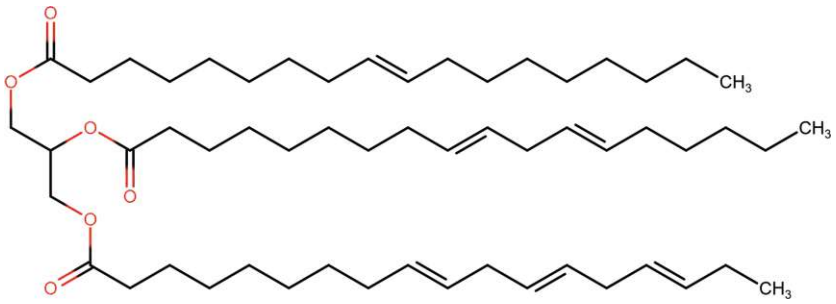 | **Vegetable oil**<br>$CH_2$-OOC-$R_1$<br>\|<br>$CH_2$-OOC-$R_2$<br>\|<br>$CH_2$-OOC-$R_3$<br>$R_{1-3}$ = C-length dependent on source |

**Table 1.1:** Simplified display and general formula of structural similarities and differences of petroleum diesel (top), biodiesel or fatty acid methyl ester (middle), and vegetable oil or triglyceride (bottom; here: unsaturated with an oleic C18:1, linoleic C18:2, and linolenic C18:3 acid chain).

Regulations on fuels like diesel and biodiesel are required to evaluate certain machinery compatibility and performance properties, to ensure quality levels for efficiency and longevity, to provide safety (e.g., for transportation, handling, and use), and to assess the environmental impact of such. Within Europe, the following standard methods for the analysis of diesel and biodiesel are employed:

- **Cetane number (CN)** is measured according to EN ISO 5165 [22] for gaseous and liquid fuels and lubricants (petroleum-, bio-based, and synthetic) using a standard single-cylinder, four-stroke cycle with variable compression ratio and an indirect injected diesel engine for a range of 0 to 100 CN. Paraffinic diesel (from synthesis or hydrotreatment) blends with up to 7 vol% fatty acid methyl ester (FAME) can be tested with this method. The CN measures the ignition quality of diesel fuel when injected into the combustion chamber within a diesel engine. A higher CN indicates that the fuel ignites more quickly, which is the case with biodiesel compared to petroleum-based diesel, as biodiesel mostly comprises long, unbranched hydrocarbon chains and no aromatics. Saturation in biodiesel feedstocks also affects the CN, as a higher amount of saturated fatty acids results in higher CN fuels [23].

- **Density** of fuels at 15 °C is determined by EN ISO 3675 [24] using a glass hydrometer having a Reid vapor pressure of a maximum of 100 kPa. The density of biodiesel is mostly slightly higher than that of petroleum-based diesel and it is increasing with its degree of unsaturation [23].

- **Viscosity** is measured for a range of 0.2 to 300,000 $mm^2/s$ within a temperature range of -20 to 150 °C by EN ISO 3104 [25] using manual or automatic viscometry. With increasing carbon numbers, the viscosity of biodiesel increases. The alcohol for transesterification might also affect the viscosity (methanol < ethanol < propanol) of the biodiesel.

A correlation of the type and the degree of unsaturation and viscosity is observed. A higher unsaturation results in a lower viscosity. Whereas the position of the double bond within the fatty acid chain has little influence, the configuration (cis, trans) shows a bigger influence. Trans double bonds lead to a higher viscosity compared to cis, hence most natural oils are less viscous, as cis double bonds are dominant [23].

- **Water content** EN ISO 12937 [26]: The water content of diesel and biodiesel is measured by coulometric Karl Fischer titration within 0.003 to 0.1 wt%. Water content is also a quality factor that might increase with increasing oil degradation and contamination, which influences the viscosity range of the oils. Regarding oil degradation, chain branching through hydrocarbon oxidation occurs, leading to water formation [27].
- **Ash content** is determined by EN ISO 6245 (petroleum-based) [28] within a range of 0.001 and 0.18 wt% for hydrocarbon diesel fuels, whereas bio-based fuel ash should be determined by ISO 3987 (bio) [29] with a minimum of 0.005 wt%, containing an additional step to produce sulfated ash of higher melting point. The ash content of petroleum-based fuels is generally quite low; a low ash content in fuels is preferred, and it might be increased by certain additives (inorganics). Specific biodiesel norms allow an ash content slightly higher, as it may contain inorganic impurities from the production process.
- **Flash point** EN ISO 2719 [30]: The flash point is evaluated in a temperature range of 40 to 370 °C using a Pensky-Martens closed-up tester, three procedures A-C are described where A is for distillate fuels (diesel, biodiesel blends), B for residual fuel oils and used lubricating oils, and C for biodiesel. The flash point is an important measure, especially for biodiesel, as it simultaneously demonstrates if the purity is ensured after methanol removal or whether there are highly volatile impurities, such as methanol, significantly depressing the flash point. Flash point and volatility are in a direct inverse relationship. With ongoing oxidation (chain branching) and the formation of low-molecular-weight components (alcohols, aldehydes, ketones), the physical properties will change, increasing the volatility of the oil [31].
- **Corrosiveness to copper** EN ISO 2160 [32]: Copper corrosion is measured using the copper strip test method for 3 h at 50 °C. The degree of corrosion is separated into four degrees: 1. slight tarnish, 2. moderate tarnish, 3. dark tarnish, and 4. severe corrosion.
- **Oxidative stability** is determined according to EN 14112 (bio) [33], EN ISO 12205 (petroleum-based) [34], and EN 15751 or EN 16091 (blends) [35, 36]. The oxidation stability of biodiesel is measured at 110 °C in an accelerated oxidation test. The determination by EN ISO 12205 is only allowed for middle-distillates with an initial boiling point above 175 °C and a 90 vol% recovery point below 370 °C. For blends, two different methods are valid: oxidation stability can be determined within 48 h of the induction period with up to 2 vol% biodiesel by EN 15751 (Rancimat method) and under accelerated conditions at 140 °C for an induction period to the specific breakpoint in a reaction vessel by EN 16091 (PetroOxy method). Especially for plant-derived oils, oxidative stability is an important factor for fuel performance. The oxidative stability and cold flow properties are influenced by the number of double bonds or free fatty acids (also represented in the acid number). In general, it can be stated that the higher the degree of unsaturation, the poorer the oil stability. The use of additives or structural modifications of the oils might be necessary to overcome these limitations [23].

  During the oxidation of hydrocarbons (oils), oil thickening (formation of high-molecular-weight hydrocarbons) and formation of carbonyl compounds (acids, aldehydes, ketones)

and alcohols take place, which can additionally modify the volatility and polarity of the oils. With the progression of degradation, sludge, deposit, and varnish can be formed, affecting the general lubricity. Auto-oxidation includes chain initiation, propagation, branching, and termination by free-radical chain reaction. The oxidation is initiated by exposure to oxygen and/or energy (heat, UV light, mechanical stress), where an allylic hydrogen atom is removed, and alkyl radicals are created. Carbon atoms connected to two vinyl groups (doubly allylic in poly-unsaturated oils) are especially susceptible to experiencing this form of oxidative instability. Subsequently, chain propagation occurs, where peroxyl radicals are formed and react with a hydrocarbon molecule to hydroperoxide and more alkyl radicals. The hydroperoxide initiates chain branching where alcohols and water are formed. Branching can also lead to the formation of aldehydes and ketones. Upon a specific oil viscosity, where oxygen diffusion is limited, two alkyl radicals will form a hydrocarbon molecule, causing chain termination [23, 31].

- **Cold flow properties:** Cold filter plugging point (CFPP) is determined using either a stepwise (EN 116) [37] or linear (EN 16329) [38] cooling bath method; EN 23015 is still stated as the standard method for cloud point (CP) measurement in biodiesel, but was replaced and unified with petroleum-based fuels by EN ISO 3015 [39] in 2019. The CP of a fuel is used to assess the temperature, where crystals start to form in the liquid. According to EN ISO 3015, a CP below 49 °C can be determined for diesel, biodiesel, paraffinic diesel blends with up to 7 vol% biodiesel and petroleum-based diesel with up to 30 vol% biodiesel being transparent in layers of 40 mm thickness. Furthermore, EN ISO 22995 [40], using a stepwise cooling technique, can determine the CP of petroleum-based fuels.

  Given significant variations in seasonal and geographical temperatures, specific restrictions on the low-temperature performance of diesel, biodiesel, and blends may not be universally applicable, despite the importance of these properties. Wax formation and insoluble precipitates can cause fuel filter blocking and engine starvation. As can be seen, more than one method is needed to give away viable information about the low-temperature performance of a fuel. For biodiesel, the CP increases with increasing saturation and chain lengths in fatty acid esters, leading to higher melting points and poorer cold flow properties. An investigation of more recent research is the formation of low-quantity insoluble, such as saturated monoglycerides and steryl glycosides, above the CP affecting the low-temperature operability [23].

- **Sulfur content** within a range of 3 to 500 mg/kg is estimated by EN ISO 20846:2019 [41] for diesel fuels and blends with up to 30 vol% biodiesel content using an ultraviolet fluorescence test method. The sulfur content of diesel, biodiesel, and 10 wt% blends can also be determined by EN ISO 20884 [42] using wavelength-dispersive X-ray fluorescence spectrometry within 5 to 500 mg/kg or by EN ISO 13032 [43] using energy-dispersive X-ray fluorescence spectrometry from 8 to 50 mg/kg.

- **Total contamination** is determined according EN 12662 [44] for diesel and blends with up to 30 vol% biodiesel content within 12 to 26 mg/kg.

Moreover, the following methods are necessary for evaluating diesel quality in addition to the methods mentioned above:

- **Cetane index** four-variable calculation by EN ISO 4264 [45] is only valid for petroleum-based diesel. It should not be applied to biodiesel, as it depends on the fuel's density and

distillation properties, which are non-comparable between the two fuel classes. The cetane index is used to estimate the CN of petroleum-derived middle-distillate fuels when test engines are unavailable.

- **Lubricity** is assessed according to EN ISO 12156-1 [46] using a high-frequency reciprocating rig measuring the wear scar diameter within 350 to 700 µm with a digital camera. The method validates petroleum-based middle distillate fuels, paraffinic diesel fuels, and biodiesel blends. A good fuel lubricity is essential, preventing surface damage within fuel injection systems. The lubrication can be of either hydrodynamic or boundary nature – hydrodynamic lubrication occurs when a liquid film separates two surfaces, e.g., the diesel fuel in the injector. In contrast, boundary lubrication is when the surfaces come in contact with each other; the lubricant adheres to the surfaces, forming a thin, protective layer.

  While modern injection systems need fuels with better lubricity, methods like hydrotreating to reduce the sulfur content of fuels show a negative impact on the overall lubricity of the fuel, as it removes lubricity-improving O-, N-, and S-heteroatomic molecules (decreasing in the order of O > N > S > C). Biodiesel naturally shows excellent lubricity due to its ester groups and trace impurities, such as free fatty acids and monoglycerides; thus, the purification of biodiesel to reduce impurities is at the expense of losing lubricity. The lubricity of neat biodiesel is not further regulated. Moreover, blending hydrotreated ultra-low sulfur diesel with low amounts (1-2 vol%) of biodiesel significantly improves the overall lubricity of the blend [23].

- **Manganese content** is determined within a range of 0.5 to 7.0 mg/l by EN 16576 [47] using inductively coupled plasma (ICP)-optical emission spectroscopy (OES) for diesel fuels with up to 10 vol% biodiesel content.

- **Polycyclic aromatic hydrocarbons** (mono-, di-, tri+-aromatic) in middle distillates containing up to 30 vol% biodiesel can be identified by EN 12916 [48] using high-performance liquid chromatography (HPLC).

- **Carbon residue** evaluation is feasible within ranges of 0.10 to 0.30 wt% according to EN ISO 10370 [49] after evaporation and pyrolysis under specified conditions.

And finally, the specific quality of biodiesel is further assessed using the following methods:

- **Linolenic acid methyl ester (C18:3)** is evaluated by gas chromatography (GC)-flame ionization detector (FID) according to EN 14103 [50] with an expected range of 90 to 100 wt%. The reason for specifically testing for this type of linolenic acid methyl ester is that it is composed of doubly-allylic sites, causing instability through auto-oxidation. Comparing the auto-oxidation rates of C18:1, C18:2, and C18:3 gives values of 1:41:98 [23].

- **Polyunsaturated FAME** with ≥ four double bonds are analyzed according to EN 15779 [51] using GC-mass spectrometry (MS). FAME of eicosatetraenoic acid (C20:4 (n-6)), eicosapentaenoic acid (C20:5 (n-3)), docosapentaenoic acid (C22:5 (n-3), and docosahexaenoic acid (C22:6 (n-3) within a range of 0.6 to 3.0 wt%.

- **Acid number** is determined by neutralizing free fatty acids in the biodiesel, which often are naturally present in the biodiesel feedstock, by titration with potassium hydroxide (KOH) within the range of 0.1 to 1 mg KOH/g according to EN 14104 [52].

- **Iodine value** is determined by EN 14111 [53] using a titrimetric method in the range of 111 to 129 g iodine/100 g. It simply measures the amount of iodine reacting with C=C double bonds, being proportional to the degree of unsaturation.
- **Methanol** content as a residue from the transesterification process is measured according to EN 14110 [54] using headspace GC-MS for ranges of 0.01 to 0.5 wt%. Already small amounts of residual methanol will have significant effects on the flash point of the fuel.
- **Glycerin (free and total)** (or glycerol), a by-product from transesterification, can be determined by GC-FID according to EN 14105 [55] down to 0.001 wt% in biodiesel originating from rapeseed, sunflower, soy, palm or animal oils and fats. Biodiesel from coconut and palm kernel derivatives is not compliant.
- **Glycerides** such as mono-, di-, and triglycerides can be determined down to 0.1 wt% by GC-FID along with glycerin [55]. Unreacted triglycerides from the transesterification process are measured along with impurities of mono- and diglycerides, as they are responsible for poor low-temperature operability problems.
- **Metal** content such as Ca, K, Mg and Na within fuels is determined within a range of 1 to 10 mg/kg using ICP-OES by EN 14538 [56] or using atomic absorption spectroscopy by EN 14108 [57] (sodium content $\geq$ 1 mg/kg) and EN 14109 [58] (potassium content $\geq$ 0.5 mg/kg).
- **Phosphorous** content is evaluated by EN 14107 from 4 to 20 mg/kg using ICP-OES [59].

The here-stated ranges (e.g., for GC-MS) are the threshold values for the analytical methods, not the quality limitations of the fuels. The threshold values required to meet the quality standards for diesel, biodiesel, and blends, as outlined in the mentioned regulations, are precisely discussed in Chapter *1.4.1 Diesel* and Chapter *1.4.2 Biodiesel*. Further methods for evaluation of fuels and lubricants not included in these norms are discussed in Chapter *1.7 Advanced structural elucidation for fuels and lubricants*.

It can be concluded that chemical components with negative effects in one direction might give beneficial properties in another. For example, monoglycerides contained in biofuel might lead to poorer cold flow properties while improving lubricity. Apart from complying with the regulations above regarding fuel quality, it is essential to investigate the efficiency and performance of a fuel during its use. Therefore, the fuel's rheological (flow) and tribological (friction and wear) characteristics are explored under varied conditions tailored to the particular application's requirements, including different materials, temperatures, loads, or additive packages. Along with lubricity/wear and abrasion, corrosion, and deposits on the engine compartments, fuel lifetime (stability and cleanliness) and fuel emissions can be tracked. Details are discussed in Chapter *1.4.4 Tribology* and Chapter *1.7 Advanced structural elucidation for fuels and lubricants [60]*.

While conventional petroleum sources decline, both present and future challenges for the global economy will be governed by decarbonization and advanced energy storage. A change to renewable energy sources is indispensable, drop-in products with increased sustainability using the available infrastructure or higher blends of biodiesel could serve as a bridge during the transition between phases of research, development, and industrial implementation. Drop-in products are bio-derived alternatives that can be integrated into fossil-based pathways at early stages, provided they are functionally and chemically equivalent and compatible with existing

infrastructure and used fuel additive packages. By reducing the requirement for conventional diesel and largely aligning with existing industrial infrastructure, these blends offer potential compatibility and support for the evolving energy landscape.

### 1.4.1 Diesel

Diesel has been used as a fuel since the end of the 19$^{th}$ century, and with progressing industrialization also the demand for fuel increased proportionally [61]. Conventional petroleum-based diesel is collected by the fractional distillation of crude oil. It consists of a complex hydrocarbon mixture of alkanes (n-, iso-paraffins), alkenes (olefins), cycloalkanes (naphthenes), and aromatics. It primarily comprises long-chain alkanes with its main fraction between $C_{10}$ and $C_{15}$ [62]. Paraffin waxes (branched chain hydrocarbons) tend to solidify at low temperatures, affecting the low-temperature operability of the fuel and its pour point and cloud point. To evaluate the fuel's low-temperature performance, the following tests are applied: ASTM D 2500 (cloud point) [63], ASTM D 97 (pour point) [64], ASTM D 6371 (cold filter plugging point) [65], and ASTM D 4539 (low-temperature flow test) [66]. The pour point is where the fuel starts to gel, whereas the cloud point is where the fuel starts forming crystals. These wax crystals may lead to fuel filter blocking. The cloud point of a fuel demonstrates low-temperature operability and can be improved by certain additives, mainly polymers interacting with the wax-crystal formation. The point when the fuel starts to block the filters is not solely based on the presence of crystals but more on their size and shape. To avoid issues with wax crystal formations, less waxy crudes or blends with lower wax content are used. Furthermore, diesel fuel can be manufactured at lower distillation end points to eliminate higher boiling wax contents, and certain additives can improve low-temperature performance [60].

Burning of diesel releases harmful environmental emissions such as GHGs, particulate matter, sulfur dioxide, and other pollutants [67]. Sulfur emitted from the fuel can react to sulfur dioxide, which can form particulate matter in the atmosphere, harming the respiratory system of humans and animals. But first, sulfur must be present in the fuel to form sulfur dioxide [68]. Low sulfur content increases the stability of a fuel; unstable fuel can cause filter blocking due to the formation of gums and organic particulates. Regulations address this issue and limit the content of sulfur in on-road fuels (ultra-low sulfur fuels) to 10 ppm within the EU [19, 69] and 15 ppm by U.S. EPA [70]. Along with sulfur, organic acids are reduced by fuel hydrotreating, reducing the fuel's overall acidity and its capability of corrosive damage at the expense of naturally occurring antioxidant and lubricating compounds. Hydrotreated fuel requires the addition of sophisticated performance additives, providing oxidative stability and lubricating properties [60].

Further specific requirements for diesel fuel are given by ASTM D975 [18] (USA) and EN 590 [19] (Europe). Fuel quality is given without limitation by a minimum CN, flash point, and a certain viscosity range. The ash content, consisting of metallo-organic compounds and inorganic particles, is limited to a maximum of 0.01 wt%, i.e. 100 ppm, enhancing the oil's lubricity since mainly inorganic particles contribute to increased wear. Furthermore, the water content is limited to a maximum of 0.05 wt% (USA) and 0.02 wt% (Europe) to limit corrosion within the engine system and upon storage [60].

| Property | Unit | ASTM D975 | | EN 590 | |
|---|---|---|---|---|---|
| | | Min | Max | Min | Max |
| Cetane number (CN) | | 40 | - | 51.0 | - |
| Cetane index | | 40 | - | 46.0 | - |
| Aromaticity | vol% | - | 35 | - | - |
| Polycyclic aromatic hydrocarbons | wt% | - | - | - | 8.0 |
| Sulfur content | mg/kg | - | 15 | - | 10.0 |
| Manganese content | mg/l | - | - | - | 2.0 |
| Flash point | °C | 38 | - | > 55.0 | - |
| Carbon residue | wt% | - | 0.35 | - | 0.3 |
| Ash content | wt% | - | 0.01 | - | 0.010 |
| Water content | wt% | - | 0.05 | - | 0.020 |
| Total contamination | mg/kg | - | - | - | 24 |
| Copper strip corrosion (3 h, 50 °C) | | - | Class 3 | - | Class 1 |
| FAME content | vol% | - | - | - | 7.0 |
| Oxidation stability | $g/m^3$ | - | - | - | 25 |
| Lubricity, wear scar at 60 °C | µm | - | 520 | - | 460 |
| Viscosity at 40 °C | $mm^2/s$ | 1.9 | 4.1 | 2.000 | 4.500 |
| Conductivity | pS/m or C.U. | 25 | - | | |

**Table 1.2:** Relevant threshold levels for diesel fuel specifications according to ASTM D975 [18] and EN 590 [19].

The here-stated ASTM D975 [18] values (Table 1.2) are for No. 2-D S15 fuels: general-purpose middle distillate fuels for use in diesel engine applications requiring a fuel with maximum 15 ppm sulfur. Furthermore, for both norms, CP or CFPP have to be determined and restricted depending on the climate.

As conventional diesel is not readily biodegradable, leaks and spills result in environmental consequences and damage. The biodegradability is assessed according to ASTM D5864 [71], ASTM D731 [72] or OECD 301 [73], stating that a product is readily biodegradable if at least 60 % of it is fully biodegraded within 28 days. Petroleum-based fluids do not fulfill this criterion [31]. Moreover, diesel fuel is non-renewable, and crude oil reserves are limited and expected to be depleting [74]; this is why it is often blended with or replaced by sustainable alternatives such as biodiesel.

The following specified limitations in regulations, including the Renewable Energy Directive (RED) and the Land-Use Change (ILUC) provisions, establish current and future foundations and frameworks for renewable fuels and energy carriers. Biofuels are required to achieve a reduction in GHG emissions of at least 50 % compared to fossil fuels since 2017. Moreover, by 2020, every European member state was obligated to substitute at least 10 % of the fossil energy used in transportation with renewable energy sources, including biofuels and electricity from renewable energy sources. Starting in 2023, detailed regulations for renewable fuels of non-biological origins (RFNBOs) have been established, specifying when electricity used to produce liquid or gaseous renewable fuels for transport is considered fully renewable and ensuring a GHG emissions reduction of at least 70 % compared to fossil fuels. By 2030, each member state is supposed to have a minimum share of 29 % renewable energy in their final transport energy consumption or a reduction of at least 14.5 % GHG transport intensity. Additionally, the share of advanced biofuels and biogas must increase to at least 1 % by 2025 and 5.5 % (at least 1 % of

RFNBOs) by 2030 for transport energy supply. Furthermore, the EU directive related to road transport was transposed into Austrian national law (fuel regulation, KVO), which states an obligated minimum annual GHG reduction of 6.0 % compared to the base fuel value of 94.1 g/MJ $CO_2$-equivalent by 2020. In Austria in 2022, the average GHG intensity of all fuels and energy carriers supplied to the Austrian market compared to the 2010 reference value results in a 3.05 % reduction (2.97 % attributable to biofuels and 0.08 % to renewable electricity), meaning that only half of the GHG reduction target was achieved through the use of fuel alternatives to fossil diesel and gasoline (60 % biodiesel GHG intensity) [75].

### 1.4.2 Biodiesel

Biodiesel is a renewable fuel from biological sources, typically vegetable oils or animal fats. Common feedstocks include soybean oil (largest source in the U.S.), canola oil (mostly used in Europe), used cooking oil, Jatropha, coconut and palm oil (common in Asia and Africa). Biodiesel comprises FAME and is produced by transesterification (see Figure 4) of those oils. Triglycerides (found in oils and fats) react with methanol (FAME) or ethanol (fatty acid ethyl ester (FAEE)), often catalyzed by an acid or base catalyst, to produce FAME and glycerol. Glycerol is used as animal feedstock, food or cosmetic industry. Further byproducts like water, catalysts, unreacted triglycerides, and alcohol must be removed from the biodiesel as they might have a huge impact on the quality and performance properties of the fuel. The resulting FAME alkyl chain lengths result from the original triglyceride structure and are typically within 12 to 22 carbons [60].

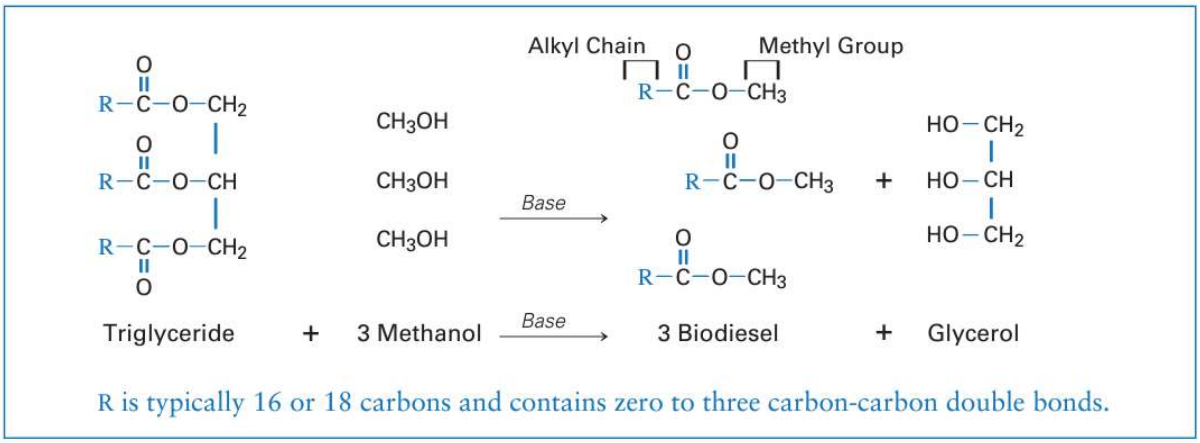


**Figure 4:** Scheme of transesterification of vegetable oil with methanol to biodiesel [60].

Biodiesel has similar physical and chemical properties as conventional petroleum-based diesel fuel, making it suitable for blending. The composition of biodiesel will vary significantly depending on the used source for the biodiesel. The most prominent fatty acids within vegetable oils and animal fats are palmitic acid (16:0), stearic acid (18:0), mono-unsaturated oleic acid (18:1), di-unsaturated linoleic acid (18:2), and tri-unsaturated linolenic acid (18:3), with huge variations within the different plant types. Canola (a breed of rapeseed) and rapeseed are mostly composed of C18:1 (up to 60 %), followed by C18:2 and C18:3 (adding up to $\sim$ 30 %). Oils like corn, safflower, soy and sunflower mainly contain C18:2, followed by C18:1. Jatropha oil contains almost equal parts of C18:1 and C18:2 ($\sim$ 40 %); Divergent from the other oils, palm

and coconut oil are mostly composed of saturated fatty acids; palm oil contains an equal share of C16:0 and C18:1 (∼ 40 %) and coconut oil is mostly containing shorter chain fatty acids, such as C12:0 (∼ 50 %) and C14:0 (∼ 20 %). The main component of tallow and yellow grease is C18:1 (∼ 40 %); followed by C16:0 > C18:1 (tallow) and C18:2 > C16:0 (yellow grease) [23].

Unsaturated fatty acids improve cold flow performance (e.g., as in rapeseed oil) but are less stable towards oxidation. Supposedly, unsaturated fatty acids cause lower CN and higher iodine values. Highly saturated fatty acid feedstocks (e.g., tallow and palm oil) tend to have poor low-temperature properties. As can be concluded, changes in the single compositional features of FAMEs can simultaneously have desirable and undesirable effects since they often behave antagonistically. Moderate unsaturation levels are favorable for biodiesel since saturated fatty acids are structurally more similar to conventional diesel than unsaturated ones. The cold flow performance of biodiesel is crucial for determining its suitability as a fuel or blend feedstock [23].

Potential sustainable biodiesel sources that are not so obvious as common vegetable oils might be oils from agricultural or other plant-derived waste types such as spent coffee grounds oil (SCGO). SCGO was investigated within this work as waste-derived feedstock that does not primarily compete with the food industry as other vegetable oils do (see Chapter *2.2 Publication II - Moving towards green lubrication: tribological behavior and chemical characterization of spent coffee grounds oil*). The composition and properties of the spent coffee grounds oil appear suitable for biodiesel production via transesterification. Now, there are just a few applications for spent coffee grounds, including coffee composites [76] or growing mushrooms [77]; most of the grounds are disposed of at landfills, with their potential as high-quality feedstock for biofuel or bio-lubricant production. However, as coffee has widespread popularity as a modern beverage with an increasing demand and Europe holds the biggest market share for coffee consumption, there is a big industrial potential to locally collect spent coffee grounds and process them into novel valuable products [78].

Specific requirements for biodiesel fuel are given by ASTM D6751 [20] (USA) and EN 14214 [21] (Europe). The ash content limit of 200 ppm for biodiesel is higher than that of conventional diesel, resulting from soluble metallic soaps or abrasive solids and remains of catalyst all derived from the transesterification process. Further maximum limits are on water content, a by-product from transesterification, with 0.05 wt%, sulfur with 15 ppm and 10 ppm for USA and Europe, respectively. Metals group I (Na, K) and group II (Ca, Mg) are limited to 5 ppm in each group, indicating the presence of residual catalysts or metallic soaps, as they could raise the ash content and participate in the precipitate formation, hence increase the filter blocking probability [60].

Compared to conventional diesel, for biodiesel, higher viscosity is permitted, which is usually more viscous. For Europe, thresholds are regulated more strictly (3.5 to 5.0 $mm^2/s$) compared to the U.S. (1.6 to 6.0 $mm^2/s$), especially at lower limits. In general, viscosity correlates with the degree of unsaturation; higher unsaturation causes lower viscosity (except for coconut-derived FAME). Most biodiesel types fall within a range of 4 to 5 $mm^2/s$, meeting both ASTM D6751 and EN 14214 viscosity specifications. Some biodiesel types (e.g., coconut-derived) are below the limit of EN 14214, but would still meet ASTM D6751 criteria due to tolerating very low viscosity levels [23].

From the reaction of triglycerides with methanol, unreacted glycerin might still be left, total glycerin content is therefore limited to 0.024 wt% and 0.25 wt% for USA and Europe, respectively; a low amount of free glycerin (max. 0.02 wt%) in the fuel ensures a high FAME conversion. Also, methanol could still be left from the reaction and is limited to 0.2 wt%, causing a decrease of flash point. A high content of total glycerin in biodiesel or blends can cause the formation

of precipitates, leading to injector deposits and system or filter blocking. The same problem occurs with higher mono-, di- or triglyceride levels. Therefore, they are limited to 0.4 wt% and 0.7 wt% for monoglycerides, for USA and Europe, respectively, and 0.2 wt% for di- and triglycerides for Europe. The acid number for biodiesel, determining free fatty acids, is limited to 0.5 mg KOH/g; it is expected that due to the presence of natural organic acids, this value is higher than that of conventional diesel. Furthermore, biodiesel unsaturation is also restricted within Europe: the maximum iodine value, a measure of total unsaturation, is 120 g $I_2$/100 g biodiesel; linolenic acid methyl ester (C18:3), commonly contained in vegetable oils, is limited to 12 wt% and polyunsaturated FAMEs (four or more double bonds) are limited to 1 wt%. Furthermore, CP and CFPP have to be reported and limitations depend on the climate classifications.

| Property | Unit | ASTM D6751 | | EN 14214 | |
|---|---|---|---|---|---|
| | | Min | Max | Min | Max |
| Cetane number (CN) | | 47 | - | 51.0 | - |
| Kinematic viscosity at 40 °C | $mm^2/s$ | 1.9 | 6.0 | 3.5 | 5.0 |
| Density at 15 °C | $kg/m^3$ | - | - | 860 | 900 |
| Sulfur content | mg/kg | - | 15 | - | 10.0 |
| Flash point | °C | 130 | - | 101 | - |
| Carbon residue | wt% | - | 0.050 | - | - |
| Sulfated ash content | wt% | - | 0.020 | - | 0.02 |
| Water content | wt% | - | 0.050 | - | 0.050 |
| Total contamination | mg/kg | - | - | - | 24 |
| Copper strip corrosion (3 h, 50 °C) | | - | Class 3 | - | Class 1 |
| FAME content | wt% | - | - | 96.5 | - |
| Oxidation stability at 110 °C | h | 3 | - | 8.0 | - |
| Acid number | mg KOH/g | - | 0.50 | - | 0.5 |
| Iodine value | g iodine/g | - | - | - | 120 |
| Linolenic acid methyl ester | wt% | - | - | - | 12.0 |
| Polyunsaturated FAME | wt% | - | - | - | 1.00 |
| Methanol content | wt% | - | 0.2 | - | 0.20 |
| Monoglyceride content | wt% | - | 0.4 | - | 0.70 |
| Diglyceride content | wt% | - | - | - | 0.20 |
| Triglyceride content | wt% | - | - | - | 0.20 |
| Free glycerin | wt% | - | 0.020 | - | 0.02 |
| Total glycerin | wt% | - | 0.240 | - | 0.25 |
| Metals I (Na+K) | mg/kg | - | 5 | - | 5.0 |
| Metals II (Ca+Mg) | mg/kg | - | 5 | - | 5.0 |
| Phosphorous content | mg/kg | - | 10 | - | 4.0 |
| Distillation 100 % removed | °C | - | 360 | - | - |

**Table 1.3:** General performance and quality requirements for biodiesel.

ASTM D6751 [20] values (provided in Table 1.3) are relevant for No. 2-B S15 fuels: general-purpose biodiesel blends stocks for use in middle distillate fuel engine applications requiring a fuel with maximum 15 ppm sulfur and a good low-temperature operability.

Biodiesel generally has a lower carbon footprint compared to conventional diesel. It produces fewer GHG emissions during combustion and can be considered a more environmentally friendly

alternative. Biodiesel can be used in diesel engines with little to no modification. However, higher blends may require engine modifications. One of the significant drawbacks of biodiesel is that it currently cannot completely replace diesel. Due to biodiesel's higher pour point (increased viscosity at low ambient temperatures) compared to conventional diesel, its use is limited in colder climates. Also, components such as glycerin, glycerides, and unsaturated FAME may precipitate above the cloud point, causing filter blocking and injector coking [23, 60]. This also affects blends of diesel and biodiesel, which is further investigated in the next Chapter *1.4.3 Blends and applicability*.

### 1.4.3 Blends and applicability

It is known that diesel fuel can gel at frigid temperatures (crystallization of paraffin wax), potentially causing engine issues [79]. Still, biodiesel shows even slightly poorer cold-weather performance (saturated components can increase the crystallization temperature) [80]. Therefore, biodiesel (B100) is often blended with conventional diesel (B0) in different ratios. The nomenclature for such blends indicates the percentage of biodiesel in the blend, e.g., B5, B7, B20, indicating 5, 7, and 20 % biodiesel mixed with pure diesel, respectively. Fuel quality is assessed by monitoring the CFPP, a measure of the lowest temperature where a specific fuel volume passes a standardized filter within a certain time period [81], by EN 116 (stepwise cooling bath method) [37] of the seasonal fuel (temperature limitations for biodiesel according to EN 14214:2019-05 [21] and B0-B7 blends according to EN590:2022-05 [19]). The specific properties and regulations regarding biodiesel blends vary by region and depend on the feedstocks used in biodiesel production.

Some biodiesel constituents are expected to impact the cold flow properties, such as unsaturated FAME [50, 51], steryl glycosides [82], glycerin [55], water [26], and mono-, di- and triglycerides/soaps [55], and most of them are regulated [21]. Even though biodiesel is used in blends with diesel and complies with the limit set in the norms, sedimentation and filter blocking still occur at petrol stations and in combustion engines. EN 14214:2019-05 [21] explicitly advises a further limitation of total saturated monoglyceride (SMG) content, but no established testing method was available at the time of disclosure. The standard procedure combines multiple testing methods of undefined precision based on multilevel correlation, giving a high measurement error (± 50 %). The main cause for filter blocking was considered to relate to the occurrence of saturated monoglycerides as published in one preliminary study [83].

The total SMGs content in biodiesel is limited to 7000 ppm [21], theoretically resulting in 490 ppm in a B7 mixture. These levels do not prevent filter blocking, nor does the regulation of individual SMG concentrations. A reliable detection of SMGs 1-C16:0, 2-C16:0, 1-C18:0 and 1-C19:0 by GC-FID in the range of 200 to 1500 ppm in biodiesel (theoretically 14 to 105 ppm for B7) is possible according to EN 17057:2018-03 [84]. Both norms only apply to detecting SMGs in biodiesel, but not for blends with diesel. An adaption for the GC-FID method is necessary for SMG detection in diesel blends reducing overlapping signals in the complex matrix, which gave the starting point for the third publication within this thesis (*2.3 Publication III - Advanced Method for the Detection of Saturated Monoglycerides in Biodiesel using GC-EI-MS/MS*), aiming to introduce a GC-electron ionization (EI)-tandem MS method to properly detect SMGs in biodiesel-diesel blends and correlate those amounts with the filter blocking behavior of the fuel (also see Chapter *1.7.1 Gas chromatography coupled to mass spectrometry*).

### 1.4.4 Tribology

The word tribology consists of the two Greek words 'tribos' $\tau\rho\iota\beta\omega\sigma$ meaning "rubbing" and 'logia' $\lambda o\gamma\iota\alpha$ for "science of" [85, 86]. So, tribology describes the science and engineering of interacting surfaces in relative motion. It plays a crucial role in energy management, as motion can cause friction and wear, and lubrication may be needed. The so-called tribosystem is made of a body, a counter-body, an intermediate medium (e.g., a lubricant; not compulsory), an applied normal force, and a specific type of movement (sliding, rolling, impact, oscillating). These bodies and counter-bodies can be of various materials mimicking the intended application such as different metals, ceramics, synthetic materials, etc. [87].

#### 1.4.4.1 Tribology of different diesel blends

The application of tribological principles is essential for various industries, including automotive, aerospace, manufacturing, and energy. In terms of a motorized vehicle, reduced fuel and oil consumption, low maintenance, high reliability and durability, reduced exhaust emissions, etc., are crucial not only in terms of optimized machine operation (energy efficiency, safety, and lifetime) but also in minimizing environmental impact [88]. In essence, greenifying in the context of tribology involves implementing practices that prioritize environmental sustainability, energy efficiency, and reduced environmental impact in the study and application of friction, wear, and lubrication. This involves incorporating a) environmentally friendly lubricants (EFLs) being bio-based, recyclable and biodegradable, b) minimizing friction and wear through improved materials and technology to extend lifespans, c) enhanced surface design and nanotechnology [89], d) (standardized) life cycle assessments (LCAs) to evaluate the environmental impact and e) restrictions through regulations and standards [90]. A transition towards more sustainable processes is challenging; substantial infrastructure changes need massive investments parallel to creating a sufficient demand and overcoming market resistance for petroleum-based products. Supportive policies and regulatory frameworks on a global level are mandatory to ensure economic viability and facilitate advancements in green, sustainable technologies.

Since vegetable oils have good natural lubricity, it is not regulated for biodiesel. The wear scar for conventional diesel fuels must be determined according to ASTM D6079 [91], ASTM D7688 [92] or EN ISO 12156-1 [46] using a high-frequency reciprocating rig. For diesel fuels, it can be normally said that the less processed (e.g., hydrotreated) it is, the better the lubricity. To enhance the lubricity of diesel fuel, surface-active polar additives can be added to attach to the metal surfaces and act as boundary lubricants [60].

To study the effectiveness of a lubricant, friction and wear tests are conducted. A common friction test is recording the coefficient of friction as a function of sliding speed giving the Stribeck curve (see Figure 5. The curve is sectioned in the following regimes [93, 94]:

- Boundary regime: at low speeds or high loads, when the surfaces come in direct contact and the lubricant is squeezed out of the contact zone and fails to form a load-bearing film, wear is expected
- Mixed lubrication regime: within increasing speed, the lubricant can enter the gap between the surfaces, reducing friction and wear, asperity contact is possible
- Elastohydrodynamic regime: a thin lubricant film starts forming between opposing surfaces, elastic deformation of the bodies in contact takes place, the viscosity of the lubricant increases and hydrodynamic action is enhanced [95]

- Hydrodynamic regime: at higher speeds or lower loads, the lubricant separates the two opposing surfaces forming a load-bearing film; as the film thickness increases, so does friction, with the rheological properties of the lubricant being the primary influence in this scenario

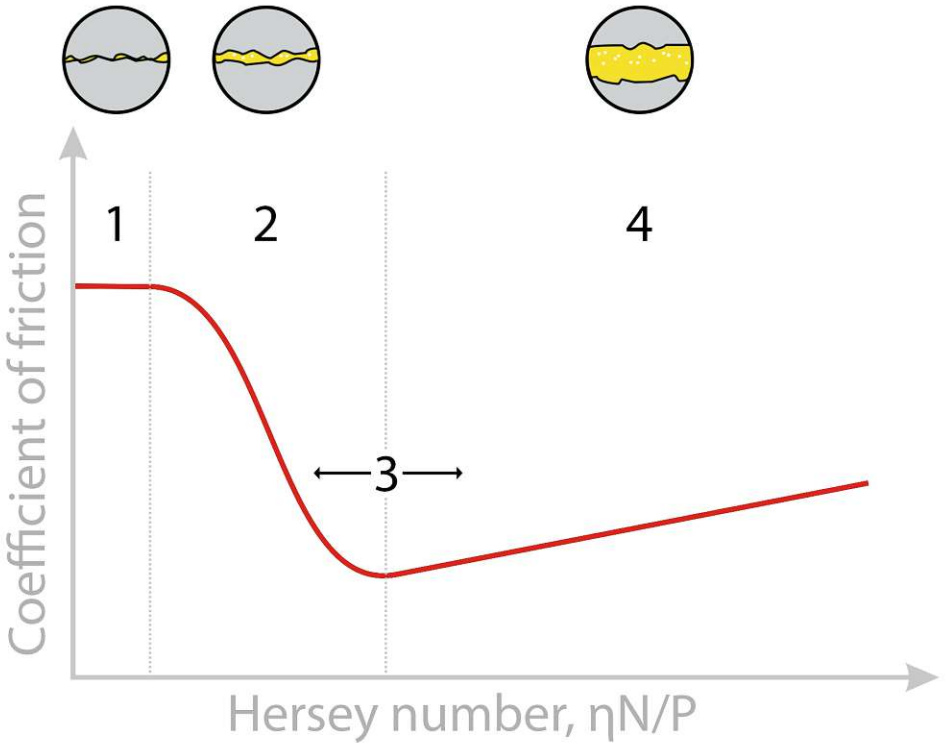


**Figure 5:** Schematic Stribeck curve showing 1. boundary lubrication, 2. mixed lubrication, 3. elastohydrodynamic lubrication, and 4. hydrodynamic lubrication. Adapted from [96].

The shear-induced friction is dependent on the viscosity ($\eta$), the rotational speed (N), and the applied load (P), giving the Hersey number:

$$Hersey\ number = \frac{\eta N}{P}\ in\ Pa * s \tag{1.1}$$

As actual field tests for tribological investigation of a system's efficiency are time-consuming, often not easily controllable concerning conditions, and expensive, test rigs are used. There are multiple tribological test systems available for the evaluation of lubricant and fuel performance; the according test rig can be chosen based on standardized test methods or available equipment. Moreover, the most suitable selection needs a definition of the problem identified in the field (heat, wear, failure, etc.) [97]. Then the field application of interest has to be simulated concerning test parameters and expected test results. This step includes the selection of materials for base- and counter-body (composition, hardness, surface design, coatings, etc.), intermediate medium, type of motion (sliding, rolling, unidirectional, oscillating), velocity (ramp, constant, alternating), load (constant, ramp, cycling), contact pressure, and duration (fixed or until failure) [87]. As a result, the wear scar, volume, and weight loss can be determined combined with the coefficient of friction, the friction force, and lubricant analysis (change in properties, decline of additives, increased wear particle count). Furthermore, test results can be correlated with the field results [97].

The geometry of the tribo-contact influences the applied load, the contact area, and the shape. Whether it is characterized as point, line, or area contact, this geometry plays a crucial role alongside other factors like sliding speed, material chemistry, and lubricant properties, shaping the distinct tribological challenge. The selection of contact geometry for wear testing depends on the particular tribological situation being mimicked, whether to assess particular lubricant characteristics, such as additive performance, with designated material combinations or to model wear mechanisms observed in real industrial machinery [97].

Tribological tests suitable for evaluating lubricant performance include those conducted with a four-ball wear tester, pin- or ball-on-disc, plate, or three-plate configuration.

- **Four-ball:** features three lower balls, which can be held stationary or allowed to roll in a race, while the upper ball rotates for a set duration. The stationary ball configuration is the most commonly used in these tests. Lubricant is added to the tank, and the fixed balls are pressed against the rotating one, initiating sliding wear in an initial three-point contact. This system offers precise loading but has a limited range of test loads. As motion begins, the contact area transitions from point to area contact. At the test's conclusion, the wear scar width on each ball is microscopically measured and averaged. Testing with balls ensures consistency in shape and properties, although the material being tested must be available in ball form. Alternatively, the ball-on-three-plates setup can be used for other geometries. This test is often used to assess the anti-wear properties of diesel fuels containing lubricity additives, providing wear prevention characteristics and coefficient of friction at various test loads [97, 98].

- **Unidirectional/rotational pin- or ball-on-disc:** A fundamental and widely used wear testing method involving a rotating disc and a loaded pin or ball creating wear tracks. Primarily used to assess the endurance and wear rates of coatings, film lubricants, and the effectiveness of liquid lubricants, measuring wear progression and friction coefficients by observing material removal or transfer between the pin (or ball) and disc. Both bodies are analyzed after the test for wear extent and material transfer, typically through wear scar measurements and surface profiling of the scar's depth and width. A drawback of the pin-on-disc test is that the wear results often deviate from those observed in field tests, primarily due to differences in configuration compared to typical field components [97].

- **Reciprocating/oscillating pin- or ball-on-plate:** also referred to as pin- or ball-on-flat, the test is commonly used to investigate reciprocating sliding motion, which is valuable for studying friction, wear, and lubrication films appearing in applications like piston rings on cylinder walls. Reciprocating motion can occur in point, line, or area contacts, with vertical load application. The speed, controlled by reciprocation rate, stroke length, and machine design, follows a sinusoidal wave shape due to the start-stop reversal of reciprocation. The test can be run at a high repetition rate to reach steady-state friction and wear conditions rapidly or at longer stroke distances, with fewer oscillations in a specific duration, to focus on initial wear stages. Longer strokes may affect the reciprocation rate depending on the test design. The reciprocation rate is measured in Hertz (cycles per second), and it needs to be specified along with stroke length, load, and temperature for the conduction of the test. Wear is evaluated by measuring wear scars on the ball and plate. This test is commonly employed to assess the lubricating properties of diesel fuels and lubricants, including extreme pressure performance, friction, and wear [97, 98].

- **Ball-on-three-plates:** also referred to as ball-on-pyramid; A ball in rotational or reciprocal movement is placed on three stationary, 45° tilted plates or discs under equal, predetermined

load. This test is similar to the four-ball test. Also here, lubricant can be added to the tank, and the rotation of the upper ball against the fixed plates induces sliding wear at an initial three-point contact. But differently to the four-ball tester, a wider selection of material combinations is available. At the end of the test, the wear scar can be determined and averaged for the three plates. For the lubricant, the friction and wear performance, additive reactivity, and lubrication regimes (boundary, mixed, hydrodynamic) can be assessed with this method [97, 99].

- **Block-on-ring:** A rectangular block is placed against a rotating ring under a predetermined load, initially establishing Hertzian line contact. As movement begins, a load-carrying bearing surface develops, allowing for the formation of anti-wear and/or extreme pressure films on the surface. This setup is adaptable to various test fixtures for point, line, ellipsoid, and area contact. Measurements of the coefficient of friction, wear scar width and potential volume loss (which may be challenging for identical metals) of both the block and the ring are taken as the ring rotates at a specified rate. Additionally, oscillating drive mechanisms can be investigated to assess wear protection provided by lubricant films, utilizing a steel ring oscillating against a steel block [97, 99]. Testing ball-on-ring combinations can support the monitoring of the friction force of extreme pressure additives in lubricants to predict load limits [97]. In general, block-on-ring tribometers can be utilized to simulate wheel wear (with the ring representing the wheel and the block serving as the brake) [98] and to explore nanolubricants, solid lubricants, coatings, and other materials. This tribometer configuration enables the evaluation of wear and coefficient of friction between sliding surfaces in contact, such as lubricating films, rings, and bearings [99].
- **Pin and Vee Block:** Its basic design involves two opposing Vee blocks loaded against a rotating journal pin, typically operating in four-line contact unless C-Blocks are used to provide a conformal area contact. It is utilized for assessing the lubricating and wear-reduction properties of various lubricants, such as metalworking fluids, automotive and industrial lubricants, and solid film lubricants. During testing, the pin and blocks are immersed in the lubricant and with either constant load (for anti-wear properties) or increasing load (until failure assess lubricating effects at different load levels) applied. Monitoring torque with respect to the test load can provide insights into the lubricating properties of the tested fluid and its interaction with the selected materials. Changes in the torque curve slope can indicate variations in the lubrication regime and a detailed examination of torque, load, and wear values offers information on the anti-wear and extreme pressure properties of the tribological system [97, 98].

Wear can be quantified using various methods, including gravimetrically, volumetrically, or by measuring the affected area over time or under increasing loads. The gradual reduction in wear, eventually stabilizing at a low level, is described as "running-in wear". The concept of failure analysis elaborates on potential functionality concerns, particularly for assessing tool and machine element failures arising from wear, lubrication issues, plastic deformation, and fracture. Practical tests oriented towards such analysis are employed [100, 101].

Wear damage through tribological contact can cause alterations in form and materials and lead to wear particle formation. Wear is characterized by four mechanisms: adhesive wear, abrasive wear, fatigue wear, and corrosive wear, and their damage patterns are depicted in Figure 6. They can occur individually or frequently as a combination of these mechanisms and are described the following [87]:

- **Adhesive wear**: wear caused by material transfer between two surfaces under high pressure (and the generated frictional heat), allowing atomic bonding. The material will detach from one surface and adhere to the opposite surface, typically at low progression rates. When two metals are used, this wear phenomenon is called cold welding. To protect the surfaces from adhesive wear, intermediate media such as lubricants can be used, separating the surfaces at their contact positions [87, 94]. Adhesive wear can result in particle formation and transition into abrasive wear, and both types of wear can be minimized by employing metal combinations less prone to bonding, enhancing the formation of low-shear-strength additive layers, and increasing the lubricant film thickness [102].

- **Abrasive wear**: wear is provoked by materials with significantly different hardness levels, hard particles, or surface bumps causing material removal from the surface. Due to relative motion, channels and scratches form, and in severe cases, material breaks away from the surface, leading to extensive wear. Material abrasion involves multiple simultaneous microstructural changes such as micro-plowing (plastic deformation), micro-cutting (formation of shavings), micro-fracture (formation of cracks), and micro-fatigue (local material fatigue) [87, 101]. Considering the abovementioned factors, abrasive wear can be minimized by enhancing surface hardness, decreasing surface roughness, and applying soft coatings for abrasive particle embedding [102].

- **Fatigue wear**: also referred to as fretting wear; wear caused by surface fracture through rolling or sliding surfaces under contact stress in an oscillating motion. When the applied load surpasses the elastic limit, plastic deformation takes place. The caused displacements are migrated along the slip planes, pile up at transition points and eventually block each other's movements. This accumulation of dislocations at obstacles contributes to the strain hardening of the material, and contact fatigue induces surface fretting and flaking [87, 101]. Damage can be mitigated by augmenting lubricant film thickness, incorporating fatigue-reducing additives, or minimizing sliding relative to rolling motion in the contact [102].

- **Corrosive wear**: wear within the tribo-contact area caused by chemical reaction of surfaces with the ambient medium (e.g., atmosphere, humidity, ...) or intermediate material (e.g., the lubricant) promoting particle or layer formation [87]. The predominant form of this type of wear is oxidative wear, although it could also be derived from other corrosive species such as water, carbon dioxide, sulfuric compounds, acids (due to combustion or oxidation), and performance additives (anti-wear or extreme pressure) [102]. The reaction products, whether naturally occurring or resulting from tribochemical reactions, are often hard and brittle, such as metal oxides. If these products detach due to mechanical stress, they exacerbate wear (abrasion), perpetuating the tribochemical reactions [87, 101]. Corrosive wear can be reduced by applying lubricant additives designed to prevent corrosion, rust, and oxidation. Additionally, restricting water access to the surface and employing overbased detergents for neutralization are advantageous [102].

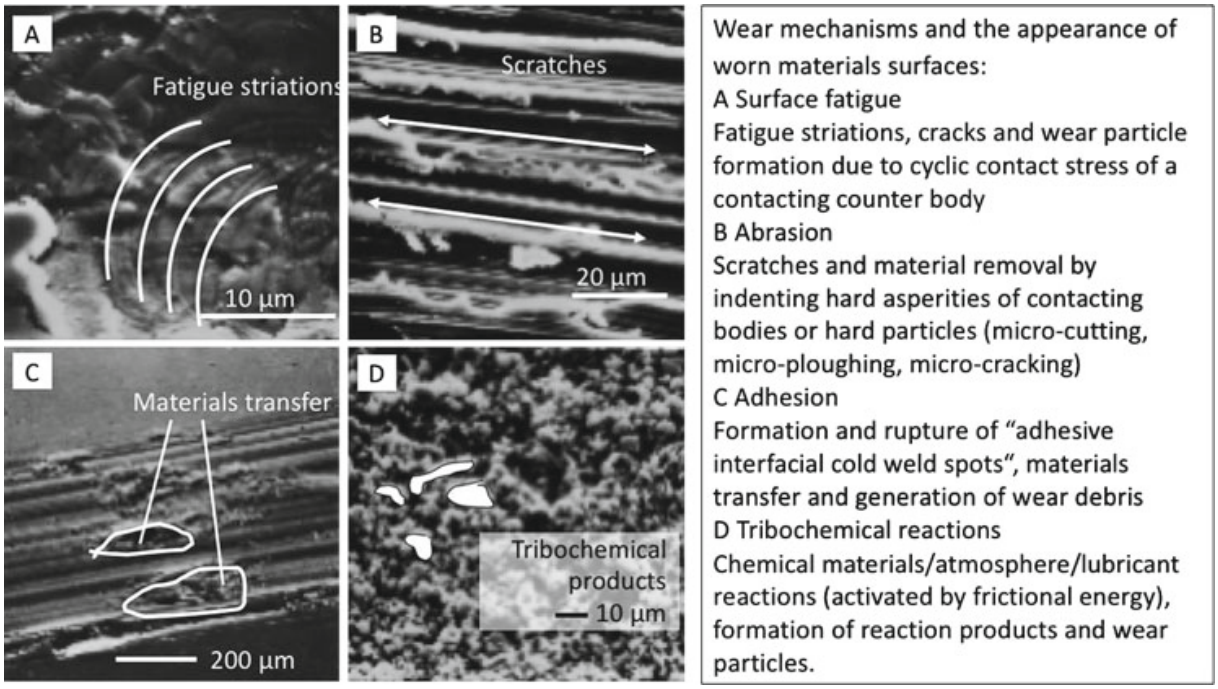


**Figure 6:** Damage patterns occurring from four different wear mechanisms [103].

### 1.4.5 Lubricants

Lubricants are used in a wide range of applications such as transportation, power generation, food processing, medical devices, marine and space, etc. for different machinery. These include engines, bearings, gears, transmissions, pumps, turbines, and so on to reduce friction between moving surfaces, minimize wear, and extend machinery life. They come in various types: mineral oil-based, synthetic, ester- and bio-based. A lubricant's task is to reduce friction and wear between surfaces, ensure efficient heat transfer and cooling, protect the surface (sealing), e.g., from corrosion, and provide a transfer of material, e.g., wear debris (cleaning effect). For a functional lubricant, it is therefore important to have high thermo-oxidative stability, low volatility, good lubricity, suitable thermal viscosity properties, low foam building tendency, and minimized tendency to form deposits.

At least 70 vol% of a lubricant is composed of a specific base oil of varying origin giving specific basic properties (see Table 1.4; the rest is a variation of additives being able to affect the lubricant's properties (enhancing, suppressing, or adding to existing base oil properties) to ideally be better performing for a particular field of application. Different materials with great potential as lubricant base oils of industrial relevance and benign or biomimetic to the environment were intensely studied within the first manuscript - Chapter *2.1 Publication I - A comprehensive review of sustainable approaches for synthetic lubricant components* which includes structures derived from fatty-acids, fermentation, lignin, polysaccharides and glycans, polyalcohols, ionic liquids, proteins, vitamins, lecithin and a few more.

| Characteristic | Petroleum Oil | Vegetable Oil | Saturated Ester | PAO |
|---|---|---|---|---|
| Lubricity | Low | High | High | Low |
| Oxidative Stability RPVOT | 300 | 50 | 180 | 300 |
| Viscosity Index (VI) | 100 | 200 | 165 | 150 |
| Hydrolytic stability | High | High | Low | High |
| Polarity | Low polar | Highly polar | Polar | Low polar |
| Saturation | Saturated | Unsaturated | Saturated | Saturated |
| Flash point (°F/°C) | 200/95 | 450/235 | 400/205 | 350/180 |
| Pour point (°F/°C) | -35/-38 | -35/-38 | -40/-40 | -50/-45 |

**Table 1.4:** Characteristics of different base fluids for lubricant formulation. Adapted from [31].

Lubricant additives are used for alterations in:

- Viscosity: viscosity modifier, e.g., thickener, to improve the resistance to flow
- Friction performance: friction modifier, to enhance the lubricity
- Wear properties: anti-wear or extreme pressure, to protect the surface from wear damage
- Corrosion behavior: corrosion inhibitor, to prevent rust and corrosion as a destructive reaction between water or acids and metals
- Degradation mechanisms: antioxidant, to reduce deposit precursors (radicals, hydroxides)
- Foam formation: foam inhibitor, to prevent air from reacting with the lubricant
- Pour point: pour point depressant, to improve cold flow properties
- Dispersibility: dispersant, to control the deposit and keep it suspended
- Contamination: detergent, to control the deposit and act as acid neutralizer

Often, these additives are based on structures that are not readily biodegradable or even harmful to the environment, are toxic, cause hazardous emissions upon production or use, or contaminate wastewater. Additionally, additives designed for non-polar petroleum-based oils are unsuitable for highly polar vegetable-based oils, often leading to solubility issues. Ongoing efforts aim to develop eco-friendly lubricants with minimal environmental impact [104].

Antioxidants are one of the most common lubricant additives, as lubricant oxidation occurs when hydrocarbons come in contact with oxygen or heat. This process can be further catalyzed by transition metals such as copper, iron, and nickel, which are present in, e.g., internal combustion engines, making them perfect chemical reactors. Antioxidants are often sulfur-, nitrogen-, phosphor-based or containing metals, which do not comply with the environmental regulations to reduce $SO_2$, $NO_x$, soot and ash content [31].

One group is zinc diorganodithiophosphates (ZDDPs), a common lubricant additive, representing critical multi-functional additives, mainly for automotive engine oils, that provide oxidation inhibition and anti-wear/extreme pressure properties [31, 104]. Looking more closely into ZDDPs, they release the toxic gas hydrogen sulfide in their first reaction step upon production, requiring careful handling and high-quality equipment. ZDDPs might decompose, forming volatile phosphorous species, causing coating and clogging in catalytic converters [105, 106]. A complete omission

of ZDDPs is not yet feasible concerning their superior anti-wear properties. Still, the trend moving is towards ZDDP species, causing less volatile phosphorous formation upon decomposition. Other engine oil additives comprise over-based calcium sulfonates, succinimide dispersants, and polymeric VI improvers, all causing hazardous emissions like $H_2S$ and HCl during production [31, 104].

More eco-friendly antioxidants could include lecithin (a phosphatide and by-product from soybean oil production), ashless alkylated aromatic amines and hindered phenols, or phosphorus-based and boron-based ones (as a replacement for ZDDPs) [31]. Due to their inherently good viscosity, vegetable oils typically do not require the addition of viscosity modifiers. However, using common viscosity modifiers, such as long-chain polymers and persisting microbial catabolism, may compromise the biodegradability and overall sustainability of the lubricant. Bio-based polyesters such as polyricinoleate, polyhydroxystearate [107], $TiO_2$ nanoparticles [108], and polymer composites synthesized from vegetable oil with different monomers, such as alkyl acrylates, 1-decene, and styrene [109] are investigated as environmentally friendly viscosity modifiers. Enhancing the wear behavior of vegetable oils is rarely needed due to their superior lubricity properties; if needed, amine phosphate compounds work well in vegetable oils. Silicon, dimethylsiloxane and alkyl acrylates are used for foam inhibition. For anti-rust and anti-corrosion, sulfonates can be applied. Pour point depressants, such as styrene esters, methacrylates, and alkylated naphthalenes, can hinder crystal growth in vegetable oils. Dispersants are mainly designed for petroleum oils and possible environmental alternatives, such as polyisobutylene succinimides [110], are still under research. Phenates and sulfonates attached to heavy metals are typically used as detergents, which are toxic to the environment. Instead, metal-free phenates, sulfonates, phosphates, and phosphate esters could be used [31].

Apart from the tribological characterization of lubricants, structural identification can be achieved using techniques such as attenuated total reflection (ATR)-Fourier transform infrared spectroscopy (FTIR), GC-MS, and high-resolution (HR)-MS. In contrast to the other methods, ATR-FTIR is a very time-efficient method, with no sample preparation and only a minimum sample volume (a drop) required. This technique assesses how the primary chemical groups of a lubricant sample interact with infrared light, generating a spectrum based on absorbance intensity across a spectral range. This straightforward method facilitates the identification of structural similarities or differences among samples within the same group and enables the assessment of aging effects (fresh vs. aged comparison). Furthermore, ICP-OES and CHNSO elemental analysis can be used for a combined insight into the elemental composition. The ICP-OES traces metal contents of acidified samples prior to nebulization and ionization by plasma, which can lead to the identification of certain additives or indicate their depletion. The CHNSO elemental analysis is conducted by sample combustion (CHNS mode) or pyrolysis (O mode), and the resulting gases are reduced, dried, and chromatographically separated by columns before thermal conductivity detection. Using the Boie adaptation of Dulong's formula and combining CHNSO values with water levels by methods like Karl Fischer, the lower heating value of a sample can be calculated [111, 112].

Depending on its intended use, a lubricant must exhibit specific physical properties to meet minimum performance standards. These properties include viscosity and viscosity index, cloud and pour point, foaming, air and water release, oxidation, flash point, thermal stability, rust prevention, and particle counting. For instance, the thermal stability of a lubricant or fuel can be explored using simultaneous thermogravimetric analysis (TGA) and differential scanning calorimetry (DSC) analysis in different atmospheres (e.g., synthetic air, inert gas, oxidative gas). A known initial amount of sample is gradually heated (isobaric) in the thermo-gravimetric

analyzer until a set temperature limit, the mass loss (TGA) and the change in the heat flow (DSC, indicating endothermic or exothermic reaction) of the sample are recorded as a function of time and displayed as so-called thermograms. Furthermore, additional information on the absorption, adsorption, desorption, dehydration, phase transitions, ignition, etc. can be collected by TGA [113] and on crystallization, melting, chemical kinetics, heat change capacity, purity, glass change temperature, thermal curing, and decomposition process by DSC [114]. The first derivative of the thermo-gravimetric signal over time can be drawn for additional information on intermediate formation. Vegetable oils, often containing unsaturated fatty acids, appear weak to oxidation and hydrolyzation, resulting in a lower melting temperature (but better low-temperature properties), which can be studied using TGA/DSC [111]. Additionally, bio-derived oils can be assessed based on their acid number (AN), the saponification value (SV), the peroxide value (PV), and the iodine value (IV) which indicate the content of free fatty acids, triglycerides, rancidity, and degree of unsaturation, respectively [115]. All the methods described above can also be used to assess the performance of fuels.

## 1.5 Carbon footprint

### 1.5.1 Emission reduction – decarbonization

The term decarbonization implies either the general substitution of carbon-based energy carriers by using renewable energy, electrification, and hydrogen or the phase-out of the fossil-derived energy forms natural gas, coal, and petroleum (defossilization). Especially in the material sector, general decarbonization cannot take place, as sustainable forms of energy are also carbon-based. Cellulose, sugars, starch, fat and oil, protein, etc., from biomass-derived alternatives (wood, grazed biomass, crop production, or other residues) can be used for substitution of fossil-based energy [116].

At the COP28, the Global Carbon Budget showed the following trend for global fossil $CO_2$ emissions (Figure 7): China at the 1st place (11.9 Gt), more than doubling its emissions over the last 20 years; followed by the USA (4.9 Gt), India (3.1 Gt) and EU27 (2.6 Gt). It reached 37.4 Gt of total $CO_2$ emission by the end of 2023 [117], even though in some regions, including the USA (-3 %) and EU27 (-7.4 %), fossil $CO_2$ emissions show a downward trend. To avoid surpassing the 1.5 °C global warming target set by the Paris Agreement, the pace of decarbonization must accelerate. Furthermore, the global financial crisis of 2007-2009 and the COVID-19 pandemic of 2020 are clearly reflected as dips in the curve, highlighting the significant impact of human behavior on the data [4, 17, 118].

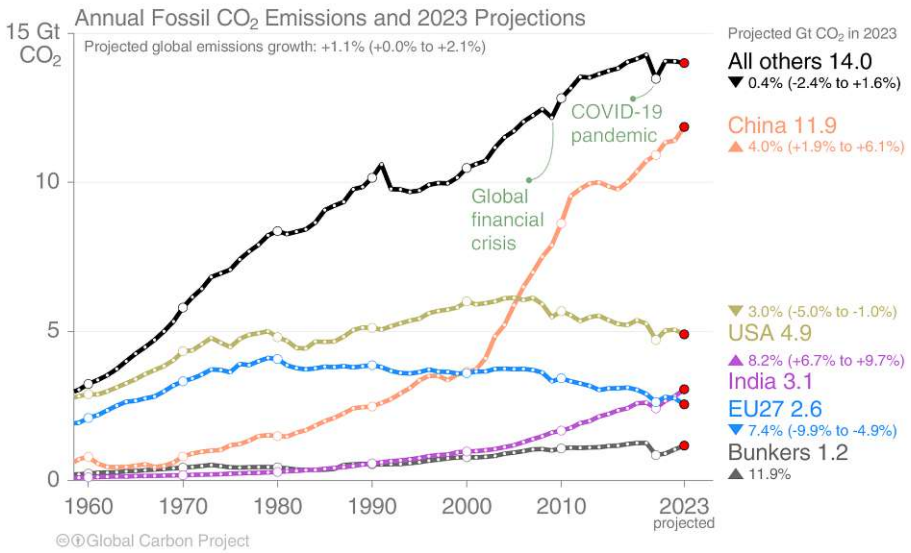


**Figure 7:** Regional annual fossil $CO_2$ emissions between 1960 and 2023 from EU27, USA, China, India and others expressed in gigatons (Gt). Adapted from [4].

The upward trend of global $CO_2$ emissions is not surprising when considering the consumption of fossil-derived energy forms (oil, coal, gas) in comparison to sustainable forms of energy (Figure 8). While natural gas use declined by the end of 2022, oil consumption almost recovered from its COVID-19 pandemic losses. Renewable energy consumption continues to grow, but too slow for a proper replacement of fossil-based energy forms. As of 2021 in the US, the largest source of $CO_2$ emissions was coming from the combustion of fossil fuels within the transport sector, being accountable for 35 % of the national $CO_2$ emissions and 28 % of GHG emissions. This is followed by 31 % of total $CO_2$ emissions within the electricity sector (24 % of GHG emissions) and 15 % $CO_2$ (12 % of GHG) emissions derived from industrial processes, all caused by the combustion of fossil fuels [8]. For Europe (2021), the majority of the $CO_2$ emissions are coming from electricity generation, with 49 % contributing to 24 % of GHG emissions. The second place of $CO_2$ emissions is occupied by transport with 21 % (24 % GHG emissions), and the industrial sector reaches 11 % (12 % GHG emissions). Most of these $CO_2$ emissions are related to the burning of fossil fuels like oil (40 %), gas (31 %), and coal (26 %) to generate electricity and heat, fuel vehicles and machinery [119, 120]. Reducing fossil fuel consumption directly and positively affects the $CO_2$ emissions within these sectors.

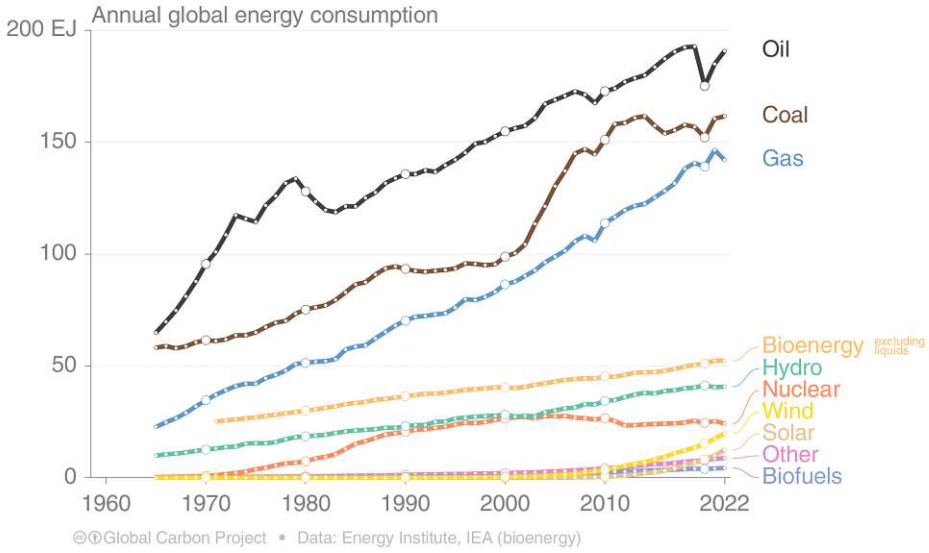


**Figure 8:** Global primary energy use in exajoules by category [4].

Decarbonizing the transport sector and transitioning from petroleum-based products to sustainable solutions can be supported by rapidly deploying low-emission fuels. Using the same industrial pathways, low-emission e-fuels and electrolytic hydrogen are fit for a quick scale-up by 2030, and meanwhile, further decarbonization possibilities like biofuels can mature to a market-penetrating scale [121].

Apart from the energy and transport sector, the materials and chemicals sector is still, in large part, based on fossil carbon (52 %); organic-based carbon from biomass contributes 37 % and recycling 11 % (Figure 9). The sectors predominantly reliant on fossil-based feedstocks include the heavy oil fraction (comprising bitumen, lubricants, and paraffin waxes) as well as chemicals and derived materials. Notably, the latter represents the largest sector, constituting 44 % of the total, with a significant 88 % sourced from fossil-based carbon and 4 % from recycling based on fossil feedstocks. Bio-based feedstocks contribute a mere 8 %, while carbon capture and utilization (CCU) technologies account for just 0.03 %. Future initiatives must prioritize phasing out fossil feedstocks and transitioning to renewable sources, a challenging task given the ongoing growth in material and chemical consumption. Additionally, the limited availability of agricultural and forestry areas, coupled with concerns about biodiversity loss, present further obstacles. In upcoming scenarios, the crucial roles will be played by recycling and the advancement of $CO_2$-based (CCU) technologies [116].

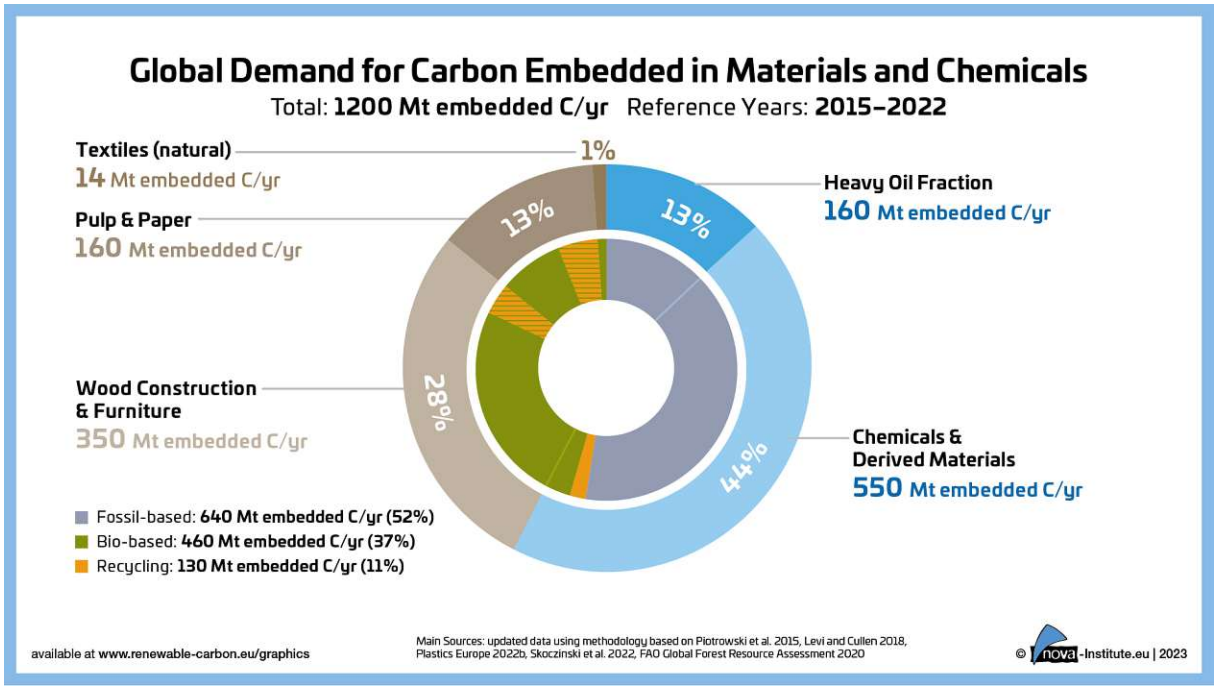


**Figure 9:** Global demand for carbon embedded in materials and chemicals over a period of seven years (2015-2022) [116].

### 1.5.2 Substitution projects

In coming years, there is a need to reduce the reliance on fossil-based feedstocks. To achieve this, it is imperative to incorporate bio-based feedstocks as well as expand recycling efforts. The following recent at least pilot-stage projects concerning fossil-based diesel fuel and lubricant substitution have given this their top priority:

- Waste-to-fuel or biomass-to-liquid technologies involve the conversion of different types of waste (industrial, agricultural, plastics, ...) into usable liquid fuels. This can be achieved through various processes such as pyrolysis, gasification, Fischer-Tropsch synthesis, fermentation, and hydrothermal liquefaction. Complex organic compounds are degraded into simpler hydrocarbons, which can be further refined into liquid hydrocarbon fuels like biodiesel or synthetic fuels (also electrofuels, e-fuels) as drop-in replacement fuels.
  - Daka ecoMotion™: Biodiesel is produced from waste-derived animal fat and waste cooking oil by pre-esterification, transesterification, and distillation. About 71,100 t/a of waste materials can be turned into 65,300 t/a fuel [122, 123].
  - Neste MY Renewable Diesel using NExBTL™ technology: Waste cooking oils and fats are turned into drop-in diesel fuel; oxygen is removed by the usage of hydrogen in the hydrodeoxygenation step, resulting in a pure hydrocarbon mixture. The following tunable isomerization process simulates the properties of fossil-based diesel fuel. Production facilities are placed in Singapore, Finland, and the Netherlands with a 65 % waste-based biogenic share [124–126].
  - ReNew™ Fuel using ALDUO™ and NExBTL™ technology: Algae is grown and harvested in bio-photoreactors or open ponds, and algae oil is collected and used as an alternative feedstock for the production of renewable diesel and biodiesel [127].

  - UPM biofuels – BioVerno: Crude tall oil, a by-product of pulp production, undergoes hydrotreatment to produce a low-emission, sulfur-free biodiesel with properties similar to those of fossil diesel [128].
  - Gela pilot plant using Eni Waste to Fuel technology: The organic share of municipal solid waste and waste from the food industry are used for the production of bio-oil by thermoliquefication. The obtained bio-oil can be further processed into biofuels [129].
  - bioliq®: Biomass is transformed into liquid pyrolysis oil by fast pyrolysis before gasification and Fischer-Tropsch synthesis into biofuels [130].
  - Sierra BioFuels: An estimated 42 million liters per year of synthetic crude oil is produced from 175,000 tons of landfill waste, which is shipped to a refinery for low-carbon fuel production [131].
  - BioForming®: A big variety of biomass and sugars are used to produce drop-in hydrocarbons, which can be blended in high concentrations with fuels (co-processing) using existing infrastructure [132].
  - ReOil®: Instead of incineration, plastics-based waste is chemically recycled by converting it into pyrolysis oil, which is then utilized in the production of fuels and new plastics. This process saves primary fossil-based feedstocks and promotes the idea of a circular economy [133, 134].

- Carbon is captured as a by-product from industrial processes or as atmospheric GHG in CCU technologies and converted into synthesis gas in combination with other gases. It can be used as a precursor in the production of various fuels and chemicals. For example, synthesis gas (syngas; $CO+H_2$) can be converted into liquid hydrocarbons through Fischer-Tropsch synthesis, which can then be used as transportation fuels. Syngas can also be used as a feedstock in the production of methanol, ammonia, or other chemical products. Applying CCU technologies offers a potential pathway to reduce GHG emissions, contributing to an increased environmental sustainability and resource efficiency.
  - Waste2Value: Syngas is processed from sewage sludge, by-products of the pulp and paper industry and damaged timber by a thermochemical gasification process, which can then be synthesized into various types of liquid fuels (green diesel, green natural gas, green hydrogen, ...) [135].
  - ReCarbon: The emitted GHGs $CO_2$ and $CH_4$ are converted by a plasma carbon conversion unit into hydrogen and syngas, which can be used for the production of e-fuels, chemicals, and energy. This method enables the fermentation of syngas into ethanol through bio-fermentation, in a process free of $CO_2$ emissions. Typically, ethanol is obtained from source crops, leading to competition for resources such as land and water with food and agriculture [136].
  - Carbon to product Austria (C2PAT+): A combined effort of internationally known companies from industrial sectors to capture $CO_2$ from a cement plant, electrolysis of $H_2$ using renewable energy, synthesis to hydrocarbons and further processing into renewable fuels and plastics [137, 138].
  - CirclEnergy: $CO_2$ is collected as a waste stream from ferrosilicon, coke oven gas, limestone kiln, or ethylene oxide productions. $H_2$ is produced from electrolysis using renewable energy. Both gases are then converted via emissions-to-liquid (ETL) technology into renewable e-methanol, which can be used for the production of fossil-mimicking fuel components or biodiesel [139].

- Biomass balance approach: Co-processing of conventional fossil-based feedstocks with bio-based feedstocks during the first steps of chemical production (e.g., steam cracker or syngas) represents a biomass-balance approach. It is used to produce bio-based products, including biofuels, chemicals, and materials, reduces the demand for fossil-based resources, and contributes to less $CO_2$ emissions [140].
  - Biogenic oil co-processing technology: Co-processing of biogenic feedstocks with petroleum intermediates (e.g., gas oil) is used to create hydrocarbon fuels with a higher renewable content using existing infrastructures. The biogenic feedstock may originate from domestically sourced rapeseed oil, sunflower oil, used cooking oil, or algae oil. This co-processing makes it possible to reduce GHGs by up to 85 % [141].
  - bioCRACK: Co-processing of cheap petrochemical by-products (such as vacuum gas oil) and solid lignocellulosic biomass from wood and straw through fluid-phase pyrolysis into second-generation biomass-to-liquid diesel fuel with a 20 % biogenic share. This technology can save up to 85 % of GHGs [142].

On the one hand, named technologies incorporate reducing general waste disposal, diversifying fuel sources, and mitigating GHG emissions by utilizing renewable and low-carbon feedstocks. On the other hand, industrial scalability, cost-efficiency, and true environmental sustainability throughout the production process remain challenging. Close collaboration of research and industrial development stakeholders is necessary for a sophisticated and resource-efficient process design.

### 1.5.3 The sustainability evaluation toolbox

LCA is a powerful tool to evaluate a product's environmental footprint, process, or system involving an entire life cycle perspective, from raw material extraction to end-of-life disposal. LCA can evaluate supply chains comparable between products, processes, or systems. Furthermore, the most significant environmental, social, and economic impacts, as well as the life cycle stages that contribute most to these impacts, can be identified. Recognizing ecological and social hotspots connected with significant environmental implications within goods, services, systems, technologies, innovations, and infrastructures is essential. Another key aspect of the analysis is the assessment of unintended consequences, such as burden shifting between environmental and socio-economic impacts (reducing one impact while increasing another) or changes across life cycle stages [143].

Basically, LCA consists of 1) the definition of goal and scope, 2) life cycle inventory (LCI) analysis, 3) life cycle impact assessment (LCIA), and 4) data interpretation in an iterative approach, and is described according to ISO 14044 as the following steps [144, 145]:

- Defining the product system: unit processes, inputs, and outputs; the product can be a processed material, hardware, software, or a service
- Specifying the functions of the product system, the functional unit, and the reference flows: The functional unit provides a quantifiable value for standardizing input and output flows. Reference flows must be utilized to compare systems based on the same functions quantified with the same functional units.
- Setting system boundaries (cut-off criteria): The part of the process that is considered and how detailed it is elaborated within the LCA is defined here. This has to agree with the stated aim of the LCA. The cut-off criteria can be mass- or energy-based or selected according to their environmental relevance.

- Allocation procedures are required when the same process is used for multiple product systems and a direct assignment of flows to the defined product system is not possible. Allocation should be avoided wherever possible. If it cannot be avoided, allocating inputs and outputs between different products or functions should be as precise as possible.
- Environmental impact assessment: The impact categories, impact indicators, and characterization models are specified.
- Data requirements are given based on the essential quality criteria (time interval, geographic range, precision, completeness, etc.), as well as any underlying assumptions and constraints.
- Critical review considerations: The necessity of a critical review is declared, how it is performed and who will conduct it.
- Type and format of the report are declared. The report must contain a statement on the modifications of the initial investigation framework, selection of system boundaries, a description of the process units, including a decision on allocation, and finally, information on the data, including decisions, specifics regarding individual data and requirements for data quality.
- Inventory includes the data collection (validation, energy analysis, and allocation) and data compiling. It is explained in more detail below.
- Impact of categories: The results from the inventory analysis are assigned to the selected impact categories, and the values for the impact indicators (as a mathematical unit per functional unit) are calculated. As the impact of the categories is reconciled with the other phases, it is important to disclose whether ...
  - ... the inventory data quality and outcomes are adequate for the impact assessment, aligning with the study's defined objectives and scope.
  - ... the system boundary and cut-off criteria have been sufficiently examined to guarantee the availability of inventory data crucial for computing the impact assessment indicator values.
  - ... the environmental significance of the impact assessment results has decreased due to the functional unit calculations, system-wide averaging, aggregation, and allocation carried out during the inventory process.
- Interpretation of LCA: Significant parameters are identified and evaluated, considering their completeness, sensitivity and consistency, according to the results based on the inventory and impact assessment phases of the LCA. Conclusions are drawn from the data interpretation while providing insights into limitations and offering recommendations.

Different scenarios can be calculated to help understand a product or system's environmental impact: cradle-to-cradle (C2C), cradle-to-gate, or cradle-to-grave. Which approach is used often depends on the data availability or the assessment's scope. The C2C highlights a closed-loop product design, where materials are continuously repaired, reused, or recycled without any loss in value. The cradle-to-gate focuses on the resource collection and manufacturing process. In contrast, the cradle-to-grave additionally considers the use and disposal stages, providing a holistic view of a product's environmental impact [143].

The LCI is a complex analysis step that concerns material inventory, energy and energy forms, co-products, production waste, operating and auxiliary materials, transport to or from the plant,

etc. All data regarding the flows in and out of the product system is gathered and applied to the process and functional unit. Furthermore, the data is divided into a foreground process (e.g., manufacturing and packaging of the product) and a background process (e.g., manufacturing of materials, transportation of goods, electricity for production) [144].

Within the LCIA, the environmental impact from resource extraction over manufacturing and use to disposal of the LCI is assessed. It includes the functional unit, system boundary and allocation procedures. The LCIA involves classifying the inventoried in- and outputs and characterizing how each categorized in- and output contributes to its respective impact category, then combining these contributions within each category. The impact is displayed in categories such as climate change, ozone depletion, ionizing radiation, formation of fine particulate matter, generation of photochemical oxidants affecting ecosystem quality and human health, terrestrial acidification, freshwater and marine eutrophication, water consumption, scarcity of mineral and fossil resources, human toxicity (cancer and noncancer), ecotoxicity on terrestrial, freshwater, and marine ecosystems, as well as land use [144, 146].

The EU recommends the implementation of environmental footprints, based on LCA methods, to assess the sustainability performance and quantify the environmental impacts of a product, process, service, or organization [147]:

- Product carbon footprint (PCF): The PCF is a measure to quantify the GHG emissions associated with the life cycle of a chemical product. As different methodologies and technologies contain different levels of data quality and uncertainties, a guideline with specific and harmonized rules and methodologies was established to make chemical products comparable [148]. The guideline also proposes strategies if carbon-reduction technologies, such as CCU or chemical recycling, were considered within a product or process [149].
- Product environmental footprint (PEF): The European Commission (EC) introduced the PEF for LCA assessment of the environmental performance of products with a standardized and harmonized set of methods and category rules. It aims to ensure consistency and comparability across different products and industries. In addition to the classification and characterization steps of the LCIA, the PEF also includes normalization and weighting of the analysis results. The PCF is incorporated within the PEF [144, 150].
- Organization environmental footprint (OEF): The OEF, proposed by the EC, is a LCA-based method to quantify the environmental impact of an organization, including their supply chain activities (from raw material extraction to production and application, to the final management of waste). The PEF is supplemented by the OEF [147].

## 1.6 The road ahead

When using renewable sources, drawbacks, e.g., through differences in chemical or physical properties, faster degradation mechanisms, industrial resource availability, lack of established infrastructure, slow technological progress, etc., are to be expected. A better understanding of the degradation mechanisms of renewable resources will play an essential part, as biomass or organic waste undergoes degradation over time (spoilage, fermentation, microbial proliferation, etc.), and stricter handling and storage regulations will be necessary to minimize degradation and preserve product quality [151]. When discussing product quality, the diversity in the composition of plant matter can present another challenge. During the lifespan of plants, their composition undergoes changes influenced by factors such as exposure to elements (sun, wind, rain, temperature),

seasonal variations, and age [152]. This variability results in higher fluctuations compared to fossil-based products. For example, for biodiesel, the different composition causes poorer cold flow properties compared to conventional diesel, as trace impurities like SMGs start to precipitate, provoking filter blocking incidents (more details see Chapter *2.3 Publication III - Advanced Method for the Detection of Saturated Monoglycerides in Biodiesel using GC-EI-MS/MS*). Therefore, a more considerate application and storage of biodiesel is necessary.

Envisioning a full implementation of the SDGs for future fuels, they must deliver on climate action, affordable and clean energy, responsible consumption and production, life below water and on land, and zero hunger. The utilization of more sustainable resources will reduce the overall carbon footprint and minimize hazardous emissions to land and water. As climate change progresses, glaciers will melt, sea levels will rise, and available land, including areas for agricultural activities, will decrease [153]. With harsher climatic conditions, the shortage of food supplies will exacerbate. Hence, it is crucial to refrain from competing with the food industry for energy solutions. Instead, we should focus on utilizing waste streams to foster a complete circular economy [154]. As changes on industrial levels are slow, resource- and cost-efficient, renewable drop-in products will provide a feasible interim solution. Adapted or even stricter methods for property and quality assessment may be necessary to increase the efficiency of products and processes; the assessment of a product's life cycle will possibly play a key part from now on. Finally, policy and regulatory frameworks are crucial in supporting the transition to renewable energy sources. Inadequate policies or inconsistent regulations can hinder renewable technology investment and deployment, limiting their ability to reduce GHGs and mitigate climate change.

## 1.7 Advanced structural elucidation for fuels and lubricants

Fuels are well suitable for GC-MS analyses, as they comprise molecules with relatively low molecular weight and high volatility. On the contrary, lubricants exhibit a wide range of compositions, such as water-based solutions, emulsions, or polymers, which presents a challenge for conventional GC-MS analysis due to their high polarity, molecular weight, and low volatility. Electrospray ionization (ESI)-high-resolution (HR)-mass spectrometry (MS) analysis would be more suitable for analyzing these lubricants, highlighting that a single analysis method may not meet all the requirements for studying complex samples.

The following sections describe ionization techniques and mass analyzers primarily used throughout this thesis and emphasize the respective combinations used in the available instrumentation.

### 1.7.1 Gas chromatography coupled to mass spectrometry

GC-EI-MS is a well-established technique for efficiently separating complex samples and determining the structure of lower molecular weight oil-based lubricants. It is a highly suitable method for sensitive quantification but also for identifying unknowns.

#### 1.7.1.1 Gas chromatography

GC is a separation method of volatile and complex sample mixtures. The operable GC instrument consists of a temperature-programmable oven equipped with a column that connects the inlet and the detector, an injector, and a carrier gas as mobile phase (He, $H_2$, $N_2$, or Ar). Upon small

volume sample injection (1-10 $\mu$l), the sample is evaporated in the heated inlet and transported into the oven by the carrier gas. Non-volatile and solid particles are collected in the inlet. Then, the separation of the compound mixture happens due to gradually increasing the temperature gradient (chromatographic principle), which influences the interactions of the compounds with the stationary phase. The smallest, most volatile components evaporate first, being less retarded on a common GC column (5 % diphenyl/95 % dimethyl polysiloxane phase), followed by larger, less volatile ones, and finally, the least volatile molecules, typically those with higher masses. The latter compounds show high interaction with the column leaving it at the end of the temperature gradient due to strong interaction with the separation material. The method is limited by the molecular weight of compounds ($<$ 1000 g/mol) due to the necessity of boiling points being below 350 °C to evaporate from the inlet. To increase the volatility of non-volatile compounds and make them measurable by GC-MS, derivatization is an option, modifying the chemical structure by replacing polar groups (e.g., -OH, -SH, -$NH_2$) and establishing a higher volatility of the molecule, while often also stabilizing the molecules and enhancing the detection limits [155].

**Selection of separation column** For GC separations, a huge variation of separation columns is available on the market, differing in phase constitution/polarity, length, inner diameter, and phase thickness. It is necessary to chose the appropriate system depending on the analytes of interest. This paragraph examines the different chemical and physical properties of GC columns and explores why these characteristics are particularly important for analyzing highly complex fuel matrices. In general, for fuels and lubricants containing numerous non-polar compounds, a low polarity GC column, e.g., with a 5% diphenyl/95% dimethyl polysiloxane phase, is a good match.

The selection of the most suitable column depends on the respective analytical question. A polyimide layer on the outside usually coats fused silica ($SiO_2$) capillaries for stability, flexibility, and the stationary phase on the inside. The internal walls of the capillary are deactivated to cover functional silanol groups. The stationary phase is either non-polar, polar or a mix of both. Standard non-polar columns are 100 % dimethylpolysiloxane, whereas polar columns are 100 % polyethylene glycol. Substituting methyl groups with other functional groups, such as phenyl, trifluoropropyl, or cyanopropyl, changes the polarity and selectivity. The separation resolution of two peaks (analytes) depends on phase interactions caused by dipole-dipole interaction, dispersion, acid-base, or hydrogen bonds. The interaction is exclusively due to weak dispersibility for nonpolar phases, while more polar phases cause stronger polar interactions [156, 157].

Apart from the phase selection, other parameters concerning the column's dimensions, such as length, inner diameter, and film thickness, which affect the sample capacity and separation efficiency, can be chosen. The length determines the separation efficiency; increasing the length by two times enhances the efficiency of separation by $\sim$ 40 % while simultaneously prolonging the analysis time and, thus, the retention time. Advancing the film thickness decreases efficiency but enhances the sample capacity. The sample capacity also increases with the increasing inner diameter of a column. Thus, a bigger inner diameter allows the analysis of samples with more significant concentration differences but reduces the separation efficiency [157, 158].

To conclude, the best choice of column depends on the sample matrix, the compounds of interest, and the desired preciseness and duration of the analysis, which leaves us with a wide range of columns to choose from. To maintain adequate gas flows, inner diameters of $\leq$ 0.25 mm (or not higher than 0.32 mm) are preferred. Lower film thicknesses are better for fuels, as they are composed of high boiling analytes (e.g., 0.25 $\mu$m and lower); higher film thicknesses (e.g., 1 $\mu$m) would be favorable for highly volatile analytes. Depending on the analytical question, a good column selection for diesel fuels and blends giving an overview of the main constituents,

could be maintained, e.g., a column with parameters within the range of 15 m to 30 m length, 0.25 mm or 0.32 mm inner diameter, and 0.25 µm phase thickness with a low polarity (0 to 5 %). When the focus is more on the aromatic compounds found in the diesel matrix, a highly polar wax column should be used; one column alone will not be sufficient for the complete identification and quantification of fuel components, a problem that could be overcome by multidimensional GC-MS systems [157].

#### 1.7.1.2 Two-dimensional gas chromatography systems

Modern systems combine different GC columns within one oven or a combined oven system (oven within another oven) as a so-called multi-dimensional GC system that can be used as comprehensive GCxGC or heartcut GC-GC. For both the comprehensive and the heartcut 2D-GC systems, two columns are connected in series by means of a modulator and coupled to a detector (or a combination of detectors, e.g., atmospheric FID and an MS). The difference between the two systems is that for the heartcut 2D-GC, a detector (e.g., FID) is connected between the two columns for the selection of a specific fraction of interest, which is cut from the initial separation of the first column and transferred to the second column connected to an MS. For the comprehensive 2D-GC the entire sample is subjected to a separation in both dimensions. Mostly, the focus is on separation orthogonality (independent separation mechanisms) provided by columns with different physicochemical properties, including size, charge, and polarity [159, 160].

This results in a highly increased separating capacity using two columns with different parameters. Especially for fuels and lubricants with their highly complex matrix, this leads to a precise structural evaluation that is almost impossible with single GC-MS due to overlapping peaks of, e.g., aromatics and hydrocarbons. So, connecting two columns with different polarities makes it feasible to distinguish, identify, and quantify the signals of compound groups with varying polarities too similar for a single GC-MS separation. Furthermore, due to the increased separation capability, further analyses for structural elucidation might become negligible, saving material and energy resources [159].

#### 1.7.1.3 Electron ionization

EI is most commonly used in GC-MS interfaces to determine the structure of small molecules by "hard" ionization. Gaseous, neutral molecules enter a heated chamber under a high vacuum through a sample hole and are ionized by collision with accelerated electrons emitted from a heated filament. The collision of the molecules and the electrons creates radical ions of the molecule, missing an electron and therefore, forming a positively charged radical cation. Kinetic energy is transferred from the electron to the molecular ion during this process, resulting in considerable fragmentation. These fragments and potentially survived molecular ions are exiting through a hole to the MS. In many cases, the molecular ions do not survive the process of EI, leading to an informational loss regarding the chemistry of the intact analyte. Still, at the same time, new fragments are gained that are characteristic of the respective structure of the molecule. Lowering the acceleration potential of the electron beam decreases over-fragmentation at the cost of ionization efficiency and, thus, lowers sensitivity, which impacts the reproducibility of the mass spectra. Ionization by EI creates highly reproducible mass spectra, enabling automated, reliable compound identification by mass spectral libraries. Not only can a molecule be identified by its m/z ratio, but its elemental composition creates a specific isotopic pattern. As the EI needs gaseous molecules, the process is limited to compounds of lower molecular weight and

less polarity. The volatility of polar compounds can be increased by derivatization techniques, improving ionization and allowing sensitive detection through particular product ions [155].

#### 1.7.1.4 Quadrupole

Quadrupoles are built of four parallel metal electrodes, either cylindrical or hyperbolic in shape. Opposite electrodes are connected and share a combined potential (each pair has the same potential but opposite polarity), resulting in a direct current with radiofrequency voltage. When voltage is applied, an electric field with a hyperbolic shape forms, enabling the separation of ions based on their m/z values by stabilizing their oscillatory trajectory toward the detector within the electric field. Adjusting the direct potential and alternating the voltage at a defined frequency makes a selection of specific m/z ratios possible. The pairs of electrodes serve as filters, blocking molecules with mass-to-charge ratios (m/z) higher or lower than the selected m/z from passing through the detector. When considering the effect of both direct current and radiofrequency voltages on ion behavior, ions with higher m/z primarily respond to the direct current voltage, as the rapid changes of the radiofrequency voltage have little impact on their movement. These ions can be thought of as too heavy to react to such rapid fluctuations. Conversely, ions with lower molecular weights predominantly respond to the radiofrequency voltage, being agile enough to react to its oscillations [155].

The quadrupole is well suitable for integration in GC-MS or liquid chromatography (LC)-MS systems, as it is capable of both the monitoring of one or several selected m/z values instead of measuring the entire spectrum and rapid switching between selected m/z values for sensitive qualitative and quantitative ion determination. The quadrupole can be operated as a mass filter in the selected ion monitoring (SIM) mode; instead of recording the whole spectrum, only specific m/z values of the compounds of interest are traced, which results in increased selectivity and sensitivity for quantitative determination. In general, for mass analysis, a combination of each individual ion spectrum is summed up as a total ion current (TIC) chromatogram as a function of the retention times of individual compounds or spectrum numbers. Compared to other traps, the quadrupole has only a limited measurement range (approximately m/z 50 to 4,000), enabling the detection of low molecular weight compounds [155].

#### 1.7.1.5 Triple Quad

Quadrupoles can be combined into a triple quad (QqQ) system, which can be used for four main MS/MS scan modes: (1) product ion scan, (2) precursor ion scan, (3) neutral loss scan, and (4) selected reaction monitoring (SRM). Primarily, the first quadrupole (Q1) is used as the analyzer of precursor ions, the second (q2) as a collision cell, and the third (Q3) as the analyzer of fragments [155].

The most common scan type used is the (1) product ion scan. A specific m/z ratio of a precursor ion is selected in the first quadrupole (Q1). After collision and fragmentation in the second quadrupole (q2), the resulting products (fragment ions) are analyzed in the third quadrupole (Q3). The fragment ions serve as a unique fingerprint of the previously selected precursor ion, facilitating the identification of the molecule [155]. For the precursor ion scan (2), product ions at specific m/z values are scanned in Q3 after the collision, allowing the identification of all precursor ions (as molecules contained in the analyzed mixture), creating the exact product ion. This mode is used to screen for structural similarities in the analyzed compounds [155]. The neutral loss scan (3) provides an analysis of ions with constant mass offset in both Q1 and Q3. The precursor ion passes through the first mass analyzer and is detected by Q3, given

that it produces a product resulting from the loss of a particular fragment (such as a specific group) from the precursor ion. This collision-induced loss could be a water molecule, phosphate, carbon dioxide, etc., and makes identification of molecules possible due to distinct structural characteristics [155].

In the SRM mode (4), both the Q1 and the Q3 are analyzing specific ions with preset m/z values, and only if those specific ion transitions are occurring are they allowed to transmit from fragmentation. In contrast to SIM mode, where only a single quadrupole is necessary, the SRM mode brings higher selectivity and sensitivity due to improved signal-noise-ratio of only detecting particular ions. The SRM mode is also referred to as multiple reaction monitoring (MRM) mode if multiple m/z values for ion transitions are scanned. This mode is especially interesting for low-abundant species in samples with complex matrices such as fuels. As for the detection of SMGs in biodiesel (refer to Chapter *2.3 Publication III - Advanced Method for the Detection of Saturated Monoglycerides in Biodiesel using GC-EI-MS/MS*), the SIM mode alone would not have been sufficient for the determination of the specific SMGs, as the signals coming from the SMGs overlap with the ions of biodiesel matrix itself. The MRM mode allowed a precise determination of the concentration of SMGs in the biodiesel matrix by tracing particular precursor ion > product ion transitions, the supplementary use of ESI-HR-MS is not essential anymore in this case [155].

### 1.7.2 Electrospray ionization-high-resolution-mass spectrometry

In MS, a key aim is to determine the chemical formula of a compound under investigation. This is achieved by accurately determining the molecular mass, which helps narrow down the possible atomic compositions, especially with increasing mass accuracy. Mass spectrometers with high resolution and accuracy, surpassing 1 ppm, are particularly valuable for analyzing larger molecules, such as those found in complex mixtures in petroleum fractions. The Orbitrap is used for high-resolution and accurate analysis of compounds, and structural evaluation is possible by MS and MSn (also called MS/MS or $MS^2$; breaking down precursor ions into fragments/product ions). For direct-infusion analysis, the Orbitrap provides a fast method for the identification of unknown compounds in liquid samples, such as fuels and lubricants. Typically, only minimum sample preparation is needed, e.g., a dilution in a suitable solvent. Solvents with low boiling point temperatures and low surface tension are preferable [155].

#### 1.7.2.1 Electrospray ionization

ESI is a "soft" ionization technique applicable at atmospheric pressure. In contrast to EI, ESI does not produce unwanted fragmentation, and excessive sample pre-treatment is not necessary, making it suitable for coupling with, e.g., HPLC. When the solution is introduced into the ionization chamber through a capillary, a Taylor cone is formed as a result of the electrostatic force created due to the high voltage being applied between the ESI tip and the MS inlet. The solvent is sprayed into droplets, which are dried by heated sheath gas as they move away from the source, causing solvent evaporation and increasing the charge density at the droplet's surface. When the electrical repulsion overcomes the surface tension of the droplet, it undergoes Coulomb fission, breaking into smaller droplets. This process repeats until only a single charged analyte molecule or ion is remaining, which is then ready for mass spectrometric analysis. Depending on the potential of the heated capillary, the ESI source can be used to create positively charged ions (positive ion mode) or negatively charged ions (negative ion mode) [155].

Suitable solvents for ESI-MS include water (in a mixture of other solvents), alcohols (methanol, ethanol, isopropanol, and n-propanol), acetonitrile, and chloroform (usually mixed with methanol). Additional ions, such as salts and metal ions, negatively influence the ionization process (ion suppression effect) by masking analyte ions or forming clusters of unpredictable charge [155].

#### 1.7.2.2 Linear ion trap

The linear ion trap can be used for the storage of ions or for their detection. Its structure is similar to that of a quadrupole, consisting of four radiofrequency electrodes. When a potential is applied to the electrodes, ions can be focused and their movement along x- and y-axes is controlled. Additional electrodes positioned at the end of the trap regulate the movement of the ions along the z-axis, allowing the entering and trapping of ions in the center of the trap. A collision with neutral gas particles reduces the kinetic energy of the ions towards zero (ion cooling). The ion cloud can be spread along the entire length of the trap, facilitating a higher number of ions to be present (improved signal-to-noise ratio, hence the limit of detection) without causing repulsion between equally charged ions (space charge effect). For detection of the ions, their trajectory at the defined m/z range is destabilized, and they are ejected toward the detector, assessing their number at specific m/z values. The ion trap is well performing in storing ions long enough suitable for, e.g., accumulation to a sufficient number for detection, fragmentation, and combination with pulsed mode mass analyzers like the Orbitrap. The linear ion trap provides a simple, low-priced instrumentation for fast ion scanning without the need for a high vacuum. The mass range of the ion trap is similar to the quadrupole with m/z 50 to 4,000 (sometimes extending to m/z 6,000) and is suitable for low mass analysis of organic and inorganic compounds [155].

#### 1.7.2.3 Orbitrap mass analyzer

The Orbitrap detects the m/z values of trapped, oscillating ions previously collected by an ion trap (C-trap or linear ion trap), as the Orbitrap alone cannot perform fragmentation on ions. The principle of ion capturing and detection in the Orbitrap is similar to Fourier transform (FT)-ion cyclotron resonance (ICR) and quite different from all other conventional mass spectrometers. Where in an Orbitrap analyzer, the oscillatory frequency of ions traveling in circular orbits around the inner electrode is measured by the outer electrodes and calculated into m/z ratios, in the ICR, a magnetic field is used to trap and oscillate ions at their specific cyclotron frequencies, which can be calculated to the referring m/z ratios. Both are using FT for converting single frequencies detected from an amplified image current into the correlating m/z values. The FT-ICR is not further discussed within this chapter [155].

The Orbitrap consists of three electrodes: two outer barrel-shaped ones surrounding an inner axial spindle-shaped one. A thin layer of insulator separates the electrodes. The ions are injected far away from the equatorial plane of the Orbitrap, inducing axial oscillations of the ion cloud along the z-axis. The specific m/z values for the ions can be obtained from the frequency of the oscillations. The Orbitrap analyzer offers a high resolution, combined with exceptional mass accuracy (1 to 5 ppm) and a large capacity for space charge. The higher mass range of the Orbitrap from m/z 50 to 6,000 (or even up to m/z 10,000), allows analysis of bigger molecules in contrast to the ion trap [155].

#### 1.7.2.4 Hybrid mass spectrometry

Modern Orbitrap instrumentation incorporates a hybrid trap–trap combination of a linear ion trap and the Orbitrap mass analyzer. The Orbitrap's high-resolution and accurate mass detection

capabilities are integrated with the sensitive ion detection, precursor isolation, and fragmentation functionalities of the linear ion trap. Additionally, the instrument can be equipped with a C-trap, collision cells for ion fragmentation based on techniques such as higher-energy collisional dissociation (HCD), collision-induced dissociation (CID) or electron-transfer dissociation (ETD), and a quadrupole mass filter. The mass filtering and isolation of the precursor ions can be conducted by the quadrupole or the ion trap, with subsequent fragments created by either HCD, CID, or ETD, providing different structural information. The combination of the rapid and effective quadrupole isolation with HCD fragmentation and Orbitrap detection enhances the quality of data obtained. Furthermore, precursor and product ions can be detected through the Orbitrap or the ion trap, making it possible to fully operate in parallel. The collision cell or the C-trap is filled with ions during the ongoing MS-MSn detection cycle. While one analyzer is busy detecting targeted product ions, the other can simultaneously detect untargeted ions, maximizing the use of the ion current and providing complex sample analysis. One way to conceptualize this is as follows: The linear ion trap is used to collect multiple, low-resolution MSn spectra, and meanwhile, the Orbitrap records high-resolution, high-mass accuracy spectra. Especially the application of direct infusion ESI-MS, where no upstream separation technique such as HPLC was used and, therefore, chronological correlation of compounds can be disregarded, benefits greatly from parallel detection and an in-depth structural elucidation [155, 161].

# Chapter 2

# Publications

This chapter was carried out as part of the COMET Centre InTribology project (FFG no. 872176 and 906860), funded in the COMET – Competence Centres for Excellent Technologies Programme by the federal ministries BMK and BMAW as well as Niederösterreich and Vorarlberg. COMET is managed by FFG. It was conducted in collaboration with the Institute of Chemical Technologies and Analytics (CTA) at TU Wien.

## Publication I - A comprehensive review of sustainable approaches for synthetic lubricant components

This review discusses the growing importance of EFLs in the context of global sustainability initiatives like the European Green Deal. It introduces the concepts of green chemistry and tribology, emphasizing the need for products and processes that reduce environmental impact. The term "sustainable lubrication" is explored regarding what criteria are needed for a lubricant to be sustainable, e.g., concerning biodegradability, renewability, and toxicity. The focus is on lubricant components derived from renewable and recycled feedstocks that would be available on industrially relevant scales and aligned with principles of green chemistry.

Moreover, the legal landscape surrounding EFLs is continually evolving, and stringent criteria through initiatives such as the European Green Deal, the European Ecolevel, the environmentally acceptable lubricant (EAL) definition by the EPA, and the Vessel Incidental Discharge Act are expounded on. Regulations classifying lubricants and components as safe or potentially harmful are needed for bio-based lubricants to enter the market. Commercializing such lubricants from lab and pilot scale to mass production involves gaining and maintaining market share, often achieved by directly substituting fossil-based products with comparable price and quality.

This systematic review focuses on recent developments in biolubricants from 2015 to 2022, particularly emphasizing benign lubricant components derived from bio-originated or bio-derived sources and their tribological properties for industrial applications. The presented alternative structures include fatty acid-based estolide esters, fermentation-based farnesene, polysaccharides, glycans, lignin and lignin-derived components, hydrogels, polyalcohols, ionic liquids, proteins, vitamins, lecithin, $\alpha$-lipoic acid esters, and benzoic acid. All of them are supposed to be sustainably collectible, focusing on non-toxic and non-bioaccumulative degradation. However, toxicology data was not always available for the proposed structures, and results vary highly depending on the type of organism used. The tribological response of these structures, such as friction and wear behavior, is highlighted throughout the work. Resources studied for water-based lubrication and humane/medicinal applications were not of interest for this review. Discussions are limited to non-edible and waste-based feedstocks for lubricant components, omitting processing steps and their environmental impacts.

My contribution to this publication included the following tasks: conceptualization and visualization of the research; literature investigation and curation for all sections; sections that were entirely written by me (original draft): abstract, introduction, regulations for commercial lubricants and lubricant components, vegetable oil-derived lubricants, carbohydrate polymer, waste lubricant oil, industrial waste, plastic waste and miscellaneous, as well as the conclusions; sections that I partly wrote together with another co-author: ionic liquids and waste of animal origin; design of the graphical abstract; reviewing, editing and proofreading of all sections

## Publication II - Moving towards green lubrication: tribological behaviour and chemical characterization of spent coffee grounds oil

On the search for alternative resources for lubricants, which comply with the SDGs and, thus, do not primarily compete with the food and pharmaceutical industry as other vegetable oils do. The search for an industrial-scale waste stream was the basis for the second publication. Sustainability, local availability, easy access in big volumes, and fast extraction of liquids were prioritized when screening waste resources. Coffee is consumed in large numbers in Europe; therefore, coffee waste is available en masse but collecting and processing structures have yet to be established. At this point, spent coffee grounds (SCG) seemed like a promising resource, as all the mentioned criteria were given, and the physicochemical properties already published in the literature were similar to those of mineral oils. Still, the information on the tribological behaviour of SCGO was scarce.

Spent coffee grounds oil was extracted by Soxhlet extraction (SE) using n-hexane as a solvent. The choice of solvent has a huge impact on the overall sustainability of the extraction process, which was determined by the conducted LCA. N-hexane was selected as the solvent for the SE-extraction in this publication, as it showed the highest oil yields discovered in the literature, and the impairment of the sustainability of the process was neglected. The collected SCGO was then further used to show whether it had suitable properties for use as a lubricant base oil and compared to polyalphaolefin (PAO) as a synthetic, petroleum-derived base oil reference. Tests like ATR-FTIR, acid number, CHNSO elemental analysis, TGA-DSC, GC-EI-MS, HR-ESI-MS were conducted for the investigation of physicochemical properties of the SCGO. These tests resulted in a higher oxygen content and a higher number of free fatty acid groups of SCGO in contrast to PAO, as it naturally contains functional ester and acid groups. These lead to enhanced lubricity but will cause faster oxidation if not stabilized by, e.g., antioxidant additives. The thermal stability of SCGO and PAO were comparable for both inert $N_2$ and oxidative atmospheres; thermal decomposition started well after 240 °C.

Especially the tribological properties of the SCGO were of interest. So, they were extensively studied in a pin-on-disc (oscillatory motion) and a ball-on-three-plates (unidirectional and oscillatory motion) tribological configuration on different material pairings. Tests were conducted of pure SCGO and a 5 % dilution in PAO to show its suitability as an additive and provide a further scenario for the early stage of coffee ground collection, where amounts of oils were not yet available in large volumes. A typical Stribeck curve was recorded, demonstrating excellent friction-reducing properties and a broad speed range with constant friction for the SCGO for both, as pure base oil and as 5 % additive, in contrast to the PAO reference. Topographic analysis of the tribo-contact zones showed abrasive wear for all oil types, but least for SCGO.

The life cycle of SCGO was evaluated by LCA in a cradle-to-grave approach, including collection and transport of SCGs, oil extraction, its use as lubricant, and finally, re-collection and disposal of the used lubricant. Given the extrapolation of values from lab-scale to industrial-scale production, these figures provide an indication rather than precise, realistic values shedding light on the fundamental challenges of oil production from SCGs. Since the oil extraction involved SE and the use of n-hexane as a solvent, there was an increase in toxicity and freshwater pollution values attributed to the chosen solvent, which is listed in the SIN list of hazardous substances to be avoided [162].

My contribution to this publication included the following tasks: conceptualization and visualization of the research; literature investigation and curation; conducting of the following experiments: collection of sample and SE, CHNSO analysis, and nanotribometer and GC-MS measurements; data interpretation of the following experiments: ATR-FTIR, CHNSO, rheometer viscosity, TGA/DSC, GC-MS, nanotribometer and rheometer tribological behavior; design of the graphical abstract and figures; sections, that were entirely written by me (original draft): abstract, introduction, experimental, tribological experiments, results and discussion, and conclusion

## Publication III – Advanced Method for the Detection of Saturated Monoglycerides in Biodiesel using GC-EI-MS/MS

Depending on the type of FAME used, the cold flow properties of the resulting biodiesel vary. B7 biodiesels, comprising 7 % FAME mixed with mineral oil-based diesel, can cause fuel filter blockages due to poor cold weather behavior even when meeting the required quality regulations, which prevents diesel from being blended with a higher bio-content share. Key contributors identified to cause filter blocking by precipitation are SMGs. According to regulations, only the initial biodiesel stock is evaluated according to its SMG concentration, and a determination within blends by norms is also unnecessary. Moreover, only the total SMG concentration is limited (as a sum of single contents of 1-C16:0, 2-C16:0 and 1-C18:0), but single SMGs are not further regulated, even though an anomalous behavior within SMG species could be disclosed within this publication. Until now, a method for precise detection and quantification of SMGs in a highly complex matrix of diesel-biodiesel blends was unavailable. Before the presented advanced GC-EI-tandem MS method, a less sophisticated GC-EI-FID-SIM-MS method was used in-house.

Comparing those two methods, specific precursor ions of the SMGs were selected for the SIM mode and scanned throughout the entire fuel matrix. At the retention time where these precursor ions were confirmed by MS, the corresponding FID peak, being not specific to the precursor ion, was integrated for quantification. However, this method also integrates the fuel matrix, leading to a potentially inflated SMG concentration due to the inclusion of additional, non-targeted ions. Adapting the method to use SRM with a triple quadrupole MS/MS system could address this issue. In this approach, precursor ions were chosen and fragmented in the first and second quadrupoles before detecting specific product ions in the third quadrupole. Detection only occurred when the correct transition from the selected precursor to the designated product ions occurred, enabling a highly sensitive and selective analysis that effectively mitigated most matrix effects.

Furthermore, the standardized procedure [84] used for SMG determination by GC-FID states a lower quantification limit of 200 ppm in FAME. B7 samples confirmed to cause filter blocking were found well below concentrations of 200 ppm. Therefore, this method would not have been applicable. As the fuel manufacturing industry and distributors are under pressure to assess the potential for filter blocking as part of quality assurance measures, the objective of this research was to provide a precise quantification method for single SMG determination in both petroleum-based and bio-based fuels, as well as their blends within only one analytical instrument. The refined method involved optimizing sample preparation and calibration for low concentrations, utilizing SRM for specific ion detection, incorporating time segments and enhancing scan time, and determining limits of detection and quantification, ultimately yielding a highly sensitive and accurate detection technique for SMGs in biodiesel.

My contribution to this publication included the following tasks: conceptualization and visualization of the research; literature investigation and curation; conducting of the following experiments: GC-EI-MS/MS method development; design of the graphical abstract and figures; sections that were entirely written by me (original draft): abstract, introduction, materials and methods, results and discussion, conclusion

# Bibliography


[1] European Commission. *Consequences of climate change*. URL: https://climate.ec.europa.eu/climate-change/consequences-climate-change_en (visited on 04/06/2024).

[2] United Nations. *THE 17 GOALS*. URL: https://sdgs.un.org/goals (visited on 01/29/2024).

[3] World Health Organization. *Petroleum Products in Drinking-water*. Research rep. WHO, 2008. 20 pp.

[4] P. Friedlingstein et al. "Global Carbon Budget 2023". In: *Earth System Science Data* 15.12 (2023), pp. 5301–5369. DOI: 10.5194/essd-15-5301-2023. URL: https://essd.copernicus.org/articles/15/5301/2023/ (visited on 01/02/2024).

[5] European Commission. *Energy, Climate change, Environment*. URL: https://commission.europa.eu/energy-climate-change-environment_en (visited on 01/29/2024).

[6] United Nations. *Sustainable Development Goals*. URL: https://upload.wikimedia.org/wikipedia/commons/a/a7/Sustainable_Development_Goals.svg (visited on 09/16/2024).

[7] The National Aeronautics and Space Administration (NASA). *What is the greenhouse effect?* 2024. URL: https://climate.nasa.gov/faq/19/what-is-the-greenhouse-effect/ (visited on 01/02/2024).

[8] EPA. *Overview of Greenhouse Gases*. URL: https://www.epa.gov/ghgemissions/overview-greenhouse-gases (visited on 01/29/2024).

[9] EPA. *Understanding Global Warming Potentials*. URL: https://www.epa.gov/ghgemissions/understanding-global-warming-potentials (visited on 01/29/2024).

[10] NOAA Climate.gov. *Climate Change: Atmospheric Carbon Dioxide*. URL: https://www.climate.gov/news-features/understanding-climate/climate-change-atmospheric-carbon-dioxide (visited on 01/29/2024).

[11] ENERGY STAR by EPA. *Sources of Industrial Greenhouse Emissions*. URL: https://www.energystar.gov/industrial_plants/decarbonizing_industry/sources_industrial_greenhouse_emissions (visited on 01/29/2024).

[12] EPA. *Greenhouse Gas Reporting Program (GHGRP) Chemicals*. URL: https://www.epa.gov/ghgreporting/ghgrp-chemicals (visited on 01/29/2024).

[13] United Nations. *COP26: Together for our planet*. URL: https://www.un.org/en/climatechange/cop26 (visited on 01/29/2024).

[14] Climate Analytics and NewClimate Institute. *UAE 2030 climate plan keeps firm focus on fossil fuels*. 2023. URL: https://climateactiontracker.org/press/uae-2030-climate-plan-keeps-firm-focus-on-fossil-fuels/ (visited on 01/29/2024).

[15] Visual Capitalist. *Global Carbon Budget 2023*. 2021. URL: https://www.visualcapitalist.com/sp/the-paris-agreement-is-the-worlds-climate-action-plan-on-track/ (visited on 01/29/2024).

[16] MSCI Inc. *Global Progress Towards the Paris Agreement*. 2021. URL: https://www.msci.com/research-and-insights/visualizing-investment-data/paris-agreement-global-progress (visited on 01/02/2024).

[17] Global Carbon Project (GCP). *The Paris Agreement: Is The World's Climate Action Plan on Track?* URL: https://globalcarbonbudget.org/carbonbudget2023/ (visited on 01/29/2024).

[18] *ASTM D975-21: Standard Specification for Diesel Fuel*. English. West Conshohocken, PA: ASTM International, 2022. DOI: 10.1520/D0975-21. URL: https://www.astm.org/.

[19] *EN 590:2022: Automotive fuels – Diesel – Requirements and test methods*. Deutsch. Berlin: DIN Deutsches Institut für Normung e. V., 2022. DOI: 10.31030/3337114.

[20] *ASTM D6751-23a: Standard Specification for Biodiesel Fuel Blendstock (B100) for Middle Distillate Fuels*. English. West Conshohocken, PA: ASTM International, 2023. DOI: 10.1520/D6751-23A. URL: https://www.astm.org/.

[21] *EN 14214:2012+A2:2019: Liquid petroleum products – Fatty acid methyl esters (FAME) for use in diesel engines and heating applications – Requirements and test methods*. Deutsch. Berlin: DIN Deutsches Institut für Normung e. V., 2019. DOI: 10.31030/3005309.

[22] *EN ISO 5165:2020-11: Petroleum products – Petroleum products – Determination of the ignition quality of diesel fuels – Cetane engine method (ISO 5165:2020)*. Deutsch. Berlin: DIN Deutsches Institut für Normung e. V., 2020. DOI: 10.31030/3157992.

[23] S. K. Hoekman, A. Broch, C. Robbins, E. Ceniceros, and M. Natarajan. "Review of biodiesel composition, properties, and specifications". In: *Renewable and Sustainable Energy Reviews* 16.1 (2012), pp. 143–169. ISSN: 1364-0321. DOI: 10.1016/j.rser.2011.07.143. URL: https://www.sciencedirect.com/science/article/pii/S136403211100390X.

[24] *EN ISO 3675:1999-11: Crude petroleum and liquid petroleum products – Laboratory determination of density – Hydrometer method (ISO 3675:1998)*. Deutsch. Berlin: DIN Deutsches Institut für Normung e. V., 1991. DOI: 10.31030/8382849.

[25] *EN ISO 3104:2021-01: Petroleum products – Transparent and opaque liquids – Determination of kinematic viscosity and calculation of dynamic viscosity (ISO 3104:2020)*. Deutsch. Berlin: DIN Deutsches Institut für Normung e. V., 2021. DOI: 10.31030/3163720.

[26] *DIN EN ISO 12937:2002-03: Petroleum products – Determination of water – Coulometric Karl Fischer titration method (ISO 12937:2000)*. Deutsch. Berlin: DIN Deutsches Institut für Normung e. V., 2002. DOI: 10.31030/9131845.

[27] C.-I. Chen and S. M. Hsu. "A Chemical Kinetics Model to Predict Lubricant Performance in a Diesel Engine. Part I: Simulation Methodology". In: *Tribology Letters* 14.2 (2003), pp. 83–90. DOI: 10.1023/A:1021748002697. URL: https://link.springer.com/article/10.1023/A:1021748002697.

[28] *EN ISO 6245:2003-01: Petroleum products – Determination of ash (ISO 6245:2001)*. Deutsch. Berlin: DIN Deutsches Institut für Normung e. V., 2003. DOI: 10.31030/9429191.

[29] *ISO 3987:2010-11: Petroleum products – Determination of sulfated ash in lubricating oils and additives*. Deutsch. Berlin: DIN Deutsches Institut für Normung e. V., 2003.

[30] *EN ISO 2719:2016+A1:2021-06: Determination of flash point – Pensky-Martens closed cup method (ISO 2719:2016 + Amd 1:2021)*. Deutsch. Berlin: DIN Deutsches Institut für Normung e. V., 2021. DOI: 10.31030/3261194.

[31] L. R. Rudnick, ed. *Lubricant Additives: Chemistry and Applications, Third Edition*. 3. Boca Raton, FL, USA: Taylor & Francis Group, LLC, 2017. ISBN: 978-1-4987-3172-0.

[32] *EN ISO 2160:1999-04: Petroleum products – Corrosiveness to copper – Copper strip test (ISO 2160:1998)*. Deutsch. Berlin: DIN Deutsches Institut für Normung e. V., 1999. DOI: 10.31030/8069636.

[33] *EN 14112:2021-02: Fat and oil derivatives – Fatty Acid Methyl Esters (FAME) – Determination of oxidation stability (accelerated oxidation test)*. Deutsch. Berlin: DIN Deutsches Institut für Normung e. V., 2021. DOI: 10.31030/3180257.

[34] *EN ISO 12205:1996-11: Petroleum products – Determination of the oxidation stability of middle-distillate fuels (ISO 12205:1995)*. Deutsch. Berlin: DIN Deutsches Institut für Normung e. V., 1995. DOI: 10.31030/7293923.

[35] *EN 15751:2014-06: Automotive fuels – Fatty acid methyl ester (FAME) fuel and blends with diesel fuel – Determination of oxidation stability by accelerated oxidation method*. Deutsch. Berlin: DIN Deutsches Institut für Normung e. V., 2014. DOI: 10.31030/2057812.

[36] *EN 16091:2022-12: Liquid petroleum products – Middle distillates and fatty acid methyl ester (FAME) fuels and blends – Determination of oxidation stability by rapid small scale oxidation test (RSSOT)*. Deutsch. Berlin: DIN Deutsches Institut für Normung e. V., 2022. DOI: 10.31030/3360235.

[37] *DIN EN 116:2018-04: Diesel and domestic heating fuels – Determination of cold filter plugging point – Stepwise cooling bath method*. Deutsch. Berlin: DIN Deutsches Institut für Normung e. V., 2018. DOI: 10.31030/2826727.

[38] *EN 16329:2023-01: Diesel and domestic heating fuels – Determination of cold filter plugging point – Linear cooling bath method*. Deutsch. Berlin: DIN Deutsches Institut für Normung e. V., 2023. DOI: 10.31030/3368417.

[39] *EN ISO 3015:2019-09: Petroleum and related products from natural or synthetic sources – Determination of cloud point (ISO 3015:2019)*. Deutsch. Berlin: DIN Deutsches Institut für Normung e. V., 2019. DOI: 10.31030/3030982.

[40] *EN ISO 22995:2019-09: Petroleum products – Determination of cloud point – Automated step-wise cooling method (ISO 22995:2019)*. Deutsch. Berlin: DIN Deutsches Institut für Normung e. V., 2019. DOI: 10.31030/3032590.

[41] *EN ISO 20846:2019-12: Petroleum products – Determination of sulfur content of automotive fuels – Ultraviolet fluorescence method (ISO 20846:2019)*. Deutsch. Berlin: DIN Deutsches Institut für Normung e. V., 2019. DOI: 10.31030/3062531.

[42] *EN ISO 20884:2019+A1:2021: Petroleum products – Determination of sulfur content of automotive fuels – Wavelength-dispersive X-ray fluorescence spectrometry (ISO 20884:2019 + Amd 1:2021)*. Deutsch. Berlin: DIN Deutsches Institut für Normung e. V., 2019. DOI: 10.31030/3309129.

[43] *EN ISO 13032:2012-06: Petroleum products – Determination of low concentration of sulfur in automotive fuels – Energy-dispersive X-ray fluorescence spectrometric method (ISO 13032:2012)*. Deutsch. Berlin: DIN Deutsches Institut für Normung e. V., 2012. DOI: 10.31030/1860429.

[44] *EN 12662:2014-07: Liquid petroleum products – Determination of total contamination in middle distillates, diesel fuels and fatty acid methyl esters*. Deutsch. Berlin: DIN Deutsches Institut für Normung e. V., 2014. DOI: 10.31030/2056268.

[45] *EN ISO 4264:2018-10: Petroleum products – Calculation of cetane index of middle-distillate fuels by the four variable equation (ISO 4264:2018)*. Deutsch. Berlin: DIN Deutsches Institut für Normung e. V., 2018. DOI: 10.31030/2832285.

[46] *EN ISO 12156-1: Diesel fuel – Assessment of lubricity using the high-frequency reciprocating rig (HFRR) – Part 1: Test method (ISO 12156-1:2018)*. Deutsch. Berlin: DIN Deutsches Institut für Normung e. V., 2019. DOI: 10.31030/3016425.

[47] *EN 16576:2015-02: Automotive fuels – Determination of manganese and iron content in diesel – Inductively coupled plasma optical emission spectrometry (ICP OES) method*. Deutsch. Berlin: DIN Deutsches Institut für Normung e. V., 2015. DOI: 10.31030/2153440.

[48] *EN 12916:2019+A1:2022-10: Petroleum products – Determination of aromatic hydrocarbon types in middle distillates – High performance liquid chromatography method with refractive index detection*. Deutsch. Berlin: DIN Deutsches Institut für Normung e. V., 2022. DOI: 10.31030/3371612.

[49] *EN ISO 10370:2015-03: Petroleum products – Determination of carbon residue – Micro method (ISO 10370:2014)*. Deutsch. Berlin: DIN Deutsches Institut für Normung e. V., 2015. DOI: 10.31030/2144607.

[50] *EN 14103: Fat and oil derivatives – Fatty Acid Methyl Esters (FAME) – Determination of ester and linolenic acid methyl ester contents*. Deutsch. Berlin: DIN Deutsches Institut für Normung e. V., 2020. DOI: 10.31030/3086493.

[51] *DIN EN 15779:2013-12: Petroleum products and fat and oil derivates – Fatty acid methyl esters (FAME) for diesel engines – Determination of polyunsaturated (≥ 4 double bonds) fatty acid methyl esters (PUFA) by gas chromatography*. Deutsch. Berlin: DIN Deutsches Institut für Normung e. V., 2013. DOI: 10.31030/2065043.

[52] *EN 14104: Fat and oil derivates – Fatty acid methyl ester (FAME) – Determination of acid value*. Deutsch. Berlin: DIN Deutsches Institut für Normung e. V., 2021. DOI: 10.31030/3192558.

[53] *EN 14111:2022-08: Fat and oil derivatives – Fatty Acid Methyl Esters (FAME) – Determination of iodine value*. Deutsch. Berlin: DIN Deutsches Institut für Normung e. V., 2022. DOI: 10.31030/3365188.

[54] *EN 14110:2019-06: Fat and oil derivatives – Fatty Acid Methyl Esters – Determination of methanol content*. Deutsch. Berlin: DIN Deutsches Institut für Normung e. V., 2019. DOI: 10.31030/2853780.

[55] *EN 14105: Fat and oil derivatives – Fatty Acid Methyl Esters (FAME) – Determination of free and total glycerol and mono-, di-, triglyceride contents*. Deutsch. Berlin: DIN Deutsches Institut für Normung e. V., 2020. DOI: 10.31030/3181185.

[56] *EN 14538:2006-09: Fat and oil derivatives – Fatty acid methyl ester (FAME) – Determination of Ca, K, Mg and Na content by optical emission spectral analysis with inductively coupled plasma (ICP OES)*. Deutsch. Berlin: DIN Deutsches Institut für Normung e. V., 2006. DOI: 10.31030/9703804.

[57] *EN 14108:2015-06: Fat and oil derivatives – Fatty Acid Methyl Esters (FAME) – Determination of sodium content by atomic absorption spectrometry*. Deutsch. Berlin: DIN Deutsches Institut für Normung e. V., 2015. DOI: 10.31030/2315946.

[58] *EN 14109:2003-10: Fat and oil derivatives – Fatty acid methylesters (FAME) – Determination of potassium content by atomic absorption spectrometry*. Deutsch. Berlin: DIN Deutsches Institut für Normung e. V., 2003. DOI: 10.31030/9393320.

[59] *EN 14107:2003-10: Fat and oil derivatives – Fatty acid methylesters (FAME) – Determination of phosphorus content by inductively coupled plasma (ICP) emission spectrometry*. Deutsch. Berlin: DIN Deutsches Institut für Normung e. V., 2003. DOI: 10.31030/9393419.

[60] J. Bacha, J. Freel, A. Gibbs, L. Gibbs, G. Hemighaus, K. Hoekman, J. Horn, A. Gibbs, M. Ingham, L. Jossens, D. Kohler, D. Lesnini, J. McGeehan, M. Nikanjam, E. Olsen, R. Organ, B. Scott, M. Sztenderowicz, A. Tiedemann, C. Walker, J. Lind, J. Jones, D. Scott, and J. Mills. *Diesel Fuels Technical Review*. Research rep. Chevron Corporation, 2007. 116 pp. URL: https://www.chevron.com/-/media/chevron/operations/documents/diesel-fuel-tech-review.pdf (visited on 03/10/2024).

[61] M. Zöldy and Á. Török. "Road Transport Liquid Fuel Today and Tomorrow: Literature Overview". In: *Periodica PolytechnicaTransportation Engineering* 43.4 (2015), pp. 172–176. DOI: 10.3311/PPtr.8095.

[62] G. D. Todd, R. L. Chessin, and J. Colman. *Toxicological Profile for Total Petroleum Hydrocarbons (TPH)*. Research rep. U.S. Department if Health and Human Services, 1999. 315 pp.

[63] *ASTM D 2500-23: Standard Test Method for Cloud Point of Petroleum Products and Liquid Fuels*. English. West Conshohocken, PA: ASTM International, 2023. DOI: 10.1520/D2500-23. URL: https://www.astm.org/.

[64] *ASTM D 97-17b(2022): Standard Test Method for Pour Point of Petroleum Products*. English. West Conshohocken, PA: ASTM International, 2022. DOI: 10.1520/D0097-17BR22. URL: https://www.astm.org/.

[65] *ASTM D 6371-17a: Standard Test Method for Cold Filter Plugging Point of Diesel and Heating Fuels*. English. West Conshohocken, PA: ASTM International, 2017. DOI: 10.1520/D6371-17A. URL: https://www.astm.org/.

[66] *ASTM D 4539-22: Standard Test Method for Filterability of Diesel Fuels by Low-Temperature Flow Test (LTFT)*. English. West Conshohocken, PA: ASTM International, 2022. DOI: 10.1520/D4539-22. URL: https://www.astm.org/.

[67] EPA. *DERA – Learn About Impacts of Diesel Exhaust and the Diesel Emissions Reduction Act (DERA)*. 2023. URL: https://www.epa.gov/dera/learn-about-impacts-diesel-exhaust-and-diesel-emissions-reduction-act-dera (visited on 03/20/2024).

[68] EPA. *Sulfur Dioxide (SO2) Pollution – Sulfur Dioxide Basics*. 2024. URL: https://www.epa.gov/so2-pollution/sulfur-dioxide-basics (visited on 03/20/2024).

[69] The European Parliament and the Council of the European Union. "Directive 2009/30/EC of the European Parliament and of the Council of 23 April 2009 amending Directive 98/70/EC as regards the specification of petrol, diesel and gas-oil and introducing a mechanism to monitor and reduce greenhouse gas emissions and amending Council Directive 1999/32/EC as regards the specification of fuel used by inland waterway vessels and repealing Directive 93/12/EEC (Text with EEA relevance)". In: *Official Journal of the European Union* 140 (2009), pp. 88–113. URL: http://data.europa.eu/eli/dir/2009/30/oj.

[70] EPA. *Diesel Fuel Standards and Rulemakings*. URL: https://www.epa.gov/diesel-fuel-standards/diesel-fuel-standards-and-rulemakings (visited on 01/08/2023).

[71] *ASTM D5864-23: Standard Test Method for Determining Aerobic Aquatic Biodegradation of Lubricants or Their Components*. English. West Conshohocken, PA: ASTM International, 2023. DOI: 10.1520/D5864-23. URL: https://www.astm.org/.

[72] *ASTM D731-22: Standard Test Method for Molding Index of Thermosetting Molding Powder*. English. West Conshohocken, PA: ASTM International, 2022. DOI: 10.1520/D0731-22. URL: https://www.astm.org/.

[73] OECD. *Test No. 301: Ready Biodegradability*. Research rep. Paris: OECD Guidelines for the Testing of Chemicals, Section 3, 1992. 62 pp. DOI: 10.1787/2074577x.

[74] S. Sorrell, J. Speirs, R. Bentley, A. Brandt, and R. Miller. *Global Oil Depletion – An assessment of the evidence for a near-term peak in global oil production*. Research rep. UKERC – UK ENERGY RESEARCH CENTRE, 2009. 288 pp.

[75] S. Aichmayer, R. Mitterhuemer, and R. Winter. *Erneuerbare Kraftstoffe und Energieträger im Verkehrssektor in Österreich 2023*. Research rep. Bundesministerium für Klimaschutz, Umwelt, Energie, Mobilität, Innovation und Technologie, 2024. 108 pp. URL: https://www.bmk.gv.at/themen/energie/publikationen/biokraftstoffbericht.html (visited on 09/15/2024).

[76] B. Boldt. *Vielseitige Verbundwerkstoffe aus Kaffeesatz*. 2020. URL: https://biooekonomie.de/foerderung/foerderbeispiele/vielseitige-verbundwerkstoffe-aus-kaffeesatz (visited on 12/20/2023).

[77] Hut und Stiel GmbH. *Die Austernpilze von heute wachsen auf dem Kaffeesatz von gestern*. URL: https://www.hutundstiel.at/ (visited on 12/20/2023).

[78] Centre for the Promotion of Imports from developing countries (CBI). *What is the demand for coffee on the European market?* 2022. URL: https://www.cbi.eu/market-information/coffee/what-demand (visited on 04/06/2024).

[79] L. F. Cavalheiro, M. Y. Misutsu, R. C. Rial, L. H. Viana, and L. C. S. Oliveira. "Characterization of residues and evaluation of the physico chemical properties of soybean biodiesel and biodiesel: Diesel blends in different storage conditions". In: *Renewable Energy* 151 (2020), pp. 454–462. ISSN: 0960-1481. DOI: 10.1016/j.renene.2019.11.039. URL: https://www.sciencedirect.com/science/article/pii/S0960148119317203.

[80] G. M. Chupka, J. Yanowitz, G. Chiu, T. L. Alleman, and R. L. McCormick. "Effect of Saturated Monoglyceride Polymorphism on Low-Temperature Performance of Biodiesel". In: *Energy & Fuels* 25.1 (2011), pp. 398–405. DOI: 10.1021/ef1013743.

[81] Y. Sugami, S. Yoshidomi, E. Minami, N. Shisa, H. Hayashi, and S. Saka. "The Effect of Monoglyceride Polymorphism on Cold-Flow Properties of Biodiesel Model Fuel". In: *Journal of the American Oil Chemists' Society* 94 (2017), pp. 1095–1100. DOI: 10.1007/s11746-017-3016-9.

[82] *EN 16934:2017: AAutomotive fuels and fat and oil derivates – Determination of steryl glycosides in fatty acid methyl esters (FAME) – Method by GC-MS with prior purification by SPE*. Deutsch. Berlin: DIN Deutsches Institut für Normung e. V., 2017. DOI: 10.31030/2627337.

[83] M. Frauscher, J. Pichler, A. Agócs, B. Dewitz, T. Drexler, and A. Orfaniotis. "Root causes for low-temperature filter blocking at petrol stations – A field study". In: *Fuel* 366 (2024), p. 131304. DOI: 10.1016/j.fuel.2024.131304. URL: https://www.sciencedirect.com/science/article/pii/S0016236124004514.

[84] *EN 17057:2018: Automotive fuels and fat and oil derivates – Determination of saturated monoglycerides content in Fatty Acid Methyl Esters (FAME) – Method by GC-FID*. Deutsch. Berlin: DIN Deutsches Institut für Normung e. V., 2018. DOI: 10.31030/2811679.

[85] TriboNet. *What is Tribology?* 2016. URL: https://www.tribonet.org/wiki/what-is-tribology/ (visited on 03/20/2024).

[86] Douglas Harper. *-logy.* URL: https://www.etymonline.com/word/-logy (visited on 03/20/2024).

[87] T. Mang, K. Bobzin, and T. Bartels. *Industrial Tribology – Tribosystems, Friction, Wear and Surface – Engineering, Lubrication.* Weinheim, Germany: WILEY-VCH Verlag & Co. KGaA, 2011. ISBN: 978-3-527-32057-8.

[88] AZoM.com Limited. *Tribological Performance Within the Automotive Industry.* URL: https://www.azom.com/article.aspx?ArticleID=13763 (visited on 09/09/2024).

[89] M. Nosonovsky and B. Bhushan. "Green tribology: principles, research areas and challenges". In: *Phil. Trans. R. Soc. A.* 368.1929 (2010), pp. 4677–4694. DOI: 10.1098/rsta.2010.0200. URL: https://royalsocietypublishing.org/doi/10.1098/rsta.2010.0200.

[90] American Petroleum Institute. *Lubricants Life Cycle Assessment and Carbon Footprinting—Methodology and Best Practice.* Tech. rep. Washington: API, 2023. 53 pp.

[91] *ASTM D6079-22: Standard Test Method for Evaluating Lubricity of Diesel Fuels by the High-Frequency Reciprocating Rig (HFRR).* English. West Conshohocken, PA: ASTM International, 2022. DOI: 10.1520/D6079-22. URL: https://www.astm.org/.

[92] *ASTM D7688-18: Standard Test Method for Evaluating Lubricity of Diesel Fuels by the High-Frequency Reciprocating Rig (HFRR) by Visual Observation.* English. West Conshohocken, PA: ASTM International, 2018. DOI: 10.1520/D7688-18. URL: https://www.astm.org/.

[93] Anton Paar GmbH. *Basics of tribology.* URL: https://wiki.anton-paar.com/en/basics-of-tribology/ (visited on 03/20/2024).

[94] Y. Wang and Q. J. Wang. "Stribeck Curves". In: *Encyclopedia of Tribology.* Ed. by Q. J. Wang and Y.-W. Chung. Boston, MA, USA: Springer Science+Business Media, 2013, pp. 3365–3370. ISBN: 978-0-387-92896-8. DOI: 10.1007/978-0-387-92897-5_148. URL: https://link.springer.com/referenceworkentry/10.1007/978-0-387-92897-5_148.

[95] G. L. Doll. "Chapter Four – Lubricants and lubrication". In: *Rolling Bearing Tribology – Tribology and Failure Modes of Rolling Element Bearings.* Amsterdam, Netherlands: Elsevier, 2023, pp. 87–119. ISBN: 978-0-12-822141-9. DOI: 10.1016/B978-0-12-822141-9.00003-0. URL: https://www.sciencedirect.com/science/article/pii/B9780128221419000030?via%3Dihub.

[96] Wikimedia Foundation, Inc. *Schematic Stribeck curve.* URL: https://upload.wikimedia.org/wikipedia/commons/9/91/Curva_di_Stribeck.svg (visited on 03/01/2024).

[97] G. E. Totten, S. R. Westbrook, and R. J. Shah., eds. *Fuels and Lubricants Handbook: Technology, Properties, Performance, and Testing.* West Conshohocken, PA, USA: ASTM International, 2003. ISBN: 0-8031-2096-6.

[98] G. W. Stachowiak, A. W. Batchelor, and G. B. Stachowiak, eds. *Experimental Methods in Tribology.* Vol. 44. Amsterdam, Netherlands: Elsevier B.V., 2004. ISBN: 0-444-51589-5.

[99] A. Morshed, H. Wu, and Z. Jiang. "A Comprehensive Review of Water-Based Nanolubricants Lubricants". In: *Lubricants* 9.9 (2021), p. 89. DOI: 10.3390/lubricants9090089. URL: https://www.mdpi.com/2075-4442/9/9/89.

[100] T. Mang and W. Dresel, eds. *Lubricants and Lubrication*. 2. Weinheim, Germany: WILEY-VCH Verlag & Co. KGaA, 2007. ISBN: 978-3-527-31497-3.

[101] S. Wen and P. Huang, eds. *Principles of Tribology*. 2. Solaris South Tower, Singapore: WILEY-VCH Tsinghua University Press, 2018. ISBN: 978-1-119-21491-5.

[102] R. M. Mortier, M. F. Fox, and S. T. Orszulik, eds. *Chemistry and Technology of Lubricants, Third Edition*. 3. London, United Kingdom: Springer Science+Business Media B.V., 2010. ISBN: 978-1-4020-8661-8. DOI: 10.1023/b105569.

[103] H. Czichos and K.-H. Habig. *Tribologie-Handbuch – Tribometrie, Tribomaterialien, Tribotechnik*. 5. Weinheim, Germany: Springer Fachmedien Wiesbaden GmbH, 2020. ISBN: 978-3-658-29483-0. DOI: 10.1007/978-3-658-29484-7.

[104] J. M. Herdan. "Lubricating oil additives and the environment — an overview". In: *Lubrication Science* 9.2 (1997), pp. 161–172. DOI: 10.1002/ls.3010090205. URL: https://onlinelibrary.wiley.com/doi/abs/10.1002/ls.3010090205.

[105] N. Dörr, J. Brenner, A. Ristić, B. Ronai, C. Besser, V. Pejaković, and M. Frauscher. "Correlation Between Engine Oil Degradation, Tribochemistry, and Tribological Behavior with Focus on ZDDP Deterioration". In: *Tribology Letters* 67.62 (2019). DOI: 10.1007/s11249-019-1176-5. URL: https://link.springer.com/article/10.1007/s11249-019-1176-5.

[106] N. Dörr, A. Agocs, C. Besser, A. Ristić, and M. Frauscher. "Engine Oils in the Field: A Comprehensive Chemical Assessment of Engine Oil Degradation in a Passenger Car". In: *Tribology Letters* 67.68 (2019). DOI: 10.1007/s11249-019-1182-7. URL: https://link.springer.com/article/10.1007/s11249-019-1182-7.

[107] H. Méheust, J.-F. L. Meins, E. Grau, and H. Cramail. "Bio-Based Polyricinoleate and Polyhydroxystearate: Properties and Evaluation as Viscosity Modifiers for Lubricants". In: *ACS Appl. Poly. Mater.* 3.2 (2021), pp. 811–818. DOI: 10.1021/acsapm.0c01153. URL: https://pubs.acs.org/doi/10.1021/acsapm.0c01153.

[108] N. R. N. Roselina, N. S. Mohamad, and S. Kasolang. "Evaluation of TiO2 nanoparticles as viscosity modifier in palm oil bio-lubricant". In: *IOP Conference Series: Materials Science and Engineering* 834 (2020), p. 012032. DOI: 10.1088/1757-899X/834/1/012032. URL: https://iopscience.iop.org/article/10.1088/1757-899X/834/1/012032.

[109] G. Karmakar, K. Dey, P. Ghosh, B. K. Sharma, and S. Z. Erhan. "A Short Review on Polymeric Biomaterials as Additives for Lubricants". In: *Polymers* 13.8 (2021), p. 1333. DOI: 10.3390/polym13081333. URL: https://www.mdpi.com/2073-4360/13/8/1333.

[110] A. K. Singh and R. K. Singh. "A Search for Ecofriendly Detergent/Dispersant Additives for Vegetable-Oil Based Lubricants". In: *Journal of Surfactants and Detergents* 15.4 (2012), pp. 399–409. DOI: 10.1007/s11743-011-1321-0. URL: https://aocs.onlinelibrary.wiley.com/doi/10.1007/s11743-011-1321-0.

[111] L. R. Rudnick, ed. *Synthetics, Mineral Oils, and Bio-Based Lubricants – Chemistry and Technology*. 3. Boca Raton, FL, USA: Taylor & Francis Group, LLC, 2020. ISBN: 978-1-138-06821-6.

[112] S. Rönsch and H. Wagner. *Calculation of heating values for the simulation of thermochemical conversion plants with Aspen Plus*. Research rep. Deutsches Biomasseforschungszentrum DBFZ, 2011. 7 pp. URL: https://www.dbfz.de/fileadmin/prozesssimulation/data/downloads/workshop_juni2011/Roensch_und_Wagner_2012_Calculation_of_heating_values_with_Aspen_Plus.pdf (visited on 09/09/2024).

[113] Innovation-el. *TGA/Thermogravimetric Analysis*. URL: https://innovation-el.net/tool/tga-thermogravimetric-analysis/ (visited on 04/09/2024).

[114] E. Ghanbari, S. J. Picken, and J. H. van Esch. "Analysis of differential scanning calorimetry (DSC) determining the transition temperatures, and enthalpy and heat capacity changes in multicomponent systems by analytical model fitting". In: *Journal of Thermal Analysis and Calorimetry* 148.22 (2023), pp. 12393–12409. DOI: 10.1007/s10973-023-12356-1. URL: https://link.springer.com/article/10.1007/s10973-023-12356-1.

[115] M. R. Molla, A. K. M. Asaduzzaman, M. A. R. Mia, M. Uddin, S. Biswas, and M. S. Uddinn. "Nutritional Status, Characterization and Fatty Acid Composition of Oil and Lecithin Isolated from Fresh Water Fish Shoul (Channa striata)". In: *International Journal of Food Sciences and Nutrition* 5.1 (2016), pp. 9–15. DOI: 10.11648/j.ijnfs.20160501.12. URL: https://www.sciencepublishinggroup.com/article/10.11648/j.ijnfs.20160501.12.

[116] F. Kähler, O. Porc, and M. Carus. *RCI Carbon Flows Report: Compilation of supply and demand of fossil and renewable carbon on a global and European level*. Research rep. Renewable Carbon Initiative, 2023. 92 pp. URL: https://renewable-carbon.eu/publications/product/the-renewable-carbon-initiatives-carbon-flows-report-pdf/ (visited on 03/01/2024).

[117] International Energy Agency (IEA). *CO2 Emissions in 2023 – Executive Summary*. URL: https://www.iea.org/reports/co2-emissions-in-2023/executive-summary (visited on 03/01/2024).

[118] Global Carbon Project (GCP). *Fossil CO2 emissions at record high in 2023*. 2023. URL: https://globalcarbonbudget.org/fossil-co2-emissions-at-record-high-in-2023/ (visited on 01/29/2024).

[119] International Energy Agency. *Total CO2 emissions*. URL: https://www.iea.org/regions/europe/emissions (visited on 04/06/2024).

[120] Eurostat. *Greenhouse gas emissions by source sector, EU, 2021*. URL: https://ec.europa.eu/eurostat/statistics-explained/images/5/52/Greenhouse_gas_emissions_by_source_sector%2C_EU%2C_2021.png (visited on 04/06/2024).

[121] International Energy Agency (IEA). *The Role of E-fuels in Decarbonising Transport*. Research rep. IEA, 2023. 76 pp. URL: https://www.iea.org/reports/the-role-of-e-fuels-in-decarbonising-transport (visited on 03/01/2024).

[122] Daka Denmark A/S. *For the Purpose of Automotive Fuel*. URL: https://www.dakaecomotion.dk/en/products/product-overview/automotive-fuel/ (visited on 09/09/2024).

[123] REMONDIS Sustainable Services GmbH. *Biodiesel is way ahead of fossil fuels*. URL: https://www.remondis-lippe-plant.com/production-of-biodiesel/ (visited on 09/09/2024).

[124] Neste Oyj. *NEXBTL technology turns renewable oils and fats into high-quality products*. URL: https://www.neste.com/products-and-innovation/innovation/nexbtl (visited on 03/01/2024).

[125] ETIP-B-SABS 2. *Waste oils and fats as feedstocks for biofuels production*. URL: https://www.etipbioenergy.eu/value-chains/feedstocks/waste/waste-oils-and-fats (visited on 03/01/2024).

[126] ETIP-B-SABS 2. *HVO/HEFA*. URL: https://www.etipbioenergy.eu/value-chains/products-end-use/products/hvo-hefa (visited on 03/01/2024).

[127] Cellana Inc. *Algae Will Help Meet the Growing Demand for Biofuels for Transporation and Energy*. URL: https://cellana.com/products/renew-fuel/ (visited on 03/01/2024).

[128] UPM-Kymmene Corporation. *UPM BioVerno diesel – a genuine fuel choice for the future*. URL: https://www.upmbiofuels.com/traffic-fuels/upm-bioverno-diesel-for-fuels/ (visited on 03/01/2024).

[129] Eni Rewind S.p.A. *Giving new life to organic waste to create energy*. URL: https://www.eni.com/enirewind/en-IT/water-waste/waste-to-fuel.html (visited on 03/01/2024).

[130] KIT – Karlsruhe Institute of Technology. *bioliq® – Cluster Project of the Profilregion Mobilitätsysteme Karlsruhe*. URL: https://www.bioliq.de/english/ (visited on 03/01/2024).

[131] Fulcrum BioEnergy, Inc. *NET-ZERO CARBON PLANTS – A network of fuels plants across the U.S.* URL: https://www.fulcrum-bioenergy.com/plants-overview (visited on 03/01/2024).

[132] Virent, Inc. *BioForming*. URL: https://www.virent.com/technology/bioforming/ (visited on 09/09/2024).

[133] OMV Aktiengesellschaft. *ReOil: Getting crude oil back out of plastic*. 2018. URL: https://www.omv.com/en/blog/reoil-getting-crude-oil-back-out-of-plastic (visited on 09/09/2024).

[134] OMV Aktiengesellschaft. *Recycling technologies*. URL: https://www.omv.com/en/recycling-technologies (visited on 09/09/2024).

[135] BEST – Bioenergy and Sustainable Technologies GmbH. *Green fuel from residual waste*. URL: https://smartcity.wien.gv.at/en/waste2value/ (visited on 03/01/2024).

[136] ReCarbon, Inc. *Discover ReCarbon*. URL: https://www.recarboninc.com/ (visited on 03/01/2024).

[137] C. Markowitsch, M. Lehner, J. Kitzweger, W. Haider, S. Ivanovici, M. Unfried, and M. Maly. "C2PAT – Carbon to Product Austria". In: *EnInnov2022; 17. Symposium Energieinnovation; Kurzfassungsband*. 17. Symposium Energieinnovation (Feb. 16–18, 2022). Graz, Austria, 2022.

[138] Holcim (Österreich) GmbH. *Mit C2PAT+ zur Klimaneutralität*. URL: https://www.holcim.at/nachhaltigkeit/mit-c2pat-plus-zur-klimaneutralitaet (visited on 09/09/2024).

[139] Carbon Recycling International (CRI). *A proven carbon utilisation solution*. URL: https://carbonrecycling.com/ (visited on 03/01/2024).

[140] BASF SE. *BASF's biomass balance approach*. URL: https://www.basf.com/global/en/who-we-are/sustainability/we-drive-sustainable-solutions/circular-economy/mass-balance-approach/biomass-balance/biomass-balance.html (visited on 03/01/2024).

[141] OMV Aktiengesellschaft. *Biogenic oil co-processing*. 2020. URL: https://omv.online-report.eu/en/sustainability-report/2019/focus-areas/innovation/biogenic-oil-co-processing.html (visited on 03/01/2024).

[142] Green Tech Valley Cluster GmbH. *BDI bioCRACK – Biomass-to-Liquid-Treibstoffe*. URL: https://www.greentech.at/produkte/biocrack-biomass-to-liquid-treibstoffe/ (visited on 03/01/2024).

[143] G. Sonnemann and M. Margni, eds. *LCA Compendium – The Complete World of Life Cycle Assessment*. London, United Kingdom: Springer Science+Business Media B.V., 2015. ISBN: 978-94-017-7220-4. DOI: 10.1007/978-94-017-7221-1.

[144] European Commission. *Life Cycle Assessment (LCA)*. URL: https://eplca.jrc.ec.europa.eu/lifecycleassessment.html (visited on 01/29/2024).

[145] *DIN EN ISO 14044:2021-02: Environmental management – Life cycle assessment – Requirements and guidelines (ISO 14044:2006 + Amd 1:2017 + Amd 2:2020)*. Deutsch. Berlin: DIN Deutsches Institut für Normung e. V., 2021. DOI: 10.31030/3179656.

[146] European Commission. *ILCD Handbook: Recommendations for Life Cycle Impact Assessment in the European context*. Research rep. European Union, 2011. 159 pp. DOI: 10.278/33030. URL: https://eplca.jrc.ec.europa.eu/uploads/ILCD-Handbook-Recommendations-for-Life-Cycle-Impact-Assessment-in-the-European-context.pdf (visited on 03/10/2024).

[147] European Commission. *Environmental Footprint*. URL: https://eplca.jrc.ec.europa.eu/EnvironmentalFootprint.html (visited on 01/29/2024).

[148] CEFIC. *Measuring The Emissions Impact In The Chemical Sector: A Guide On Product Carbon Footprint*. URL: https://cefic.org/media-corner/newsroom/measuring-the-emissions-impact-in-the-chemical-sector-a-guide-on-product-carbon-footprint/ (visited on 01/29/2024).

[149] TfS – Together for Sustainability. *Scope 3 GHG Emissions Programme*. URL: https://www.tfs-initiative.com/how-we-do-it/scope-3-ghg-emissions (visited on 01/29/2024).

[150] European Commission. *Environmental Footprint methods*. URL: https://green-business.ec.europa.eu/environmental-footprint-methods_en (visited on 01/29/2024).

[151] A. Majumdar, N. Pradhan, J. Sadasivan, A. Acharya, N. Ojha, S. Babu, and S. Bose. "Chapter 5 – Food Degradation and Foodborne Diseases: A Microbial Approach". In: *Microbial Contamination and Food Degradation – Handbook of Food Bioengineering*. Ed. by A. M. Holban and A. M. Grumezescu. London, UK: Elsevier Inc., 2018, pp. 109–148. ISBN: 978-0-12-811515-2. DOI: 10.1016/B978-0-12-811515-2.00005-6. URL: https://www.sciencedirect.com/science/article/pii/B9780128115152000056?via%3Dihub.

[152] E. Reszczyńska and A. Hanaka. "Lipids Composition in Plant Membranes". In: *Cell Biochemistry and Biophysics* 78 (2020), pp. 401–414. DOI: 10.1007/s12013-020-00947-w. URL: https://link.springer.com/article/10.1007/s12013-020-00947-w.

[153] The National Aeronautics and Space Administration (NASA). *Understanding Sea Level*. URL: https://sealevel.nasa.gov/understanding-sea-level/global-sea-level/overview/ (visited on 09/15/2024).

[154] Ellen MacArthur Foundation. *Food and the circular economy -– deep dive*. URL: https://www.ellenmacarthurfoundation.org/food-and-the-circular-economy-deep-dive (visited on 09/15/2024).

[155] M. Smoluch, G. Grasso, P. Suder, and J. Silberring, eds. *Mass Spectrometry – An Applied Approach*. 2. Hoboken, NJ, USA: John Wiley & Sons, Inc., 2019. ISBN: 978-1-119-37730-6.

[156] Merck KGaA. *How to Choose a Capillary GC Column*. URL: https://www.sigmaaldrich.com/AT/de/technical-documents/technical-article/analytical-chemistry/gas-chromatography/column-selection (visited on 04/06/2024).

[157] Merck KGaA. *Gas Chromatography (GC) Column Selection Guide*. URL: https://www.sigmaaldrich.com/AT/de/technical-documents/technical-article/analytical-chemistry/gas-chromatography/gc-column-selection-guide (visited on 04/06/2024).

[158] Altmann Analytik GmbH & Co. KG. *GC-Säulen: Erläuterung und Anwendung*. URL: https://www.analytics-shop.com/de/gc-saeulen (visited on 04/06/2024).

[159] H.-J. Hübschmann, ed. *Handbook of GC-MS – Fundamentals and Applications*. 3. Weinheim, Germany: Wiley-VCH Verlag GmbH & Co. KGaA, 2015. ISBN: 978-3-527-33474-2. DOI: 10.1002/9783527674305.

[160] P. Q. Tranchida, I. Aloisi, and L. Mondello. "Chapter Three – Heart-cutting and comprehensive multidimensional gas chromatography: Basic principles". In: *Comprehensive Analytical Chemistry*. Ed. by C. E. I. Cordero. Vol. 96. Netherlands: Elsevier B.V., 2022, pp. 69–92. ISBN: 978-0-323-98881-0. DOI: 10.1016/bs.coac.2021.10.003.

[161] R. Romero-González and A. G. Frenich, eds. *Applications in High Resolution Mass Spectrometry – Food Safety and Pesticide Residue Analysis*. Oxford, United Kingdom: Elsevier Inc., 2017. ISBN: 978-0-12-809464-8.

[162] The International Chemical Secretariat (ChemSec). *SIN List Chemical*. URL: https://sinsearch.chemsec.org/chemical/110-54-3 (visited on 04/07/2024).

## 2.1 Publication I - A comprehensive review of sustainable approaches for synthetic lubricant components

Authors: Jessica Pichler, Rosa Maria Eder, Charlotte Besser, Lucia Pisarova, Nicole Dörr, Martina Marchetti-Deschmann & Marcella Frauscher

Journal: Green Chemistry Letters and Reviews, 16:1, 2185547, 2023
DOI: 10.1080/17518253.2023.2185547

The publication is reprinted on the following pages.

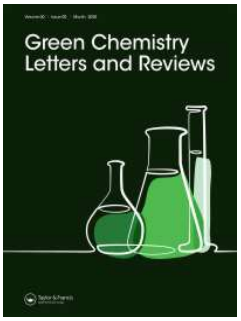

Green Chemistry Letters and Reviews

ISSN: (Print) (Online) Journal homepage: www.tandfonline.com/journals/tgcl20

# A comprehensive review of sustainable approaches for synthetic lubricant components

Jessica Pichler, Rosa Maria Eder, Charlotte Besser, Lucia Pisarova, Nicole Dörr, Martina Marchetti-Deschmann & Marcella Frauscher

**To cite this article:** Jessica Pichler, Rosa Maria Eder, Charlotte Besser, Lucia Pisarova, Nicole Dörr, Martina Marchetti-Deschmann & Marcella Frauscher (2023) A comprehensive review of sustainable approaches for synthetic lubricant components, Green Chemistry Letters and Reviews, 16:1, 2185547, DOI: 10.1080/17518253.2023.2185547

**To link to this article:** https://doi.org/10.1080/17518253.2023.2185547



Published online: 16 Mar 2023.

GREEN CHEMISTRY LETTERS AND REVIEWS
2023, VOL. 16, NO. 1, 2185547
https://doi.org/10.1080/17518253.2023.2185547

Taylor & Francis
Taylor & Francis Group

REVIEW

OPEN ACCESS Check for updates

# A comprehensive review of sustainable approaches for synthetic lubricant components

Jessica Pichler [a,b], Rosa Maria Eder [a], Charlotte Besser [a], Lucia Pisarova [a], Nicole Dörr [a], Martina Marchetti-Deschmann [b] and Marcella Frauscher [a]

[a]AC2T Research GmbH, Wiener Neustadt, Austria; [b]Faculty of Technical Chemistry, Institute of Chemical Technologies and Analytics, TU Wien, Vienna, Austria

**ABSTRACT**

In the last few years, there is a general shift observable toward greener lubrication, fueled amongst others by policy initiatives such as the European Green Deal in consistency with the UN Sustainable Development Goals. At least 70 vol% of a lubricant is composed of a specific base oil, the rest is a variation of additives altering the lubricant properties (enhancing or suppressing existent base oil properties or adding new properties) to be operational for a particular field of application. So, in terms of sustainability, biodegradability, bioaccumulation, and toxicity the type of base oil plays a major role, which makes environmentally harmful petroleum-based lubricant formulations highly problematic for future applications. Hence, this leads to an ever-growing demand of environmentally friendly lubricant alternatives. Within the scope of this review lies the investigation of bio-based, bio-derived, and other sustainable lubricant components that could serve as promising replacements for conventional petroleum-based formulations, in accordance with the principles of green chemistry and tribology. As recycling is embraced by the term sustainability, waste-derived components of non-biological origin are also included in this work. An overview of studies on the tribological performance such as friction and wear properties of these sustainable and benign lubricant components is given.

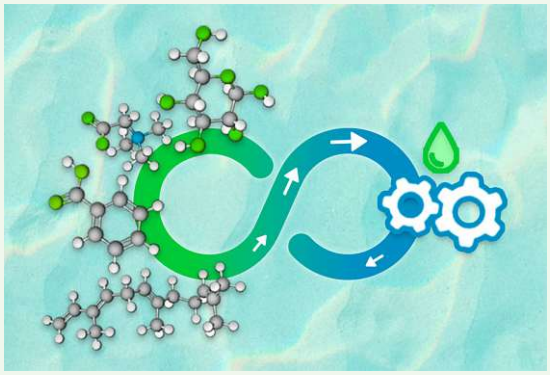

**ARTICLE HISTORY**
Received 23 January 2023
Accepted 24 February 2023

**KEYWORDS**
Environmentally acceptable; tribology; synthetic lubricants; sustainability; European Green Deal

## Introduction

During the last decade lubricants with low environmental impact have been the subject of research activities and numerous products are available on the market. This is fueled globally due to sustainable development goals (SDGs) to which countries are committed. To give an example, the President of the European Commission, Ursula von der Leyen, has proclaimed the European Green Deal in December 2019 (details see chapter Legal issues) (*1*).

Measures to implement climate and environmental protection in governmental agendas are given more emphasis. Hence, several foundations have already been laid, accompanied by the propagation of a number of definitions:

*What is green chemistry?* The concept of green chemistry is defined as 'the design of chemicals and products and processes that reduce or eliminate the use or generation of hazardous substances' by the US Environmental Protection Agency (EPA) (*2*). Most important in this sense

**CONTACT** Jessica Pichler jessica.pichler@ac2t.at AC2T research GmbH, Viktor-Kaplan-Straße 2/C, 2700 Wiener Neustadt, Austria
This article has been corrected with minor changes. These changes do not impact the academic content of the article.

is the life cycle of a chemical product, to help with the design of such next-generation products, 12 principles of green chemistry are formulated (*3*):

(1) Prevent waste instead of treating or cleaning up in hindsight.
(2) Maximize atom economy so that few or no atoms are wasted through synthesis.
(3) Design less hazardous chemical syntheses to pose little or no health risk for humans and the environment.
(4) Reduce toxicity by a safer chemical product design.
(5) Solvents and auxiliaries should be safer when needed and avoided when possible.
(6) Increase energy efficiency to reduce the negative impact on the environment and economy, chemical syntheses should be conducted at room temperature and ambient pressure.
(7) Use renewable raw materials and feedstocks.
(8) Minimize or completely avoid unnecessary derivatization products.
(9) Use catalysts instead of stoichiometric reagents.
(10) Design chemical substances for degradation at the end of their function.
(11) Implement real-time, in-process monitoring, and control to prevent hazardous product formation.
(12) Minimize the potential risk of accidents such as fires, explosions, releases, etc. by choosing safer chemistry.

How green chemistry is implemented in today's economy and the resulting regulations are addressed in detail in chapter Legal issues.

*What is green tribology?* Tribology – the science of interacting surfaces in relative motion – in general, comprises friction, wear reduction, and lubrication improvement, with the intention to save energy and materials (*4*). The term green tribology implicates 'the science and technology of the tribological aspects of ecological balance and of environmental and biological impacts' and combines the areas of green engineering and green chemistry. The areas of green tribology incorporate (i) biomimetic surfaces, (ii) environmentally friendly and biodegradable lubrication, and (iii) tribology of renewable sources. The performance of a tribological system plays the most important role in terms of efficiency improvement including prevention of heat pollution, energy dissipation, and protection of material by controlling friction and wear (*5*). Green tribology becomes increasingly important when heading toward a low-carbon economy and dealing with issues such as environmental pollution, climate crisis, and global energy shortage (*4*). In this work, we focus on sustainable lubrication as a contributing factor toward greener tribology.

*What is sustainable lubrication?* The term 'sustainable' lubrication is not yet universally defined, but it incorporates amongst others 'biodegradable,' 'environmentally friendly,' and 'environmentally acceptable' (bio)lubricants. For a lubricant to be considered as environmentally friendly, it must fulfill the following key criteria to satisfy EPA standards and EU Ecolabel limitations: 1. biodegradability according to OECD 301 and ASTM tests D5864 and D6731 (easily biodegradable), 2. renewability according to ASTM D6866 (carbon content is less than 5 years old and products must have 25% of renewable content) implying a general low carbon footprint, and 3. toxicity according to OECD 201-203 (acute toxicity) and OECD 210-211 (chronic toxicity) tests, or in other words being non-toxic to humans and the environment. Besides, it must be non-bioaccumulative (also see Vessel Incidental Discharge Act) and producible in large quantities in sustainable production. The ideas range from vegetable oils over microbial biofilms and biopolymers to hydration lubrication. Moreover, amongst others the use of minimum quantities (e.g. avoid spills due to specific bottle shape), recyclable packaging, and excluded or limited substances (e.g. for lubricant additives) are addressed within the EU Ecolabel criteria (*4,6*).

Within this work lubricant components such as base oils and additives of bio-based or bio-derived renewable feedstocks producible in an industrially relevant scale are chosen, which should contribute to less toxicity, an enhanced biodegradation, and promote sustainability of the final product, in line with the green chemistry principles. As a supplementary topic recycled feedstocks are addressed, as they fit within the scope of reducing the environmental impact (circular economy) and maintaining an ecological balance (less primary resource use). Furthermore, a special focus is laid on the tribological performance of formulations proven for industrial applications, while sheer bio-tribological applications are only mentioned briefly and not expanded on.

## Legal issues

The year 2021 marked the beginning of the action plan set by the European Green Deal, which works toward a more sustainable economy of the European Union (EU), according to Regulation (EU) No 2018/1999 of the European Parliament and of the Council. In addition, Regulation (EEC) No 880/1992 of the Council of the European Communities describes the European Ecolabel for Lubricants that supports the achievement of those essential climate goals until 2030 (*7*).

Several national and regional ecolabels, such as the Blue Angel (Germany) or the Nordic Swan (Denmark, Sweden, Norway, Finland, and Iceland) have been replaced and/or harmonized with the European Ecolabel (*8*). Essentially, it requires (1) the absence of dangerous materials, referring to the European Union Dangerous Preparations Directive; (2) the passing of toxicity tests (OECD 201, 202, 210, 211); (3) biodegradability; (4) low bioaccumulation; (5) a renewable content; and (6) the restriction of certain substances. European Ecolabel Lubricants shall guarantee high technical performance while replacing petroleum-based base oils with alternatives to achieve an energy portion of 32.5% from renewable sources until 2030. By 2050, the long-term strategy of the EU includes the goals to be climate neutral, having an economy with net-zero greenhouse gas emissions, and pursuing efforts to limit global warming below 1.5°C (global average temperature). These goals are in line with the COP21, the climate conference from December 2015 in Paris, and the European Green Deal (*7*,*9*).

In the USA, the definition of EAL (Environmentally Acceptable Lubricant) published by the EPA (Environmental Protection Agency) is dominant (*9*). In comparison to the European Ecolabel, the EPA only includes bioaccumulation, biodegradability, and aquatic toxicity and is only valid for marine applications.

Regarding waste management, Directive (EU) 2018/851, being an amendment to Directive 2008/98/EC, promotes the idea of a circular economy by planning improved waste management requirements and guidance including the whole life cycle of products. Goals of the European Circular Economy sustainability roadmap include a recycling rate of 55% of municipal waste by 2025 and a separate collection of hazardous household waste by 2022 and biowaste by 2023. Additionally, the Directive is advising Member States to either prevent waste generation in general or to implement a suitable long-term recovery strategy for both re-use and recycling (*10*).

For US water waste management, the Vessel Incidental Discharge Act (VIDA), formerly named VGP (Vessel General Permit), aims to reduce the environmental impact of discharges (e.g. ballast water), proposing a CWA (Clean Water Act). The CWA regulates discharges of pollutants into the waters of the US and further aims to regulate the quality standards for surface waters (*11*).

## Regulations for commercial lubricants and lubricant components

Only a small number of bio-based lubricants explored at lab and pilot scale will make it to commercial production. After establishing commercialization, the bio-based lubricant must gain and maintain a market share. The easiest way for a bio-based product to accomplish the market entrance is when it is directly substituting a fossil-based product with matching price and quality and using the same infrastructure (*12*).

For lubricants and lubricant components, there are lists available classifying their use either as safe for humans and the environment or as potentially harmful. One of those lists is provided by FDA as the 21 CFR § 178.3570 'Lubricants with incidental food contact and limitations of H1 food-grade lubricant components (base stocks and additives), not updated since 1977.' Suitable base stocks and additives for biolubricant formulation might also be found in the White Book™ – Nonfood Compounds Listing Directory of NSF (National Science Foundation), listing countless lubricant components by brand names that are compliant with food safety regulations. Another contemporary (regularly updated) and a comprehensive list is supplied by the European Commission as Lubricant Substance Classification list (LuSC-list) mentioning various substances and base oil brands along with their EEL (EU Ecolabel Lubricant) biodegradability and aquatic toxicity, reaching over various sugars to different glycerides, oil extractives, and fatty acids. Only substances with 100% classification A (ultimately aerobically biodegradable) EEL biodegradation and 100% classification D (nontoxic) EEL aquatic toxicity are approved for the list. Other lists such as the OSPAR List of Chemicals for Priority Action (LCPA), first adopted in 2004, are comprising priority chemicals that pose a concern to the marine environment such as (organo-)metallic compounds, organohalogens, pesti- or biocides, phenols, and others. The list is announced to be updated in 2022 (*13*–*16*).

The European Commission lists 37 producers of 138 fully formulated lubricants (by January 2022) in the LuSC list complying with the criteria of the EU Ecolabel according to Commission Decision (EU) 2018/1702. These criteria cover no addition or formation of hazardous substances or substances of very high concern (≤0.010 wt.% in the final product), requirements for technical performance and packaging, and strict regulations on aquatic toxicity, bioaccumulation, and biodegradability. Latter demands, that > 90 wt.% of hydraulic and closed gear lubricants, and metalworking fluids, >75 wt.% of stern tube, open gears, and two-stroke lubricants, and >95% of chainsaw, and other total loss lubricants and greases are readily aerobically biodegradable. A minimum of 25% bio-based carbon content (corresponding to EN 16807) is mandatory in the final product (*17*,*18*).

## Recent research activities

In view of the large amount of research on biolubricants, this systematic review mainly focuses on developments within a time frame of the last seven years (2015–2022) particularly in the field of biologically benign lubricant components for base oil formulations (as in either bio-originated, or bio-derived) from synthetic or modified organic structures, as well as their tribological properties, friction, and wear behavior, and possible field of applications as lubricants. These abovementioned key issues are complemented by the following restriction criteria:

- Inclusion criteria: benign or biomimetic structures, industrial tribology, tribological findings (concerning friction and wear), oil-based lubrication, water-based lubrication, accessibility in industrial quantities.
- Exclusion criteria: publicized research findings older than 2015, without tribological tests, limited to water lubrication applications, limited to human/bio-tribology.

Only those vegetable oil (VO)-derived lubricant components are discussed, that are not primarily in competition with biodiesel production or the food industry, thus will not comply with UN global malnutrition programs as they may serve as food source. Therefore, only non-edible and/or waste-based feedstocks are investigated here but not the entire area of VOs. Furthermore, this work is not enlarging upon the processing steps (synthesis, catalysis, …) of the mentioned lubricant components and thus, not discussing their environmental impact caused by production processes.

### *Vegetable oil-derived lubricants*

#### *Fatty acid-based components: estolide esters*

Estolides are esters synthesized from fatty acids by homopolymerization, creating secondary ester linkages of one fatty acid to the alkyl backbone of another fatty acid. They are mostly produced from vegetable oils but can be synthesized from animal fats or fatty wastes too. Synthetic estolides are classified into (i) glyceride-based, (ii) ester-based, and (iii) fatty acid-based. Estolides are further characterized by the degree of polymerization and the estolide number (EN), which describes the extent of oligomerization (EN = $n + 1$). They show unique physical properties due to different structures and synthesis pathways, convincing with excellent biodegradability, hydrolytic stability, natural detergency, low volatility, high viscosity, and improved oxidation stability and cold flow properties, which promotes their use as lubricating fluids (*19*).

The higher viscosity indices (VI) of estolides result in excellent wear protection behavior. Furthermore, due to a high degree of saturation, estolides maintain a very good oxidative stability comparable to other high-end synthetics, for example, when determined by rotating pressurized vessel oxidation test (RPVOT) in (*19*). Because of the branched structure of estolides, also short chain lengths (C2-C10) show good pour point ranges from −12 to −30°C, awakening the interest to use estolides also as thickening agents. Large hydrophobic branches on both sides of the estolides create a stearic barrier, resulting in very good hydrolytic stability comparable to those of polyalphaolefin (PAO) base oils (*19*). Naturally occurring estolides are found in various plant seed oils, secretions from the glandular hair of a caterpillar, as well as in human meibomian glands (within the eyelid) as wax esters (*19–21*).

The structure of estolides and, consequently, the physical properties such as pour point, cloud point, and viscosity, can be affected by the use of catalysts and synthetic conditions. This enables a targeted adaption based on different fields of applications, such as personal care, automotive, industrial, and marine lubricant base oils (*21*).

To give some examples of tribological use of estolides, castor oil-derived estolides are investigated with similar properties compared to the already established enhanced lubricity of triacylglycerol (TAG)-based estolides from *Orychophragmus violaceus* (Ov) seed oil. Friction and wear tests are conducted on a macroscale pin-on-disk (steel/steel) tribometer, in a reciprocating motion. The lubricants are tested in the boundary lubrication regime with a maximum contact pressure of 1.5 GPa. Uncapped natural OvTAG estolides (hydroxy fatty acids at the terminal end of the estolide branch chain) show a lower coefficient of friction (COF) at 25°C, whereas capped OvTAG estolides (non-hydroxy fatty acids at the terminal end) show a lower COF at 100°C. Mixing uncapped and capped OvTAG estolides leads to an even lower COF, suggesting that both types have a positive impact on tribological performance. Synthetic castor estolides produce less wear volume on the wear scar for surface and ball track width compared to natural castor oil surface/ball track width (*22*).

Since the use of vegetable oil (VO) as a biolubricant is limited by poor cold flow properties and oxidative stability, manipulation of the chemical structure of VO overcomes these limitations. The modification of vegetable oil-based oleic acid and further conversion to estolide esters and amides via lauric acid-capped estolides is studied along with tribological tests on a four-ball

tester (steel). The anti-wear properties evaluated by wear scar diameter (WSD) are comparable or even better for all estolide ester and amide samples in contrast to commercial lubricants. The lowest wear with the smallest WSD could be established by octyl estolide ester, followed by estolide amides (*23*).

### *Fermentation-based components: farnesene*

Farnesene ($C_{15}H_{24}$), a sesquiterpene, is an unsaturated hydrocarbon, that holds great potential as a future lubricant feedstock for base oils since it can be biotechnologically produced from any kind of fermentable sugar feedstock using adapted microbial cells by metabolic engineering. Co-oligomerization of hydrogenated $\beta$-farnesene with (petroleum derived) linear alpha olefins, LAOs, (>90% saturates, VI > 120, sulfur < 0.03%) leads to a base oil (farnesene-derived base oil, FDBO) with 30 carbon atoms, that is ready to compete with Group III mineral oils and Group IV PAOs as renewable, low toxic and biodegradable alternative. Furthermore, FDBO applies to the criteria of the EU Ecolabel and the US EPA VGP (Vessel General Permit) (*6*).

In recent approaches it is demonstrated that farnesene can be produced from sources not competing with the food industry, for example, as $\alpha$-farnesene from engineered yeast such as *Yarrowia lipolytica* using waste lipid feedstock (*24*) or *Saccharomyces cerevisiae* (*25*) and as $\beta$-farnesene from bacteria (*26*). Farnesene could already be successfully produced on an industrial scale from sugar feedstock using genetically modified *S. cerevisiae* yeast strains (*6*). Moreover, engineered cyanobacteria can be used for $\alpha$-farnesene production utilizing $CO_2$ as feedstock (*27*).

So far, the oligomerization step with the LAOs is the limiting factor for FDBOs biodegradability and environmental friendliness (which is still above those of PAOs), but squalane, a C30-saturated hydrocarbon, might provide the solution. Squalane, a 4 cSt base oil, naturally found in shark livers and olive oil, can be obtained by the dimerization of two farnesene molecules and exhibits superior biodegradability (86% for farnesene+farnesene-derived FDBO, 74% for LAO+farnesene-derived FDBO, 48% for LAO-derived PAO) (*6*). Squalane is often used in studies as model fluid e.g. as lubricant base oil investigating molecular dynamics with certain additives (*28*), in EHL traction prediction for rolling bearing applications (*29*), or for density and viscosity estimation for high-pressure industrial equipment applications (*30*). Furthermore, it is tested as a lubricant base oil e.g. in mixtures of polyisoprene for gear-mixed lubrication (*31*). However, general tribological studies of farnesene-derived lubricant base oils are still rare. Bio-based PAO is discussed in detail in chapter PAO.

### *Carbohydrate polymers*

The trend is leading toward plant-based substitutes for petroleum products, due to the renewability aspect contributing to sustainable industry development in line with SDGs. However, this does not necessarily represent also a low environmental impact pointing out, for example, deforestation for palm oil production. Therefore, these feedstocks are excluded in this review. The discussed substitutes include materials originating from biomass such as (hemi-)cellulose, chitosan, and lignin (see chapter Lignin and lignin-derived lubricant components), and non-polymeric materials such as phospholipids and triglycerides. Biomass means organic matter composed of carbon, hydrogen, oxygen, and nitrogen, often having a similar chemical structure as fossil-derived products (*32, 33*). Carbohydrate-based lubricants are naturally found in the skeletal joints of animals and humans (*34*) but can also be produced by plants (*35*), bacteria (*36*), and fungi (*37*).

### *Polysaccharides and glycans*

The Pacific Northwest National Laboratory (PNNL) and the National Renewable Energy Laboratory (NREL) supply lists for 'Top Value-Added Chemicals from Biomass,' referring to the top feasible biological or chemically converted pathways for chemical building blocks from biomass sugars, synthesis gas (Vol 1, released 2004), and lignin (Vol 2, released 2007). More than 300 potential compounds from sugar pathways were screened and the top 12 candidates are specified (*38,39*).

The amphiphilic nature of cellulose makes it interesting for the use as lubricant or additive, since it is interacting with both polar material surface and a non-polar lubricant. Compared to cellulose, which is a homopolysaccharide only built from glucose monomers, hemicellulose is a heteropolymer of five different saccharides. Cellulose can be a precursor for glucose, hydroxymethyl furfural (HMF), levulinic acid, or formic acid (*32*). Hemicellulose is used for the production of furfural (Top 30 biomass-derived compounds (*38*)), which provides a stock for 2-methyltetrahydrofuran (MTHF), a potential fuel additive. (*40*) Cellulose is often used as bio-based lubricant additive, in castor oil or other vegetable oils e.g. as thickener in the form of epoxidized cellulose pulp (ECP) (*41*), methylcellulose and cellulose pulp, as well as chitin (*42*), cellulose acetate butyrate (CAB) in acetyl tributyl citrate (ATBC) (*43*), or as friction-reducing and anti-wear additive in the form of fibrillated or crystalline nanocellulose (*44*). Also, the potential of dielectric constant variation to control friction behavior with different concentrations of nanocellulose particles is

studied (45). Others discuss the potential biolubricant base oil production from lignocellulose-derived 5-hydroxymethylfurfural (HMF) (46), or 2-alkylfurans and ketones (47). Even superlubricity (COF < 0.004) could be achieved with hydroxyethyl cellulose (HEC) in water for 0.25–2 wt.% and applied loads of 5–9 N on quartz glass in a rotary micro-tribometer (48).

When it comes to lubricating greases, products based on nanocellulose oleogels produced from castor oil are compared to common lithium-based lubricant greases for industrial application. Rheological and linear viscoelastic behavior in a parallel plate-plate setup with a shear rate from $10^{-2}$ to $10^{2}$ $s^{-1}$ and 0.08 to 100 rad/s dynamic shear frequency sweep range show the comparable performance of 1.4 wt.% oleogels and the synthetic lithium soap, even though latter contained 8 wt.% of thickener (49).

The influence on thermal, rheological, and tribological effects of ionic and non-ionic gelating agents (originating from cellulose derivates) in water-polyethylene glycol (PEG) mixtures as base fluids are of interest as the effect of starch polymers on the lubricity, where the ionic gelator showed lower friction and wear than to the non-ionic gelator (50). The impact on friction by the addition of carboxymethylated, hyaluronic acid-based polymers or fatty acids such as stearic acid to methylcellulose compounds result in a decrease of friction-induced wear using a ball-on-disk tribology setup (51,52).

Amongst the polysaccharides fructose and chitosan have to be mentioned as promising lubricants components. Similar to the mentioned tribo-experiments with HEC, superlubricity is also achieved with fructose dissolved in ethylene glycol and 1,3-proanediol in weight ratios from 0.1 to 0.5. At loads between 3 and 6 N in a steel-steel ball-on-disk setup, COF ranging as low as 0.004–0.01 (at 0.5 wt.%) are measured (53).

Chitosan is a polysaccharide consisting of acetylated and deacetylated glucosamine-units, collected by deacetylation of chitin from shells of crustaceans and fungal cell walls, making it the second most abundant natural polysaccharide right after cellulose (33). However, chitosan-derived multifunctional lubricant additives utilized as antioxidant, anti-friction, anti-wear, and anti-corrosion additive, have potential to be an environmentally friendly bio-based alternative to existing non-biodegradable additives such as zinc dialkyldithiophosphate (ZDDP). Chitosan and its derivates are also promising bio-replacement for vegetable oils as thickeners and modifiers in greases and oleogels (54). Addition of 4% sugar-derived N-octadecyl-D-gluconamides (NOG) gelator to polyethylene glycol (PEG) base oil shows an improvement of the thermal stability and reduction of friction and wear (55).

Similarly, saccharides do not only serve as promising green additives but also provide potential as environmentally friendly lubricant base oil, for example, xylose from sugarcane bagasse can be effectively used as feedstock for oleaginous yeast to produce single cell oil (SCO) (56). Comprehensive overviews of carbohydrate-based biolubricants from algae and bacteria focusing on extracellular polysaccharides, such as agar, carrageenan, and alginic acids are available (35).

Glycans are complex carbohydrates, linking monosaccharide units through glycosidic bonds, forming linear or branched polymers. They can be either free oligo- or poly-saccharides or bound to proteins (e.g. glycoproteins) and lipids (e.g. glycolipids) (57), and can be found in animals, plants, and fungi (37). As highly functional glycoproteins, so-called mucins, they play a significant part in the field of implant and cartilage wear reduction or prevention, contact lenses, cosmetics, oral salivary (58), synovial fluid (hyaluronan, a glycosaminoglycan) (59), or reducing friction between cornea and eyelid as tear fluid (60,61). In bio-medical application lubricin, a mucin-like glycoprotein lubricin-like synthetic polymers are important boundary lubricants, and naturally occurring alongside hyaluronic acid in the synovial fluid like mucin, lubricin can bind to surfaces and trap water close to the surface, enhancing gliding and reducing friction at the same time (62). Outside the field of bio-tribology, base oils from glycans are not yet studied for their industrial tribological relevance.

### *Lignin and lignin-derived lubricant components*

Lignin is a complex heterogeneous polymer, naturally found in wood, of cross-linked phenolic moieties, mainly p-coumaryl, coniferyl, and sinapyl alcohols, varying in concentration based on the plant source (63). The structure of lignin is diverse, affected by the source of wood and recovery methods (64). Due to the many functional sites within its structure, lignin has a wide range of applications, for example, its amphiphilic nature makes it a good anti-corrosion agent (33). Based on various pathways, modifications on aliphatic and aromatic hydroxy groups of lignin are possible, and different applications for lignin acquired from different sources are known (65).

Various feedstocks are discussed in the literature, ranging from kraft lignin functionalized with laccase SilA from *Streptomyces ipomoeae* (66), lignin-enriched fractions from sugarcane bagasse waste (67) or NCO-functionalized residual lignin fractions from eucalypt and pine wood in castor oil (68). Recently, a new method for low energy-consuming electrochemical

depolymerization method of lignin by using levulinic acid as a sustainable bio-based component for the solvent system is reported, Figure 1 shows the insoluble fraction of kraft lignin (*69*).

Lignin is mainly studied as additive in lubricants, for example, as a thickener in the form of epoxide-functionalized alkali lignins (*70*), and as friction and wear improver (*71–73*). It has been found that the broader the distribution of lignin's macromolecules and the higher the concentration of lignin's hydroxy groups, the better the lubricant properties when using it as a biodegradable additive with polyethylene glycol (*64*). Organosolv lignin has an outstanding adhesion character on metal surfaces as well as excellent film strength and is a good non-corrosive green lubricant additive alternative (*74*).

Blending with polyethylene glycol (PEG) results in enhanced thermal stability, while wear loss could be reduced up to 93.8% compared to pure PEG when mixed with lignin (*63*), or by 89% when mixed with ethylene glycol (EG) (*72*). Recent research also implies the usage of lignin as a biolubricant base oil by converting lignin-derived monomers and aldehyde into branched benzene and branched cyclic lubricant base oils (*75*). In the last five years, lignin becomes increasingly interesting as a green component in lubricant formulations, but tribological data for lignin-based base oils are still scarce.

## Hydrogels

A hydrogel is a macromolecular polymer, which can absorb large amounts of fluids within its interstitial space while remaining insoluble in water due to present physical or chemical cross-linking. Biomimicry refers to biological methods and systems found in nature, typically environmentally friendly, that is emulated by modern engineering and technology design. Biomimetic lubrication is often used in the sense of water-based lubrication as in bio-tribology (*5*). In general, hydrogels are used as biomimetic lubricating materials in biomedical applications such as drug delivery (*76*) and tissue engineering, for example, for articular cartilage repair, since they show good biocompatibility, viscoelasticity, permeability, and therefore, biomimetic properties, but lack in friction and wear properties (*77, 78*). They can be synthesized from plant-derived materials including cellulose, hemicellulose, lignin, polysaccharides (starch, pectin, gum), and proteins (*76*).

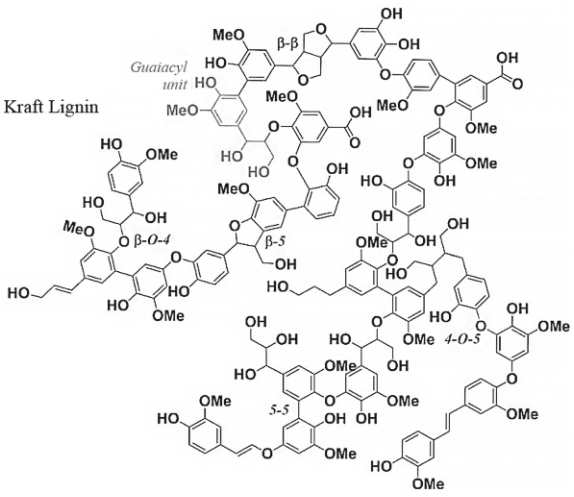


**Figure 1.** Structural characteristic of kraft lignin from industrial spent pulping liquor. With permission from (*69*).

Recent biomedical tribological examinations are conducted with hydrogel in the form of cross-linked alginate-polyacrylamide in invasive joint implants (*79*), being agarose-hyaluronan based (*80*), as anisotropic sugarcane composite replacing biological tissues (*81*), as material for contact lenses (*82–84*), or basil-based lubricant gels with ethanol as an additive in catheters and gastric tubes (*85*).

Besides that, the tribological properties of gel-like, glycol-based lubricants for application in, for example, water-based bearings or high load conditions are of interest. The lubricating gels are functionalized with nitrogen and phosphorus small molecules in mixtures of water-glycol and water-diethylene glycol, forming a 3D network structure with self-assembly functions. These gels show good anti-wear and friction properties with low wear volume losses at 400 N compared to the base fluids without gels, especially for the 4% gels. Also, for the increasing frequency at 400 N, the 4% gels could maintain a lower friction coefficient throughout the experiment time of 30 min. (*86*). Furthermore, sugar-based low-molecular-weight gelator hydrogels are studied as environmentally friendly lubricants (*87*).

## Polyalcohols

About 75% of polyalcohols (polyols) belong to the group of polyether polyols, whereas the remaining 25% belong to the group of polyesters and other polyols (*88*). The representatives of the polyol group range from the simplest ethylene glycol over diethylene glycol, triethylene glycol, and tetraethylene glycol to polyethylene glycol (*89*). Renewable polyols can derive from plants-based components such as carbohydrates (monosaccharides, starch), proteins, and essential oil extracts. In addition, polyols can be recollected from agro-residue or waste from households and the food processing industry, to not compete with possible food sources in the first place (*90*). In the lubricating industry, neopentyl polyol

esters composed of a central quaternary carbon atom with attached primary alcohol methylol groups are usually used as base oils for synthetic lubricant production. This relates especially to neopentyl glycol (NPG), pentaerythritol (PE), and trimethylolpropane (TMP) (*6*).

Research on the usability of polyalcohols as sustainable lubricants mainly focusses on their tribological behavior. PE ester, NPG ester, and a formulated lubricant are compared to a commercially available non-bio-based one. The formulated lubricant is made from PE and palm oil methyl ester with extreme pressure, anti-wear, and corrosion inhibitor additives. The coefficient of friction is determined in a four-ball steel/steel tribometer, in mixed and boundary lubrication regime from 50°C to 100°C. Concerning friction and wear, the formulated lubricant gives the best results compared to PE base oil (*91*). Similarly, the tribological behavior of PE, NPG, and trimethylolpropane (TMP) as vegetable oil-based polyol ester lubricants originating from waste mango seed kernel oil is investigated with a four-ball tribometer according to ASTM D4172. PE ester shows a lower coefficient of friction and a smaller wear scar diameter related to its higher viscosity compared to NPG ester and TMP ester (*92*). In another approach, TMP is used to enzymatically esterify the microbial lipid of the yeast *Rhodotorula gultinis* to produce a biolubricant with excellent low temperature, and good friction (COF < 0.1) and wear properties (*93*). Palm oil-based polyol is investigated as a green lubricant concerning its viscosity, viscosity index, flash point, coefficient of friction, and wear properties. The tribological tests are run on a four-ball tribometer (steel/steel) showing a higher COF for the polyol sample (COF = 0.071), but a decreased wear scar (WSD = 624 µm) compared to palm-oil (COF = 0.064, WSD = 660 µm) (*94*). Tribological investigation on a ball-on-disk tribometer, rolling bearing tests, and wear tests with a combination of glycerol and sorbitan monooleate as base oil with additives such as chitosan, glyceryl monostearate, and calcium phosphate lead to a decrease in the COF. For the combination of high-oleic sunflower oil (HOSO) with glycerol and cellulose ether as additive this effect could not be observed (*95*). Glycerol monooleate can efficiently reduce the COF as a 5 wt.% additive in PAO in boundary lubrication (*96*). Glycerol in mixtures with propanediol shows superlubricity performance with a coefficient of friction below 0.01 and 723–871 MPa Hertzian pressure for steel tribo-pairs in a ball-on-disk setup (*97*). Additionally, polyols such as 1-decanol are studied in the elastohydrodynamic lubrication regime, contact conditions that are found inside bearings and gears. The coefficient of friction is evaluated in a ball-on-disk setup (steel-steel, steel-glass, and glass-glass), a load between 1 and 50 N with Hertzian pressure from 0.1 to 1.1 GPa and macroscale superlubricity is observed for all surfaces (*98*).

### Ionic liquids

Ionic liquids (ILs) are composed of a positively charged bulky organic cation, and an organic or inorganic anion (*99*). The room temperature ionic liquids are liquid at ambient conditions due to poorly coordinated asymmetric moieties and are most suitable for base oil lubricant design. The ILs generally exhibit high thermo-oxidative stability, non-flammability, and strong affinity to metallic surfaces, which predetermines them as promising lubricant candidates especially for highly demanding applications. ILs can be also recovered in high yields (>95%) which fulfills the circular economy demands to limit resource consumption, waste, and pollution (*100*). Their physicochemical properties can be tuned due to immense cation and anion structural variability. These characteristics make ILs a promising class of substances for the development of potentially high-performing and eco-friendly lubricants. As the structural variability of ILs is immense, the determination of structure–activity relationships is crucial to pre-design ILs with low environmental impact.

#### Structural recommendations from toxicity and biodegradability perspective

Since ionic liquids are composed of diverse chemistries and the ions are often of non-biological sources, the toxicity of these mixtures is of special concern. In general, a quick classification is mostly not possible and therefore, this topic is covered with particular care in this chapter. The IL toxicity mainly depends on the nature of cation and its alkyl chain length. The longer the side chain the higher the toxicity, due to increased lipophilicity enabling cell membrane disruption (*101*). The antimicrobial toxicity increases especially for $C_{12}$–$C_{14}$ chain lengths but polar functional groups, for example, ester, can reduce the toxicity of long side chains (*102*). The aromatic imidazolium and pyridinium-containing ILs have tendency to inhibit enzyme activities (*103*). The non-aromatic cations, such as quaternary ammonium exhibit lower toxicity compared to aromatic moieties (*100*). Morpholinium and dicationic IL moieties are also featuring low toxicity effects due to reduced lipophilicity (*104*). Especially polyfluorinated anions $BF_4$, $PF_6$, and favored $[(CF_3SO_2)_2N]$ are more toxic compared to, for example, $Br^-$ and $Cl^-$ halides due to increasing overall IL hydrophobicity leading to cell membrane damage (*105*). In general, the influence of the anion moieties on toxicity is less predictable than that of cations (*106*).

Biodegradability aspect is crucial to avoid issues related to bioaccumulation or high mobility. Unfortunately, the opposing trend to toxicity recommendations exists, with preference for longer alkyl chain lengths. The short-chain imidazolium cations, such as $C_1$–$C_4$ have been reported to exhibit poor biodegradability [*107*). Functionalization of ILs with e.g. ester-, carboxyl- or terminal hydroxyl-group significantly enhances biodegradability due to the possibility of enzymatic attacks (*104*). The cyclic side chains are causing the drop in the enzymatic activity and cause lower biodegradability (*100*). Also, branched side chains are more resistant to biodegradability (*107*). Aromatic functional groups and symmetric side chains of the same length cause bulkier or symmetric moieties and are not biodegradable, while polar functional groups improve the biodegradability of at least short side chains. The imidazolium-based ILs undergo very limited biodegradation as well as dicationic moieties in contrast to ammonium and pyrrolidinium undergoing full mineralization (*104*). The inorganic anions do not contribute directly as a carbon source to biodegradation, as they are already in their mineralized form. Anions with high carbon content, such as octyl sulphate, feature excellent biodegradability due to being modeled on sodium dodecyl sulphate used as a positive control in biodegradation tests (*107*). The fluorinated anions with a large portion of highly stable C–F bonds are not biodegradable while carboxylic acids with linear $C_4$–$C_{10}$ chains are generally biodegradable but shorter chains are toxic (*104*).

Thus, it is difficult to reconcile the opposing structural demands from toxicity and biodegradability perspective. However, some overlap of recommended structural features can be identified to comply with both requirements. The eco-friendly IL design should focus on non-aromatic cations with non-halogenated counter anion and the side chains should be kept below $C_{12}$ length, while functionalization by polar groups (carboxy-, ester-, terminal hydroxyl-group) is preferential, as summarized in Figure 2.

As the cation and anion have distinctive structural features, their toxicity and biodegradation as well as mobility and bioaccumulation in environment can significantly vary. Thus, it is not sufficient to design ILs with only one moiety (cation or anion) derived from, for example, naturally occurring sources to ensure their environmental benignity, while neglecting the impact of the counter ion (*104*). Unfortunately, this trend is seen in the majority of publications from tribological field claiming the green IL formulation, so these will be omitted herein. Apart from deliberate IL structure modeling bound to the need of extensive toxicity and biodegradability studies, is the utilization of naturally occurring bio-derived cation and anion moieties. Hence, tribological performance will be described only for ILs with both bio-based moieties.

### *Tribological performance of ILs with bio-based moieties*

From tested choline-based ILs with amino acid anions, the choline L-phenylalanine [ChPhe] achieve the lowest wear volume and 46% wear reduction compared to 1-hexyl-3-methylimidazolium bis(trifluoromethane sulfonyl)imide $[C_{6mim}][NTf_2]$ reference while leading to a thicker film exhibiting more effective anti-wear properties although displaying the highest COF (*108*,*109*). Excellent anti-wear and friction reduction properties are reported for choline ILs with aspartic [Ch][Asp] and glutamic acid [Ch][Glu] anions (*109*,*110*). Promising anti-corrosion properties and 70% lower friction than for paraffin-based reference oil are shown by choline L-proline [Ch][Pro] under full film elastohydrodynamic lubrication (EHL) regime (*111*).

Additionally, superlubricity (COF < 0.01) can be achieved by [Ch][Pro] in glycerol aqueous solution applied between 1-3 wt.%, while 3 wt.% concentration displayed the lowest COF (*112*). Addition of lignin into [Ch][Pro] results in low friction and good wear protection of both DLC and steel surfaces (*73*). Also, choline monocarboxylate acids exhibit excellent lubrication properties similar to amino acid-based counterparts even for difficult to lubricate copper and aluminum-based surfaces (*113*). Furthermore, choline with ricinoleic fatty acid anion, found in castor seed oil (*44*), can reduce COF in comparison to plain glycerol solution (*114*).

Further, ILs based on naturally occurring quaternary ammonium, being also identified as preferential cation for ILs with low environmental impact (see Structural recommendations from toxicity and biodegradability perspective), are designed with fatty acid counter anions. Fatty acid anions hexanoate ($C_{6:0}$), octadecanoate ($C_{18:0}$), and octadec-9-enoate ($C_{18:1}$) with ammonium-based ($N_{8881}$) cation are investigated for their tribological and corrosion performance on steel-steel, steel-aluminum alloy, steel-bronze, steel-cast iron, and steel-tungsten carbide surfaces. After 21 days of corrosion testing, only steel-bronze shows corrosion activity for $[N_{8881}][C_{18:0}]$ and $[N_{8881}][C_{18:1}]$ ILs. The three ILs show comparable friction behavior on the same counter-pair materials, the COF of 0.06 and lowest wear is measured on tungsten carbide (*115*). When ammonium ($N_{1444}$) octanoate ($C_{8:0}$) is compared to fluorinated L-F104 imide it exhibited lower friction and much less wear at loads of 200 N for steel/steel and 100 N for steel/copper and steel/aluminum contacts (*116*). In another study, oleate ($C_{18:1}$)

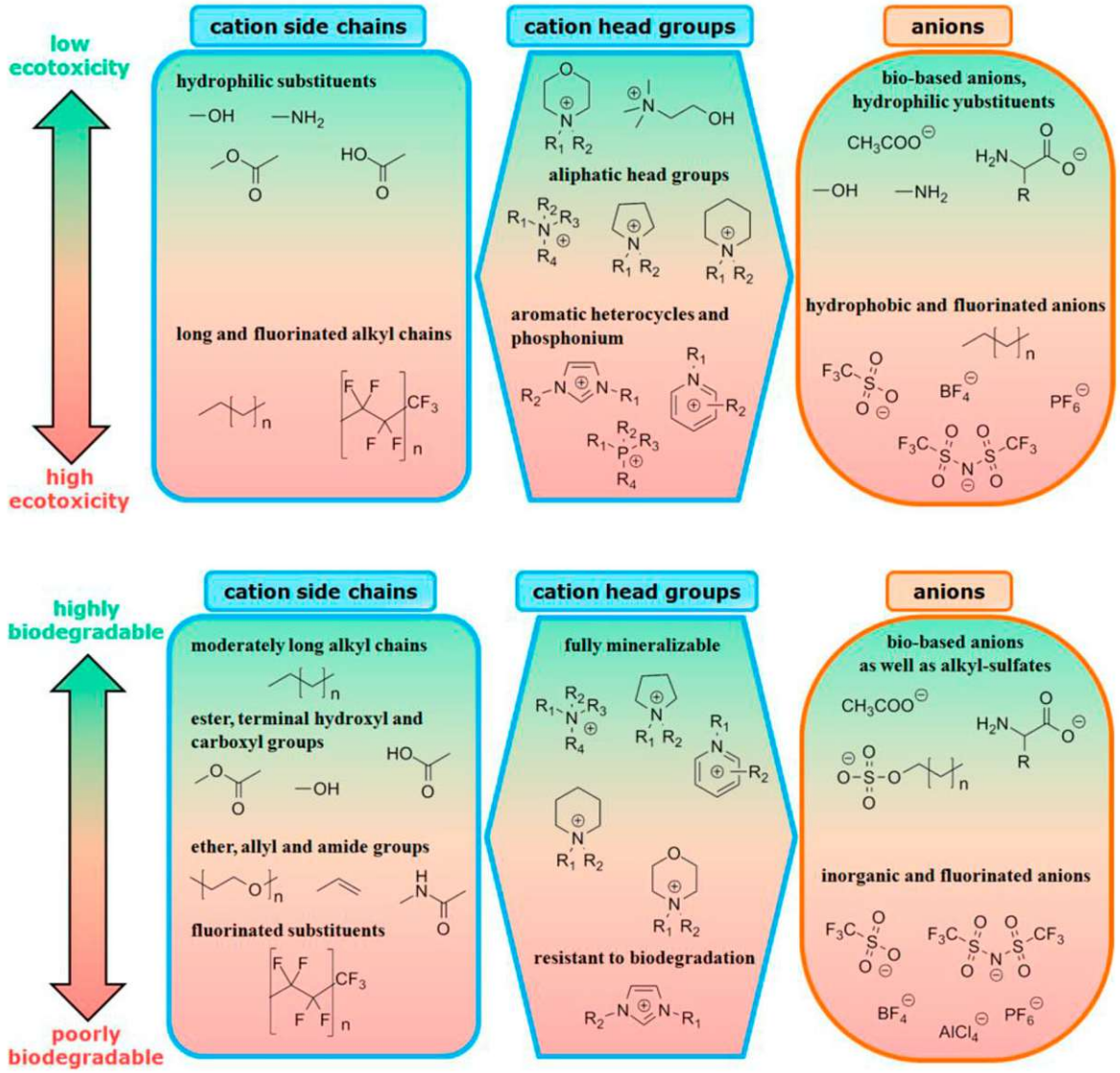


**Figure 2.** Structural recommendations for IL's design with the lowest environmental impact. With permission from (*104*).

tetrabutylammonium ($N_{4444}$) performs as the best anti-wear and friction-reducing anion under boundary lubrication when compared to other tested $C_6$, $C_8$, and $C_{18:2}$ anions (*117*). When studying ILs based on ($N_{4444}$) cation and $C_{10}$, $C_{12}$, $C_{14}$, $C_{16}$, and $C_{18:1}$ fatty acid anions as 1% additives in mineral oil, it is observed that COF slightly increases with alkyl chain length increase but decreases with unsaturation as a result of changes in viscosity and in van der Waals interaction triggered by these structural differences (*118*). Preliminary studies propose that longer alkyl chains of cations lead to higher viscosity accompanied by an increase in van der Waals interactions but this effect is also influenced by interactions between cation and anion and the anion moieties (*119*). Thus, when comparing $[N_{6666}][C_{8:0}]$ and $[N_{6666}][C_{16:0}]$, the latter has a lower viscosity, a higher viscosity index, and a lower COF. The $[N_{6666}][C_{8:0}]$ is shifting from EHL to mixed lubrication regime at higher speeds and temperatures leading to an increase in COF, whereas $[N_{6666}][C_{16:0}]$ remains in EHL regime most of the time. Ball-on-disk tribo-tests show slightly better friction performance of $[N_{6666}][C_{8:0}]$ over $[N_{6666}][C_{16:0}]$ (*120*). Adding protic long-chain palmitate-based ($C_{16:0}$) IL in 1 wt.% to protic short-chain citrate IL, both with ammonium-based cation, increases the viscosity and improves the tribological performance (*121*). Furthermore, excellent anti-wear and good friction reduction properties (COF ~ 0.1) are accomplished with 2% palmitate ammonium IL in water, without any signs of tribo-corrosion (*122*).

Further potential bio-moieties for IL design, such as glycine betaine present in plants or sweeteners, for example, saccharinate, acesulfamate, or medically proven docusate might be explored. When both cation and anion are naturally based, the ILs have the highest chance to comply with rigorous toxicology and biodegradability criteria. However, as for all bio-derived lubricants, the IL design must ensure not only the non-toxic and biodegradable features but must prove to deliver desired performance under particular application conditions (*101*,*104*).

### Other natural compounds with tribological potential

The following structures were chosen due to being benign and contributory to the field of sustainable lubrication, most of them are researched as lubricant additives in the field of bio-tribology. Furthermore, they are industrially synthesized in commercial-scale productions with long-standing expertise. While they are not yet investigated as industrial lubricant components, they might be considered as environmentally friendly lubricant additives, for example, in micro-tribology applications (for low load contacts like in micro electromechanical systems, MEMS).

#### Proteins

Often proteins such as albumin, globulin, mucin, and lectin are studied in the context of human bio-tribology for prosthetics and implants (*123*,*124*), joints and cartilages (*125*,*126*), oral tribology (dryness, response to food, …) (*127–131*), contact lenses (*132*,*133*), etc. Within a biomimetic approach, bovine serum albumin (BSA) is investigated as a potential additive in concentrations from 0.1 to 0.6 mg/ml in rice bran oil (RBO) for bio-cutting fluid formulations. Tribo-tests are carried out on a four-ball tester (steel-steel), where the coefficient of friction and wear scar diameter values are the lowest for 0.4 mg/ml BSA in RBO. The green cutting fluid could further outperform a commercial cutting fluid based on the coefficient of friction values at 400–1000 rpm disk speeds as well as in weight loss of pin using a pin-on-disk tribometer (iron-steel) with 100 N constant load in a rotating motion (*134*).

#### Vitamins

Vitamins are a natural component in various plant-based oils, but their influence on tribological performance especially outside of bio-tribology is hardly investigated. A fully formulated biolubricant from esterified rubber seed oil (E-RSO) is tested with 1.5% .-tocopherol (vitamin D) and 1% L-ascorbic acid (vitamin C) as antioxidant additives and compared to the plain rubber seed oil and commercial mineral oil (SAE20W40). The values for (bio-)chemical oxygen demand of E-RSO are within the accepted ranges of biodegradability. A combination of the named vitamin-based antioxidants along with butylated hydroxylanisole (BHA) shows better oxidative stability of the fully formulated E-RSO than plain E-RSO and RSO and is comparable to the commercial SAE. Furthermore, the friction and wear properties of fully formulated E-RSO are superior to SAE (*135*).

#### Lecithin

Lecithins are glycerophospholipids. Phosphatidyl choline, phosphatidyl inositol, phosphatidyl ethanolamine, and phosphatidic acid form the main phospholipids in lecithin from soya and sunflower. The soybean lecithin is obtained by degumming the extracted oil of the used soybean seeds. Lecithin is non-toxic, well tolerated, and can be entirely metabolized by humans (*136*). Soy-derived lecithin is used as gel-forming thickener, due to its ability to self-assemble into vesicles in polar solvents like glycerol, formamide, and ethylene glycol, which might be of interest in biolubricant applications (*137*). Moreover, lecithin is used as an anti-wear additive in hydrotreated mineral oil (10 cSt) and diester, where 0.5 wt.% of lecithin reduces the wear scar diameter by 21 times and the 1.5 wt.% solution by 45%, it has better friction and anti-wear properties than ZDDP (*136*,*138*).

#### α-lipoic acid esters

The α-lipoic acid (5-[1,2]-dithiolan-3-yl-pentanoic acid) occurs naturally in plants and animals. It is a cofactor of several enzymes and possesses antioxidative properties. Derivatives of lipoic acids are potential natural and environmentally friendly alternatives to toxic additives due to their cyclic disulfide moiety. First tribological tests of selected lipoyl esters in synthetic base fluid indicate good anti-wear properties (*139*).

#### Benzoic acid

Benzoic acid occurs naturally in many plants. It is reported that the addition of benzoic acid to titanium greases improves anti-wear properties (*140*). Low friction coefficient and high anti-wear properties are observed for the new category of titanium complex grease using titanium tetraisopropanolate, 12-hydroxystearic acid, and benzoic acid as additives in naphthenic mineral oil (KN 4010)/polydimethylsiloxane as base oil. (*141*). Good anti-wear properties and low coefficient of friction are observed for 2 wt.% benzoic acid tested in Jatropha

vegetable oil when compared to mineral oils SAE 5W-30 and SAE 10W-30 (*142*).

### Common synthetics

Unlike mineral oils, which are mainly classified by their performance, synthetic (bio)lubricants can be categorized according to several approaches, for example, according to the feedstock or the synthesis. The most widely used classification is according to their chemical composition (*143*,*144*). Due to the wide range of various chemistries, several groups can be defined. However, in the following, only some of the most common synthetic lubes shall be discussed. This includes (a) synthetic esters, (b) synthetic hydrocarbons, particularly polyalphaolefins, and (c) (poly)ethers.

#### Synthetic esters

In the first decades after the invention of synthetic ester lubricants the focus was primarily on their ability to provide equipment protection advantages under extreme operating conditions, including very low or very high temperatures, and their ability to resist oxidation. In the past decades, the interest shifted more and more toward their ability to minimize the impact on the environment and use them as so-called 'biolubricants' (*143*). Hereby, the term biolubricant is assigned to lubricants either made from bio-based raw materials or other environmentally benign hydrocarbons (*145*,*146*).

These fully synthetic esters may be differentiated into two groups, both of them showing high biodegradability and low toxicity: (1) diacid esters and (2) polyol ester (*144*,*147*). While this does not mean ester oils automatically show environmentally benign characteristics when fully formulated, there are certain classifications for additivated synthetic esters for this purpose, for example, the HEES type classification for hydraulic applications (*148*).

One major aspect when it comes to stability is the crucial knowledge of structure-stability relationships (*149*). With this knowledge, nearly tailor-made lubricant components for each application can be synthesized. Based on targeted synthesis via long-chain alcohols and acids, the resulting completely saturated synthetic esters show high thermo-oxidative and hydrolytic stability as well as more stable ageing characteristics (*145*). For example, feedstocks include C6–C13 alcohols (i.e. n-hexanol, n-heptanol, isonal, and decanol), C5–C18 mono acids (i.e. valeric, heptanoic, pergalonic, and oleic acid) with neopentyl polyols, such as pentaerythritol (PE), polyol esters, diacids (i.e. adipic acid, azelaic, sebacic, and dodecanedioic), and various dimer acids (*145*).

In the production of esters from non-edible animal fats those having less saturated acids improve oxidation stability as well as better lubricity properties. However, the lower amount of unsaturated acids increases the pour-point. When it comes to applications, where a low ash-content of the base-oil is beneficial, synthetic esters with shorter-chain alcohols are better performing (*150*).

Besides chemistry concerns, the tribological performance of synthetic esters is a main area of research. Different isomers of isooctyl naphthatate-based oils show, compared to isooctyl sebacate as a reference, higher oxidation stability as well as lubricity. It is found that the introduction of a naphthalene ring improves the flash points, stability, and lubrication properties due to the large $\pi$-electron conjugate system. Tribotests with an SRV ball-on-disk tribometer show a positive effect in terms of lubrication of the naphthalene ring system, additionally (*151*).

When the friction performance of synthetic esters is measured with a pin-on-disk tribometer a correlation with the molecular structure of the lubricant is revealed. Esters with branched-chain structures show an improvement in low-friction performance with an increasing number of branches or carbon atoms. For esters with phenyl-groups, 1,3-benzene esters seem to be better performing than orthophthalic esters. Tribological performance of the esters with the chain structures seems to be better than those with the phenyl group when the difference in their viscosities is small (*152*).

Based on one of the 12 priority chemicals identified by the US Department of Energy for the establishment of a 'green' chemical industry (*38*), 5-furandicarboxylic acid, an isooctyl furan dicarboxylate (FD) as lubricating oil is synthesized. Tribo-experiments with a 4-ball tribometer (steel ball) and SRV tribometer (steel/steel, steel/copper, steel/aluminum) show the superior performance of Isooctyl-FD to the references isooctyl sebacate and isooctyl adipate in terms of anti-wear and friction behavior. However, viscosity–temperature and low-temperature properties are inferior. These properties should be improved by additives (*153*).

Synthetic esters do not only act as a base oil but can also be applied as additives. A pentaerythritol rosin ester (PRE) is synthesized from abietic acid, an abundant renewable natural resource, to act as an environmentally friendly multifunctional additive in rapeseed and soybean oil. In blends with 20 wt.% PRE, the onset temperature of oxidation as well as the oxidation induction time are increased significantly, which proves the potential of PRE as a substitute to common additives in eco-friendly bio-based lubricants (*154*).

In addition to conventional and commonly used surfaces, the performance of biodegradable oils on special

coatings is a topic of high interest, as so far, the tribological behavior is not fully investigated (*155*).

### PAO

Polyalphaolefines (PAO) can be designed with higher biodegradability but since their industrial-scale production is not necessarily based on renewable materials they are not considered as bio-based in general. However, if they fulfill this criterion, they can be counted as an important class of high-performing synthetic environmentally friendly lubricants base oils, in particular in Europe (*147*).

There are numerous studies comparing the performance characteristics of different synthetic biodegradable lubricants such as esters or PAOs with mineral oils in order to increase the knowledge on similarities and differences in tribological performance. The friction behavior and wear protection ability of these selected base lubricants are compared using a pin-on-disk tribometer. Based on the results it can be concluded that the viscosity has the predominant influence on the friction and wear-protection properties of PAO and mineral oils, contrary to ester oils where these properties are influenced by their polar functional groups. All tested lubricants generally obey the trend of a typical Stribeck curve, and the increase in viscosity decreases the minimum friction coefficient at the valley (between mixed and fill-film lubrication regime) of each Stribeck curve (*152*).

To investigate the effect of the structure on the performance, a bio-based PAO-40 synthesized from complex vegetable oils is compared to a non-functionalized mineral-based commercial PAO-40 synthesized only from alpha olefins. The effect of methyl ester functionalization on physicochemical properties and tribological performance is investigated. A beneficial influence of the methyl ester groups on several parameters is revealed, amongst them a higher density between 40° C and 100°C, higher viscosity index, lower COF, and lower wear scar diameter when using 4-ball tribometer, and a higher elastohydrodynamic (EHD) lubricant film thickness under boundary conditions. However, in terms of oxidation stability evaluated by pressurized DSC and total acid number, the performance of the conventional mineral-based PAO without methyl ester groups is better (*156*).

In applications with nano-grained stainless steel, which shows a higher susceptibility for oxidative wear due to the increase of grain boundaries, PAO 4 shows an effective improvement of the wear-resistance and friction-reduction compared to dry conditions. Under lubricated conditions, the tribological performance ranges from severe oxidative to mild adhesive wear (*157*).

One issue related to synthetic lubricants is the compatibility with elastomers. PAO-based synthetic oils with different additives are investigated based on a new method for lubricant-elastomer compatibility. It is revealed that static tests give an indication of possible chemically active additives, but the dynamic test is necessary for the simulation of real application conditions. Test results are dependent not only on the oil but as well as on the additive combination (*158*).

### Ethers

Ether-type synthetic oils show outstanding characteristics, especially for certain special applications where their excellent heat resistance, oxidation, and radiation resistance and low vapor pressures are of importance. This makes them suitable for high-temperature and high-vacuum applications, and for locations subjected to radiation (*144*,*159*). This particularly concerns polyphenyl ethers, which are used as lubricants in extreme environments such as nuclear power plants, space satellites, nuclear submarines, food sterilization equipment, radiation chemistry laboratories, and medical imaging systems. Besides liquid lubricants, they are commercially available as greases (*160*). Ether-based lubricants may be produced from renewable biomass-derived feedstocks, for example, through direct or reductive etherification of pyrolysis oils, plant, and algal oils, or C5–C6 sugars (*161*).

The lubrication properties and mechanisms of ethers, compared to various other oxygenated compounds, for example, ketone, alcohols, and esters, are investigated in detail to study the effects of the functional group, carbon-chain length, and ambient humidity on the lubricity of the oxygenated compounds. For this purpose, the high-frequency reciprocating rig is used to measure the lubricity, and microscopic observation of disk specimens with a scanning electron microscope is done. The significant effect of the functional group on the enhancement of lubricity is shown. However, the increase in ambient humidity worsens the lubricity of the oxygenated compounds since the water absorbed by the oxygenated compounds tends to compete with the lubricating compounds in the adsorption process and prevents the formation of the lubricating film. This leads in the case of oxygenated compounds with hydroxyl, ester, and ether groups to abrasive wear with corrosion (*162*).

### Waste

There are different types of waste which can be used as feedstock for sustainable lubricant production from the viewpoint of circular economy even though they might not be from a bio-derived source. The following

section gives an overview over the main approaches for the reuse of products that are normally being discarded.

### *Waste cooking oil (WCO)*

Due to the growing world population, the increasing demand for food led to a higher production of kitchen waste. Among other things, WCO and grease pose a problem, as these wastes have a low degradability, commonly enter the environment due to improper disposal and, hence, result in water pollution and sewer clogging. However, they are produced in large quantities in households, restaurants or in the industry. To overcome their disposal problems, scientists work on its conversion into cheap, easily available, and eco-friendly biolubricants. Besides the growing interest in new applications such as value-added product development leading to financial benefits, actions are taken to overcome the mismanagement of WCOs and to meet public policies (*163–165*). In Europe (EU + UK), almost all the collected WCOs (0.7–1.2 million tons/year) and additionally a high amount of imported ones are used for biodiesel production, being the third most used feedstock with a share of approx. 19% (2.8 million tons), after rapeseed oil (37%) and palm oil (30%) (*166*).

WCOs consist of triglycerides, which can be chemically modified to enhance their lubrication performance, for example, make them more stable against oxidation. Figure 3 shows possible chemical modification pathways for the triglycerides such as (trans)esterification, estolide formation, epoxidation, and further ring-opening and acetylation reactions to improve the physicochemical properties (*163*).

Water extraction of contamination of the crude WCO is a common pre-treatment step within WCO recycling methodologies. The condition of this procedure is crucial as it has a great influence on the quality of the resulting oil. Thus, the analytical determination of optimum conditions is of great interest (*167*). Edible sunflower oils in fresh and used condition as well as after four different recycling treatments with different pH and temperature are compared to find the best procedure for natural regenerated oleic acid bases. Based on their data and available data from literature, they design a prototype recycling machine for WCO with the possibility to tune the resulting oil depending on pH and temperature (*168*). Moreover, they successfully use multivariate surface responding analysis (SRA) to find optimum conditions for the water treatment with special regard to density and flash point temperature (*167*).

A promising application of WCO is the production of environmentally friendly greases. It is possible to produce biodegradable greases from used frying oils in optimal concentrations of 10–15 wt.% in the base oil exhibiting the same quality level as greases from fresh rapeseed oil. However, upscaling or commercializing is difficult as the composition and condition of the used oils highly depend on its source and usage (*169*). Greases formulated with WCO and spent bleaching earth (solid waste generated from the bleaching process in the palm oil industry) possess promising performance characteristics for future utilization (*170*).

Additional research is done on the development of new processes for the transformation of waste into value-added products. A new green and efficient method for preparing octylated branched biolubricants from WCO is presented by hydrolyzation to unsaturated fatty acids with subsequent esterification, epoxidation, and nucleophilic reaction. They obtained a product with excellent lubricant properties in terms of a low pour point, high viscosity index, high thermo-oxidative stability, and enhanced lubricity in a high-frequency reciprocating rig (HFRR) (*171*).

As mentioned, besides chemical and process considerations, the tribological performance of resulting compounds has to be sufficient. Investigating the tribological performance of mixtures of soybean oil and used frying oil proves that these mixtures are promising candidates for eco-friendly lubricants accompanied by low friction coefficients in boundary and/or mixed lubrication regimes. Especially with the addition of additives, their lubrication performance can be further enhanced (*164*). Introducing the green synthesis of pentanal-derived alkyl ester dioxolanes with used frying oil as feedstock and determination of density, viscosity, TAN, TBN, and IV (iodine value) prove methyl 8-(2-butyl-5-octyl-1,3-dioxolan-4-yl)octanoate as promising biolubricant candidate (*172*).

However, there are some issues that need to be overcome for enabling industrial implementation. For example, the supply chain plays a significant role and requires the deployment of effective policies and regulated practices for WCOs recycling and collecting. It has to be ensured that the consumed resources for recycling do not surpass those from the obtained WCOs (e.g. transportation routes). A second challenge of WCOs reuse is their highly heterogeneous nature exhibiting a large variability in physicochemical and sensory properties and significant amounts of various impurities (*165*).

### *Waste lubricant oil (WLO)*

Lubricants are either consumed during mechanical processing or partly lost due to, for example, evaporation, combustion, but about 50% of the lubricant remains as waste oil (*173*). About 97% of all lubricants are

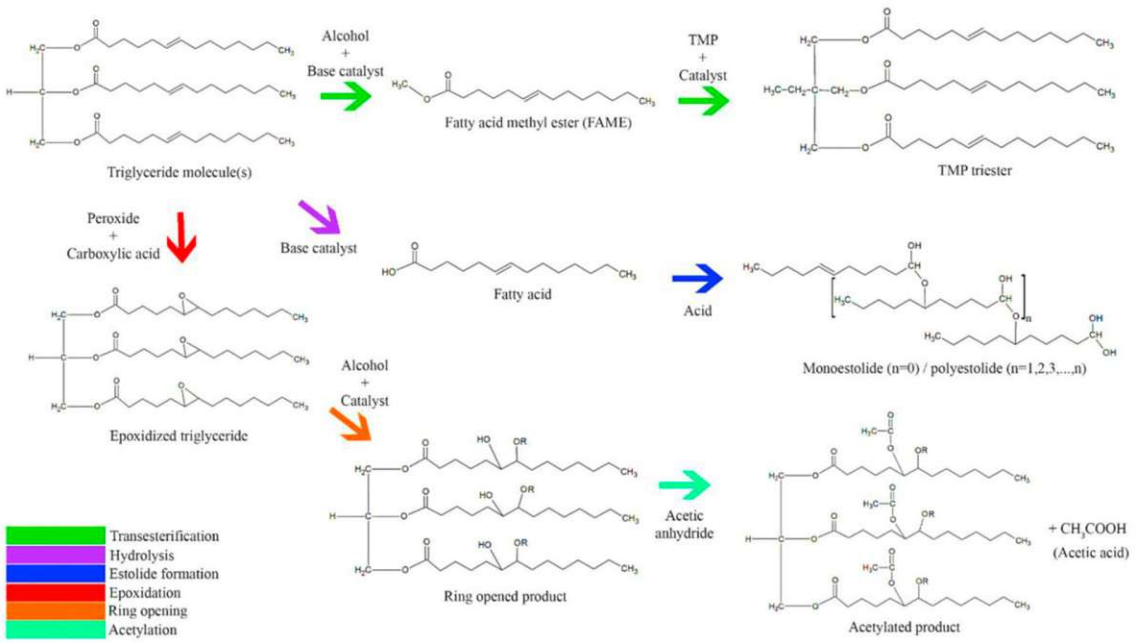


**Figure 3.** Different chemical reaction pathways for the modification of triglycerides. With permission from (*163*).

originating from mineral-based oils, being considered as hazardous waste after use (*174*). WLOs are usually toxic and non-biodegradable, contaminating soil, water, and air, and therefore, causing serious problems for the ecosystem, when not properly disposed (*173*). Though WLOs are not considered as biofriendly lubricants, they can be recycled instead of just disposing them, which increases their sustainability. This cannot only be seen as a more environmentally friendly approach but can also be applied to WLOs from bio-derived sources in the future.

Depending on their field of application, in Europe, WLOs are laundered, reclaimed, regenerated, burned, mildly or severely reprocessed, and thermally cracked, for energy recovery or re-oil processing purposes. Regeneration of WLOs can lead to lubricating oils with similar properties as the virgin lube base oils when cleaned from contaminants, oxidation products, and additives (*173*).

Diverse methods are proposed to produce recycled lubricants in the required quality, for example, when discussing the removal of organic compounds, including alkanes, aliphatic amines, alcohols, and aromatics, from waste lubricant oil distillate with microbubble-ozonation with elevated temperature and stable pH (*175*). A green way to recover base oil from truck engines by applying mechanical stirring and ultrasound is presented as promising recovery yields could be proven, showing an effective removal of Ca, Mg, Na, and Zn and almost 100% elimination of Al, Cr, Fe, and Mo (*176*).

There are various possibilities in the reuse of WLOs, for example:

- Production of lubricating greases: Rheological and physicochemical properties of greases based on used motor oils are studied while substances interfering with the grease structure are successfully removed resulting in a quality base stock comparable with commercial base oils (*177*).
- Production of base oils: used mineral-based lubricating oils are recovered by extraction with polar organic solvents. The physicochemical and thermal properties of the obtained oils are further investigated, such as density, viscosity, ash content, acid number, and thermal and oxidative decomposition profiles (*178*).

However, also life cycle assessments have to be taken into account. Various WLO management scenarios are evaluated for future implementation in Serbia. They investigate the re-refining of used oil for the recovery of base oils, WLO as a substitute for fossil fuels in cement kilns, and combusting WLOs in waste incinerators with energy recovery. It is found that no single WLO application meets all desired requirements. Moreover, they propose four possible WLO management scenarios with an anticipated annual saving of up to 22,100 t $CO_2$ equivalent and 34,300 t oils equivalent which would contribute to the sustainable industry development (*179*).

### Industrial waste

The demand for recycling of industrial wastes, for example, in terms of recovery of valuable materials like hydrocarbons, that can be upgraded into fuels, base oil, and greases, is not only rising on the governmental side, but also from society (*180*). In general, waste minimization, disposal, and environmental impact are the most important new factors, which are shaping the market (*144*).

Research is done on various types of waste processing. For example, food processing side streams from confectioneries and wheat mills are used for their further fermentation with yeast and fungi to produce microbial oil. The various physicochemical properties of these microbial oils are measured, such as pour point, cloud point, acid value, viscosity, and oxidative stability, illustrating their suitability as a sustainable feedstock for biolubricant production (*181*). The production of lubricants from industrial waste contains high amounts of sulfur when using polyaddition and polycondensation methods (*182*).

### Agro-industrial waste

One drawback of biolubricants from plant-based feedstock is the fact that they might directly compete with agricultural and food production, but the use of agro-industrial waste could solve this problem (*183*). The following section presents examples of agro-industrial wastes which can be converted into value-added products.

For example, Cardanol, the main component of cashew nutshell liquid (CNSL), consists of phenolic lipids containing mostly unsaturated aliphatic sidechain. Its amphiphilic structure makes it an alternative lubricant, as the polar group adheres to metallic surfaces leading to a monolayer formation effectively reducing friction and wear by reducing the metallic surface contact. The production of CNSL is estimated to be approximately $1 \times 10^6$ tons. This makes CNSL when using a green and efficient synthesis, a biodegradable and low-cost lubricant alternative. Tribological tests of Cardanol indicate good performance in the boundary lubrication regime showing COF values below 0.2 (*183*).

Extracted coffee waste oils are proposed as alternative raw material for biolubricant production as with 8.9 billion kg of coffee produced in 2016 it is worldwide the most popular beverage. To efficiently use the coffee waste, oil is removed and converted to biofuel products (biomass, biogas, etc.). Furthermore, hydrolysis can be used to convert waste coffee oils to fatty acids (*184*). Oil extracted from waste coffee grounds is tested as lubricant base oil and as a 5% additive in PAO, leading to significantly reduced COF values compared to pure PAO and showing very promising results as a possible friction modifier additive (*185*).

Natural wax from one of the most widely cultivated medicinal plants in Gansu Province *Codonopsis pilosula* is investigated. Tribological tests indicate that the natural wax shows excellent lubricity in a load range from 100 to 250 N and a temperature range of 25–150° C, which is comparable to synthetic PAO 8 oil and plant oils, like hydrotreated rapeseed oil (*186*).

Litesea Cubeba kernels are waste products of essential oil production from litsea cubeba. By applying litsea cubeba kernel oil as feedstock trimethylolpropane fatty acid triester (TFATE) could be synthesized as biolubricant base oil. They found that the obtained TFATE possesses promising properties as an alternative biolubricant feedstock due to its good oxidative stability and low-temperature performance (*187*).

Lastly, supercritical extraction of waxes from sugarcane waste (leaves, rind, and bagasse) is proposed as an alternative biolubricant but tribological tests are not performed (*188*).

### Waste of animal origin

The lubricity of conventional synthetic lubricants is not only compared to these from agro-industrial waste, mainly of plant-based origin but also to lubes from the waste of animal origin (*189*). In contrast to plant-based lubricants, lubricants of animal origin are completely water insoluble as they are derived from animal fats and therefore hydrophobic. These animal fats include hard fats (i.e. stearin) and soft fats (i.e. lard) and are structurally composed of triglycerides (glyceryl esters of fatty acids) (*189*). Possible sources of animal waste are wide-ranging.

Two fresh commercial synthetic cutting oil emulsions against a new metalworking bio-based oil derived from slaughtering waste are assessed. Focus is laid on the impact of the lubricants on the emulsion treatment of metal working wastewater. In these terms, best results are obtained with the emulsion produced with the bio-based lubricant, however, tribological tests are not performed (*189*).

Bio-paraffin production by special hydrocracking of pre-treated waste lard from processing plant represents an alternative to synthetic lubricants and can be further used in versatile ways. During the treatment of waste lard, only 2–4% of secondary waste is formed and even this waste can be used as feedstock for biogas production (*190*).

Furthermore, fish oil residue is considered as non-edible waste and a possible source of biolubricant production. The non-edible waste caused by the fish

industry is estimated to 5.2 million tons per year. Lipids extracted from these fish oil wastes, with good acid values and oxidation parameters, are successfully converted into trimethylpropane fatty esters with kinematic viscosities in the ISO VG 22 range (*191*).

The tribological properties of unmodified and modified synthesized beef tallow grease are studied. The effects of modifications, such as antioxidant additives, anti-wear additives, waste PET polymer compound, and thermally processed graphite additive, are studied on the synthesized beef tallow. Tribological tests are carried out using a four-ball geometry proving that synthesized beef tallow modified with 20% of PET waste and anti-wear additives shows enhanced friction and wear properties. Additionally, adding thermally processed graphite to the grease compound shows improved tribological performance (*192*).

The physical and chemical properties of esterified housefly larva lipids are studied for the application as biolubricants. Tribological tests are carried out according to ASTM D4172-94(2010) for measuring the wear scar diameter (WSD) of the gained 2-ethylhexyl fatty acid esters indicating good anti-wear properties of the ester. Assessment of typical oil parameters proves promising chemical properties of the esters for biolubricant base oil utilization (*193*).

Lubricant additives derived from poultry chicken feathers are showing good antioxidant characteristics and anti-corrosion performance in polyol as the base oil, but only moderate anti-wear potential which using a four-ball tester (*194*).

### *Plastic waste*

More than 75% of annually produced plastic materials are discarded as single-use plastics, ending up in landfills, polluting the environment through uncontrolled discharge, or incinerated for electricity production (*195*). Conventional plastics are non-biodegradable and accumulative in the environment, posing a serious threat to any species at a global scale. Thus, the conversion of plastic waste into value-added products, such as lubricants, is of high interest in order to enforce circular economy principles and to support sustainable industry developments. Some process conversion strategies and the resulting products are discussed in the following section.

Focusing on the chemical upcycling of polyethylene by hydrogenolysis via Pt/$SrTiO_3$-catalyst conversion leads to a break-up of long hydrocarbon chains into narrowly distributed oligomeric chains, and therefore, to high-quality liquid products, such as lubricants and waxes (*195*).

Plastic waste is treated and converted into lubricant additives via copolymerization for engine oil enhancement. More specific, the change in physicochemical properties of three synthetic esters created from poly propylene, high-density polyethylene (HDPE), and low-density polyethylene (LDPE) is studied, when added to different mineral base oils. Polypropylene ester as a lubricant additive shows the best impact on viscosity index and pour point (*196*).

Recycled polypropylene and lubricant oil are used for synthetic bitumen formulation, as an alternative to the common disposal of these materials. Rheological tests, such as dynamic oscillatory, creep-recovery, and shear steady tests, are carried out in parallel-plate geometry with a frequency range of 0.01–100 rad/s, 1 Pa constant stress (linear viscoelastic region), and temperatures between 25°C and 150°C (*197*).

Alternative high-quality liquid lubricants (HQL) originating from pre- and post-consumer polyolefin waste are investigated regarding their tribological behavior. They found that HQLs exhibited similar performance to synthetic base oils (e.g. PAOs) in terms of wear scar volume and even a superior performance compared to Group III mineral oils. Moreover, they discovered synergistic effects on friction and wear by blending the upcycled plastic lubricant with synthetic mineral oils. Life cycle assessments and techno-economic analyses prove that this novel technology represents a cost-saving method to reduce the detrimental environmental impact of plastic waste (*198*).

A comparative study on the hydroconversion of polyolefin plastic waste to fuels, lubricants, and waxes by hydrogenolysis and hydrocracking of model alkanes to obtain basic knowledge for engineering better catalysts and processes is carried out. A direct comparison of results from different laboratories is highly challenging due to aspects like complex and varying feedstock, impurities, additives, and various processing issues (*199*).

A method for the selective conversion of polyolefins originating from single-use plastics to fuels is presented, with a process that could be adapted for the conversion of different common plastic wastes as well as composite plastics to fuels and light lubricants (*200*).

A new route for the chemical recycling of polyethylene from plastic waste to α,ω-divinyl-functionalized oligomers (Figure 4) via a sequence of bromination, dehydrobromination, and olefin metathesis reactions is proposed. By techno-economic assessments, it could be proven that this process could be applied on an industrial scale for upcycling plastic waste into value-added chemicals which can be utilized as feedstock for lubricant synthesis (*201*).

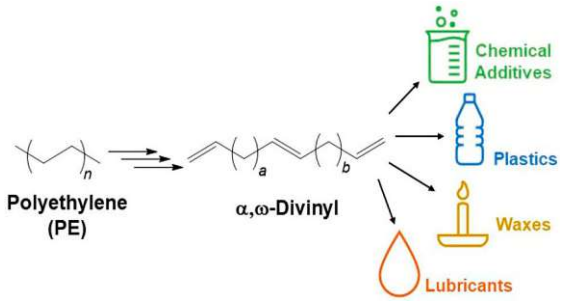


**Figure 4.** Conversion scheme of polyethylene to $\alpha,\omega$-divinyl-oligomers and possible applications. With permission from (*201*).

### *Miscellaneous*

Besides the above-mentioned sources to produce sustainable lubricants, there are some special niche feedstocks which can successfully be converted into value-added products.

Kitchen chimney dump lard recycling into biolubricant is investigated along with its rheological and tribological properties. These measurements are focusing on viscosity, wear, and friction behavior, showing no change in specific wear rate (*202*).

The production of long-chain fatty acids like erucic acid (C22:1) from crude glycerol and waste cooking oil by a recombinant yeast strain is researched. Erucic acid can be further used for lubricant, surfactant, or biodiesel production (*203*).

In another approach, the synthesis of graphite oxide from waste carbon source (e.g. paper waste) is demonstrated. Using graphite oxide as nano-additive in synthetic engine oil has a beneficial effect on the coefficient of friction and wear properties. Tribological characterization is carried out with synthetic base oil with and without the addition of graphite oxide on a four-ball tester (steel, high carbon, and high chromium alloy) (*204*).

Converting waste tires into pyrolytic oil is not only providing a possibility for waste tire recycling but also results in an improved oil suitable as base oil for lubricant applications, meeting the standard requirements for commercial lubricant oils (*205*).

## Characterization and condition monitoring

One of the most important characteristics of a lubricant, no matter if manufactured from renewable/natural or of fossil origin, is the maintenance of the desired performance properties (*206*). Exposure to elevated temperatures, leading to oxidation reactions, and contaminations from environment or machine parts are only some of the stress factors causing degradation (*207*). Based on the intrinsic properties and the structure synthetic lubes, for example, esters, can show advantages over mineral-based ones, in particular regarding high-temperature and oxidation stability (*143*). When it comes to bio-based synthetic lubes, this property may be affected by the presence of a higher degree of double bonds or free fatty acids. Thus, the stability of these products is of high concern and continuous condition monitoring to maintain and prolong the performance is key, which also facilitates proactive measures (additive addition) (*145*). For this reason, appropriate techniques have to be used to determine the impact of these structural variations on the thermo-oxidative stability and performance of the lubricants.

While routine analytics such as determination of viscosity, determination of water content, or determination of neutralization number can be done accordingly to the standards for mineral oils (*206*), the oxidation stability methods are often not fully suitable for bio-based synthetic oils and have to be modified, e.g. some tests cannot differentiate between bio-based oils with different oxidation stability (*147*). Methods inspired by food chemistry or the bio-fuel industry (*147,208*) are one promising approach, supported by analytical methods which focus not only on the determination of sum parameters, such as oxidation. Detailed analytical characterization of synthetic or bio-based (complex mixtures) lubricants has to deal with the wide variety of chemistries, from synthesized hydrocarbons like polyalphaolefins via esters to polysaccharide or protein-based lubricants. However, the well-defined molecular structure due to synthesis process enables in-depth characterization and, consequently, elaboration of the correlation between structure and thermo-oxidative stability as well as performance and property prediction in different ageing conditions, which is a challenge for bio-based lubricants consisting of complex mixtures (*209*).

By means of artificial alteration and in-depth analysis, for example, with gas chromatography coupled to mass spectrometry (GC-MS) the impact of the structure of the lubricant-oil components on the alteration behavior can be monitored. This combination of techniques is used to simulate the ongoing reactions under well-defined, reproducible, and variable conditions and to correlate the identified degradation products with the tribological performance (*151,208,210,211*). Other chromatography techniques, such as liquid chromatography combined with high-resolution MS, enable to study the degradation of synthetic biodegradable lubricants and the used additives even in more extent (*212*). However, this approach is not sufficient for a comprehensive elucidation of the main pathways of oxidative degradation

and identifying involved molecule types as well as oxidative degradation product formation over time. When it comes to oxygen-containing lubricants, such as synthetic esters, the clear identification of the oxidation reactions is even more challenging.

The use of stable isotopic tracer within an artificial alteration set-up under oxygen pressure and GC-MS enabled to obtain detailed information on the oxidation products of oxygen-containing components. In detail, the approach enables the unambiguous attribution of oxygen atoms in the degradation products and particularly hints to the mechanism of the formation of the degradation products. Hence, the involvement of specific molecule structures in the degradation process can be assigned (*149*,*213*).

## Conclusions

### *Challenges and outlook*

Heterogeneity of the biological or waste feedstock, even in the same category, compared to petroleum-based feedstock is very challenging for industrialization attempts. Based on the findings outlined above, the following summary on challenges of sustainability for lubricant formulations and the lubricant industry can be drawn:

- Need for thorough characterization and where necessary separation (compounds decreasing stability, corrosive ones, those limiting operational window, for example, waxes, etc.)
- Need for toxicity and biodegradability assessment, not only of the individual constituents but also of the whole part of the feedstock (mixed toxicity effects, for example, synergism) used in the final lubricant formulation
- To have industrial relevance and to be economically viable, it is preferential that the feedstock is compatible with the existing industrial infrastructure, especially for the transition state toward a sustainable industry by using renewable sources to replace crude oil (easiest introduction for molecules resembling the petroleum feedstock, e.g. alkenes)
- When thinking in terms of green chemistry and sustainable lubrication also production pathways and materials (and availability of those), for example, for synthesis, catalysis, etc. must be considered and regulated
- Advanced surface and material design (as a concept of green tribology) will further challenge energy consumption
- Proper disposal and/or recycling of fully formulated lubricant must be ensured → everything is toxic in large amounts and to certain organisms → biodegradability ensures it does not persist and cause long-term toxicity and it avoids the issue of bioaccumulation. Biodegradability is dependent on the type of organism and ambient conditions.

Not only the feedstock and lubricant product assessment but also the whole lubricant life cycle analyses up to the waste stage is necessary, as compounds of special concern might be detected, and proper disposal measurements are taken (complex issue as application conditions vary affecting the degradation products). The potential for recyclability even for other application(s) than the original should be assessed to limit the need for original resources and to limit the waste production.

Furthermore, in many cases, an adaption of specifications will be necessary, including:

- Common condition monitoring (see Characterization and condition monitoring) tests are optimized for the evaluation of mineral-based lubrication oils and are often not suitable for plant-derived oils (*147*).
- Biodegradability tests e.g. according to OECD301, a guideline adopted in 1992, define a lubricant as readily biodegradable (and within the EEL criteria), if at least 60% of the formulation is fully biodegraded within a period of 28 days. However, how long it does take for the remaining 40% of the lubricant to fully biodegrade is not regulated (*214*), which means up to 50% of the formulation can be of petroleum origin with high persistency and bioaccumulation potential. Even with such composition, they would still fulfill the criteria of the EU Ecolabel (*215*).
- Toxicity values of a substance are strongly varying with the type of organism used and therefore, are not consistently meaningful if not tested comprehensively.

### *Concluding remarks*

The emission of lubricant into the environment via micro drops or oil mist (e.g. in the case of metal-working fluids) is hardly preventable during use and especially accidental spills of petroleum-based lubricants cause a massive negative impact on the environment and human health. For example, contamination of the water surface through oil spills impairs the gas exchange at the water-atmosphere interface and leads to a decrease in oxygen levels in the water, threatening aquatic ecosystems (*215*).

So, it is already past due, that the focus must shift toward bio-based or bio-derived lubricant components

from renewable sources accompanied by proper eco-hazard tests (biodegradability, bioaccumulation, and toxicity), that imitate common synthetic lubricant structures and serve as intermediates in established industrial scale production (on the way to a sustainable production). For scarce and limited resources (e.g. metals) within the production processes recycling could act as a driver. In general, recycling used lubricants and enforcing a circular economy are necessary not only for harmful substances but also for renewable materials as a matter of sustainable use.

## Disclosure statement

No potential conflict of interest was reported by the author(s).

## Funding

This review paper was funded by the 'Austrian COMET-Program' (project InTribology, no. 872176) via the Austrian Research Promotion Agency (FFG) and the Provinces of Niederösterreich and Vorarlberg and has been carried out within the 'Excellence Centre of Tribology' (AC2T research GmbH).

## ORCID

*Jessica Pichler* http://orcid.org/0000-0002-5868-229X
*Rosa Maria Eder* http://orcid.org/0009-0002-3624-8422
*Charlotte Besser* http://orcid.org/0000-0003-4836-0075
*Lucia Pisarova* http://orcid.org/0000-0002-0822-6683
*Nicole Dörr* http://orcid.org/0000-0002-8378-4589
*Martina Marchetti-Deschmann* http://orcid.org/0000-0002-8060-7851
*Marcella Frauscher* http://orcid.org/0000-0001-7939-9656

## References

[1] European Commission. "A European Green Deal", 2022.
[2] United States Environmental Protection Agency. "Basics of Green Chemistry", 2022.
[3] Anastas, P.; Eghbali, N. Green Chemistry: Principles and Practice. *Chem. Soc. Rev.* **2010,** *39*, 301–312. DOI: 10.1039/b918763b.
[4] Zhang, S.-w. Green Tribology: Fundamentals and Future Development. *Friction* **June 2013,** *1*, 186–194. DOI: 10.1007/s40544-013-0012-4.
[5] Nosonovsky, M.; Bhushan, B. Green Tribology: Principles, Research Areas and Challenges. *Philos. Transact. Royal Soc. A: Math. Phys. Eng. Sci.* **October 2010,** *368*, 4677–4694. DOI: 10.1098/rsta.2010.0200.
[6] Rudnick, L.R. *Synthetics, Mineral Oils, and Bio-Based Lubricants*, L. R. Rudnick, Ed., CRC Press: Boca Raton, FL, USA, 2020. DOI: 10.1201/9781315158150.
[7] European Commission. "Energy, Climate change, Environment".
[8] European Commission. "EU Ecolabel", 2022.
[9] United States Environmental Protection Agency. "Environmentally Acceptable Lubricants", 2011.
[10] European Commission. "Directive (EU) 2018/851 of the European Parliament and of the Council of 30 May 2018 Amending Directive 2008/98/EC on Waste (Text with EEA Relevance)", *Official Journal of the European Union*, 2018.
[11] United States Environmental Protection Agency. "The Vessel Incidental Discharge Act (VIDA)", 2020.
[12] de Jong, E.; Stichnothe, H.; Bell, G.; Jørgensen, H. "Bio-Based Chemicals", 2020.
[13] Code of Federal Regulations. 21 CFR §178.3570 Lubricants with Incidental Food Contact, March 1977. [Online]. https://www.ecfr.gov/current/title-21/chapter-I/subchapter-B/part-178/subpart-D/section-178.3570 (accessed 11 02 2022).
[14] NSF - The Public Health and Safety Organization. White Book™ - Nonfood Compounds Listing Directory, February 2022. [Online]. https://info.nsf.org/usda/Listings.asp. (accessed 11 02 2022).
[15] European Commission. Lubricant Substance Classification List (LuSC-list), January 2022. [Online]. https://ec.europa.eu/environment/ecolabel/documents/LuSC-list vs 20012022 v2.pdf. (Accessed 11 02 2022).
[16] OSPAR Commission. List of Chemicals for Priority Action, 2013. [Online]. https://www.ospar.org/work-areas/hasec/hazardous-substances/priority-action (Accessed 11 02 2022).
[17] European Commission. EU Ecolabel Lubricants, 2022. [Online]. http://ec.europa.eu/ecat/category/en/49/lubricants (Accessed 11 02 2022).
[18] European Commission. 2018/1702 Establishing the EU Ecolabel Criteria for Lubricants, November 2018. [Online]. https://eur-lex.europa.eu/legal-content/EN/TXT/?qid=1542112371100&uri=CELEX:32018D1702 (Accessed 11 02 2022).
[19] Cermak, S.C.; Isbell, T.A.; Bredsguard, J.W.; Thompson, T.D., Ed.; Estolides: Synthesis and Applications. In *Fatty Acids: Chemistry, Synthesis, and Applications*; Ahmad, Moghis U., Ed.; Elsevier: San Diego, CA, US, 2017; pp 431–475. DOI: 10.1016/b978-0-12-809521-8.00015-5.
[20] Chan, C.-H.; Tang, S.W.; Mohd, N.K.; Lim, W.H.; Yeong, S.K.; Idris, Z. Tribological Behavior of Biolubricant Base Stocks and Additives. *Renewable Sustainable Energy Rev.* **October 2018,** *93*, 145–157. DOI: 10.1016/j.rser.2018.05.024.
[21] Chen, Y.; Biresaw, G.; Cermak, S.C.; Isbell, T.A.; Ngo, H.L.; Chen, L.; Durham, A.L. Fatty Acid Estolides: A Review. *J. Am. Oil Chem. Soc.* **January 2020,** *97*, 231–241. DOI: 10.1002/aocs.12323.
[22] Romsdahl, T.; Shirani, A.; Minto, R.E.; Zhang, C.; Cahoon, E.B.; Chapman, K.D.; Berman, D. Nature-Guided Synthesis of Advanced Bio-Lubricants. *Sci. Rep.* **August 2019**, *9*. DOI: 10.1038/s41598-019-48165-6.
[23] Hoong, S.S.; Arniza, M.Z.; Mariam, N.M.D.N.S.; Armylisas, A.H.N.; Ishak, S.A.; Ismail, T.N.M.T.; Yeong, S.K. Synthesis of Estolide Ester and Amide from Acetylated Polyhydroxy Estolide for Lubricant Base Oil. *Eur. J. Lipid Sci. Technol.* **August 2020,** *122* (10), 2000098, 1–12. DOI: 10.1002/ejlt.202000098.
[24] Liu, Y.; Wang, Z.; Cui, Z.; Qi, Q.; Hou, J. α-Farnesene Production from Lipid by Engineered Yarrowia

Lipolytica. *Bioresources and Bioprocessing* **August 2021**, *8*, 72, 1–12. DOI: 10.1186/s40643-021-00431-0.
[25] Wang, Z.; Zhang, R.; Yang, Q.; Zhang, J.; Zhao, Y.; Zheng, Y.; Yang, J. Recent Advances in the Biosynthesis of Isoprenoids in Engineered *Saccharomyces cerevisiae*. *Adv. Appl. Microbiol.* **2021,***114*, 1–35. DOI: 10.1016/bs.aambs.2020.11.001.
[26] Milker, S.; Holtmann, D. First Time β-Farnesene Production by the Versatile Bacterium *Cupriavidus necator*. *Microb. Cell Fact.* **April 2021**, *20*, 89, 1–7. DOI: 10.1186/s12934-021-01562-x.
[27] Lee, H.J.; Lee, J.; Lee, S.-M.; Um, Y.; Kim, Y.; Sim, S.J.; Choi, J.-i.; Woo, H.M. Direct Conversion of CO2 to α-Farnesene Using Metabolically Engineered *Synechococcus elongatus* PCC 7942. *J. Agric. Food Chem.* **November 2017,** *65*, 10424–10428. DOI: 10.1021/acs.jafc.7b03625.
[28] Tsagkaropoulou, G.; Warrens, C.P.; Camp, P.J. Interactions Between Friction Modifiers and Dispersants in Lubricants: The Case of Glycerol Monooleate and Polyisobutylsuccinimide-Polyamine. *ACS Applied Materials & Interfaces* **July 2019,** *11*, 28359–28369. DOI: 10.1021/acsami.9b05718.
[29] Liu, H.C.; Zhang, B.B.; Bader, N.; Venner, C.H.; Poll, G. Simplified Traction Prediction for Highly Loaded Rolling/Sliding EHL Contacts. *Tribol. Int.* **August 2020,** *148*, 106335, 1–13. DOI:10.1016/j.triboint.2020.106335.
[30] Bürk, V.; Pollak, S.; Quiñones-Cisneros, S.E.; Schmidt, K.A.G. Complementary Experimental Data and Extended Density and Viscosity Reference Models for Squalane. *Journal of Chemical & Engineering Data* **April 2021,** *66*, 1992–2005. DOI: 10.1021/acs.jced.0c01058.
[31] Zhao, J.; Sheng, W.; Li, Z.; Zhang, H.; Zhu, R. Effect of Lubricant Selection on the Wear Characteristics of Spur Gear Under Oil-Air Mixed Lubrication. *Tribol. Int.* **March 2022,** *167*, 107382, 1–12. DOI:10.1016/j.triboint.2021.107382.
[32] Opia, A.C.; Hamid, M.K.B.A.; Syahrullail, S.; Rahim, A.B.A.; Johnson, C.A.N. Biomass as a Potential Source of Sustainable Fuel, Chemical and Tribological Materials – Overview. *Mater. Today: Proc.* **2021,** *39*, 922–928. DOI: 10.1016/j.matpr.2020.04.045.
[33] da Cruz, M.G.A.; Budnyak, T.M.; Rodrigues, B.V.M.; Budnyk, S.; Slabon, A. Biocoatings and Additives as Promising Candidates for Ultralow Friction Systems. *Green Chem. Lett. Rev.* **April 2021,** *14*, 358–381. DOI: 10.1080/17518253.2021.1921286.
[34] Ulvskov, P. *Plant Polysaccharides, Biosynthesis and Bioengineering*; Wiley-Blackwell: Chichester, West Sussex, UK, 2011.
[35] Borah, D.; Gopalakrishnan, S.; Nooruddin, T. Carbohydrate Biolubricants from Algae and Cyanobacteria. *J. Polym. Environ.* **April 2021,** *29*, 3444–3458. DOI: 10.1007/s10924-021-02144-z.
[36] Kumar, V.; Bhatia, S.S. *Complete Biology for Medical College Entrance Examination*, 3rd ed., McGraw Hill Education: New York City, NY, USA, 2013.
[37] Yang, D.; Zhou, Z.; Zhang, L. An Overview of Fungal Glycan-Based Therapeutics. *Prog. Mol. Biol. Transl. Sci.* **2019**, *163*, 135–163. DOI: 10.1016/bs.pmbts.2019.02.001.
[38] Werpy, T.; Petersen, G. Top Value Added Chemicals from BiomassVolume I – Results of Screening for PotentialCandidates from Sugars and Synthesis Gas, August 2004. [Online]. https://www.energy.gov/sites/default/files/2014/03/f14/35523.pdf. (accessed 11 02 2022).
[39] Bozell, J.J.; Holladay, J.E.; Johnson, D.; White, J.F. Top Value-Added Chemicals from BiomassVolume II – Results of Screening for Potential Candidates from Biorefinery Lignin, October 2007. [Online]. https://www.pnnl.gov/main/publications/external/technical_reports/PNNL-16983.pdf. [accessed 11 02 2022].
[40] Silva, J.F.L.; Mariano, A.P.; Filho, R.M. Economic Potential of 2-Methyltetrahydrofuran (MTHF) and Ethyl Levulinate (EL) Produced from Hemicelluloses-Derived Furfural. *Biomass Bioenergy* **December 2018,** *119*, 492–502. DOI: 10.1016/j.biombioe.2018.10.008.
[41] Cortés-Triviño, E.; Valencia, C.; Delgado, M.A.; Franco, J.M. Thermo-Rheological and Tribological Properties of Novel Bio-Lubricating Greases Thickened with Epoxidized Lignocellulosic Materials. *J. Ind. Eng. Chem.* **December 2019,** *80*, 626–632. DOI: 10.1016/j.jiec.2019.08.052.
[42] Gallego, R.; Cidade, T.; Sánchez, R.; Valencia, C.; Franco, J.M. Tribological Behaviour of Novel Chemically Modified Biopolymer-Thickened Lubricating Greases Investigated in a Steel–Steel Rotating Ball-on-Three Plates Tribology Cell. *Tribol. Int.* **February 2016,** *94*, 652–660. DOI: 10.1016/j.triboint.2015.10.028.
[43] Gorbacheva, S.N.; Yadykova, A.Y.; Ilyin, S.O. Rheological and Tribological Properties of Low-Temperature Greases Based on Cellulose Acetate Butyrate Gel. *Carbohydr. Polym.* **November 2021,** *272*, 118509, 1–12. DOI:10.1016/j.carbpol.2021.118509.
[44] Fernández-Silva, S.D.; Delgado, M.A.; Roman, C.; García-Morales, M. Rheological and Tribological Properties of Nanocellulose-Based Ecolubricants. *Nanomaterials* **November 2021,** *11*, 2987, 1–14. DOI:10.3390/nano11112987.
[45] Delgado-Canto, M.A.; Fernández-Silva, S.D.; Roman, C.; García-Morales, M. On the Electro-Active Control of Nanocellulose-Based Functional Biolubricants. *ACS Appl. Mater. Interfaces* **September 2020,** *12*, 46490–46500. DOI: 10.1021/acsami.0c12244.
[46] Chen, S.; Zhao, C. Production of Highly Symmetrical and Branched Biolubricants From Lignocellulose-Derived Furan Compounds. *ACS. Sustain. Chem. Eng.* **August 2021,** *9*, 10818–10826. DOI: 10.1021/acssuschemeng.1c02875.
[47] Liu, S.; Bhattacharjee, R.; Li, S.; Danielson, A.; Mazal, T.; Saha, B.; Vlachos, D.G. Thiol-promoted Catalytic Synthesis of High-Performance Furan-Containing Lubricant Base Oils from Biomass Derived 2-Alkylfurans and Ketones. *Green Chem.* **2020,** *22*, 7896–7906. DOI: 10.1039/d0gc01897j.
[48] Sheng, D.; Zhou, J.; Zhang, H.; Tian, H.; Liu, X.; Qi, X.; Zhang, H.; Wang, W. Achievement of Super-Low Friction Between Ultra-Polished Quartz Lubricated by Hydrated Hydroxyethyl Cellulose. *J. Mater. Eng. Perform.* **October 2021**, *31*, 1096–1107. DOI: 10.1007/s11665-021-06284-0.

[49] Roman, C.; García-Morales, M.; Eugenio, M.E.; Ibarra, D.; Martín-Sampedro, R.; Delgado, M.A. A Sustainable Methanol-Based Solvent Exchange Method to Produce Nanocellulose-Based Ecofriendly Lubricants. *J. Cleaner Prod.* **October 2021**, *319*, 128673, 1–10. DOI:10.1016/j.jclepro.2021.128673.

[50] Shetty, P.; Mu, L.; Shi, Y. Polyelectrolyte Cellulose Gel with PEG/Water: Toward Fully Green Lubricating Grease. *Carbohydr. Polym.* **February 2020,** *230*, 115670, 1–8. DOI:10.1016/j.carbpol.2019.115670.

[51] Colter, J.; Wirostko, B.; Coats, B. Coefficient of Friction Between Carboxymethylated Hyaluronic Acid-Based Polymer Films and the Ocular Surface. *Investigative Opthalmology & Visual Science* **December 2017,** *58*, 6166, 1–9. DOI:10.1167/iovs.17-22414.

[52] Shi, S.-C.; Peng, Y.-Q. Preparation and Tribological Studies of Stearic Acid-Modified Biopolymer Coating. *Prog. Org. Coat.* **January 2020,** *138*, 105304, 1–8. DOI:10.1016/j.porgcoat.2019.105304.

[53] Ma, Q.; Wang, S.; Dong, G. Macroscale Liquid Superlubricity Achieved with Mixtures of Fructose and Diols. *Wear* **November 2021,** *484-485*, 204037, 1–8. DOI:10.1016/j.wear.2021.204037.

[54] Negi, H.; Verma, P.; Singh, R.K. A Comprehensive Review on the Applications of Functionalized Chitosan in Petroleum Industry. *Carbohydr. Polym.* **August 2021,** *266*, 118125, 1–17. DOI:10.1016/j.carbpol.2021.118125.

[55] Zhang, R.; Liu, X.; Guo, Z.; Cai, M.; Shi, L. Effective Sugar-Derived Organic Gelator for Three Different Types of Lubricant Oils to Improve Tribological Performance. *Friction* **September 2019,** *8*, 1025–1038. DOI: 10.1007/s40544-019-0316-0.

[56] Bandhu, S.; Khot, M.B.; Sharma, T.; Sharma, O.P.; Dasgupta, D.; Mohapatra, S.; Hazra, S.; Khatri, O.P.; Ghosh, D. Single Cell Oil from Oleaginous Yeast Grown on Sugarcane Bagasse-Derived Xylose: An Approach Toward Novel Biolubricant for Low Friction and Wear. *ACS. Sustain. Chem. Eng.* **November 2017,** *6*, 275–283. DOI: 10.1021/acssuschemeng.7b02425.

[57] Belicka, L. Introduction to Glycomics and Glycan Analysis. In *Glyconanotechnology: Nanoscale Approach for Novel Glycan Analysis and Their Medical Use*; 1st ed.; T. Bertók, Ed.; Pan Stanford Publishing: Singapore, **2020,** pp 33–64.

[58] Petrou, G.; Crouzier, T. Mucins as Multifunctional Building Blocks of Biomaterials. *Biomater. Sci.* **2018,** *6*, 2282–2297. DOI: 10.1039/c8bm00471d.

[59] Crouzier, T.; Boettcher, K.; Geonnotti, A.R.; Kavanaugh, N.L.; Hirsch, J.B.; Ribbeck, K.; Lieleg, O. Modulating Mucin Hydration and Lubrication by Deglycosylation and Polyethylene Glycol Binding. *Adv. Mater. Interfaces.* **September 2015,** *2*, 1500308, 1–7. DOI:10.1002/admi.201500308.

[60] Sterner, O.; Karageorgaki, C.; Zürcher, M.; Zürcher, S.; Scales, C.W.; Fadli, Z.; Spencer, N.D.; Tosatti, S.G.P. Reducing Friction in the Eye: A Comparative Study of Lubrication by Surface-Anchored Synthetic and Natural Ocular Mucin Analogues. *ACS Appl. Mater. Interfaces* **May 2017,** *9*, 20150–20160. DOI: 10.1021/acsami.6b16425.

[61] Varki, A. Biological Roles of Glycans. *Glycobiology* **August 2016,** *27*, 3–49. DOI: 10.1093/glycob/cww086.

[62] Bayer, I. Advances in Tribology of Lubricin and Lubricin-Like Synthetic Polymer Nanostructures. *Lubricants* **April 2018**, *6*, 30, 1–26. DOI:10.3390/lubricants6020030.

[63] Mu, L.; Wu, J.; Matsakas, L.; Chen, M.; Rova, U.; Christakopoulos, P.; Zhu, J.; Shi, Y. Two Important Factors of Selecting Lignin as Efficient Lubricating Additives in Poly (Ethylene Glycol): Hydrogen Bond and Molecular Weight. *Int. J. Biol. Macromol.* **May 2019,** *129*, 564–570. DOI: 10.1016/j.ijbiomac.2019.01.175.

[64] Danilov, A.M.; Antonov, S.A.; Bartko, R.V.; Nikulshin, P.A. Recent Advances in Biodegradable Lubricating Materials (A Review). *Pet. Chem.* **April 2021**, *61*, 697–710. DOI: 10.1134/s0965544121050121.

[65] Kazzaz, A.E.; Feizi, Z.H.; Fatehi, P. Grafting Strategies for Hydroxy Groups of Lignin for Producing Materials. *Green Chem.* **2019,** *21*, 5714–5752. DOI: 10.1039/c9gc02598g.

[66] Domínguez, G.; Blánquez, A.; Borrero-López, A.M.; Valencia, C.; Eugenio, M.E.; Arias, M.E.; Rodríguez, J.; Hernández, M. Eco-Friendly Oleogels from Functionalized Kraft Lignin with Laccase SilA from Streptomyces Ipomoeae: An Opportunity to Replace Commercial Lubricants. *ACS. Sustain. Chem. Eng.* **March 2021**, *9*, 4611–4616. DOI: 10.1021/acssuschemeng.1c00113.

[67] Cortés-Triviño, E.; Valencia, C.; Franco, J.M. Thickening Castor Oil with a Lignin-Enriched Fraction from Sugarcane Bagasse Waste via Epoxidation: A Rheological and Hydrodynamic Approach. *ACS. Sustain. Chem. Eng.* **July 2021,** *9*, 10503–10512. DOI: 10.1021/acssuschemeng.1c02166.

[68] Borrero-López, A.M.; Martín-Sampedro, R.; Ibarra, D.; Valencia, C.; Eugenio, M.E.; Franco, J.M. Evaluation of Lignin-Enriched Side-Streams from Different Biomass Conversion Processes as Thickeners in bio-Lubricant Formulations. *Int. J. Biol. Macromol.* **November 2020,** *162*, 1398–1413. DOI: 10.1016/j.ijbiomac.2020.07.292.

[69] da Cruz, M.G.A.; Gueret, R.; Chen, J.; Piątek, J.; Beele, B.; Sipponen, M.H.; Frauscher, M.; Budnyk, S.; Rodrigues, B.V.M.; Slabon, A. Electrochemical Depolymerization of Lignin in a Biomass-Based Solvent∗∗. *ChemSusChem.* **June 2022**, *15*, 1–9. DOI:10.1002/cssc.202200718.

[70] Delgado, M.A.; Cortés-Triviño, E.; Valencia, C.; Franco, J.M. Tribological Study of Epoxide-Functionalized Alkali Lignin-Based Gel-Like Biogreases. *Tribol. Int.* **June 2020,** *146*, 106231, 1–8. DOI:10.1016/j.triboint.2020.106231.

[71] Mu, L.; Shi, Y.; Guo, X.; Ji, T.; Chen, L.; Yuan, R.; Brisbin, L.; Wang, H.; Zhu, J. Non-Corrosive Green Lubricants: Strengthened Lignin–[Choline][Amino Acid] Ionic Liquids Interaction via Reciprocal Hydrogen Bonding. *RSC Adv.* **2015,** *5*, 66067–66072. DOI: 10.1039/c5ra11093a.

[72] Mu, L.; Shi, Y.; Hua, J.; Zhuang, W.; Zhu, J. Engineering Hydrogen Bonding Interaction and Charge Separation in Bio-Polymers for Green Lubrication. *J. Phys. Chem. B* **May 2017,** *121*, 5669–5678. DOI: 10.1021/acs.jpcb.7b03194.

[73] Hua, J.; Shi, Y. Non-Corrosive Green Lubricant With Dissolved Lignin in Ionic Liquids Behave as Ideal Lubricants for Steel-DLC Applications. *Front. Chem.* **December 2019**, *7*, 1–8. DOI:10.3389/fchem.2019.00857.

[74] Mariana, M.; Alfatah, T.; E, A.K.H.P.S.; Yahya, B.; Olaiya, N.G.; Nuryawan, A.; Mistar, E.M.; Abdullah, C.K.; Abdulmadjid, S.N.; Ismail, H. A Current Advancement on the Role of Lignin as Sustainable Reinforcement Material in Biopolymeric Blends. *Journal of Materials Research and Technology* **November 2021,** *15*, 2287–2316. DOI: 10.1016/j.jmrt.2021.08.139.

[75] Ebikade, E.O.; Sadula, S.; Liu, S.; Vlachos, D.G. Lignin Monomer Conversion Into Biolubricant Base Oils. *Green Chem.* **2021,** *23*, 10090–10100. DOI: 10.1039/d1gc03350f.

[76] Mohammadinejad, R.; Maleki, H.; Larrañeta, E.; Fajardo, A.R.; Nik, A.B.; Shavandi, A.; Sheikhi, A.; Ghorbanpour, M.; Farokhi, M.; Govindh, P.; Cabane, E.; Azizi, S.; Aref, A.R.; Mozafari, M.; Mehrali, M.; Thomas, S.; Mano, J.F.; Mishra, Y.K.; Thakur, V.K. Status and Future Scope of Plant-Based Green Hydrogels in Biomedical Engineering. *Applied Materials Today* **September 2019,** *16*, 213–246. DOI: 10.1016/j.apmt.2019.04.010.

[77] Gombert, Y.; Simič, R.; Roncoroni, F.; Dübner, M.; Geue, T.; Spencer, N.D. Structuring Hydrogel Surfaces for Tribology. *Adv. Mater. Interfaces.* **October 2019,** *6*, 1901320, 1–9. DOI:10.1002/admi.201901320.

[78] Osaheni, A.O.; Finkelstein, E.B.; Mather, P.T.; Blum, M.M. Synthesis and Characterization of a Zwitterionic Hydrogel Blend with Low Coefficient of Friction. *Acta Biomater.* **December 2016,** *46*, 245–255. DOI: 10.1016/j.actbio.2016.09.022.

[79] Arjmandi, M.; Ramezani, M.; Nand, A.; Neitzert, T. Experimental Study on Friction and Wear Properties of Interpenetrating Polymer Network Alginate-Polyacrylamide Hydrogels for Use in Minimally-Invasive Joint Implants. *Wear* **July 2018,** *406-407*, 194–204. DOI: 10.1016/j.wear.2018.04.013.

[80] Hafezi, M.; Qin, L.; Mahmoodi, P.; Yang, H.; Dong, G. Releasable Agarose-Hyaluronan Hydrogel with Anti-Friction Performance and Enhanced Stability for Artificial Joint Applications. *Tribol. Int.* **January 2021,** *153*, 106622, 1–9. DOI:10.1016/j.triboint.2020.106622.

[81] Xu, R.; Zhao, X.; Ma, S.; Ma, Z.; Wang, R.; Cai, M.; Zhou, F. Hydrogen Bonding Induced Enhancement for Constructing Anisotropic Sugarcane Composite Hydrogels. *J. Appl. Polym. Sci.* **July 2021,** *138*, 51374, 1–10. DOI:10.1002/app.51374.

[82] Su, C.-Y.; Yeh, L.-K.; Fan, T.-W.; Lai, C.-C.; Fang, H.-W. Albumin Acts as a Lubricant on the Surface of Hydrogel and Silicone Hydrogel Contact Lenses. *Polymers* **June 2021,** *13*, 2051, 1–9. DOI:10.3390/polym13132051.

[83] Iwashita, H.; Itokawa, T.; Suzuki, T.; Okajima, Y.; Kakisu, K.; Hori, Y. Evaluation of In Vitro Wettability of Soft Contact Lenses Using Tear Supplements. *Eye & Contact Lens: Science & Clinical Practice* **May 2020,** *47*, 244–248. DOI: 10.1097/icl.0000000000000698.

[84] Korogiannaki, M.; Samsom, M.; Matheson, A.; Soliman, K.; Schmidt, T.A.; Sheardown, H. Investigating the Synergistic Interactions of Surface Immobilized and Free Natural Ocular Lubricants for Contact Lens Applications: A Comparative Study Between Hyaluronic Acid and Proteoglycan 4 (Lubricin). *Langmuir* **January 2021,** *37*, 1062–1072. DOI: 10.1021/acs.langmuir.0c02796.

[85] Liu, W.; Wang, K.; Song, J.; Zhang, L.; Liu, Y. Ultralow Friction of Basil-Based Gel in the Presence of Ethanol as a Green Lubricant for Biomedical Applications. *Tribol. Int.* **January 2022,** *165*, 107320, 1–8. DOI:10.1016/j.triboint.2021.107320.

[86] Wang, Y.; Wu, Y.; Yu, Q.; Zhang, J.; Ma, Z.; Zhang, M.; Zhang, L.; Bai, Y.; Cai, M.; Zhou, F.; Liu, W. Significantly Reducing Friction and Wear of Water-Based Fluids with Shear Thinning Bicomponent Supramolecular Hydrogels. *Adv. Mater. Interfaces.* **October 2020,** *7*, 2001084, 1–10. DOI:10.1002/admi.202001084.

[87] Wen, F.; Li, J.; Wang, L.; Li, F.; Yu, H.; Li, B.; Fan, K.; Guan, X. Novel Self-Healing and Multi-Stimuli-Responsive Supramolecular gel Based on d-Sorbitol Diacetal for Multifunctional Applications. *RSC Adv.* **2021,** *11*, 32459–32463. DOI: 10.1039/d1ra05605k.

[88] Avar, G.; Meier-Westhues, U.; Casselmann, H.; Achten, D. Polyurethanes. *Polym Sci: A Comprehens. Ref.* **2012 ,***10*, 411–441. DOI: 10.1016/b978-0-444-53349-4.00275-2.

[89] S. Arulmani, S. Anandan and M. Ashokkumar, Introduction to Advanced Nanomaterials. In *Nanomaterials for Green Energy*, B. A. Bhanvase, V. B. Pawade, S. J. Dhoble, S. H. Sonawane and M. Ashokkumar, Eds.; Elsevier: Cambridge, MA, USA, 2018; pp 1–59. DOI: 10.1016/c2017-0-00368-3.

[90] Malani, R.S.; Malshe, V.C.; Thorat, B.N. Polyols and Polyurethanes from Renewable Sources: Past, Present, and Future—Part 2: Plant-Derived Materials. *J. Coat. Technol. Res.* **January 2022,** *19*, 361–375. DOI: 10.1007/s11998-021-00534-5.

[91] Aziz, N.A.M.; Yunus, R.; Rashid, U.; Zulkifli, N.W.M. Temperature Effect on Tribological Properties of Polyol Ester-Based Environmentally Adapted Lubricant. *Tribol. Int.* **January 2016,** *93*, 43–49. DOI: 10.1016/j.triboint.2015.09.014.

[92] Arumugam, S.; Baskar, S.; Subramanian, V.S.; Shivasankaran, G. Polyolester Based Lubricant from Waste Feedstock for Sustainable Environment: A Tribological Investigation. *IOP Conf. Ser.: Mater. Sci. Eng.* **October 2020,** *954*, 012021, 1–5. DOI:10.1088/1757-899x/954/1/012021.

[93] Ma, X.; Zhang, Y.; Song, Z.; Yu, K.; He, C.; Zhang, X. Enzyme-catalyzed Synthesis and Properties of Polyol Ester Biolubricant Produced from *Rhodotorula glutinis* Lipid. *Biochem. Eng. J.* **September 2021,** *173*, 108101, 1 –9. DOI:10.1016/j.bej.2021.108101.

[94] Lubis, A.M.H.S. *Tribological Properties Characterization of Green Polyol*, In Proceedings of Mechanical Engineering Research Day 2019, Abdollah, M. F. B., Ed.; Centre of Advanced Research on Energy (CARe),**2019** ; pp. 340–341.

[95] Acar, N.; Franco, J.M.; Kuhn, E.; Gonçalves, D.E.P.; Seabra, J.H.O. Tribological Investigation on the Friction and Wear Behaviors of Biogenic Lubricating Greases in Steel–Steel Contact. *Appl Sci* **February 2020,** *10*, 1477, 1–17. DOI:10.3390/app10041477.

[96] Wang, W.; Shen, B.; Li, Y.; Ni, Q.; Zhou, L.; Du, F. Friction Reduction Mechanism of Glycerol Monooleate-Containing Lubricants at Elevated Temperature – Transition from Physisorption to Chemisorption. *Sci. Prog.* **January 2021,** *104* (1), 1–15. DOI:10.1177/0036850421998529.

[97] Ma, Q.; Wang, W.; Dong, G. Achieving Macroscale Liquid Superlubricity Using Lubricant Mixtures of Glycerol and Propanediol. *Tribol. Lett.* **November 2021**, *69*, 1–12. DOI:10.1007/s11249-021-01519-6.

[98] Reddyhoff, T.; Ewen, J.P.; Deshpande, P.; Frogley, M.D.; Welch, M.D.; Montgomery, W. Macroscale Superlubricity and Polymorphism of Long-Chain n-Alcohols. *ACS Appl. Mater. Interfaces* **February 2021,** *13*, 9239–9251. DOI: 10.1021/acsami.0c21918.

[99] Welton, T. Room-Temperature Ionic Liquids. Solvents for Synthesis and Catalysis. *Chem. Rev.* **July 1999,** *99*, 2071–2084. DOI: 10.1021/cr980032t.

[100] Rahman, M.H.; Khajeh, A.; Panwar, P.; Patel, M.; Martini, A.; Menezes, P.L. Recent Progress on Phosphonium-Based Room Temperature Ionic Liquids: Synthesis, Properties, Tribological Performances and Applications. *Tribol. Int.* **March 2022,** *167*, 107331, 1–31. DOI:10.1016/j.triboint.2021.107331.

[101] Flieger, J.; Flieger, M. Ionic Liquids Toxicity – Benefits and Threats. *Int. J. Mol. Sci.* **August 2020,** *21*, 6267, 1–41. DOI:10.3390/ijms21176267.

[102] Gonçalves, A.R.P.; Paredes, X.; Cristino, A.F.; Santos, F.J.V.; Queirós, C.S.G.P. Ionic Liquids – A Review of Their Toxicity to Living Organisms. *Int. J. Mol. Sci.* **May 2021,** *22*, 5612, 1–50. DOI:10.3390/ijms22115612.

[103] Dong, X.; Fan, Y.; Zhang, H.; Zhong, Y.; Yang, Y.; Miao, J.; Hua, S. Inhibitory Effects of Ionic Liquids on the Lactic Dehydrogenase Activity. *Int. J. Biol. Macromol.* **May 2016,** *86*, 155–161. DOI: 10.1016/j.ijbiomac.2016.01.059.

[104] Beil, S.; Markiewicz, M.; Pereira, C.S.; Stepnowski, P.; Thöming, J.; Stolte, S. Toward the Proactive Design of Sustainable Chemicals: Ionic Liquids as a Prime Example. *Chem. Rev.* **September 2021,** *121*, 13132–13173. DOI: 10.1021/acs.chemrev.0c01265.

[105] Jing, B.; Lan, N.; Qiu, J.; Zhu, Y. Interaction of Ionic Liquids with a Lipid Bilayer: A Biophysical Study of Ionic Liquid Cytotoxicity. *J. Phys. Chem. B* **March 2016,** *120*, 2781–2789. DOI: 10.1021/acs.jpcb.6b00362.

[106] Oulego, P.; Blanco, D.; Ramos, D.; Viesca, J.L.; Díaz, M.; Battez, A.H. Environmental Properties of Phosphonium, Imidazolium and Ammonium Cation-Based Ionic Liquids as Potential Lubricant Additives. *J. Mol. Liq.* **December 2018,** *272*, 937–947. DOI: 10.1016/j.molliq.2018.10.106.

[107] Jordan, A.; Gathergood, N. Biodegradation of Ionic Liquids – A Critical Review. *Chem. Soc. Rev.* **2015,** *44*, 8200–8237. DOI: 10.1039/c5cs00444f.

[108] Jiang, C.; Li, W.; Nian, J.; Lou, W.; Wang, X. Tribological Evaluation of Environmentally Friendly Ionic Liquids Derived from Renewable Biomaterials. *Friction* **November 2017,** *6*, 208–218. DOI: 10.1007/s40544-017-0170-x.

[109] Wu, G. *Amino Acids Biochemistry and Nutrition*, 2; Taylor & Francis Group: Boca Raton, FL, USA, 2022; p 720.

[110] Aathira, M.S.; Khatri, P.K.; Jain, S.L. Synthesis and Evaluation of Bio-Compatible Cholinium Amino Acid Ionic Liquids for Lubrication Applications. *J. Ind. Eng. Chem.* **August 2018,** *64*, 420–429. DOI: 10.1016/j.jiec.2018.04.004.

[111] Björling, M.; Bair, S.; Mu, L.; Zhu, J.; Shi, Y. Elastohydrodynamic Performance of a Bio-Based, Non-Corrosive Ionic Liquid. *Applied Sciences* **September 2017,** *7*, 996, 1–14. DOI:10.3390/app7100996.

[112] Hua, J.; Björling, M.; Larsson, R.; Shi, Y. Controllable Superlubricity Achieved with Mixtures of Green Ionic Liquid and Glycerol Aqueous Solution via Humidity. *J. Mol. Liq.* **January 2022,** *345*, 117860, 1–6. DOI:10.1016/j.molliq.2021.117860.

[113] Fan, M.; Zhang, S.; Ma, L.; Lu, Y.; Ai, J.; Du, X.; Sun, W.; Yang, D.; Zhou, F.; Liu, W. The Ecotoxicity and Tribological Properties of Choline Monocarboxylate Ionic Liquid Lubricants. *Lubr. Sci.* **August 2019,** *32*, 1–9. DOI: 10.1002/ls.1480.

[114] Zheng, D.; Wang, X.; Zhang, M.; Ju, C. Synergistic Effects Between the Two Choline-Based Ionic Liquids as Lubricant Additives in Glycerol Aqueous Solution. *Tribol. Lett.* **April 2019**, *67*, 1–13. DOI:10.1007/s11249-019-1161-z.

[115] Faes, J.; González, R.; Battez, A.H.; Blanco, D.; Fernández-González, A.; Viesca, J.L. Friction, Wear and Corrosion Behavior of Environmentally-Friendly Fatty Acid Ionic Liquids. *Coatings* **December 2020,** *11*, 21, 1–16. DOI:10.3390/coatings11010021.

[116] Fan, M.; Ma, L.; Zhang, C.; Wang, Z.; Ruan, J.; Han, M.; Ren, Y.; Zhang, C.; Yang, D.; Zhou, F.; Liu, W. Biobased Green Lubricants: Physicochemical, Tribological and Toxicological Properties of Fatty Acid Ionic Liquids. *Tribol. Trans.* **March 2017,** *61*, 195–206. DOI: 10.1080/10402004.2017.1290856.

[117] Gusain, R.; Khatri, O.P. Fatty Acid Ionic Liquids as Environmentally Friendly Lubricants for Low Friction and Wear. *RSC Adv.* **2016,** *6*, 3462–3469. DOI: 10.1039/c5ra25001c.

[118] Gusain, R.; Khan, A.; Khatri, O.P. Fatty Acid-Derived Ionic Liquids as Renewable Lubricant Additives: Effect of Chain Length and Unsaturation. *J. Mol. Liq.* **March 2020,** *301*, 112322, 1–9. DOI:10.1016/j.molliq.2019.112322.

[119] Yu, G.; Zhao, D.; Wen, L.; Yang, S.; Chen, X. Viscosity of Ionic Liquids: Database, Observation, and Quantitative Structure-Property Relationship Analysis. *AIChE J.* **October 2011,** *58*, 2885–2899. DOI: 10.1002/aic.12786.

[120] Sernaglia, M.; Blanco, D.; Battez, A.H.; Viesca, J.L.; González, R.; Bartolomé, M. Two Fatty Acid Anion-Based Ionic Liquids – Part I: Physicochemical Properties and Tribological Behavior as Neat Lubricants. *J. Mol. Liq.* **May 2020,** *305*, 112827, 1–10. DOI:10.1016/j.molliq.2020.112827.

[121] Avilés, M.-D.; Pamies, R.; Sanes, J.; Carrión, F.-J.; Bermúdez, M.-D. Fatty Acid-Derived Ionic Liquid Lubricant. Protic Ionic Liquid Crystals as Protic Ionic Liquid Additives. *Coatings* **October 2019,** *9*, 710, 1–10. DOI:10.3390/coatings9110710.

[122] Avilés, M.-D.; Cao, V.D.; Sánchez, C.; Arias-Pardilla, J.; Carrión-Vilches, F.-J.; Sanes, J.; Kjøniksen, A.-L.; Bermúdez, M.-D.; Pamies, R. Effect of Temperature on the Rheological Behavior of a New Aqueous Liquid Crystal Bio-Lubricant. *J. Mol. Liq.* **March 2020,** *301*, 112406, 1–8. DOI:10.1016/j.molliq.2019.112406.

[123] Taufiqurrakhman, M.; Bryant, M.G.; Neville, A. Tribofilms on CoCrMo Alloys: Understanding the Role of the Lubricant. *Biotribology* **September 2019,** *19*, 100104, 1–20. DOI:10.1016/j.biotri.2019.100104.

[124] Sapawe, N.; Samion, S.; Ibrahim, M.I.; Daud, M.R.; Yahya, A.; Hanafi, M.F. Tribological Testing of Hemispherical

Titanium Pin Lubricated by Novel Palm Oil: Evaluating Anti-Wear and Anti-Friction Properties. *Chin. J. Mech. Eng.* **April 2017,** *30*, 644–651. DOI: 10.1007/s10033-017-0126-0.

[125] Goh, A.S.M.; Chuah, B.S.; Nguyen, K.C.. Rheological Properties of Personal Lubricants . In *Rheology of Biological Soft Matter. Soft and Biological Matter.*; Kaneda, Isamu, Ed.; Tokyo, Japan, 2017; pp 323–336. DOI: 10.1007/978-4-431-56080-7_12.

[126] Nadein, K.; Kovalev, A.; Thøgersen, J.; Weidner, T.; Gorb, S. Insects Use Lubricants to Minimize Friction and Wear in Leg Joints. *Proc Royal Soc B: Biological Sci* **July 2021,** *288*, 20211065, 1–7. DOI:10.1098/rspb.2021.1065.

[127] Watrelot, A.A.; Kuhl, T.L.; Waterhouse, A.L. Friction Forces of Saliva and Red Wine on Hydrophobic and Hydrophilic Surfaces. *Food Res. Int.* **February 2019,** *116*, 1041–1046. DOI: 10.1016/j.foodres.2018.09.043.

[128] Xu, F.; Liamas, E.; Bryant, M.; Adedeji, A.F.; Andablo-Reyes, E.; Castronovo, M.; Ettelaie, R.; Charpentier, T.V.J.; Sarkar, A. A Self-Assembled Binary Protein Model Explains High-Performance Salivary Lubrication from Macro to Nanoscale. *Adv. Mater. Interfaces.* **November 2019,** *7*, 1901549, 1–17. DOI:10.1002/admi.201901549.

[129] Hu, J.; Andablo-Reyes, E.; Mighell, A.; Pavitt, S.; Sarkar, A. Dry Mouth Diagnosis and Saliva Substitutes – A Review from a Textural Perspective. *J. Texture. Stud.* **December 2020,** *52*, 141–156. DOI: 10.1111/jtxs.12575.

[130] Blakeley, M.; Sharma, P.K.; Kaper, H.J.; Bostanci, N.; Crouzier, T. Lectin-Functionalized Polyethylene Glycol for Relief of Mucosal Dryness. *Adv. Healthcare Mater.* **November 2021,** *11*, 2101719, 1–11. DOI:10.1002/adhm.202101719.

[131] Sarkar, A.; Soltanahmadi, S.; Chen, J.; Stokes, J.R. Oral Tribology: Providing Insight Into Oral Processing of Food Colloids. *Food Hydrocolloids* **August 2021,** *117*, 106635, 1–17. DOI:10.1016/j.foodhyd.2021.106635.

[132] Samsom, M.; Korogiannaki, M.; Subbaraman, L.N.; Sheardown, H.; Schmidt, T.A. Hyaluronan Incorporation Into Model Contact Lens Hydrogels as a Built-in Lubricant: Effect of Hydrogel Composition and Proteoglycan 4 as a Lubricant in Solution. *J Biomed Mater Res Part B: Appl Biomater* **September 2017,** *106*, 1818–1826. DOI: 10.1002/jbm.b.33989.

[133] Chang, Y.-C.; Su, C.-Y.; Chang, C.-H.; Fang, H.-W.; Wei, Y. Correlation Between Tribological Properties and the Quantified Structural Changes of Lysozyme on Poly (2-Hydroxyethyl Methacrylate) Contact Lens. *Polymers* **July 2020,** *12*, 1639, 1–10. DOI:10.3390/polym12081639.

[134] Sukumaran, A.K.; Thampi, A.D.; Sneha, E.; Arif, M.; Rani, S. Effect of Bovine Serum Albumin on the Lubricant Properties of Rice Bran oil: A Biomimetic Approach. *Sādhanā* **October 2021**, *46*, 1–10. DOI:10.1007/s12046-021-01717-x.

[135] Aravind, A.; Nair, K.P.; Joy, M.L. Formulation of a Novel Biolubricant with Enhanced Properties Using Esterified Rubber Seed Oil as a Base Stock. *J Eng Tribology* **February 2018,** *0*, 1–11. DOI: 10.1177/1350650118756243.

[136] Li, W.; Wu, Y.; Wang, X.; Liu, W. Study of Soybean Lecithin as Multifunctional Lubricating Additives. *Ind Lubrication and Tribol* **September 2013,** *65*, 466–471. DOI: 10.1108/ilt-06-2011-0050.

[137] Agrawal, N.R.; Omarova, M.; Burni, F.; John, V.T.; Raghavan, S.R. Spontaneous Formation of Stable Vesicles and Vesicle Gels in Polar Organic Solvents. *Langmuir* **June 2021,** *37*, 7955–7965. DOI: 10.1021/acs.langmuir.1c00628.

[138] Singh, R.; Kukrety, A.; Chouhan, A.; Atray, N.; Ray, S. Recent Progress in the Preparation of Eco-Friendly Lubricant and Fuel Additives Through Organic Transformations of Biomaterials. *Mini-Rev. Org. Chem.* **February 2017,** *14*, 44–55. DOI: 10.2174/1570193(13666161102151906.

[139] Kontham, V.; Padmaja, K.V. Tribological Studies of α-Lipoic Acid Esters as Effective Environmentally Friendly Multifunctional Lubricant Additives. *Energy Sources Part A* **September 2018,** *41*, 700–712. DOI: 10.1080/15567036.2018.1520352.

[140] Bhat, S.A.; Charoo, M.S. Effect of Additives on the Tribological Properties of Various Greases – A Review. *Mater. Today: Proc.* **2019,** *18*, 4416–4420. DOI: 10.1016/j.matpr.2019.07.410.

[141] Li, J.; Zhai, C.; Yin, H.; Wang, A.; Shen, L. Impact of Polydimethylsiloxanes on Physicochemical and Tribological Properties of Naphthenic Mineral Oil (KN 4010)-Based Titanium Complex Grease. *Chin. J. Chem. Eng.* **April 2019,** *27*, 944–948. DOI: 10.1016/j.cjche.2018.09.002.

[142] Ramesh, G.C.; Nagaraju, T.; Chowgi, S. Synthesis and Study of Bio-Lubricant from Jatropha Vegetable Oil. *SSRN Electronic J* **2018**. DOI: 1–4. DOI:10.2139/ssrn.3328410.

[143] Pirro, D.M.; Webster, M.; Daschner, E. *Lubrication Fundamentals, Revised and Expanded*; Boca, Raton: CRC PR INC, 2016.

[144] Rudnick, L.R.; Rudnick, L.R. *Synthetics, Mineral Oils, and Bio-Based Lubricants*, Boca, Raton: CRC Press, 2013. DOI: 10.1201/b13887.

[145] Reeves, C.J.; Siddaiah, A.; Menezes, P.L. A Review on the Science and Technology of Natural and Synthetic Biolubricants. *J Bio- and Tribo-Corrosion* **January 2017**, *3*, 1–27. DOI:10.1007/s40735-016-0069-5.

[146] Eastwood, J. Esters, The Most Versatile of Base Stock Technologies. *Lube Magazine* **October 2015**, *129*, 32–35.

[147] Honary, L.; Johnston, P.; Richter, E. *Biobased Lubricants and Greases: Technology and Products*; West Sussex: Wiley & Sons, Ltd., 2011.

[148] DIN EN ISO 6743-4:2015-11 Schmierstoffe, *Industrieöle und verwandte Erzeugnisse (Klasse L) – Klassifizierung – Teil 4: Familie H (Hydraulische Systeme) (ISO 6743-4:2015); Deutsche Fassung EN ISO 6743-4*:2015, 2015. DOI: 10.31030/2274814.

[149] Frauscher, M.; Besser, C.; Allmaier, G.; Dörr, N. Oxidation Products of Ester-Based Oils with and Without Antioxidants Identified by Stable Isotope Labelling and Mass Spectrometry. *Appl Sci* **April 2017,** *7*, 396, 1–18. DOI:10.3390/app7040396.

[150] Matiliunaite, M.; Paulauskiene, T. From Concept to Practice: Manufacturing of Bio-Lubricants from Renewable Resources. *Biomass Conversion and Biorefinery* **November 2018,** *9*, 353–361. DOI: 10.1007/s13399-018-0356-0.

[151] Fan, M.; Ai, J.; Hu, C.; Du, X.; Zhou, F.; Liu, W. Naphthoate Based Lubricating Oil with High Oxidation Stability and Lubricity. *Tribol. Int.* **October 2019,** *138*, 204–210. DOI: 10.1016/j.triboint.2019.05.039.
[152] Zhang, X.A.; Zhao, Y.; Ma, K.; Wang, Q. Friction Behavior and Wear Protection Ability of Selected Base Lubricants. *Friction* **March 2016,** *4*, 72–83. DOI: 10.1007/s40544-016-0106-x.
[153] Fan, M.; Ai, J.; Zhang, S.; Yang, C.; Du, X.; Wen, P.; Ye, X.; Zhou, F.; Liu, W. Lubricating Properties of Ester Oil Prepared from Bio-Based 2,5-Furandicarboxylic Acid. *Friction* **March 2019,** *8*, 360–369. DOI: 10.1007/s40544-019-0264-8.
[154] Xu, Z.; Lou, W.; Zhao, G.; Zhang, M.; Hao, J.; Wang, X. Pentaerythritol Rosin Ester as an Environmentally Friendly Multifunctional Additive in Vegetable Oil-Based Lubricant. *Tribol. Int.* **July 2019,** *135*, 213–218. DOI: 10.1016/j.triboint.2019.02.038.
[155] de Medeiros Castro, R.; Curi, E.I.M.; Inácio, L.F.F.; da Silva Rocha, A. Analysis of the Tribological Performances of Biodegradable Hydraulic Oils HEES and HEPR in the Sliding of Cu–Zn/WC–CoCr Alloys Using the Stribeck Curve. *J Braz Soc Mech Sci Eng* **November 2019**, *42*, 2, 1–20. DOI:10.1007/s40430-019-2080-5.
[156] Biresaw, G. Biobased Polyalphaolefin Base Oil: Chemical, Physical, and Tribological Properties. *Tribol. Lett.* **May 2018**, *66*, 76, 1–16. DOI:10.1007/s11249-018-1027-9.
[157] Qin, W.; Li, J.; Mao, Q.; Liu, Y.; Liu, Y.; Jiang, W.; Kang, J. Evolution of Tribological Mechanisms of Nano-Grained 304L Stainless Steel Under dry and Polyalphaolefin Lubrication Conditions. *Mater. Lett.* **May 2019,** *242*, 147–151. DOI: 10.1016/j.matlet.2019.01.135.
[158] Bulut, D.; Krups, T.; Poll, G.; Giese, U. Lubricant Compatibility of FKM Seals in Synthetic Oils. *Ind Lubrication and Tribol* **July 2019,** *72*, 557–565. DOI: 10.1108/ilt-02-2019-0065.
[159] Dresel, W.; Mang, T., Eds. *Lubricants and Lubrication*, Wiley-VCH Verlag GmbH & Co. KGaA: Weinheim, Germany, 2017. DOI: 10.1002/9783527645565.
[160] Hamid, S.; Burian, S.A. Polyphenyl Ether Lubricants. In Synthetics, *Mineral Oils, and Bio-Based Lubricants*; Rudnick, Leslie R., Ed.; CRC Press: Boca Raton, FL, USA, 2020; pp 181–188. DOI: 10.1201/9781315158150-9.
[161] Shylesh, S.; Gokhale, A.A.; Ho, C.R.; Bell, A.T. Novel Strategies for the Production of Fuels, Lubricants, and Chemicals from Biomass. *Acc. Chem. Res.* **September 2017,** *50*, 2589–2597. DOI: 10.1021/acs.accounts.7b00354.
[162] Sukjit, E.; Poapongsakorn, P.; Dearn, K.D.; Lapuerta, M.; Sánchez-Valdepeñas, J. Investigation of the Lubrication Properties and Tribological Mechanisms of Oxygenated Compounds. *Wear* **April 2017**, *376-377*, 836–842. DOI: 10.1016/j.wear.2017.02.007.
[163] Almasi, S.; Ghobadian, B.; Najafi, G.; Soufi, M.D. A Review on Bio-Lubricant Production from Non-Edible Oil-Bearing Biomass Resources in Iran: Recent Progress and Perspectives. *J. Cleaner Prod.* **March 2021,** *290*, 125830, 1–18. DOI:10.1016/j.jclepro.2021.125830.
[164] Ameen, N.H.A.; Durak, E. Study of the Tribological Properties the Mixture of Soybean Oil and Used (Waste) Frying oil Fatty Acid Methyl Ester Under Boundary Lubrication Conditions. *Renewable Energy* **January 2020,** *145*, 1730–1747. DOI: 10.1016/j.renene.2019.06.117.
[165] Orjuela, A.; Clark, J. Green Chemicals from Used Cooking Oils: Trends, Challenges, and Opportunities. *Curr. Opin. Green Sustain. Chem.* **December 2020,** *26*, 100369, 1–12. DOI:10.1016/j.cogsc.2020.100369.
[166] van Grinsven, A.; van den Toorn, E.; van der Veen, R.; Kampman, B. "Used Cooking Oil (UCO) Asbiofuel Feedstock in the EU", 2020.
[167] Mannu, A.; Ferro, M.; Dugoni, G.C.; Garroni, S.; Taras, A.; Mele, A. Response Surface Analysis of Density and Flash Point in Recycled Waste Cooking Oils. *Chem Data Collections* **February 2020,** *25*, 100329, 1–5. DOI:10.1016/j.cdc.2019.100329.
[168] Mannu, A.; Ferro, M.; Dugoni, G.C.; Panzeri, W.; Petretto, G.L.; Urgeghe, P.; Mele, A. Improving the Recycling Technology of Waste Cooking Oils: Chemical Fingerprint as Tool for Non-Biodiesel Application. *Waste Manage.* **August 2019,** *96*, 1–8. DOI: 10.1016/j.wasman.2019.07.014.
[169] Buczek, B.; Zajezierska, A. Biodegradable Lubricating Greases Containing Used Frying Oil as Additives. *Ind. Lubrication Tribol.* **June 2015,** *67*, 315–319. DOI: 10.1108/ilt-07-2013-0082.
[170] Abdulbari, H.A.; Zuhan, N. Grease Formulation from Palm Oil Industry Wastes. *Waste. Biomass. Valorization.* **2018,** *9*, 2447–2457. DOI: 10.1007/s12649-018-0237-6.
[171] Zhang, W.; Ji, H.; Song, Y.; Ma, S.; Xiong, W.; Chen, C.; Chen, B.; Zhang, X. Green Preparation of Branched Biolubricant by Chemically Modifying Waste Cooking Oil with Lipase and Ionic Liquid. *J. Cleaner Prod.* **November 2020,** *274*, 122918, 1 –11. DOI:10.1016/j.jclepro.2020.122918.
[172] Kurniawan, Y.S.; Thomas, K.; Hendra, J.; Wahyuningsih, T.D. Green Synthesis of Alkyl 8-(2-Butyl-5-Octyl-1, 3-Dioxolan-4-yl)Octanoate Derivatives as Potential Biolubricants from Used Frying Oil. *ScienceAsia* **2021,** *47*, 64–71. DOI: 10.2306/scienceasia1513-1874.2021.010.
[173] Pinheiro, C.T.; Quina, M.J.; Gando-Ferreira, L.M. Management of Waste Lubricant Oil in Europe: A Circular Economy Approach. *Crit. Rev. Environ. Sci. Technol.* **June 2020 ,** *51* (18), 1–36. DOI: 10.1080/10643389.2020.1771887.
[174] Thanikachalam, J.; Karthikeyan, S. Study on Extraction of Pollutant Freeflammable Fuel from Contaminatedautomobile Waste Lube Oil. *J. Achiev. Mater Manuf. Eng.* **2020,** *100*, 78–84. DOI: 10.5604/01.3001.0014.3348.
[175] Wen, C.; Wang, H.; Wang, L.; Lou, Z.; Sun, Z.; Zhou, Z. The Reduction of Waste Lubricant Oil Distillate Through the Enhancement of Organics Degradation by Ozonation with Elevated Temperature and Stable pH for the Zero Discharge. *J. Cleaner Prod.* **December 2019,** *240*, 118194, 1–7. DOI:10.1016/j.jclepro.2019.118194.
[176] Lins, T.S.; Pisoler, G.; Druzian, G.T.; Negris, L.; Decote, P.A.P.; Vicente, M.A.; Flores, E.M.M.; Santos, M.F.P. Base Oil Recovery from Waste Lubricant Oil by Polar Solvent Extraction Intensified by Ultrasound. *Env. Sci. Pollut. Res.* **July 2021,** *28*, 66000–66011. DOI: 10.1007/s11356-021-15582-y.
[177] Ostrikov, V.V.; Sazonov, S.N.; Balabanov, V.I.; Safonov, V.A. Manufacturing of Greases Based on Deep-Cleaned

Spent Mineral and Synthetic Motor Oils. *Pet. Chem.* **July 2017,** *57*, 705–713. DOI: 10.1134/s0965544117080096.

[178] Santos, J.C.O.; Almeida, R.A.; Carvalho, M.W.N.C.; Lima, A.E.A.; Souza, A.G. Recycling of Lubricating Oils Used in Gasoline/Alcohol Engines. *J. Therm. Anal. Calorim.* **February 2019,** *137*, 1463–1470. DOI: 10.1007/s10973-018-7976-2.

[179] Dudak, L.; Milisavljević, S.; Jocanović, M.; Kiss, F.; Šević, D.; Karanović, V.; Orošnjak, M. Life Cycle Assessment of Different Waste Lubrication Oil Management Options in Serbia. *Appl. Sci.* **July 2021,** *11*, 6652, 1–20. DOI:10.3390/app11146652.

[180] Lira, H.N.F.; Rangel, E.T.; Suarez, P.A.Z. Diesel-Like Fuels and Lubricating Grease Preparation from an Industrial Oily Waste. *Waste. Biomass. Valorization.* **January 2018,** *9*, 2459–2470. DOI: 10.1007/s12649-018-0200-6.

[181] Papadaki, A.; Fernandes, K.V.; Chatzifragkou, A.; Aguieiras, E.C.G.; da Silva, J.A.C.; Fernandez-Lafuente, R.; Papanikolaou, S.; Koutinas, A.; Freire, D.M.G. Bioprocess Development for Biolubricant Production Using Microbial Oil Derived via Fermentation from Confectionery Industry Wastes. *Bioresour. Technol.* **November 2018,** *267*, 311–318. DOI: 10.1016/j.biortech.2018.07.016.

[182] Gozbenko, V.E.; Kargapoltsev, S.K.; Karlina, A.I. Synthesis and Structure of Sulfur-Containing Polymers Based on Polymer Industrial Waste Applied for Rail Lubrication. *IOP Publish.* **2019**, *229*, 012021, 1–6. DOI:10.1088/1755-1315/229/1/012021.

[183] Almeida, M.O.; Silva, L.R.R.; Kotzebue, L.R.V.; Maia, F.J.N.; Acero, J.S.R.; Mele, G.; Mazzetto, S.E.; Sinatora, A.; Lomonaco, D. Development of Fully Bio-Based Lubricants from Agro-Industrial Residues Under Environmentally Friendly Processes. *Eur. J. Lipid Sci. Technol.* **February 2020,** *122*, 1900424, 1–11. DOI:10.1002/ejlt.201900424.

[184] Unugul, T.; Kutluk, T.; Kutluk, B.G.; Kapucu, N. Environmentally Friendly Processes from Coffee Wastes to Trimethylolpropane Esters to be Considered Biolubricants. *J. Air Waste Manage. Assoc.* **October 2020,** *70*, 1198–1215. DOI: 10.1080/10962247.2020.1788664.

[185] Pichler, J.; Eder, R.M.; Widder, L.; Varga, M.; Marchetti-Deschmann, M.; Frauscher, M. "Towards Green Lubrication: Tribological Behaviour and Chemical Characterization of Spent Coffee Grounds Oil", [Manuscript submitted for publication], 2023.

[186] Xie, M.; Cheng, J.; Zhao, G.; Liu, H.; Zhang, L.; Yang, C. Natural Wax from Non-Medicinal Aerial Part of *Codonopsis pilosula* as a Biolubricant. *J. Cleaner Prod.* **January 2020,** *242*, 118403, 1–11. DOI:10.1016/j.jclepro.2019.118403.

[187] Cai, Z.; Zhuang, X.; Yang, X.; Huang, F.; Wang, Y.; Li, Y. Litsea Cubeba Kernel Oil as a Promising New Medium-Chain Saturated Fatty Acid Feedstock for Biolubricant Base Oil Synthesis. *Ind. Crops Prod.* **September 2021,** *167*, 113564, 1–9. DOI:10.1016/j.indcrop.2021.113564.

[188] Attard, T.M.; McElroy, C.R.; Rezende, C.A.; Polikarpov, I.; Clark, J.H.; Hunt, A.J. Sugarcane Waste as a Valuable Source of Lipophilic Molecules. *Ind. Crops Prod.* **December 2015,** *76*, 95–103. DOI: 10.1016/j.indcrop.2015.05.077.

[189] Spasiano, D.; Petrella, A.; Lacedra, V. Chemical Destabilization of Fresh and Spent Cutting Oil Emulsions: Differences Between an Ecofriendly and Two Commercial Synthetic Lubricants. *Sustainability* **July 2020,** *12*, 5697, 1–10. DOI:10.3390/su12145697.

[190] Oliver, V.; Andras, H.; Geza, V.; Artur, T.; Jeno, H. Bio-paraffin Mixture Production from Waste Lard. *Chem. Eng. Trans.* **2019,** *76*, 1351–1356. DOI: 10.3303/CET1976226.

[191] Angulo, B.; Fraile, J.M.; Gil, L.; Herrerías, C.I. Bio-lubricants Production from Fish oil Residue by Transesterification with Trimethylolpropane. *J. Cleaner Prod.* **November 2018,** *202*, 81–87. DOI: 10.1016/j.jclepro.2018.07.260.

[192] Padgurskas, J.; Rukuiža, R.; Mandziuk, I.; Kupcinskas, A.; Prisyazhna, K.; Grigoriev, A.; Kavaliova, I.; Revo, S. Tribological Properties of Beef Tallow as Lubricating Grease. *Ind. Lubric. Tribol.* **September 2017,** *69*, 645–654. DOI: 10.1108/ilt-01-2016-0014.

[193] Wu, S.-q.; Cai, Z.-z.; Niu, Y.; Zheng, D.; He, G.-r.; Wang, Y.; Yang, D.-p. A Renewable Lipid Source for Biolubricant Feedstock Oil from Housefly (*Musca domestica*) Larva. *Renewable Energy* **December 2017,** *113*, 546–553. DOI: 10.1016/j.renene.2017.05.094.

[194] Latha, P.P.; Singh, R.K.; Kukrety, A.; Saxena, R.C.; Bhatt, M.; Jain, S.L. Poultry Chicken Feather Derived Biodegradable Multifunctional Additives for Lubricating Formulations. *ACS. Sustain. Chem. Eng.* **February 2016,** *4*, 999–1005. DOI: 10.1021/acssuschemeng.5b01071.

[195] Celik, G.; Kennedy, R.M.; Hackler, R.A.; Ferrandon, M.; Tennakoon, A.; Patnaik, S.; LaPointe, A.M.; Ammal, S.C.; Heyden, A.; Perras, F.A.; Pruski, M.; Scott, S.L.; Poeppelmeier, K.R.; Sadow, A.D.; Delferro, M. Upcycling Single-Use Polyethylene Into High-Quality Liquid Products. *ACS. Cent. Sci.* **October 2019,** *5*, 1795–1803. DOI: 10.1021/acscentsci.9b00722.

[196] Odigure, J.O.; Abdulkareem, A.S.; Jimoh, A.; Okafor, J.O.; Abiodun, A.A. Synthesis and Characterization of Lubricant Additives from Waste Plastic. *Energy Sources Part A* **September 2015,** *37*, 1846–1852. DOI: 10.1080/15567036.2011.654314.

[197] Souza, R.S.; Visconte, L.L.Y.; da Silva, A.L.N.; Costa, V.G. Thermal and Rheological Formulation and Evaluation of Synthetic Bitumen from Reprocessed Polypropylene and Oil. *Int. J. Polym. Sci.* **August 2018,** *2018*, 1–6. DOI: 10.1155/2018/7940857.

[198] Hackler, R.A.; Vyavhare, K.; Kennedy, R.M.; Celik, G.; Kanbur, U.; Griffin, P.J.; Sadow, A.D.; Zang, G.; Elgowainy, A.; Sun, P.; Poeppelmeier, K.R.; Erdemir, A.; Delferro, M. Synthetic Lubricants Derived from Plastic Waste and Their Tribological Performance. *ChemSusChem.* **June 2021,** *14*, 4181–4189. DOI: 10.1002/cssc.202100912.

[199] Kots, P.A.; Vance, B.C.; Vlachos, D.G. Polyolefin Plastic Waste Hydroconversion to Fuels, Lubricants, and Waxes: A Comparative Study. *Reaction Chem Eng* **2022,** *7*, 41–54. DOI: 10.1039/d1re00447f.

[200] Liu, S.; Kots, P.A.; Vance, B.C.; Danielson, A.; Vlachos, D.G. Plastic Waste to Fuels by Hydrocracking at Mild Conditions. *Sci. Adv.* **April 2021**, *7*, 1–9. DOI:10.1126/sciadv.abf8283.

[201] Zeng, M.; Lee, Y.-H.; Strong, G.; LaPointe, A.M.; Kocen, A.L.; Qu, Z.; Coates, G.W.; Scott, S.L.; Abu-Omar, M.M. Chemical Upcycling of Polyethylene to Value-Added α,

ω-Divinyl-Functionalized Oligomers. *ACS. Sustain. Chem. Eng.* **October 2021,** *9*, 13926–13936. DOI: 10.1021/acssuschemeng.1c05272.

[202] Dey, S.; Deb, M.; Das, P. Chemical Characterization and Tribological Behavior of Kitchen Chimney Dump Lard (KCDL) as a Bio-Lubricant. *Revue des composites et des matériaux avancés* **August 2019,** *29*, 145–150. DOI: 10.18280/rcma.290303.

[203] Gajdoš, P.; Hambalko, J.; Slaný, O.; Čertík, M. Conversion of Waste Materials Into Very Long Chain Fatty Acids by the Recombinant Yeast Yarrowia Lipolytica. *FEMS Microbiol. Lett.* **March 2020**, *367*, 1–8. DOI:10.1093/femsle/fnaa042.

[204] Sivakumar, B.; Ranjan, N.; Ramaprabhu, S.; Kamaraj, M. Tribological Properties of Graphite Oxide Derivative as Nano-Additive: Synthesized from the Waster Carbon Source. *Tribol. Int.* **February 2020,** *142*, 105990, 1–12. DOI:10.1016/j.triboint.2019.105990.

[205] Okoro, E.E.; Erivona, N.O.; Sanni, S.E.; Orodu, K.B.; Igwilo, K.C. Modification of Waste Tire Pyrolytic Oil as Base Fluid for Synthetic Lube Oil Blending and Production: Waste Tire Utilization Approach. *J. Mater. Cycles Waste Manage.* **March 2020,** *22*, 1258–1269. DOI: 10.1007/s10163-020-01018-1.

[206] Rudnick, L.R. *Synthetics, Mineral Oils, and Bio-Based Lubricants*; Boca, Raton: CRC Press, 2006. DOI: 10.1201/9781420027181.

[207] Mang, T.; Dresel, W. *Lubricants and Lubrication*; Weinheim: Wiley-VCH John Wiley Distributor, 2007. DOI: 10.1002/9783527610341.ch7.

[208] Besser, C.; Pisarova, L.; Frauscher, M.; Hunger, H.; Litzow, U.; Orfaniotis, A.; Dörr, N. Oxidation Products of Biodiesel in Diesel Fuel Generated by Artificial Alteration and Identified by Mass Spectrometry. *Fuel* **October 2017,** *206*, 524–533. DOI: 10.1016/j.fuel.2017.06.038.

[209] Srivastava, S.P. *Developments in Lubricant Technology*; Wiley: Hoboken, 2014. DOI: 10.1002/9781118907948.

[210] Wu, Y.; Li, W.; Wang, X. The Influence of Oxidation on the Tribological Performance of Diester Lubricant. *Lubr. Sci.* **July 2013,** *26*, 55–65. DOI: 10.1002/ls.1229.

[211] Salih, N.; Salimon, J.; Abdullah, B.M.; Yousif, E. Thermo-Oxidation, Friction-Reducing and Physicochemical Properties of Ricinoleic Acid Based-Diester Biolubricants. *Arab. J. Chem.* **May 2017,** *10*, S2273–S2280. DOI: 10.1016/j.arabjc.2013.08.002.

[212] Frauscher, M.; Agocs, A.; Ristic, A.; Dörr, N. Correlation of Lubricant Degradation and Performance of a Biodegradable Hydraulic Fluid, in TAE Book of Abstracts, Ostfildern, 2020.

[213] Frauscher, M.; Besser, C.; Allmaier, G.; Dörr, N. Elucidation of Oxidation and Degradation Products of Oxygen Containing Fuel Components by Combined Use of a Stable Isotopic Tracer and Mass Spectrometry. *Anal. Chim. Acta* **November 2017,** *993*, 47–54. DOI: 10.1016/j.aca.2017.09.009.

[214] Organisation for Economic Cooperation and Development (OECD). Test No. 301: Ready Biodegradability, OECD, 1992. DOI: 10.1787/9789264070349-en.

[215] Nowak, P.; Kucharska, K.; Kamiński, M. Ecological and Health Effects of Lubricant Oils Emitted Into the Environment. *Int. J. Environ. Res. Public Health* **August 2019,** *16*, 3002, 1–13. DOI:10.3390/ijerph16163002.

## 2.2 Publication II - Moving towards green lubrication: tribological behavior and chemical characterization of spent coffee grounds oil

Authors: Jessica Pichler, Rosa Maria Eder, Lukas Widder, Markus Varga, Martina Marchetti-Deschmann & Marcella Frauscher
Journal: Green Chemistry Letters and Reviews, 16:1, 2215243, 2023
DOI: 10.1080/17518253.2023.2215243

The publication is reprinted on the following pages.

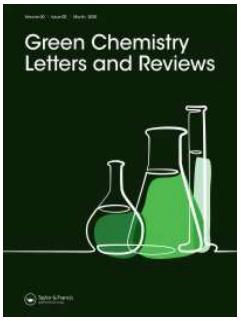

Green Chemistry Letters and Reviews

ISSN: (Print) (Online) Journal homepage: www.tandfonline.com/journals/tgcl20

# Moving towards green lubrication: tribological behavior and chemical characterization of spent coffee grounds oil

Jessica Pichler, Rosa Maria Eder, Lukas Widder, Markus Varga, Martina Marchetti-Deschmann & Marcella Frauscher

**To cite this article:** Jessica Pichler, Rosa Maria Eder, Lukas Widder, Markus Varga, Martina Marchetti-Deschmann & Marcella Frauscher (2023) Moving towards green lubrication: tribological behavior and chemical characterization of spent coffee grounds oil, Green Chemistry Letters and Reviews, 16:1, 2215243, DOI: 10.1080/17518253.2023.2215243

**To link to this article:** https://doi.org/10.1080/17518253.2023.2215243



Published online: 29 May 2023.

GREEN CHEMISTRY LETTERS AND REVIEWS
2023, VOL. 16, NO. 1, 2215243
https://doi.org/10.1080/17518253.2023.2215243

Taylor & Francis
Taylor & Francis Group



# Moving towards green lubrication: tribological behavior and chemical characterization of spent coffee grounds oil

Jessica Pichler[a,b], Rosa Maria Eder [a], Lukas Widder [a], Markus Varga [a], Martina Marchetti-Deschmann [b] and Marcella Frauscher [a]

[a]AC2T research GmbH, Wiener Neustadt, Austria; [b]Institute of Chemical Technologies and Analytics, TU Wien, Vienna, Austria

**ABSTRACT**

With the EU aiming for net-zero greenhouse gas emissions by 2050, conventional production cycles must be transformed into cradle-to-cradle approaches. Spent coffee grounds are often dumped in landfills, with their potential as high-quality feedstock for biofuel or bio-lubricant production. Spent coffee grounds oil (SCGO) was investigated for its physicochemical properties while having more free acid groups compared to the reference polyalphaolefin 8 (PAO 8), which may cause faster oxidation. TGA results displayed comparable thermal stability of SCGO and PAO 8 for inert/oxidative atmosphere. The oil composition was characterized by ATR-FTIR, elemental analysis, and GC-EI-MS, where a higher oxygen content was found for SCGO, referring to functional ester/acid groups. The tribological behavior of SCGO was studied as lubricant base oil and as a 5% additive in PAO 8. The condition of fresh and tribologically used oils was investigated with High-Resolution-ESI-MS, and the worn surfaces were evaluated by light microscopy and topographic analysis. The results showed a superior friction coefficient of pure SCGO ($\mu = 0.092$) to PAO 8 ($\mu = 0.129$). The 5% SCGO additive in PAO 8 ($\mu = 0.095$) could significantly reduce friction compared to pure PAO 8 on an unpolished 100Cr6 surface.

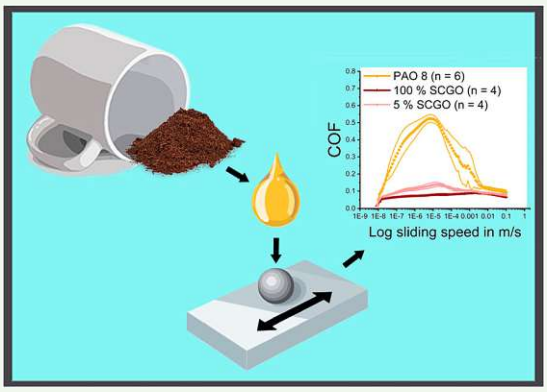


**ARTICLE HISTORY**
Received 25 January 2023
Accepted 12 May 2023

**KEYWORDS**
Tribology; sustainability; recycling; life-cycle assessment; biolubrication

## Introduction

Within the USA, the production of lubricants from renewable resources is facilitated by the USDA (U. S. Department of Agriculture) BioPreferred Program, where 139 bio-based product categories with mandatory purchasing requirements for agencies and contractors are currently listed, which is already 75 categories more than stated by Rudnick et al. in 2020 (*1*). These categories include engine oils, chain- and cable lubricants, transformer fluids, metalworking fluids, gear lubricants, intermediates, and additives for lubricant formulation and come with a minimum renewable biological content, which for lubricants lies within 25% for (wheel bearing and chassis) greases and 95% for transformer fluids (vegetable-oil based) (*2*). However, similar pull marketing strategies are currently missing in the EU.

In Europe, the year 2021 marked the beginning of a more sustainable future by bringing the European Green Deal (Regulation (EU) No 2018/1999 of the European Parliament and of the Council) (*3*) to life. Along with the Circular Economy Action Plan, the 2030 Climate Target Plan, and the Fit For 55 package, addressing the 55% of net greenhouse gas emission

**CONTACT** Jessica Pichler jessica.pichler@ac2t.at AC2T research GmbH, Viktor-Kaplan-Straße 2C, Wiener Neustadt 2700, Austria

reduction by 2030 compared to 1990 levels, Europe is heading towards climate neutrality by 2050 (*4*).

In other words, standard lubrication systems mainly of petroleum-based origin need to be adapted to reach the goals addressed by the Green Deal, such as achieving an energy portion of 32.5% from renewable sources by 2030 (*3*). There is an increasing interest in the generation of lubricants from alternative sources, e.g. lubricants from used cooking oils (UCO). However, nearly 90% of these UCOs are used as UCO methyl esters (UCOME) for biodiesel (*5*).

Within the European Union, Directive (EU) 2018/851, an amendment to Directive 2008/98/EC on waste, provides improved waste management requirements and guidance addressing the whole life-cycle of products, thus, promoting the idea of a truly circular economy (*6*). Considering waste as a valuable resource can reduce its environmental impact, which is necessary to protect, preserve and improve the quality of the environment. The sustainability roadmap of the European Circular Economy package aims at a recycling rate of 55% of municipal waste by 2025, a separate collection of hazardous household waste by 2022, and bio-waste by 2023 (*7*). The Directive advises member states to take responsibility for preventing waste generation in the first place or otherwise to implement suitable long-term recovery strategies for re-using and recycling waste material. These include processes that promote and support sustainable production and consumption, design-to-recycle or reuse, food waste reduction in primary production and food donation, reduction of industrial waste products, and the determination of primary sources of natural and marine litter (*6*).

In this regard, within the scope of this work, the focus was on SCGO as a sustainable, waste- and bio-based lubricant, or lubricant additive, which could contribute to achieving the climate goals set in the European Green Deal. Furthermore, it should comply with the concept of a circular economy and meet the high standards of the EU Ecolabel (*8*).

According to a study, almost 10,200,000 tonnes of coffee is consumed globally per year (2020); for Austria, this number is 46,000 tonnes (2018), which results in 10.1 kg (2019) of coffee per person annually (*9*). Making a rough estimation for the Austrian market, with a recycling rate of just 10%, 4,600 tonnes of spent coffee grounds (SCGs) could be collected annually, yielding 690 tonnes of SCGO (based on 15% oil content of dry SCGs).

SCGs, with a lipid content of 11-20% (dry weight basis) (*10*), are often considered a sustainable feedstock for biodiesel production (*10–14*). Efthymiopoulos (*10*) is providing a comprehensive study investigating the reuse of SCGs as an energy source, considering that SCGs contain compounds, which may be seen as pollutants when disposed of at landfills (*10*). By-products from coffee processing, such as SCGs and raw coffee husks, are described as phytotoxic due to components such as caffeine, tannins, and other polyphenols (*15,16*). An evaluation of the toxicity and/or biodegradability of SCGO could not yet be found in the literature.

Comparing the efficiency of different extraction methods, such as Soxhlet extraction (SE), ultrasonic extraction and microwave-assisted extraction (MAE), on dried SCGs with n-hexane and petroleum benzene SE provides the highest total yield of SCGO but cannot keep up with the low amounts of solvents and extraction time needed for the other methods. With supercritical fluid extraction (SFE) with $CO_2$, a change in fatty acid composition depending on temperature, pressure, type of modifier and modifier volume could be observed (*20*). These insights were confirmed when SCGs were extracted with MAE and conventional SE, where MAE seemed far superior with a 24-fold increase in efficiency, implying that less solvent per gram oil collected is needed (*21*). Another approach comprises enzymatic hydrolysis of crude SCGO to free fatty acids (FFAs) and further esterified with trimethylol-propane (TMP), which resulted in TMP esters useful for bio lubricant production (*22*).

Al-Hamamre et al. (*18*) extracted dried SCGO with different polar (isopropanol, ethanol, and acetone) and non-polar (toluene, chloroform, hexane, and n-pentane) solvents by SE before further converting free fatty acids to fatty acid methyl esters by two-step transesterification. Hexane showed the highest oil yield after 30 min of extraction with 15.28%, a low free fatty acid content and acid value. Based on these results, the herein-used extraction parameters were chosen since the proposed process is well-established.

Although many studies address different extraction methods and oil yield from SCGs, as highlighted above, only one is investigating SCGO tribologically: Grace et al. (*17*) tested SCGO as base oil with 1, 2.5 and 5 wt% of phosphonium-based ionic liquids (ILs) as an additive in a steel-steel contact on a reciprocating block-on-flat tribometer. The SCGO ILs are compared to a fully formulated commercially available wind turbine gearbox lubricant. In these experiments, ILs as additives to SCGO could reduce wear values and wear volume, and some could also reduce the coefficient of friction (COF).

Since a high potential of SCGO as a base lubricant or additive component can be assumed, tribological behavior is the main focus of this work. At first, the power of SCGOs to contribute to the greening of

industrial applications was assessed by a comprehensive SCGO life-cycle assessment from production to application. A further step was optimizing the extraction method to ensure the reproducibility and stability of the molecular content and its distribution throughout multiple extraction batches. The obtained SCGO was thoroughly examined regarding its physicochemical properties and characteristic qualities.

In this work, we want to increase knowledge in the tribological field and further evaluate the properties of SCGO in terms of friction and wear. Therefore, we applied tribological testing in steel/steel contact primarily to determine the possible operational range and operating conditions of SCGO in industrial applications and compared our findings to well-established PAO base oil. Additionally, a life cycle assessment comprised an upscaling from lab scale to industrial production to highlight critical aspects of environmental and toxicity impacts and energy consumption.

## Experimental

### Materials and consumables

SCGs from different companies (Amaroy Wiener Mischung/ Hofer, Eduscho Gala Nr. 1/Eduscho, and Spezial/ J. Hornig) were collected. PAOs were supplied by OMV, Austria. N-hexane (≥ 99%; Roth, Germany) was used for extraction, sulfanilic acid (≥ 99%; VWR Chemicals, Germany) and benzoic acid (≥ 99.5%, Merck, Germany) purchased through Elementar Analysensysteme GmbH were used as standards for CHNSO elemental analysis. Dichloromethane (DCM; ≥ 99.9%; Sigma-Aldrich, USA) and N,O-Bis-(trimethylsilyl)trifluoroacetamide with trimethylchlorosilane (BSTFA + TMCS; 99%; Sigma-Aldrich, Switzerland) were used for GC-MS analysis; the latter acted as a derivatization agent. For Karl-Fischer titration solution HYDRANAL™ – Coulomat AG-Oven (Honeywell Fluka, Germany) was used. EMSURE® KOH pellets for acid number (AN) evaluation were obtained from Supelco, Germany (≥ 85.0%). For High-Resolution (HR)-MS analyzes, isopropanol (≥ 99.95%; Roth, Germany) and methanol (≥ 99.9%; Supelco, Germany) were used. Material surfaces were cleaned threefold with isopropanol (≥ 98%; VWR, Austria), acetone (≥ 99%; VWR, Austria), and petrol ether (≥ 99.5%; VWR, France).

### Sample collection

Collected SCGs were dried in an oven for 24 h at 105 °C to remove moisture. Soxhlet extraction (SE), with n-hexane as the organic solvent, was chosen to extract crude oil from the SCGs. About 20 g of dried SCGs were weighed into a thimble in the Soxhlet extraction chamber. Extraction was performed at 140 °C device temperature (after a few rounds of optimization due to heat loss within the setup hot plate + silicon oil bath) with 200 ml of n-hexane under reflux until the solvent in the extraction chamber was fully clear/colourless (5-8 h). Afterwards, the solvent was removed on a rotary evaporator (Basis HEI-VAP ML, Heidolph, Germany) at 334 mbar, 100 rpm and 50 °C for 90 min.

The moisture content of SCG was calculated from wet weight (g) and dry weight (g) as the amount of water (g) divided by the total weight (g). The crude oil yield was calculated as the amount of oil extracted (g) divided by the amount of dry SCGs used (g).

### Characterization methods

#### Physicochemical properties of SCGO

Rheology measurements were carried out on a rheometer (MCR 302, Anton Paar, Austria) with 50 mm cone-plate measuring geometry within shear rates from 0.1 to 100 $s^{-1}$ and a temperature of 30 °C to determine similar viscosity ranges for SCGO and PAO reference oils and choose the best rheological reference fit for SCGO. The matrix of all executed measurements is shown in Table 1.

The water content was determined according to DIN 51777 (direct and indirect method) by Karl-Fischer (KF) titration (831 KF Coulomat and 890 Titrando, Metrohm Inula GmbH, Austria), the AN (mg KOH/g) was evaluated according to DIN 51558-2. The thermal stability was examined up to 450 °C under a synthetic air atmosphere and up to 500 °C under an $N_2$ atmosphere by thermogravimetric analysis (TGA) and differential scanning calorimetry (DSC)/differential thermal analysis (DTA) on a thermo-gravimetric analyser (STA 449 F3 Jupiter, Netzsch, Germany) with a heating rate of 10 °C/min and initial sample weights ~10 mg in Al crucibles. The derivative (DTG) of the TG-signal over time was drawn, and a Savitzky–Golay filter was applied.

**Table 1.** Experimental matrix for SCGO and PAO 8, selected as reference lubricant.

| | | SCGO | | | | | | Reference PAO 8 | | |
|---|---|---|---|---|---|---|---|---|---|---|
| wt% | | 100 | | | 5 | | | 100 | | |
| No. | | 1 | 2 | 3 | 1 | 2 | 3 | 1 | 2 | 3 |
| Rheometer | Stribeck | X | X | x | x | x | x | x | x | x |
| | oscillating | X | X | - | x | x | - | x | x | x |
| Nanotribo-meter | oscillating | X | X | x | x | x | x | x | x | x |
| Physico-chemical | IR | X | – | – | – | – | – | x | – | – |
| | Viscosity | X | – | – | x | – | – | x | – | – |
| | AN | x | – | – | – | – | – | x | – | – |
| | Water | x | – | – | – | – | – | x | – | – |
| TGA/DSC | | x | – | – | – | – | – | x | – | – |
| CHNSO | CHNS | x | X | x | – | – | – | x | x | x |
| | O | x | X | x | – | – | – | x | x | x |

### Determination of oil composition

The elemental composition of the oil was characterized by CHNSO elemental analysis (varioMACROcube, elementar, Germany) with He as carrier gas at 1150 °C (CHNS-mode) or 1170 °C (O-mode). Sulfanilic acid was used as the standard substance for CHNS mode, and benzoic acid was used as a standard substance for O mode. Liquid samples were weighed in tin capsules, tightly sealed under Argon atmosphere, and measured in doublet. ATR-FTIR was recorded in a spectral range of 4000-600 $cm^{-1}$ and a wavenumber resolution of 4 $cm^{-1}$ (Tenor 27, Bruker Optik GmbH, Germany).

GC-EI-MS (TQ8040; Shimadzu, Germany) determined the fatty acid distribution with AOC-20i + s autosampler diluted four wt% in dichloromethane with 18 wt% of BSTFA as a silylation agent. The sample was silylated for one h at 70 °C.

Table 2 shows the measurement conditions of the GC-MS analysis. All samples were analyzed twice in independent repetitions.

### Tribological experiments

SCGO was tested as a base oil (100%) and five wt% diluted in PAO 8 (SCGO as additive). Tribological tests were conducted on a rheometer (MCR302) and nanotribometer (NTR³) from Anton Paar, Austria. The rheometer tribo-measurements were executed in unidirectional rotation and rotational oscillating motion with a 12.7 mm diameter 100Cr6 ball vs 100Cr6 base bodies in a ball-on-three-discs (45°) geometry. The rotational motion was used to determine the frictional behavior of the lubricated interface as a so-called Stribeck curve. The rotational oscillating motion was used to compare friction and wear to results obtained using the nanotribometer with a linear oscillating motion. The parameters of the tribological tests are given in Table 3.

The nanotribometer measurements were performed linearly oscillated using a 2 mm diameter 100Cr6 ball on various base bodies (ball-on-disc setup). The base bodies included: (a) unpolished 1.4301 stainless steel plates (from now on referred to as S-SSUP); (b) unpolished 100Cr6 discs (S-CRUP); and (c) polished 100Cr6 plates (polished in-house; S-CRP) and are summarized in Table 4. Used base bodies exhibit varying surface roughness to determine more detailed insight into SCGO tribological behavior.

Since the rheometer and nanotribometer have different system setups, the rheometer parameters were adjusted to apply an identical Hertzian contact pressure in both experimental designs. The stroke distance on the rheometer for rotational oscillation was calculated through the angular deflection of 111.24 mrad (equals a stroke of 500 µm), dependent on the instrument geometry.

Tribological tests on the nanotribometer and rheometer were carried out for 900 cycles per minute for 15 and 120 min. Fifty data points were collected tip-to-tip (25 data points per stroke) per cycle on the nanotribometer and 20 data points (10 per strike) on the rheometer. The data was then treated and reduced as follows: the absolute friction values of a cycle were taken and reduced to 60% of the mean range of each stroke to discard acceleration and deceleration motion data from the stroke-end turning positions. The data was further reduced to one value per cycle. Hence, 900 (nanotribometer) and 7200 (rheometer) values in total averaged over (a) three (nanotribometer) and (b) two (rheometer) measurement repetitions. Finally, the mean value with a standard deviation of (a) three and (b) two measurements, plus the 1st decile ($Q_{0.1}$) and

**Table 2.** GC-MS instrument and method parameters for SCGO characterisation.

| Properties | Specification |
|---|---|
| Carrier gas | Helium |
| Linear velocity | 51.6 cm/s |
| Column dimensions | 5% diphenyl/95% dimethyl polysiloxane, 30 m × 0.25 mm × 0.25 µm |
| Injector | Type: PTV Split (25:1) Injection Volume: 1 µl |
| Oven temperature ramp | 1 min hold at 60, 10 °C/min to 300 °C, hold for 20 min |
| Transfer temperature | 250 °C |
| MS source temperature | 200 °C |

**Table 3.** Parameters for the rotational and linear tribological experiments on the rheometer and nanotribometer.

| | Rheometer | | Nanotribometer |
|---|---|---|---|
| Operational Mode | Unidirectional rotation | Rotational oscillation | Linear oscillation |
| Load $F_N$ in N | 5 | 20.17 | 1 |
| Temp. in °C | 30 | 30 | 25 |
| Hertzian Contact Pressure in GPa | – | 1.37 | 1.37 |
| Distance in µm | – | 500 | 500 |
| Frequency in Hz | – | 1 | 1 |
| Sliding speed in m/s | $10^{-8}$–0.1 | $10^{-3}$ | $10^{-3}$ |

**Table 4.** Material surfaces and properties for tribological measurements.

| Material | Abbrev. | Surface roughness $R_q$ in µm | Reduced valley depth $S_{vk}$ in µm | Valley material portion $S_{Mr2}$ in % |
|---|---|---|---|---|
| 1.4301 stainless steel | S-SSUP | 0.156 ± 0.035 | 0.61 ± 0.14 | 83.24 ± 1.12 |
| 100Cr6 | S-CRUP | 0.086 ± 0.007 | 0.16 ± 0.01 | 82.51 ± 0.53 |
| 100Cr6 | S-CRP | 0.007 ± 0.002 | 0.01 ± 0.00 | 90.19 ± 1.30 |

90% quantile ($Q_{0.9}$) are displayed in Figure 6. The standard deviation of uncertainty within measurement repetitions is given as error bars in the figures. For the oscillatory rheometer measurement, the wear scars of the three tested oils were further evaluated with two-dimensional microscopy and three-dimensional topographic analysis with values displayed as a mean of six surface characterizations (three discs times two runs).

For the rheometer oscillatory measurements composition of the three oils and possible ageing effects during the tribological experiments were investigated by High-Resolution (Orbitrap)-Electrospray Ionization (ESI)-MS in positive and negative ion mode. The pre- and post-rheometer test oil samples were diluted 1:1000 in methanol/isopropanol (1:1 wt%) for further mass spectrometric examinations.

Relevant surface roughness parameters for the oil retention volume, the reduced valley depth $S_{vk}$ and the valley material portion $S_{Mr2}$ were determined by three individual topography measurements of 600 µm x 600 µm scan size (Leica DCM8, Leica Microsystems GmbH, Switzerland) via the area material ratio curve or Abbott-Firestone curve and are given in Table 4.

## Results and discussion

### SCGO extraction

The crude oil yield varied between 9.5 wt% to 20.3 wt% of dry SCGO with a mean yield of approximately 14 wt%. The moisture content of the wet SCGs (before drying in the oven) showed a mean of 70 wt% (ranging from 60 wt% to 75 wt%) for different SCG types. A mixture of three different extraction batches and five SCG types was used for further analysis.

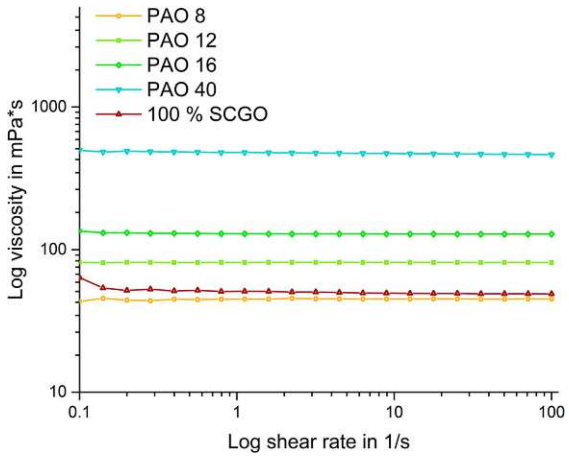


**Figure 1.** Dynamic viscosity measurement of different viscous PAOs and 100% SCGO over a shear rate of 0.1–100 $s^{-1}$.

**Table 5.** Chemical properties of SCGO and elemental composition.

| Oil Type | AN in mg KOH/g | Water in wt % | Elemental analysis in wt% | | | | |
|---|---|---|---|---|---|---|---|
| | | | C | H | N | S | O |
| PAO 8 | 0.05 | 0.007 | 85.2 | 14.1 | 0.4 | 0.1 | 0.0 |
| SCGO | 4.83 | 0.029 | 75.4 | 11.5 | 1.1 | 0.2 | 9.9 |
| SCGO (*18*) | 7.38 | – | 79.1 | 11.1 | 0.2 | 0 | 9.6[a] |

[a]Calculated.

### Physicochemical properties of SCGO

First, the SCGO's viscosity was characterized to identify a matching reference oil. The dynamic viscosity of different viscous PAOs (Figure 1) was measured on the rheometer, with PAO 8 being the best fit. Over the range of 0.1–100 $s^{-1}$ at 30 °C the mean viscosity of PAO 8 was at 44.92 mPa·s and for 100% SCGO at 51.08 mPa·s, which coincides with viscosity values for SCGOs already described in the literature: The kinematic viscosity of SCGO at 40 °C was determined between 49.6-55.5 $mm^2/s$ and 9.4-9.9 $mm^2/s$ at 100 °C when extracted with n-hexane as the solvent (*13*,*17*,*18*). The dynamic viscosity resulted in 60 mPa·s at 40 °C and 8.7 mPa·s at 100 °C (*18*).

In Table 5, the chemical properties of the SCGO and PAO 8, such as the AN, the water content, and the elemental content of carbon, hydrogen, nitrogen, sulfur, and oxygen, are given. A low AN, which determines the number of carboxylic acid groups within the oil, accounts for a more oxidatively stable oil since it contains fewer free fatty acids. The AN of SCGO measured within the scope of this work is relatively low, with a value of 4.83 mg KOH/g and considerably lower than the value of 7.38 mg KOH/g reported by Al-Hamamre et al. (*18*) which could be due to different oil extraction procedures. Nitrogen, sulfur, and hydrogen contents differ slightly for PAO 8 and SCGO; a more significant difference is visible for the oxygen content of 9.92% for SCGO (deriving from ester groups) and 0.02% for PAO 8 (a pure hydrocarbon liquid). The water content for both oils is below 0.05 wt%.

Previous research studies have found the following properties of SCGO: cloud point of 12.2 °C (ASTM D5773), pour point of 7.0 °C (ASTM D5949), lubricity at 60 °C of 180 µm (ASTM D6079), specific gravity of 0.94 (AOCS Cc 10c-95), and rancimat index (110 °C; indicating oxidative stability; EN 15751) of 8.4 h (*13*). The density at 23 °C is 0.85 $g/cm^3$, and the thermal degradation of SCGO up to 300 °C is below one wt% (*17*). With the use of different extraction solvents, the saponification value of SCGO varies from 171 to 223 mgKOH/g, the acid number from 6.5–12.8 mgKOH/g, the ester number between 167–214 mgKOH/g, the free fatty

acid content from 3.3–6.4%, and the dielectric constant was within the range of 2.6-25.7. The refractive index is at approximately 1.47 (*18*,*19*).

PAO 8 and SCGO were analysed using simultaneous thermal analysis (TGA and DSC), showing the mass loss and the change in the heat flow of a sample as a function of time in an inert atmosphere ($N_2$) up to 500 °C and synthetic air up to 450 °C with an onset temperature of mass loss defined as 0.2% within one centigrade. The oxidation sensitivity of the specimen holder is influenced by temperature limitations for the synthetic air atmosphere, which is not the case with $N_2$-atmosphere. Therefore, mass loss is not available for the whole temperature range of synthetic air. For both atmospheres, at least one intermediate is formed with SCGO, which was not further chemically analysed but might include the degradation of different saturated and unsaturated fatty acids at different temperatures before complete degradation.

When the samples were pyrolyzed in $N_2$-atmosphere (Figure 2), the onset temperatures for thermal decomposition of PAO 8 with 278.05 °C and SCGO with 274.04 °C are well comparable, the endothermic change in the DSC signal also indicates this process.

When synthetic air was applied (Figure 3), oxidative degradation of PAO 8 occurred at 244.68 °C, which is lower than the onset value of 281.28 °C for SCGO (the value might be shifted due to intermediate formation). Here, the SCGO forms multiple intermediates visible by the 1st derivative of the TGA signal (DTG) before complete combustion, again possibly deriving from the stepwise decomposition of different saturated and unsaturated fatty acids. The DSC curve indicates an exothermic reaction (upward peak).

Vegetable oils as lubricant base oils are known to have significant weaknesses in their oxidation stability, hydrolytic stability, and low-temperature properties. Saturated fatty acids are more thermodynamically stable than unsaturated fatty acids, which leads to a higher melting temperature and better oxidation stability. The bent structures of the unsaturated fatty acid moieties (such as oleic, linoleic or linolenic acid) of the SCGO are responsible for the liquidity at ambient temperature. The higher the amount of unsaturated fatty acids within the oil, the better the low-temperature properties, but the poorer the oxidative stability (*1*).

In Rudnick et al. (*1*), it is stated that the evaporation rates (in the absence of oxygen) of TGA of vegetable oils are significantly lower than those of iso-viscous hydrocarbon and synthetic base fluids. Furthermore, for the volatility in the presence of oxygen, rates were lower for vegetable oils compared to mineral oils. This observation could be confirmed with SCGO, neither for evaporation nor oxidative decomposition, since the

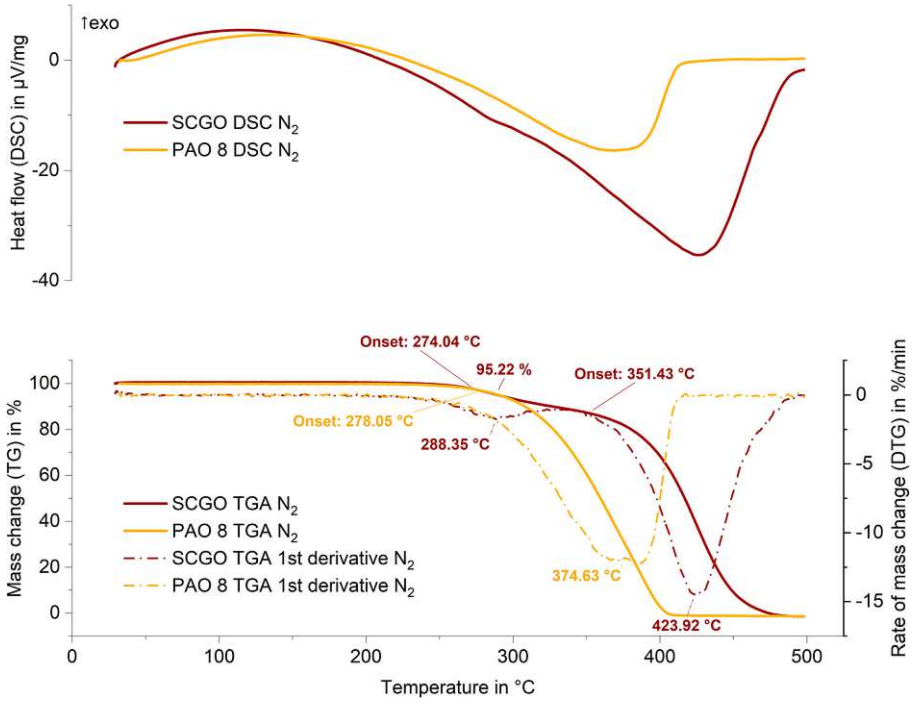


**Figure 2.** TGA (bottom, full line) and 1st derivative (dotted line) and DSC (top) **thermograms** in $N_2$ of SCGO and PAO 8. The heating rate is 10 °C/min.

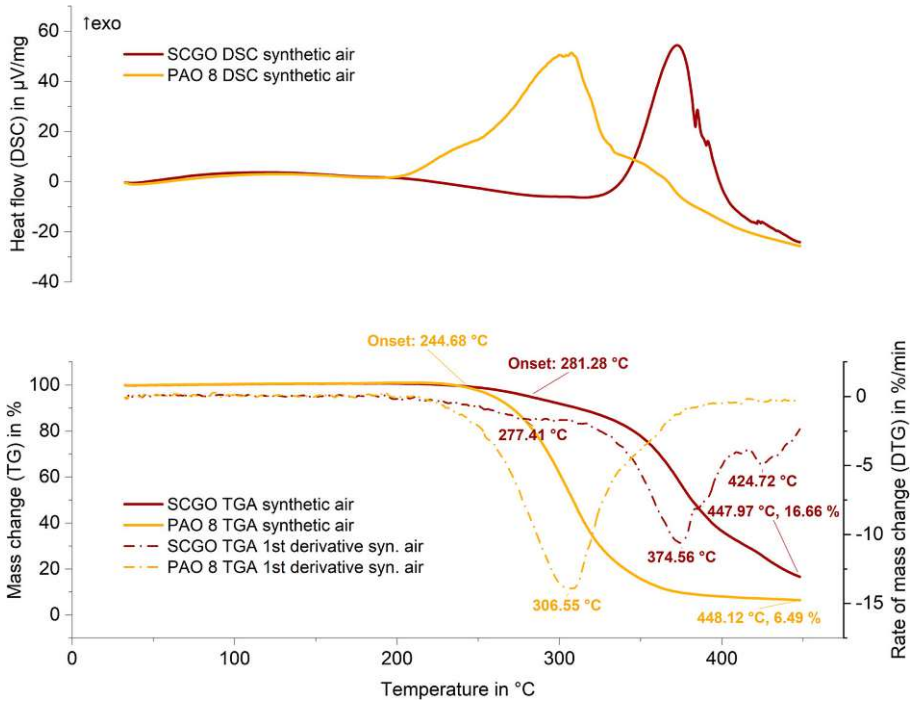


**Figure 3.** TGA (bottom, full line) and 1st derivative (dotted line) and DSC (top) **thermograms** in synthetic air of SCGO and PAO 8. The heating rate is 10 °C/min.

thermodynamic stability of PAO 8 and SCGO were always comparable. Moreover, they described a degradation mechanism of most oils with at least two steps, also present in SCGO. The good overall temperature stability of the SCGO might be due to a more balanced ratio of saturated to unsaturated fatty acids compared to other vegetable oils.

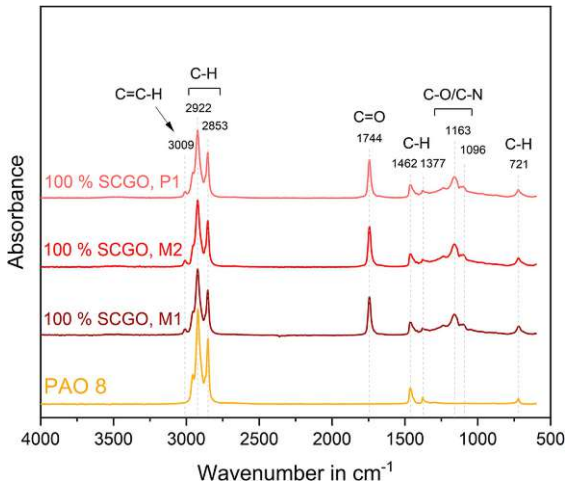


**Figure 4.** ATR-FTIR results: SCGOs compared to PAO 8 and PAO 40. M1: 100% SCGO as a mixture of two different coffee ground types; M2: 100% SCGO as a mixture of four different coffee ground types; P1: single-batch extraction: 100% SCGO of the same coffee ground type.

For ATR-FTIR (Figure 4) and GC-MS (Table 6), pure (P1: one extraction, one SCG type) and mixtures (M1: three extractions, two SCG types; M2: three extractions, five SCG types) of different SCGOs from the three coffee grounds sources were studied to identify their chemical structure. Only minor variations were observed when comparing pure SCGO to mixtures of SCGO. Therefore, a combination of different SCGO extractions was used for further investigations to increase the sample volume. Moreover, SCG as a valuable waste resource will also most likely not be available as a homogeneous single-kind fraction when disposed of at coffee shops and the like but rather as a mixture of various SCG types and grades.

The wavelength range of 1300-1000 $cm^{-1}$, as seen in Figure 4, is typical for C–O stretching vibrations characteristic for ester bonds related to the C = O carbonylic stretching vibrations at 1744$cm^{-1}$ of ester groups. The vibration band at 1163 $cm^{-1}$ reveals the presence of C–N amine bond stretching. Absorption at these wavenumbers is only found in SCGOs due to a lack of ester and amine structures in PAOs. The presence of C–H groups is shown by vibrations at 721 $cm^{-1}$ (rocking; seen only in long chain alkanes), 1462 $cm^{-1}$ (scissoring), 1377 $cm^{-1}$ (methyl rocking), as well as 2922 and 2853 $cm^{-1}$ (stretching), all appearing in the three SCGOs and synthetic PAO-based oil. The signal at 3009 $cm^{-1}$, which is only found in SCGO, represents

**Table 6.** Fatty acid distribution of SCGO detected by GC-MS and compared to literature.

| | | Peak area % | | | | |
|---|---|---|---|---|---|---|
| | | Present work | | | Literature | |
| Fatty acid | FA code | 100% SCGO, M1 | 100% SCGO, M2 | 100% SCGO, P1 | (22)[a] | (21) |
| Palmitic | C16:0 | 44 | 41 | 43 | 43 | 41.9 |
| Stearic | C18:0 | 11 | 10 | 8 | 14 | 5.65 |
| Oleic | C18:1 | 10 | 11 | 9 | 10 | 5.29 |
| Linoleic | C18:2 | 11 | 17 | 16 | 31 | 20.92 |
| Arachidic | C20:0 | 5 | 4 | 3 | – | – |
| Arachidonic | C20:4 | 4 | 4 | 3 | – | – |
| Docosanoic | C22:0 | 1 | 1 | – | – | – |
| Others | – | – | – | – | 2 | – |
| Sat./unsat. | – | 2.41 | 1.72 | 1.95 | 1.39 | 1.81 |

[a]Source is transesterified.

C = C–H stretching. With ATR-FTIR, a distinction between the three types of SCGO is impossible.

GC-MS values for fatty acid compositions vary slightly in literature and the herein performed measurements, as seen in Table 6, possibly depending on varying sample preparation procedures and measurement parameters.

The analysed fatty acid composition of SCGO shows a key peak for palmitic acid (n-hexadecanoic acid) with an area of 41-43%. According to the literature, the composition will vary slightly with the type of coffee grounds used (Arabica or Robusta) (*22*); here, mixtures of Arabica and Robusta are used. Ahangari et al. (*20*) showed that different operational conditions (e.g. extraction conditions) have quite a substantial impact on the fatty acid distribution as well.

## Tribological behavior

### Stribeck curves

Unidirectional rotation experiments were carried out on the rheometer on the S-CRUP surface, showing the variation of the COF over a sliding speed range from $8*10^{-9}$ m/s to $10^{-1}$ m/s, providing the Stribeck curve. The COF is given as an average of two measurements. The first bend of the curves of PAO 8, 100% SCGO, and 5% SCGO (Figure 5) indicates a transition from static friction to sliding friction (around $10^{-8}$ m/s). The second regime, where the COF increases, identifies as the boundary lubrication regime before the curves bend again and mixed lubrication starts. Boundary lubrication occurs until the maximum COF of the curves, which is between approx. $1.2*10^{-8}$–$6.3*10^{-6}$ m/s for PAO 8, $1.5*10^{-8}$ m/s to $5*10^{-3}$ m/s for 100% SCGO, and $1.4*10^{-8}$ m/s to $1.7*10^{-5}$ m/s for 5% SCGO. After the largest COF, the mixed lubrication regime is entered. An additional increase of COF with increasing sliding speeds due to hydrodynamic lubrication was not observed.

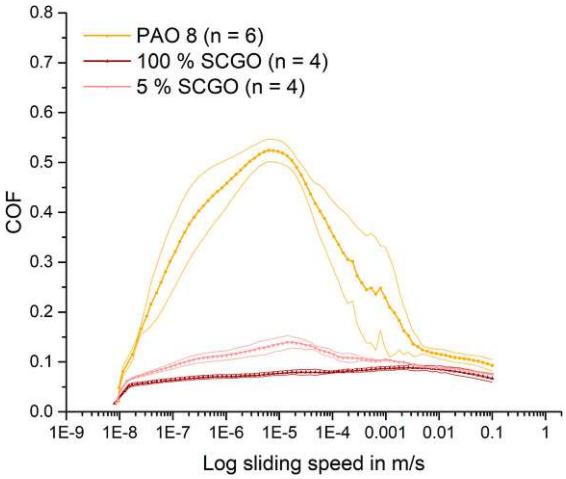


**Figure 5.** Stribeck curve of rheometer experiments using PAO 8, 100% SCGO and 5% SCGO in PAO 8 on S-CRUP.

The dedicated maximum COF ($\mu_{max}$) of 100% SCGO at 0.089 is significantly lower than that of PAO 8, being 0.524, which can be attributed to the friction-reducing properties of ester groups within this type of oil. Especially noteworthy is the low COF of 5% SCGO in PAO 8 of 0.139, indicating that SCGO works well as a boundary friction modifier additive.

Furthermore, the existence of wear also indicates boundary lubrication, which was visible for all three oil types. However, surface roughness is crucial in wear estimation due to the short measurement duration and low friction force applied. Wear volume and wear depth could not be adequately estimated for the S-CRUP surface. Thus, only surface polishing effects could be observed; the wear estimations are subjected to considerable fluctuations by the mean shift of unworn surface reference caused by the surface roughness. The mean wear scar depth of the different measurements lies within 0.02-0.13 µm Rq, which is relatively low and within the range of the original surface roughness.

### Oscillating movement

The oscillating tribological experiments were carried out on dissimilar materials with varying surface roughness. Friction and wear scars are compared on samples from rheometer (ball on three discs) and nanotribometer (ball on disc) experiments. The COF was recorded for all measurements. Additionally, wear depth and volume were determined using topography measurements.

A comparably lower COF for 100% and 5% SCGO than for PAO 8 is visible and will be discussed in detail in the following sub-chapter. An overview of the COF on the different surfaces of all executed nanotribometer and

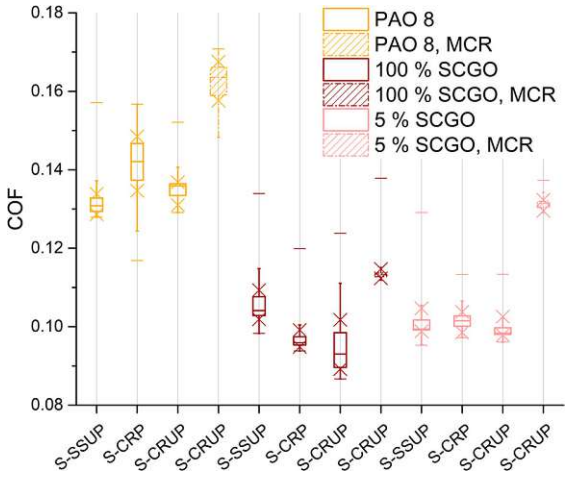


**Figure 6.** Box-and-whisker-plot of COF on different surfaces of nanotribometer and rheometer measurements. The box is giving the lower (25%) and upper (75%) quartile, whiskers are used to represent all samples lying within 1.5 times the inter-quartile range (IQR). Median line (thick horizontal line), quantiles $Q_{0.1}$ and $Q_{0.9}$ (cross), and maximum and minimum values (thin horizontal line) are displayed.

rheometer measurements is given in a box-and-whisker plot in Figure 6.

*Nanotribometer experiments on S-SSUP samples.* For the unpolished S-SSUP steel plates used in nanotribometer experiments (Figure 7), the friction coefficients of 5% SCGO in PAO 8 and 100% SCGO are in close proximity. The friction values for PAO 8 are the highest ($\mu_{mean} = 0.126$) compared to 100% SCGO ($\mu_{mean} = 0.102$) and 5% SCGO ($\mu_{mean} = 0.097$). After 15 min of measurement duration, there still is a decrease of COF observable for all three lubricants, which can be related to the system still being in the run-in phase.

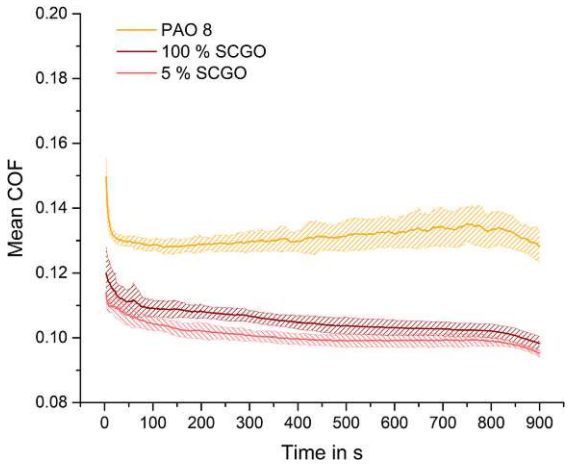


**Figure 7.** Friction values of nanotribometer experiments of different oils on unpolished S-SSUP given with standard deviation between data sets ($n = 3$).

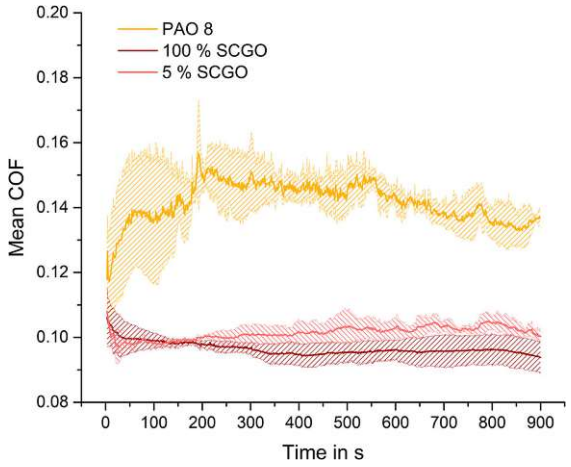


**Figure 8.** Nanotribometer measurement of COF of different oils on polished S-CRP given with standard deviation between data sets ($n = 3$).

Due to the higher surface roughness of the base body, the surface condition varies within the tested area, which might be the reason for the deviant behavior of 5% SCGO showing a smaller COF than 100% SCGO. The 5% SCGO additive and 100% SCGO samples show good repeatability and better friction stability over the measurement duration.

*Nanotribometer experiments on S-CRP samples.* Due to the low roughness induced high surface wettability, supposedly only low amounts of lubricant remain within the contact area on polished 100Cr6 surface (S-CRP) compared to the unpolished surfaces of 100Cr6 (S-CRUP) and 1.4301 stainless steel (S-SSUP). As exhibited in Figure 8, this leads to overall higher fluctuation of friction values and higher friction values for PAO 8 ($\mu_{mean} = 0.135$), probably due to the lack of, e.g. ester groups that interact with the metallic surfaces, which are present in 100% SCGO ($\mu_{mean} = 0.094$) and 5% SCGO ($\mu_{mean} = 0.097$).

Figure 9 shows the difference in wear scar appearance after nanotribometer experiments applying the three

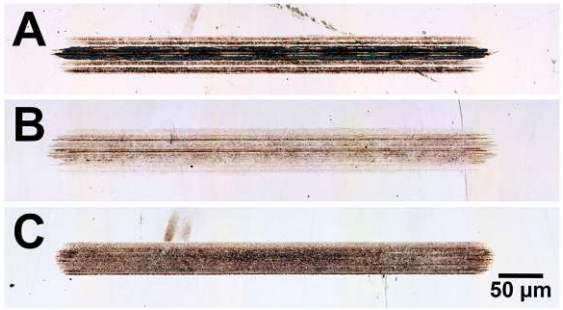


**Figure 9.** Light microscopic wear scar surface images after nanotribometer experiments of (A) PAO 8, (B) 100% SCGO, and (C) 5% SCGO in PAO 8 on polished S-CRP.

sample lubricants. The wear scar is least pronounced for 100% SCGO, thus being in good agreement with the COF.

*Nanotribometer and rheometer experiments on S-CRUP.* For the nanotribometer measurements, the lowest COF can be observed for the tribo-experiments on unpolished 100Cr6 discs S-CRUP (Figure 10). Superior to the other materials tested, S-CRUP samples display excellent repeatability with a very low margin of deviation between data points for all three applied lubricants. For this reason, the S-CRUP surface was chosen for further tribological testing on the rheometer. The SCGO exhibits lower COF deriving from long and polar fatty acid chains ($\mu_{mean} = 0.092$ 100% SCGO; $\mu_{mean} = 0.095$ 5% SCGO; $\mu_{mean} = 0.129$ PAO 8), which are strongly attracted to metallic surfaces. These components are lacking in PAO, a pure hydrocarbon base oil. The ability of SCGO to reduce friction also in the 5% dilution makes it attractive for use as friction modifying boundary lubrication additive. A common friction modifier usually consists of a polar head group and a non-polar tail, creating a cushion between the metal surfaces.

As already identified by the nanotribometer results, the friction-reducing properties of 5% SCGO in PAO 8 compared to pure PAO 8 could be confirmed by the rheometer (Figure 11). The measurements show good repeatability with a low margin of deviation between data points. Generally, the COF on the rheometer versus the nanotribometer is slightly higher but consistent, with COF values of $\mu_{mean} = 0.114$ for 100% SCGO, $\mu_{mean} = 0.131$ for 5% SCGO, and $\mu_{mean} = 0.163$ for PAO 8 for the rheometer. Since the measurement setup on both instruments is quite different, even with aligned parameters, directly comparing the results from the nanotribometer and the rheometer is impossible. This may be due

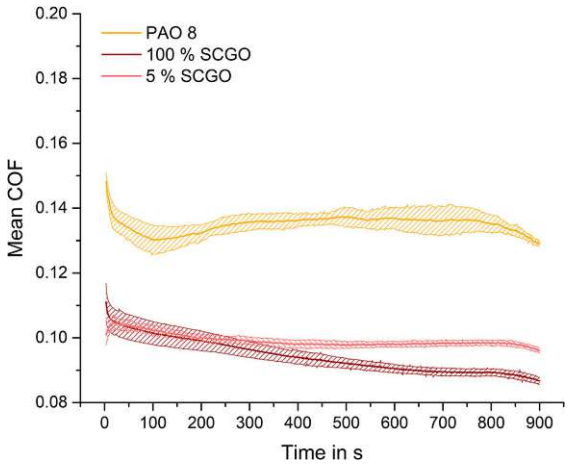


**Figure 10.** Friction values of nanotribometer experiments of different oils on unpolished S-CRUP given with standard deviation between data sets ($n = 3$).

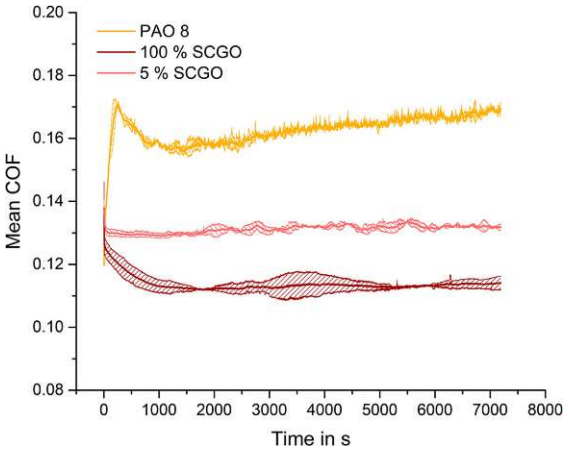


**Figure 11.** COF of rheometer experiments of different oils on unpolished S-CRUP given with standard deviation between data sets ($n = 2$).

to a better resolution of the nanotribometer with a smaller contact area (2 mm ball) within the 500 µm of testing range than the rheometer (12.7 mm ball).

Rather than only focusing on the COF, the wear volume is also relevant. Characterizing the volume and depth of the wear scar of the different oils with two-dimensional and three-dimensional topographic surface analysis (Table 7), it seemed that PAO 8 generated less wear when surface deposit was forming, leading to a distortion in comparison. This deposit is visible in 3D-topographic images as height increases (red) within the wear scar (Figure 12) and appears as a darkened surface in 2D-microscopy images (Figure 13). Therein; this effect is also slightly visible after experiments using 5% SCGO in PAO 8. Even though 100% SCGO used in rheometer experiments shows the most significant wear scar values, it must be noted that no surface deposit is visible. Instead, a surface polishing effect can be observed in the 2D images for this type of lubricant.

High resolution-MS demonstrated that for all three lubricant sample types, no significant qualitative differences were apparent when comparing pre- (fresh) and post-rheometer test (after two h of duration) samples; therefore, no specific oil degradation products were observed after two h of tribological ageing. In negative

**Table 7.** Wear track characterisation of unpolished S-CRUP surface after oscillatory rheometer measurements with PAO 8, 100% SCGO and 5% SCGO in PAO 8.

| | Linear rheometer experiments (S-CRUP) Mean wear track | | |
|---|---|---|---|
| Oil type | Width in µm | Depth in µm | Volume in µm³ |
| PAO 8 | 248 ± 9 | 0.104 ± 0.010 | 3302 ± 1023 |
| 100% SCGO | 295 ± 6 | 0.384 ± 0.021 | 22638 ± 1910 |
| 5% SCGO | 228 ± 10 | 0.140 ± 0.019 | 4876 ± 889 |

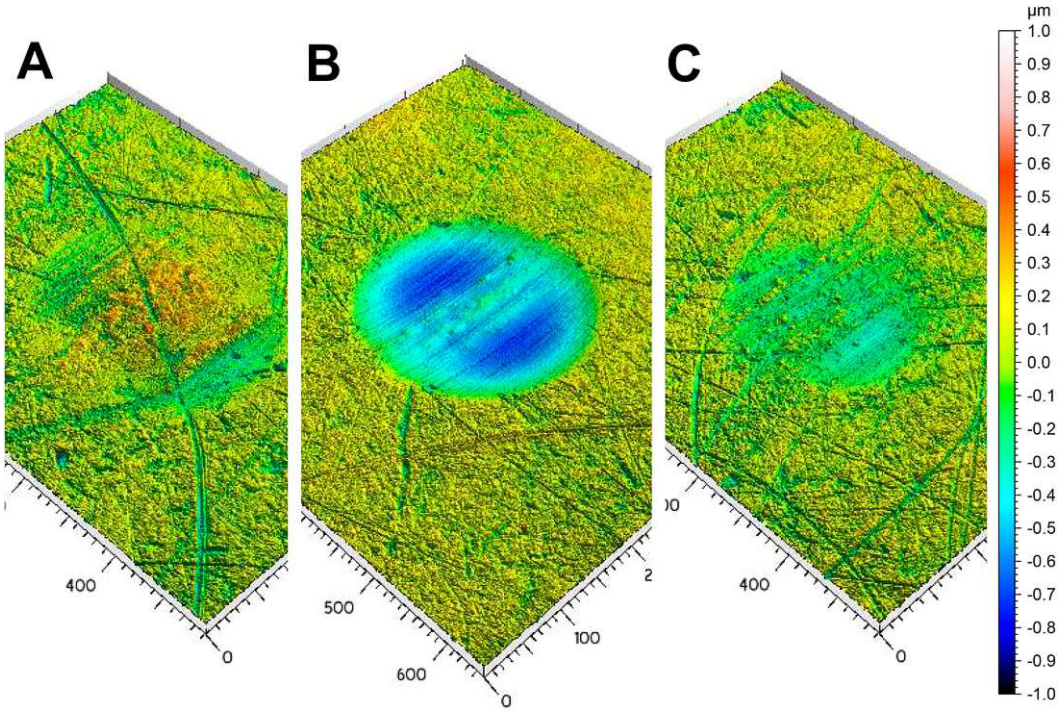


**Figure 12.** 3D-topographic surface images of wear tracks after rheometer experiments using (A) PAO 8, (B) 100% SCGO, and (C) 5% SCGO in PAO 8.

ion mode, a reduction in the intensity of about 30% of $C_{10}H_{20}$-groups for PAO 8, 90% of kahweol derivates for 100% SCGO and 50% kahweol palmitate for 5% SCGO in PAO 8 was visible for rheometer tested samples compared to the fresh samples.

Comparing 5% SCGO in PAO 8 and pure PAO 8 rheometer-tested samples, the 5% SCGO could improve the stability of PAO 8 since after tests with pure PAO 8, a loss of intensity of about 30% for the characteristic $C_{10}H_{20}$-groups was observable. In positive mode, glycerides such as mono- (MG), di- (DG), and triglycerides (TG) were visible after tests using 100% SCGO and 5% SCGO in PAO 8. DG and TG (C16:0, C18:0, C18:1 and C18:3) showed no intensity difference after tests with SCGO as a base lubricant and additive. In contrast, kahweol oleate was reduced by approximately 50% when 100% SCGO and by 70% when 5% SCGO in PAO 8 was applied. Caffeine, also found in the SCGO samples, was reduced by 40% in samples after 100% SCGO was used.

*Comparing tested base body materials*. Comparisons of the base body materials against 100Cr6 balls under the different oil types investigated are presented in Figure 14, Figure 15 and Figure 16. As can be observed, the unpolished surfaces 1.4301 stainless steel (S-SSUP)

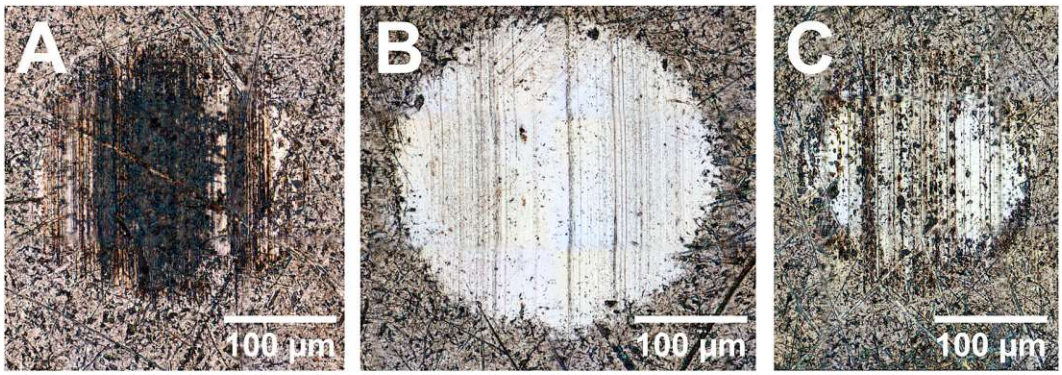


**Figure 13.** 2D-microscopic surface images of wear tracks after rheometer experiments using (A) PAO 8, (B) 100% SCGO, and (C) 5% SCGO in PAO 8 on unpolished S-CRUP samples.

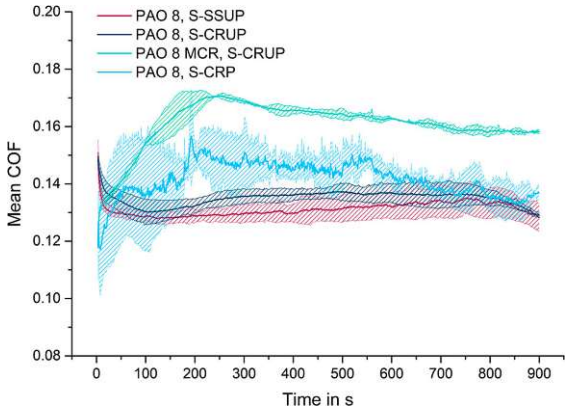


**Figure 14.** Comparison of friction values for nanotribometer and rheometer experiments applying PAO 8 on different surfaces S-SSUP, S-CRUP, and S-CRP.

and 100Cr6 (S-CRUP) seem to yield more stable friction values compared to the polished 100Cr6 (S-CRP) surface for PAO 8 (probably due to adhesion), for the SCG oils the measurements are very comparable in general. The standard deviation between measurement runs was relatively low, giving high repeatability.

For PAO 8 (Figure 14), the highest COF was reached on the rheometer with the S-CRUP. For the nanotribometer results, S-CRUP and S-SSUP showed quite comparable COF values. The S-CRP surface showed higher fluctuations between measurement repetition, indicating that PAO 8 does not adhere too well to the polished surface.

100% SCGO (Figure 15) shows good repeatability on all three surface types for all measurements. After 15 min of test duration, the COF still decreases, indicating that the materials are in the run-in phase. The lowest COF was reached with the S-CRUP surface, followed by the S-CRP surface for the nanotribometer measurements.

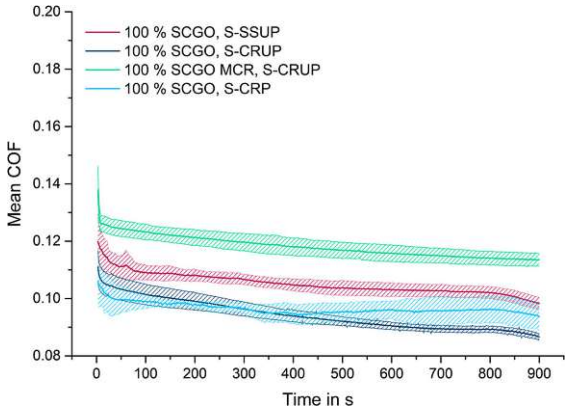


**Figure 15.** Comparison of friction values for nanotribometer and rheometer experiments applying 100% SCGO on different surfaces S-SSUP, S-CRUP, and S-CRP.

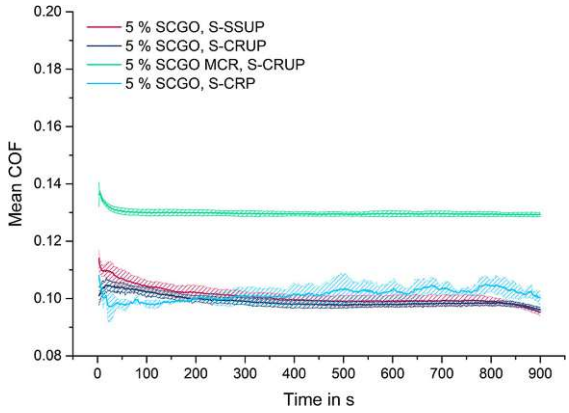


**Figure 16.** Comparison of friction values for nanotribometer and rheometer experiments applying 5% SCGO compared on different surfaces S-SSUP, S-CRUP, and S-CRP.

For 5% SCGO diluted in PAO 8 (Figure 16), the lowest COF was reached with surfaces S-SSUP and S-CRUP in the nanotribometer measurements. Experiments using S-CRP surfaces showed minor fluctuations, similar to Figure 14, where they are observed to a greater extent. Thus, they seem to derive from PAO 8.

For every oil type applied onto the S-CRUP surface, the measured COFs from experiments on the rheometer are slightly higher than those measured on the nanotribometer. However, a comparison of absolute friction values between instruments is difficult. Due to the differences in the tribo-systems, the contact area in nanotribometer experiments is considerably smaller (2 mm ball; approx. 50 µm of wear track width) and a better resolution based on data acquisition compared to the rheometer (12.7 mm ball; 250-300 µm of wear track width).

### *Life-cycle assessment case study*

A life-cycle assessment (LCA) of oil from SCGs as a future lubricant for the case study of an extruder was undertaken. It includes a scale-up from a lab scale to fit an industrial extruder (operational time 1000 h, with an amount of ~ 65 l of lubricant). The intention was to assess all tangible environmental impacts associated with various stages of SCGOs' life, ranging from raw material extraction through materials processing, industry size manufacture, distribution, and application. All values are extrapolated from the laboratory scale, including the accompanying uncertainties. For this work, the focus is laid on highlighting especially the critical segments and where process optimization might be necessary.

The LCA is divided into the life-cycle inventory (LCI) conducted with a SimaPro model and the life-cycle impact assessment (LCIA) using the ILCD 2011 Midpoint + Version 1.11 method (specific for Europe). The LCI

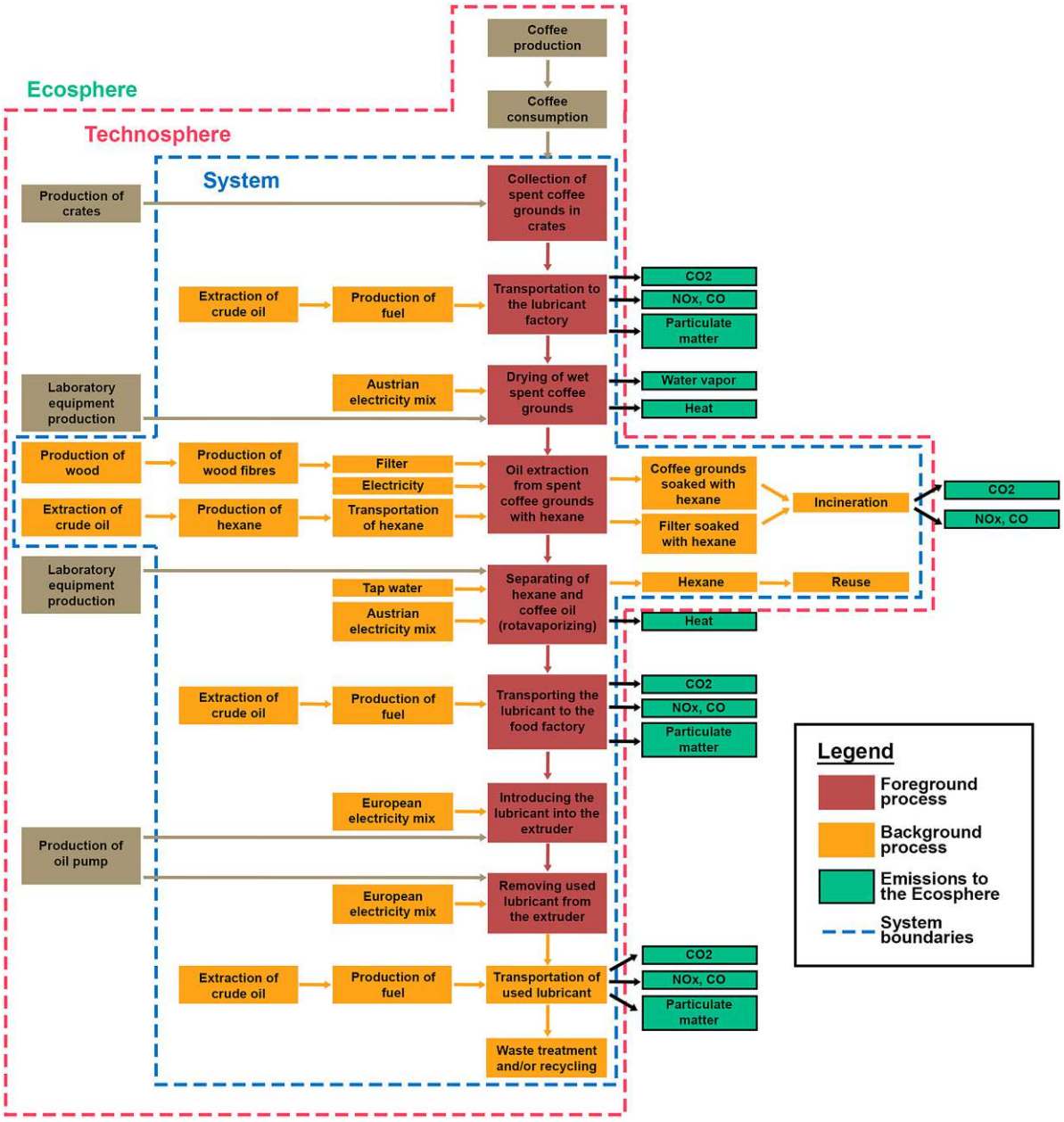


**Figure 17.** Flow chart of a cradle-to-grave life cycle of SCGO. Adapted with permission from (*23*).

involves the computational model for input and output flows, whereas the LCIA converts these flows into characterized, normalized and weighed impacts (*23*).

Figure 17 displays the whole life cycle of oil collected from SCG, including steps of coffee grounds collection and transportation, manufacturing of oil and further use as 'lubricant' in industrial machinery (certain additives are not taken into account here), as well as the recollection of solvent and disposal of used lubricant (which could be re-refined into base oil in a cradle-to-cradle approach [*24*]).

The four most affected categories (patterned) are shown in Figure 18 and include human toxicity with non-cancerous and cancerous effects, freshwater eutrophication and freshwater ecotoxicity; all derive from n-hexane as the solvent. These impacts originate from n-hexane production, mainly collected during the fractional distillation step of crude mineral oil refining. Furthermore, after extraction, hexane is lost to the environment due to evaporation from paper thimbles and extracted SCGs. This is considered an avoidable output to Technosphere, affecting ozone depletion the

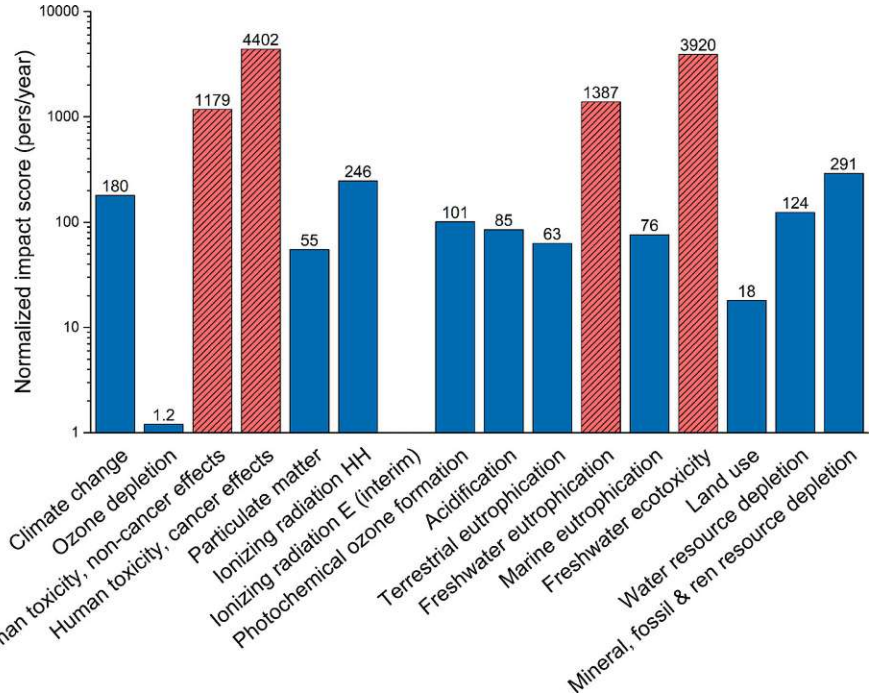


**Figure 18.** Normalized results of the cradle-to-grave analysis in number of equivalent persons per year (EU27 2010 normalization set) for each midpoint impact category. Adapted with permission from (*23*).

most of all categories (in our model resulting in 261%, with no other impact category exceeding the limit of 30%). A change of n-hexane to a more environmentally friendly solvent could restrict these effects to a minimum extent, which is discussed further in this chapter.

When comparing petroleum-based lubricants with mineral base oil and PAO base oil by a cradle-to-gate LCA approach, PAO performed even worse in all categories, with almost twice the greenhouse gas emissions and generally a more energy-consuming production process. But considering the lubricant lifetime, which is mostly higher for PAO, the impacts are reduced, and mineral oil shows the highest mark in 11 out of 15 categories (*25*).

For the assessment of the oil extraction process, the following three phases and parameters were applied:

(1) *Drying phase*: 105 °C for 24 h, electricity consumption: 4.91 kWh
(2) *Extraction phase*: 140 °C for seven h with hexane as the solvent, electricity consumption: 0.67 kWh
(3) *Rotary evaporation phase*: 50 °C for 1.5 h at 334 mbar, electricity consumption: 2.1 kWh

Values for electricity consumption in phase 3 are based on estimation and might be lower. For phases 1 and 2, the values were measured with a wattmeter.

All data was collected from small scale lab-production, with a collection of approximately 2 g of SCGO from ~ 50 g of wet SCG (~ 15 g of dry SCG).

For the collection of SCGO, the grounds were first dried for 24 h in a drying oven at 105 °C. The LCA demonstrated that the drying process was one of the main impacts concerning energy consumption for the lab-scale setup (including drying, extraction and rotary evaporation).

According to the results of TGA/DSC (Figure 19), the sample (~ 40 mg) was thoroughly dried after 16 min

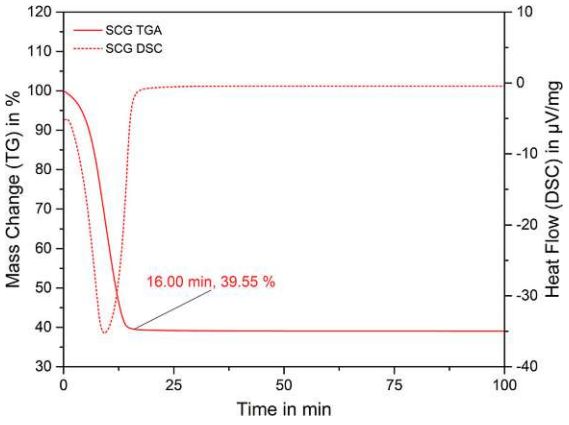


**Figure 19.** Drying rate of SCGs with TGA/DSC.

with 60.45% water evaporation. Stirring the sample during drying could even improve that process. Since SCGs are dried in more significant portions (~ 40 g) in the drying oven, the result of the TGA cannot be transferred directly, but the drying time might still be reduced by one order of magnitude. Furthermore, at an industrial scale, water vapor from the exhaust air stream could be re-collected in an exhaust head and reused.

The drying process was discussed as an energy-intensive process by Mabona et al. (*19*), which is why they assessed the dependence of moisture content on SCGO yields. They extracted SCGs with up to 20 wt% of residual moisture in non-polar solvents (hexane, toluene) and 40 wt% in polar solvents (ethanol, acetone). High moisture content was limiting for non-polar solvents, which might fail to access the SCGs properly. In contrast, polar solvents could extract more significant amounts of SCGO with higher initial water content. The best results were given by ethanol at 40 wt% with over 20% of oil yield, higher moisture contents were considered limiting. Choosing ethanol over hexane as an extraction solvent would result in a more environmentally friendly extraction process.

For the life-cycle assessment, the drying process has the most significant impact on electric power consumption. However, using n-hexane as the solvent for the extraction process introduces increased human- and eco-toxicity and freshwater eutrophication values. In addition, n-hexane evaporating from the residual waste coffee grounds after the extraction step might impact ozone depletion when not re-collected and/or disposed of properly. This conclusion is cautiously based on a direct up-scaling from the lab- to the industrial scale. Thus, a comprehensive argumentation is yet to be feasible at this point. For future LCA approaches, models could be considered, including adapted industrial process structures and more reliable values (electricity consumption, SCG amount, oil yields, etc.) for an industrial production scale.

## Conclusion

This work took a further step toward understanding the tribological applicability of waste-based SCGOs. For the first time, a broad approach to evaluate the tribological behavior of SCGO was deployed, and a wide range of tribological experiments applying SCGO was performed.

Based on experimental results, SCGO can reduce the friction coefficient as a pure oil and applied as a 5% additive in PAO 8, the latter being a common synthetic base oil that served as a reference in this study. The lowest COF and most stable friction behavior could be reached when 100% SCGO was applied on unpolished 100Cr6 (S-CRUP) samples due to ester groups within the oil that positively affect the COF. The best results for 5% SCGO in PAO 8 and pure PAO 8 were also achieved with the same surface. Therein, it could be proven that SCGO has tremendous potential when used as a base lubricant and as a friction modifier additive in a standard industrial base oil, especially when compared to PAO 8 as the reference lubricant. This outcome could interest various industrial applications, from the automotive industry to machines used, e.g. for food production.

To increase comprehension of SCGO functionalities and their influence on friction and wear, future investigations could include (a) further decreasing the amount of SCGO used as an additive without adversely affecting friction and wear modification properties (to maximize resource efficiency); (b) altering SCGOs under defined conditions for simulations of industrial applications, e.g. engine, bearing or pump devices; (c) exploring the applicable operational ranges of SCGO in tribo-tests; (d) using eco-friendly, sustainable base oils and references; (e) improving the extraction pathway to be more energy efficient; (f) estimation of environmental impact by performing biodegradability, bioaccumulation, and toxicity tests; and (g) assessment of valid values for industrial economy throughout the life cycle of SCGO.

## Acknowledgements

Our appreciation to Cesar Delafargue, Aikaterini Deli, Martine Francoise Marie-Hélène Grangé, Signe Hvidkjær, Christina Martzakli, and Adrian Müller from the Technical University of Denmark (DTU) for support on performing the life-cycle assessment of SCGO. Special thanks to Balazs Jakab, Tetyana Khmelevska, Christoph Haslehner, Marko Piljevic, Anto Puljic, Thomas Putz, and Andjelka Ristic from AC2 T research GmbH for additional support. Conceptualization, L.W., M.V., M.F., R.E., J.P.; investigation and methodology, J.P.; data curation and formal analyses, R.E., J.P.; validation, J.P.; writing – original draft, J.P.; writing – review & editing, L.W., M.V., M.F., M.M.D.; supervision, M.F., M.M.D.

## Disclosure statement

No potential conflict of interest was reported by the author(s).

## Funding

This work was funded by the 'Austrian COMET-Program' (project InTribology, no. 872176) via the Austrian Research Promotion Agency (FFG) and the Province of Niederösterreich and Vorarlberg. It was carried out within the 'Excellence Centre of Tribology' (AC2 T research GmbH).

## ORCID

*Rosa Maria Eder* http://orcid.org/0009-0002-3624-8422
*Lukas Widder* http://orcid.org/0000-0001-8297-8966
*Markus Varga* http://orcid.org/0000-0001-8272-4122
*Martina Marchetti-Deschmann* http://orcid.org/0000-0002-8060-7851
*Marcella Frauscher* http://orcid.org/0000-0001-7939-9656

## References

[1] L. R. Rudnick, In *Synthetics, Mineral Oils, and Bio-Based Lubricants*, L. R. Rudnick, Ed.; CRC Press: Boca Raton, FL, 2020. doi:10.1201/9781315158150.
[2] United States Department of Agriculture (USDA), "BioPreferred® Program", [Online]. https://www.biopreferred.gov/BioPreferred/ (accessed Jan 12, 2022).
[3] European Commission. Regulation (EU) 2018/1999 of the European Parliament and of the Council of 11 December 2018 on the Governance of the Energy Union and Climate Action, Amending Regulations (EC) No 663/2009 and (EC) No 715/2009 of the European Parliament and of the Council, Directives 94/22/EC, 98/70/EC, 2009/31/EC, 2009/73/EC, 2010/31/EU, 2012/27/EU and 2013/30/EU of the European Parliament and of the Council, Council Directives 2009/119/EC and (EU) 2015/652 and repealing Regulation (EU) No 525/2013 of the European Parliament and of the Council (Text with EEA relevance.). *Off. J. Eur. Union* **2018,** *328*, 1–77.
[4] European Union, "A European Green Deal, Striving to be the First Climate-Neutral Continent", [Online]. https://ec.europa.eu/info/strategy/priorities-2019-2024/european-green-deal_en. (accessed Jan 12, 2022).
[5] Ibanez, J.; Martín, S.M.; Baldino, S.; Prandi, C.; Mannu, A. European Union Legislation Overview about Used Vegetable Oils Recycling: The Spanish and Italian Case Studies. *Processes* **2020,** *8*, 798. doi:10.3390/pr8070798.
[6] European Commission. Directive (EU) 2018/851 of the European Parliament and of the Council of 30 May 2018 amending Directive 2008/98/EC on waste (Text with EEA relevance). *Off. J. Eur. Union* **2018**, 1–32.
[7] European Commission, "Circular Economy: New rules will make EU the global front-runner in waste management and recycling". [Online]. https://ec.europa.eu/commission/presscorner/detail/en/IP_18_3846. (accessed Oct 7, 2020), 2018.
[8] European Commission. Regulation (EC) No 66/2010 of the European Parliament and of the Council of 25 November 2009 on the EU Ecolabel (Text with EEA Relevance). *Off. J. Eur. Union* **2010,** *27*, 1–19.
[9] Tchibo and A. Liedtke, "Kaffee in Zahlen No. 9", Brand Eins. [Online]. https://de.statista.com/statistik/studie/id/75371/dokument/kaffee-in-zahlen-2020/. (accessed Jan 12, 2022), 2020.
[10] I. Efthymiopoulos, "Recovery of Lipids from Spent Coffee Grounds for use as a Biofuel", London, 2018.
[11] Abdullah, M.; Koc, A.B. Oil Removal From Waste Coffee Grounds Using Two-Phase Solvent Extractionenhanced With Ultrasonication. *Renew. Energy* **2013,** *50*, 965–970. doi:10.1016/j.renene.2012.08.073.
[12] Calixto, F.; Fernandes, J.; Couto, R.; Hernández, E.J.; Najdanovic-Visak, V.; Simões, P.C. Synthesis of Fatty Acid Methyl Esters via Direct Transesterification with Methanol/Carbon Dioxide Mixtures from Spent Coffee Grounds Feedstock. *Green Chem.* **2011,** *13*, 1196. doi:10.1039/c1gc15101k.
[13] Vardon, D.R.; Moser, B.R.; Zheng, W.; Witkin, K.; Evangelista, R.L.; Strathmann, T.J.; Rajagopalan, K.; Sharma, B.K. Complete Utilization of Spent Coffee Grounds To Produce Biodiesel, Bio-Oil, and Biochar. *ACS Sustain. Chem. Eng.* **2013,** *1*, 1286–1294. doi:10.1021/sc400145w.
[14] Uddin, M.N.; Techato, K.; Rasul, M.G.; Hassan, N.M.S.; Mofijur, M. Waste Coffee oil: A Promising Source for Biodiesel Production. *Energy Procedia* **2019,** *160*, 677–682. doi:10.1016/j.egypro.2019.02.221.
[15] Andrade, K.S.; Gonçalvez, R.T.; Maraschin, M.; do-Valle, R.M.R.; Martínez, J.; Ferreira, S.R.S. Supercritical Fluid Extraction from Spent Coffee Grounds and Coffee Husks: Antioxidant Activity and Effect of Operational Variables on Extract Composition. *Talanta* **2012,** *88*, 544–552. doi:10.1016/j.talanta.2011.11.031.
[16] Ciesielczuk, T.; Rosik-Dulewska, C.; Poluszyńska, J.; Miłek, D.; Szewczyk, A.; Sławińska, I. Acute Toxicity of Experimental Fertilizers Made of Spent Coffee Grounds. *Waste Biomass Valoriz.* **2017,** *9*, 2157–2164. doi:10.1007/s12649-017-9980-3.
[17] Grace, J.; Vysochanska, S.; Lodge, J.; Iglesias, P. Ionic Liquids as Additives of Coffee Bean Oil in Steel-Steel Contacts. *Lubricants* **2015,** *3*, 637–649. doi:10.3390/lubricants3040637.
[18] Al-Hamamre, Z.; Foerster, S.; Hartmann, F.; Kröger, M.; Kaltschmitt, M. Oil Extracted from Spent Coffee Grounds as a Renewable Source for Fatty Acid Methyl Ester Manufacturing. *Fuel* **2012,** *96*, 70–76. doi:10.1016/j.fuel.2012.01.023.
[19] Mabona, N.; Aboyade, W.; Mollagee, M.; Mguni, L.L. Effect of Moisture Content on oil Extraction from Spent Coffee Grounds. *Energy Sourc. Part A: Recov. Utiliz. Environ. Effects* **2018,** *40*, 501–509. doi:10.1080/15567036.2014.915361.
[20] Ahangari, B.; Sargolzaei, J. Extraction of Lipids from Spent Coffee Grounds Using Organic Solvents and Supercritical Carbon Dioxide. *J. Food Process. Preserv.* **2013,** *37*, 1014–1021. doi:10.1111/j.1745-4549.2012.00757.x.
[21] Hibbert, S.; Welham, K.; Zein, S.H. An Innovative Method of Extraction of Coffee oil Using an Advanced Microwave System: In Comparison with Conventional Soxhlet Extraction Method. *SN Appl. Sci.* **2019**, *1*. doi:10.1007/s42452-019-1457-5.
[22] Unugul, T.; Kutluk, T.; Kutluk, B.G.; Kapucu, N. Environmentally Friendly Processes from Coffee Wastes to Trimethylolpropane Esters to be Considered Biolubricants. *J. Air Waste Manag. Assoc.* **2020,** *70*, 1198–1215. doi:10.1080/10962247.2020.1788664.
[23] A. Müller, A. Deli, C. Delafargue, C. Martzakli, M. Grangé and S. Hvidkjær, "Lubricant Oil from Spent Coffee Grounds", Unpublished document of Technical University of Denmark, Lyngby, 2021.
[24] J. Sander, "Lubricants Can't Be Green … Can They?", Lubrication Engineers, Inc.. [Online]. Available: https://www.lelubricants.com/wp-content/uploads/pdf/news/White%20Papers/Green%20Lubricants%20white%20paper.pdf. (accessed Jul 18, 2022), 2017.
[25] Raimondi, A.; Girotti, G.; Blengini, G.A.; Fino, D. LCA of Petroleum-Based Lubricants: State of art and Inclusion of Additives. *Intern. J. Life Cycle Assess.* **2012,** *17*, 987–996. doi:10.1007/s11367-012-0437-4.

## 2.3 Publication III - Advanced Method for the Detection of Saturated Monoglycerides in Biodiesel using GC-EI-MS/MS

Authors: Jessica Pichler, Marcella Frauscher & Martina Marchetti-Deschmann
Journal: ACS Omega, 9:22, Pages 23476–23484, 2024
DOI: 10.1021/acsomega.4c00513

The publication is reprinted on the following pages.

ACS OMEGA

Open Access



http://pubs.acs.org/journal/acsodf

Article

# Advanced Method for the Detection of Saturated Monoglycerides in Biodiesel Using GC-EI-MS/MS

Jessica Pichler, Marcella Frauscher, and Martina Marchetti-Deschmann*

Cite This: *ACS Omega* 2024, 9, 23476−23484

Read Online

ACCESS | Metrics & More | Article Recommendations

**ABSTRACT:** Common B7 biodiesels consist of mixtures of mineral oil-based diesel and 7% fatty acid methyl ester (FAME). While biocontent increase can be achieved with these blends at high-quality levels during cold temperature periods, fuel filter blocking events are reported from time to time. Based on a preliminary study on fuel filters, the selection of compounds responsible for filter blocking could be narrowed down to saturated monoglycerides (SMGs). The most abundant SMGs in Europe are 1- and 2-monopalmitin (1-C16:0, 2-C16:0) and 1-monostearin (C18:0), based on the FAME origin. Until now, there has been no simple, precise, and accurate method to quantitatively detect those SMGs in the B7 matrix, which was the aim of the following work. An improved gas chromatography electron ionization tandem mass spectrometry method was developed for the quantitative detection of 1-C16:0, 2-C16:0, C18:0, and C20:0 SMGs. During the method improvement, (a) the sample preparation and (b) the calibration were optimized for low concentrations. (c) The samples were analyzed by multiple reaction monitoring focusing on specific qualifier and quantifier ions with optimized collision energies, (d) time segments and improved scan time were implemented, and (e) limits of detection and limits of quantification were determined. The time-stability of SMG standards in $CHCl_3$ with 4% neat biodiesel and the discrimination effects of the standard components were evaluated to assess method reliability. Overall, a highly sensitive and precise method for the improved detection of SMGs in biodiesel is presented.

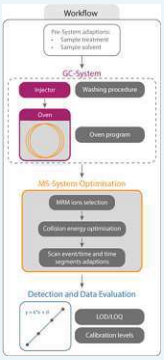


## 1. INTRODUCTION

Biodiesel (B100 or FAME) is a fuel produced from renewable resources (e.g., rapeseed, soybean, palm, corn, etc.) by transesterifying their natural oils and fats with methanol. This converts triglycerides into FAME products, with the intermediates mono- and diglycerides still being found in the final biodiesel, affecting its quality.[1] For passenger cars in Europe, the content of biodiesel is restricted to a maximum of 7 wt % in neat diesel (B0), resulting in the so-called B7 mixtures.[2]

The origin of FAME can be edible feedstock (1st generation), nonedible feedstock (2nd generation), algae feedstock (3rd generation), or microbial feedstock (4th generation). The FAME feedstock used is dependent on the geographical region[3] and mainly comprises first-generation crop oils derived from palm, rapeseed/canola, soybean, corn, and sunflower; used cooking oils (UCO); and animal fats.[4,5] The primary feedstocks in Europe are rapeseed and palm oil, UCO, and minor amounts of soybean oil, sunflower oil, and animal fats.[6] In the US, mostly soybean, corn, and canola oils are used, as well as recycled feedstocks.[7] A FAME's fatty acid profile depends on the FAME feedstock type used,[8] influencing, for example, the cold flow properties of the fuel.[9]

Unbeneficial cold flow properties of fuel can lead to the blocking of fuel filters, especially with seasonal changes. Biodiesel-related fuel filter blocking incidents have been reported recently in agricultural machinery[10] and trains,[11] although only blended with 7% mixtures in diesel. As filter blocking incidents accumulate, investigations of correlations between properties of diesel, biodiesel, and blends (including different FAME feedstocks) causing filter blocking (reduced cold flow properties, particulate matter formation, and oxidation products)[12] as well as new approaches for the analysis of fuels and filters increase, e.g., for the prediction of cold flow properties of biofuels in relation to their ester profile[13] or filter analysis with thermal desorption GC-MS providing a simple and fast method, where blocked filters showed different FAME species (mainly C16:0) and glycerol.[14]

Based on preceding studies of numerous fuel filters from all over Austria, the cause of fuel filter blocking could be narrowed down to the occurrence of SMGs, which may precipitate, i.e., at lower temperatures, attaching to the fuel filters and subsequently blocking the fuel passage. Comparing blocked filters to reference filters, high amounts of SMGs from C16:0 to C22:0 were only found on blocked filters, whereas reference filters predominately contained unsaturated C16 to C18 monoglycerides (MGs).[15]

Received: January 16, 2024
Revised: April 3, 2024
Accepted: May 9, 2024
Published: May 24, 2024





https://doi.org/10.1021/acsomega.4c00513
*ACS Omega* 2024, 9, 23476−23484

To this point, a maximum content of 0.7 wt % (7000 ppm) total SMGs in biodiesel is allowed by DIN EN 14214:2012+A2:2019,[16] resulting in 490 ppm of SMG content in ready blended B7. Even though the maximum allowed SMG amount was reduced over the years, the current levels still seem to cause unforeseeable blocking events under certain conditions. Furthermore, the amounts of individual SMG components are not regulated; the limit is given as a sum parameter of all SMGs. By EN 17057:2018-03,[17] SMGs (as a sum of single contents of 1-C16:0, 2-C16:0, and 1-C18:0) in biodiesel can be detected reliably within the range of 200 to 1500 ppm. The method is suitable for FAME derived from rapeseed, palm, and used cooking oil, but not from palm kernel or coconut derivates (applies for fuel produced and used in Europe).

When diesel needs to be stored for extended periods, e.g., at industrially used fuel stations, for storage at power security generators, or to bridge times of general constraints, in all cases, maintaining the quality of the fuel must be ensured, and therefore, studying the changes in filterability during long-term fuel storage is essential. Moreover, different storage factors (tank design/geometry, filling/extraction systems, etc.) and environmental influences during delivery and storage (mild/harsh climate, season, and temperature changes) should be considered. When storing biodiesel/diesel blends at different temperatures for 12 months, the water content significantly increased and so did the content of mono- and diglycerides and total glycerin. It also showed that the amount of biodiesel mixed with diesel impacts the filterability, especially at lower temperatures. Diesel is much more nonpolar than biodiesel, causing a reduced solubility for polar residues. This leads to more precipitates, an effect that further increases with decreasing temperature. Characterization of such precipitates by GC-FID showed a composition of mainly free glycerin and monoglycerides, especially monopalmitin and monostearin.[18] Neat B100 can tolerate more SMGs until a critical value is reached, increasing the cloud point (CP). The CP is the temperature below which a transparent solution undergoes a liquid−solid phase transition to form either a stable solution or a suspension that settles a precipitate, besides other effects. The SMG-to-B100 ratio is an essential factor for the CP. Additionally, the polymorphism of SMG crystals with different melting temperatures, solubilities, and stabilities has to be considered. SMG crystallization can occur upon rapid cooling, slow warming, or during storage and can cause fuel filter blocking above the CP.[19]

MGs are determined by GC-FID according to DIN EN 14105[20] as low as 0.001 wt % (mono-, di-, and triglycerides) along with free glycerol at 0.1 wt % in FAME from oil seeds, animal- and plant-derived fats, oils, and their residues. This method detects 1- and 2-C16:0, 1-C18:0, and 1- and 2-C18:1 to C18:3, while 1-C19:0 is used as the internal standard. In the sense of a B7 mixture, this would result in an LOQ of 70 ppm for free glycerol and 0.7 ppm for total glycerides. When analyzing different types of biodiesels for their MG content by ASTM D6584-17 using GC-FID, it was found that the method needed to be improved for nonconventional feedstocks. Improvements to the method, without changing the analysis procedure, such as using an MG stock standard from C10 to C22, adapting the relative retention time windows, and matching the profiles of MGs and FAME, led to a more accurate determination of monoglycerides.[21]

Despite filter blocking events still occurring within regulatory limits, the risk potential remains unclear for specific fuels. Both the fuel manufacturing industry and distributors are urged to evaluate the filter blocking potential as a quality assurance measure. Typically, multiple analysis methods are employed to evaluate quality criteria across various fuel matrices such as diesel, biodiesel, and blends. However, this approach can be inadequate for industries due to the use of disparate instrumentation and configurations for different matrices, leading to increased resource consumption and costs. Consequently, industrial stakeholders expressed the necessity for a fast and straightforward method to assess the filter blocking potential of petroleum- and bio-based fuels, as well as blends.

Eventually, all named complications led to the requirement of a more advanced detection method using GC-EI-MS/MS for single SMG amounts, being responsible for filter blocking events, and their limits in B0, B7, and B100 matrices, where no published method exists, providing the aim of the presented research work.

## 2. MATERIALS AND METHODS

**2.1. Chemicals, Reagents, and Consumables.** For method development of monoglyceride identification in biodiesel, the following reference materials were used: 1-monopalmitin (1-C16:0; >99%) [CAS: 542-44-9] obtained from Sigma-Aldrich (St. Louis, MO, USA) and 2-monopalmitin (2-C16:0; >98%) [CAS: 23470−00−0], monostearin (C18:0; 99%) [CAS: 123-94-4], and monoarachidin (C20:0; >99%) [CAS: 30208-87-8] all obtained from Larodan (Solna, Sweden). As internal standard (IS) rac-glycerol 1-myristate (C14:1; >99%) [CAS: 488862-82-4] obtained from Avanti Polar Lipids (Alabaster, AL, USA) was chosen, it is not naturally found in biodiesel in Europe (dependent on the FAME feedstock used). If C14:1 is present in the used biodiesel matrix, the method must be adapted by replacing it with an equivalent IS. A multicomponent standard mix was produced in different concentrations from these reference materials to set up a calibration curve.

BSTFA+TMCS (99:1; *N*,*O*-bis(trimethylsilyl)-trifluoroacetamide with trimethylchlorosilane; 99%) [CAS: 25561-30-2] obtained from Sigma-Aldrich (Buchs, Switzerland) was used as a derivatization agent. Following solvents were applied: DCM (≥99.8%) [CAS: 75-09-2] obtained from Sigma-Aldrich (St. Louis, MO, USA), $CHCl_3$ (≥99.9%) [CAS: 67-66-3] purchased from Supelco (Burlington, MA, USA), methanol (MeOH; 99%) [CAS: 67-56-1] purchased from Supelco (Darmstadt, Germany), and *n*-hexane (≥95%) [CAS: 110-54-3] obtained from Carl Roth (Karlsruhe, Germany).

**2.2. Field Sample Collection and Preparation.** Different petrol station distributors all over Austria supplied field samples (diesel and biodiesel) throughout changing seasons (varying product composition). B0, B7, and B100 samples were ultrasonicated for 15 min at room temperature and vortexed upon arrival in their original metal container to solubilize any potential precipitates. They were refilled in transparent bottles and stored at 4 °C until usage.

For GC-MS analyses, 1 mL of sample was prepared in 2 mL amber 51 vials with PFTE/silicone crimp seal (both Phenomenex; Torrance, CA, USA), diluted in the solvent, and silylated with BSTFA+TMCS in mass excess (1:4.5) at 70 °C for 1 h. Field samples (B0, B7, and B100) were added to





https://doi.org/10.1021/acsomega.4c00513
ACS Omega 2024, 9, 23476−23484

Table 1. Overview of Instrument Specificities

| | setup A | setup B |
|---|---|---|
| **instrument** | Shimadzu GC2010 (Kyoto, Japan) | Thermo Trace GC Ultra (Thermo Fisher, Bremen, Germany) |
| **injector** | Split/splitless (SSL) injector | Programmable temperature vaporizer (PTV) |
| **column parameters** | TG5MS (Thermo Fisher Scientific; Waltham, MA, USA) | |
| | length: 30 m length | |
| | internal diameter: 0.25 mm | |
| | stationary phase thickness: 0.25 $\mu$m | |
| **liner** | deactivated packed wool glass SSL inlet liner (Shimadzu, Sydney, Australia) | straight deactivated PTV metal liner (Thermo Fisher Scientific; Waltham, MA, USA) |
| **injection parameters** | injection volume: 1 $\mu$L | |
| | temperature: 300 °C | |
| | split ratio: 1:25 | |
| | carrier gas: helium | |
| **flow programming** | mode: flow control | |
| | carrier gas flow rate: 2 mL/min | |
| **oven temperature programming** | 60 °C (2 min), 10 °C/min to 300 °C (9 min) | |
| | total run time: 34 min | |
| **detectors** | TQ8040 MS (triple quadrupole) | flame ionization detector (FID), TSQ Quantum XLS MS (triple quadrupole) |
| **FID parameters** | | temperature: 300 °C |
| | | airflow: 350 mL/min |
| | | $H_2$-flow: 35 mL/min |
| | | makeup ($N_2$) flow: 30 mL/min |
| **MSD parameters** | transfer line temperature: 250 °C | |
| | electron ionization (EI) source temperature: 200 °C | |
| | electron energy: 70 eV | |
| | emission current: 60 $\mu$A | |
| | filament power switch time: 0 min off, 6 min on | |
| | monitoring ions: | |
| | 1. Full scan ($m/z$ 40 to 500); scan time: 0.3 s | |
| | 2. Multiple reaction monitoring (MRM, parameters see Figure 1); | |
| | collision gas: Argon | |
| **data acquisition and evaluation software** | GCMSsolution version 4.52 (Shimadzu) | Thermo Xcalibur 4.4.16.14 (Thermo Fisher) |

the solvent in a 4 wt % dilution (see Section 3.1 Calibration and Sample Solvent).

For determination of the water content, field samples were measured according to DIN 51777-2 (indirect method)[22] by Karl Fischer titration, where the sample is heated to 120 °C, water is evaporated, collected in a titration cell, and determined iodometrically.

**2.3. Calibration Sample Preparation.** Method used as the starting point (see Section 2.4 GC-EI-MS method): The calibration samples for detection of SMGs in the B7 field sample matrix contained 1-C16:0, 2-C16:0, C18:0, and C20:0 as a multicomponent mix in the following concentrations: 10, 50, 100, 250, 500, and 1000 ppm, plus 200 ppm of C14:1 as the internal standard (IS), in DCM. Field samples (B0, B7) were prepared as 4 wt % dilutions in DCM.

Improvement: Based on prior analyses,[15] low or very low amounts of SMGs were expected in the B7 sample matrix. The maximum total SMG content is approximately 500 ppm, which is diluted to approximately 20 ppm after sample preparation in the GC vial. For this, the concentration range had to be adapted to lower LOQs: 1, 2.5, 5, 15, 25, 50, 75, and 100 ppm of reference SMG dilutions with 100 ppm IS were prepared in $CHCl_3$ and $CHCl_3$ + 4 wt % B0 for evaluation of matrix effects and higher sensitivity. The calibration was adapted for lower or higher levels, depending on the expected SMG concentration.

**2.4. GC-EI-MS Method.** The initial method started with the GC oven preset to 60 °C, and after keeping the temperature constant for one min, it was heated to 300 °C (rate 10 °C/min) and held for 15 min (total run time 40 min). The EI ion source was operated at an electron emission current of 50 $\mu$A, and derivatized analytes were detected within the range of $m/z$ 40 to 650. Monoglyceride precursor ions of $m/z$ 341 (C14:1), 371 (1-C16:0), 218 (2-C16:0), 399 (C18:0), and 427 (C20:0) were chosen for selected ion monitoring (SIM) in separate scan events with a scan time of one s and 10 V collision energy. A full scan was conducted over the entire run time with a scan time of 0.2 s. Structural identification was done with the MS spectrum, whereas quantification was performed with the FID chromatogram. Sample solvents, washing solvents, and washing procedures were improved throughout this study and will be discussed later.

**2.5. GC-EI-MS/MS Method.** Derivatized samples were analyzed on two different GC-MS instruments (Table 1). The methods had to be slightly adapted for the specific instruments (different autosampler, syringe volume, dean switch, SSL/PTV, mass sensitive detectors (MSD)/FID, and purge flows). However, the same GC-MS column was used, an MS-compatible 5% diphenyl/95% dimethyl polysiloxane column (Thermo Fisher Scientific; Waltham, MA, USA). To prevent syringe clogging when working with field samples, the autosampler washing procedure was adapted, increasing the washing cycles before and after injection, and choosing *n*-hexane/DCM (1:1) as the washing solvent.





https://doi.org/10.1021/acsomega.4c00513
ACS Omega 2024, 9, 23476−23484

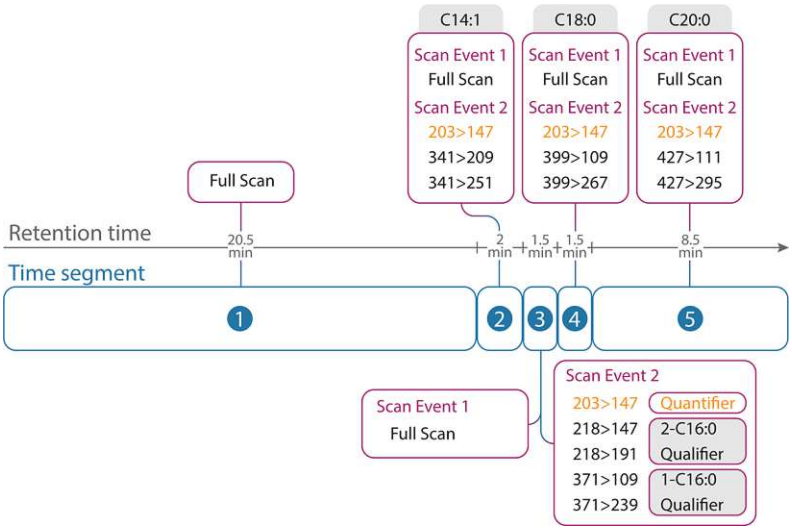


**Figure 1.** Scheme of time segments and scan events of C14:1, 1-C16:0, 2-C16:0, C18:0, and C20:0 showing full and MRM scans for the improved GC-MS/MS method. Ion transitions are displayed as $m/z$ values, and quantifier ion transitions are highlighted in orange.

Selected/multiple reaction monitoring (SRM/MRM) was used for quantitative determination, using the third quadrupole as a mass analyzer for molecular identification. The following time segments were implemented: 0 to 20.5 min full scan, 20.5 to 22.5 min—IS qualifier and quantifier ions, 22.5 to 24 min C16:0, 24 to 25.5 min C18:0, and 25.5 to 34 min C20:0 analysis (Figure 1). Analytes were scanned in individual time segments, except for 1-C16:0 and 2-C16:0 due to their very similar retention times. For every analyte, a full and a MRM scan was conducted. The full scan was run at an event time of 0.3 s, and the MRM scans (selective for specific analyte) had a scan event time of 0.2 s. The MRM events are listed in Figure 1; the MRM transition from $m/z$ 203 > 147 was selected as quantifier ions for all analytes, and the chosen qualifier ion MRM transitions of the specific analytes are stated in the figure. Qualifier ions are those specific to the analyte; quantifier ions are not specific to the analyte but show the highest intensities. Only when the qualifier response was sufficient, the quantifier response was evaluated. Analyte response was normalized to the IS. Product ions and collision energies (CE) were optimized for each analyte. The determined CE giving the best overall ion intensities was 6 V for the IS and 9 V for the SMG references. Structures were identified based on a similarity search against NIST11 and NIST20 libraries and compared to reference substances for 1-monopalmitin, 2-monopalmitin, monostearin, and monoarachidin.

Reference materials were evaluated according to their long-term stability and discrimination effects within the multi-component (single components vs multicomponent mix injections). LODs and LOQs were determined in $CHCl_3$ and $CHCl_3$ + 4 wt % B0. The LODs and LOQs were defined as the mean out of nine blank measurements (solvent) plus three times (LOD) or nine times (LOQ) the standard deviation of the blank. Details are available in 2.3 long-term stability tests, 2.4 single standard injections for discrimination effect study, and 2.6.2 LOD/LOQ determination.

**2.6. HR-ESI-MS Experiments.** Fuel samples and reference materials were analyzed qualitatively with HR-ESI-MS for contamination and purity. B7 samples and reference materials were prepared as 1:100 volumetric dilutions in a $CHCl_3$:MeOH solvent mixture (v:v, 7:3). Diesel B0 was investigated for SMG contamination in a volumetric 1:100 dilution using MeOH. The samples were injected in an LTQ Orbitrap XL hybrid tandem HR-MS (Thermo Fisher; Waltham, MA, USA) system via direct infusion at 5 $\mu$L/min and measured in positive and negative ion modes. Spectra were recorded from $m/z$ 50 to 800 for precursor ions and from $m/z$ 60 to 800 for product ions, with a resolution of 30,000. Within the ESI source, nitrogen was used as the sheath and drying gas. Helium served for cooling and as a collision gas during low-energy collision-induced dissociation (CID). Data processing and interpretation were conducted with Thermo Xcalibur 4.4.16.14, Thermo FreeStyle 1.8 SP2, and Mass Frontier 8.0 SR1 (all from Thermo Fisher Scientific Inc.).

## 3. RESULTS AND DISCUSSION

**3.1. Calibration and Sample Solvent.** The SMG standard samples showed the same solubility behavior in DCM and $CHCl_3$. Due to the easier handling of $CHCl_3$ compared to DCM concerning vapor pressure and vapor toxicity, $CHCl_3$ was chosen over DCM. Additionally, less solvent evaporation during handling improves the reproducibility of the sample preparation and makes it more independent of the temperature. It must be mentioned that both solvents are considered cancerogenic, and substitution is advised for a greener analysis approach. Furthermore, gloves that are compliant with a higher standard (EN 374[23]) than common nitrile gloves are required for DCM handling due to short breakthrough times.[24]

**3.2. MRM Optimizations.** *3.2.1. Collision Energy (CE).* A variation of CEs from 0 to 36 V (in 3 V steps) was tested using a 100 ppm mix with $CHCl_3$ plus 4 wt % B0 for every qualifier and quantifier ion of the selected SMG analytes. The CE with the best response of the quantifier ion in combination with a reasonable response for both qualifier ions was selected. The second most abundant ion ($m/z$ 203) was picked over the most abundant ion ($m/z$ 147) since the latter was present in the fuel matrix at the same retention time as SMGs, negatively impacting the signals by overlapping. A CE of 6 V was chosen for the IS, and for the SMG analytes, 9 V CE was selected (Figure 2). For 2-C16:0, 12 V CE would have given the best results concerning the quantifier ion, but since the scan was


https://doi.org/10.1021/acsomega.4c00513
ACS Omega 2024, 9, 23476−23484

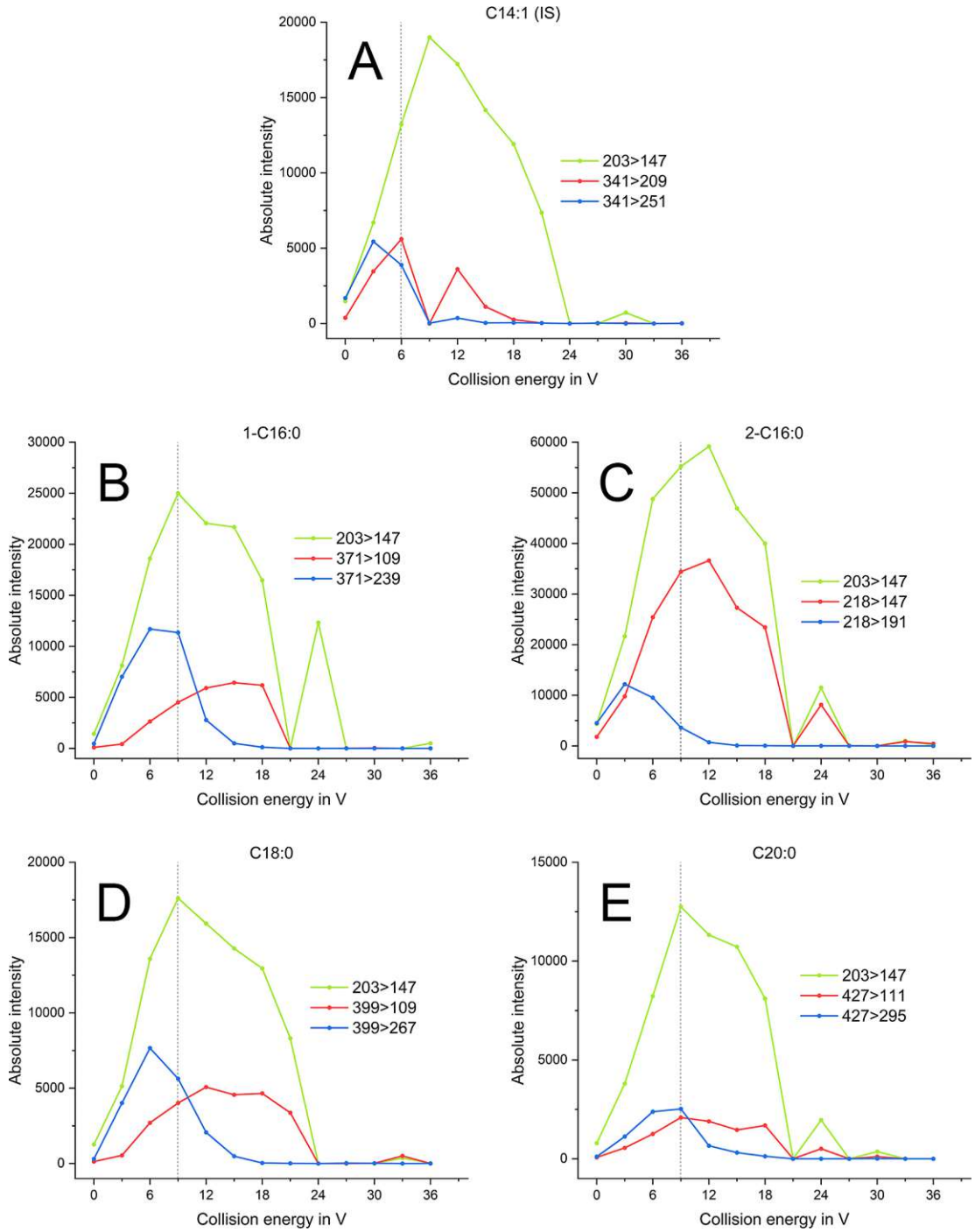


**Figure 2.** Intensities of the specific qualifier (blue and red lines) and quantifier ions ($m/z$ 203 > 147, green lines) at different collision energies are shown for the IS C14:1 (A), the single SMG standards 1-C16:0 (B), 2-C16:0 (C), C18:0 (D), and C20:0 (E). Dotted line marks the chosen collision energy at 6 V (A) or 9 V (B–E).

performed in the same time segment as 1-C16:0, due to both substances eluting within a few seconds apart, 9 V was chosen as a good compromise.[25]

*3.2.2. Scan Time and Mass Scans.* Before adaptation of the method, the peaks of the quantifier ions were evaluated in SIM mode. Typically, a default of one s is used as scan time, which is the time it takes to accomplish one scan. Multiple qualifier and quantifier ions were scanned simultaneously for only 0.2 s to improve data collection, which directly impacted peak shape quality and the number of data points per peak. The full scan time was set to 0.3 s. The scan range was reduced from $m/z$ 40 to 650 to $m/z$ 40 to 500 for an additional sensitivity increase.

The number of mass scans within a scan event influences data points over time and by this peak shape and data quality. The fewer $m/z$ values scanned per event, the more data points available per period. Therefore, the process was limited to a maximum of five masses per scan event. Furthermore, sensitivity could be considerably increased by introducing the MRM measurement in time segments.



https://doi.org/10.1021/acsomega.4c00513
ACS Omega 2024, 9, 23476−23484

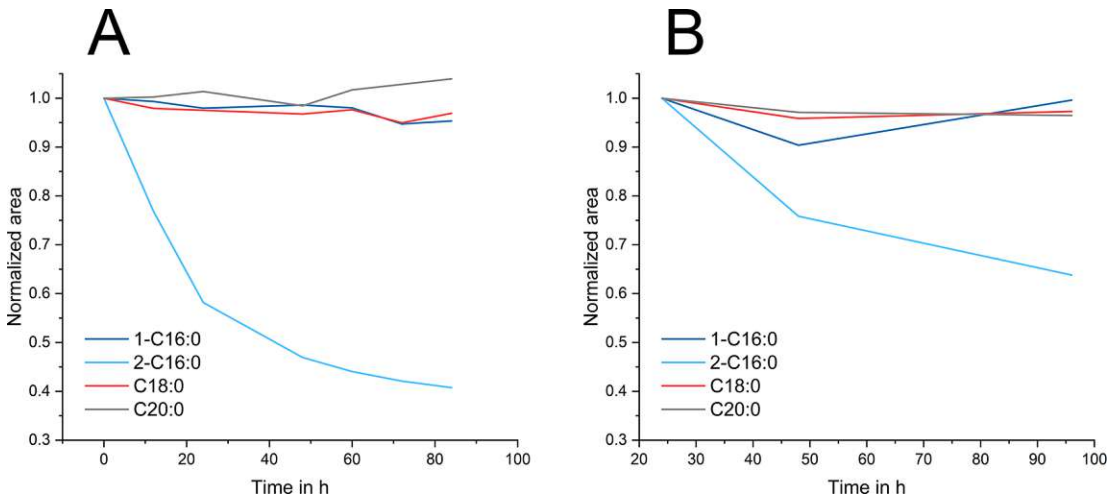


**Figure 3.** Stability of standards over (A) 82 h, sampled from the same vial, and (B) over 92 h, sampled from fresh vials to overcome solvent evaporation. Data are normalized against IS.

**3.3. Long-Term Stability Tests.** The stability of the multicomponent mix was tested in $CHCl_3$ + 4% B0 over a time period of 84 h. Solvent evaporation plays the most crucial role, which is corrected by the IS. Despite a punched vial septum, there was no decrease of area ratios observed for 1-C16:0, C18:0, and C20:0 after normalization with the IS, displaying this good stability over time. Only 2−16:0 decreases by 23% within the first 12 h, which increases to 59% signal area loss after 84 h. When sampling out of fresh, unpunched vials, there is a loss of about 36% between 24 and 96 h for 2-C16:0 (Figure 3). All other standards have more than 95% area recovery. The biggest loss of the 2−16:0 signal is expected to be within the first 20 h. The only notable structural difference between 2-C16:0 and the other SMGs is the linkage of the fatty acid to a secondary alcohol instead of a primary alcohol. This is apparently the main reason for this effect. These experiments were conducted just once to illustrate the observed deviation from other results, which affect the handling of the different SMGs. As for now, this effect was not primarily the objective of the study and, therefore, was not further investigated. The results show that a fresh preparation of the sample and immediate measurement are necessary for reliable collection of data, especially for 2-C16:0.

**3.4. Single Standard Injections for Discrimination Effect Study.** Single standards and the multicomponent mix were compared for their performance with $CHCl_3$ and $CHCl_3$ + 4% B0. For the normalized (IS and wt %) single standards, the recovery of signals in $CHCl_3$ (normalized to 100%) was slightly better than $CHCl_3$ + 4% B0, where a loss of up to 9% was observed. The same is valid for the multicomponent mix, where recovery of signals for $CHCl_3$ + 4% B0 is approximately 15−17% lower than in pure $CHCl_3$ (Table 2). Again, this aligns with the above results, confirming that $CHCl_3$ without B0 is the better solvent option. The area recovery is better for the single standards than the multistandard mix (discrimination effect). Still, a normalization by the IS area antagonized this effect. Furthermore, minor concentrations of SMGs were detected in B0 samples, where at first a carryover within GC-MS measurements was expected but was later confirmed by HR-ESI-MS (see discussion in Section 3.5 HR-ESI-MS of standards for contamination evaluation).

**Table 2. Recovery of Areas of $CHCl_3$+4% B0 Compared to Neat $CHCl_3$ (Normalized to 100%) Showing IS and wt % Normalized Areas**

| | 4% B0/$CHCl_3$ recovery | |
|---|---|---|
| standard | multi, % | single, % |
| 1-C16:0 | 83 | 99 |
| 2-C16:0 | 83 | 95 |
| C18:0 | 84 | 91 |
| C20:0 | 85 | 100 |

**3.5. HR-ESI-MS of Standards for Contamination Evaluation.** With HR-ESI-MS, the neat reference materials for SMGs 1-C16:0, 2-C16:0, C18:0, C20:0, IS C14:1, and B0 were analyzed for their purity and possible contamination. No contamination was found in the MG reference standard samples. Unexpectedly, the B0 sample showed minor impurities of C16:0 and C18:0, which are possibly due to using the same fuel trucks for B0 and B7 when delivered to the fuel station (fuel tanks at the station are always filled with the same type for all tested fuels in this study).

**3.6. Application of the Method.** *3.6.1. Calibration.* The calibrations of neat $CHCl_3$ and 4 wt % B0 in $CHCl_3$ were compared. In general, neat $CHCl_3$ showed better response ratios for all the analytes and had the advantage of a more independent sample preparation procedure (no diesel sample involved, no additional contamination introduction with the diesel sample) and fewer pipetting steps.

The expected concentration of total SMGs in prepared B7 field samples usually lay within 4 to 15 ppm. Therefore, the calibration curve was focused on the lower concentration levels and carefully evaluated between 1 and 50 ppm (six levels) instead of 10 to 1000 ppm (Figure 4). The sensitivity of the calibration function (slope) strongly affects the LOQ. All calibration curves showed a good fit above 98.8% ($R^2$ coefficient of determination) (Table 3). The more sensitive measurements for 2-C16:0 again show different behavior from the other MGs.

*3.6.2. LOD/LOQ Determination.* Blank samples were prepared as three individual sample preparations with three injections each (3 × 3; nine injections total). The area at the position of the quantifier ion was integrated for all analytes,



https://doi.org/10.1021/acsomega.4c00513
ACS Omega 2024, 9, 23476−23484

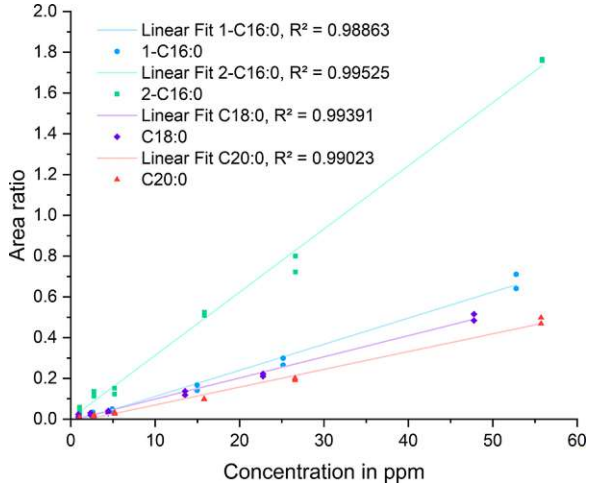


**Figure 4.** Calibration functions for 1-C16:0 (light blue), 2-C16:0 (green), C18:0 (violet), and C20:0 (red) at different concentration levels in $CHCl_3$.

giving blank areas (Table 4). The LODs and LOQs were determined in neat CHCl3, allowing the detection and quantification of SMGs to very low levels.

The following LODs and LOQs could be established:

*3.6.3. Field Samples.* Water was determined in the B7 diesel samples ($n$ = 37) with an average of 33 ± 11 ppm. The first and third quartiles are 24 and 43 ppm, giving an interquartile range of 19 ppm. The maximum or fourth quartile was defined as 51 ppm. All the values were lying below the maximum water content allowed for diesel (B0, B7), which is limited to 200 ppm by EN 590.[2] No direct influence of the water content on the filter blocking ability of the fuel was determined. This was already investigated in a prior study;[15] for the analyzed samples, no influence of water was revealed.

Twenty-eight different B7 samples were measured, providing the following data (Table 5): the total SMG content was mainly determined by 1-C16:0 and C18:0. The majority of the B7 samples are to be expected within a range of 97 to 142 ppm. The lowest total SMG concentration was 64 ppm, and the highest was 189 ppm; this can be calculated to be approximately 900 to 3200 ppm in B100 (with 7000 ppm being the upper limit for total SMGs in biodiesel by DIN EN 14214[16]). 2-C16:0 and C20:0 concentrations were below the LOQ. A decrease in SMG concentration from the time of sample preparation until their measurement has to be considered (e.g., precipitation because of crystallization), especially for 2-C16:0. Before establishing the method for routine analysis, this observation has to be further investigated and adapted if needed since a fresh preparation of samples for analysis is not always feasible.

**Table 4. LODs and LOQs of Blank Samples of $CHCl_3$**

| | concentration in ppm | | | |
|---|---|---|---|---|
| vial | 1-C16:0 | 2-C16:0 | C18:0 | C20:0 |
| LOD | ≤2.2 | ≤1[a] | ≤1.3 | ≤2.0 |
| LOQ | ≤3.4 | ≤1[a] | ≤2.4 | ≤2.1 |

[a]LODs and LOQs of 2-C16:0 were below the lowest calibration level and corrected to the concentration of the lowest calibration level.

**Table 5. Statistical Evaluation of the Total SMG Concentrations above the LOQ in 28 Different B7 Field Samples**

| sample number | 28 |
|---|---|
| | concentration in ppm |
| mean | 119.72 |
| minimum | 63.76 |
| 1st quartile | 96.86 |
| median | 119.11 |
| 3rd quartile | 141.80 |
| interquartile range | 44.94 |
| maximum | 188.89 |

For completeness, neat B0 (pure diesel) and B100 (pure biodiesel) samples were measured. The B0 sample exhibited 75 ppm of SMGs, consisting of 73 ppm of 1-C16:0 and 2 ppm of 2-C16:0, with traces of C18:0 and C20:0 below the LOQ. The 1-C16:0 value seems unusually high for a common B0 diesel, especially since it is above the median value of 72 ppm of B7. Contamination of the B0 sample was expected and confirmed by HR-ESI-MS (see Section 3.5 of HR-ESI-MS of Standards for Contamination Evaluation). For B100, a total concentration of SMGs of 771 ppm was detected; 393 ppm 1-C16:0, 25 ppm 2-C16:0, 296 ppm of C18:0, and 57 ppm of C20:0 were determined.

Regarding filter blocking, 25 differently behaved B7 samples were compared. Nonblocking samples were observed to have an interquartile SMG range from 101 to 137 ppm (median 119 ppm), partly overlapping with blocking samples within a range of 120 to 152 ppm (median 143 ppm). A differentiation was clear for blocked filters, where a high concentration of SMGs was found, whereas in nonblocked filters, mainly unsaturated MGs were discovered.[15] The blocking of a filter is caused by the accumulation of SMGs on the filter surface over time, which is dependent on the concentration of SMGs in the fuel but also on the rate of flow through the filter, resulting in a faster blocking when the concentration and/or flow rate are high.

## 4. CONCLUSIONS

Fuel manufacturers and distributors expressed the need for a precise, reliable, and efficient method to assess the filter

**Table 3. Values of Linear Fit Evaluation for the Four Different SMG Calibration Curves**

| | 1-C16:0 | 2-C16:0 | C18:0 | C20:0 |
|---|---|---|---|---|
| equation | $y = a + b \times x$ | $y = a + b \times x$ | $y = a + b \times x$ | $y = a + b \times x$ |
| intercept | −0.017 ± 0.011 | 0.003 ± 0.018 | −0.005 ± 0.006 | −0.017 ± 0.007 |
| slope | 0.013 ± 4.344 × $10^{-4}$ | 0.031 ± 6.770 × $10^{-4}$ | 0.010 ± 2.568 × $10^{-4}$ | 0.009 ± 2.741 × $10^{-4}$ |
| residual sum of squares | 0.007 | 0.020 | 0.002 | 0.003 |
| Pearson's $r$ | 0.994 | 0.998 | 0.997 | 0.995 |
| $R$-square (COD) | 0.989 | 0.995 | 0.994 | 0.990 |



https://doi.org/10.1021/acsomega.4c00513
ACS Omega 2024, 9, 23476−23484

blocking potential of diesel, biodiesel, and blends. Additionally, the demand for the ability to differentiate between high-quality and poor-quality fuels served as a driving force for the hereby established GC-EI-MS/MS method.

For improved method performance, various changes to the standard method were introduced: (a) changing the sample solvent from DCM to $CHCl_3$ improved the overall reproducibility of sample preparation, (b) changing the solvent system from a matrix-matched calibration standard (diesel plus solvent mixture) to neat solvent ($CHCl_3$) not only improved area recovery (only 83−85% area recovery of $CHCl_3$+B0 to neat $CHCl_3$ in the multicomponent standard) but also made the whole method independent from resources and better for comparability of results between different laboratories, and (c) implementing MRM with optimized collision energies and time segments into the GC-MS method resulted in a highly increased overall sensitivity for all four tested SMGs (1-C16:0, 2-C16:0, C18:0, and C20:0). For the internal standard C14:1, a CE of 9 V would have given the best result for the quantifier ions, but the two qualifier ions were not detected. Hence, 6 V was chosen as the best option for all three ions. CEs of 6−12 V for 1-C16:0 and C18:0 and 6−9 V for 2-C16:0 and C20:0 allow good detection of quantifier and qualifier ions. Scan times of 0.2 s for MRM and 0.3 s for full scan analysis gave satisfactory peak shapes. Surprisingly, the results of HR-ESI-MS showed trace impurities of C16:0 and C18:0 in neat B0 diesel.

The improved GC-MS/MS method allowed the detection of single SMG concentrations down to a minimum concentration (LOD) of 2.2 ppm and quantification (LOQ) down to at least 3.4 ppm in the GC vial, which corresponds to concentrations of 55 (LOD) and 85 ppm (LOQ) in the neat B7 sample. The total SMG concentration in B7 fuel was detectable and is expected to be between 60 and 190 ppm. B7 samples that cause filter blocking are slightly higher in their total SMG content (median of 143 ppm) than samples that do not cause filter blocking (median of 119 ppm). The water content of the fuel samples did not influence the filter blocking ability of the fuel. Still, a more extensive field sample study may be necessary for a valid comparison, including the effects leading to the accumulation of SMGs on filter surfaces over time and a comparison of the SMG concentrations accumulated on the filter and measured in the corresponding fuel for a more comprehensive picture. When comparing SMG amounts of fuels from different stations or on filters and in their related fuels, the samples might be drawn from various levels within the tank due to diverse tank geometries, which will influence the amount of precipitate collected and the resulting measured SMG concentrations, causing fluctuations when comparing nonblocked and blocked filter fuels.

The improved GC-MS/MS method generally led to a more sensitive detection of SMGs in the B0, B7, and B100 matrices. It can be used as an additional quality control for the purchase of biodiesel blend components and premixed diesel blends, for random testing, and in the event of filter blockage, as an accurate assessment based solely on current standards is insufficient. If stricter regulations for the total and single SMG amounts are to be implemented, this method may serve as a standard operating procedure. A fully automated data evaluation can also be implemented, depending on the instrument and data processing software.

A significant loss of signal of normalized 2-C16:0 over time (already within the first 12 h) was registered during long-term stability tests, while other normalized SMGs were stable over time. Various reasons can be identified for this observation: precipitation of the SMG in the original sample or sticking of 2-C16:0 to the sample container walls. More significant losses in sensitivity can still be compensated by using the peak area ratio, giving accurate results. This finding underscores the importance of fresh sample preparation and analysis.

## AUTHOR INFORMATION


### Corresponding Author

**Martina Marchetti-Deschmann** − *Institute of Chemical Technologies and Analytics, TU Wien, 1060 Vienna, Austria;* orcid.org/0000-0002-8060-7851; Email: martina.marchetti-deschmann@tuwien.ac.at

### Authors

**Jessica Pichler** − *AC2T research GmbH, 2700 Wiener Neustadt, Austria; Institute of Chemical Technologies and Analytics, TU Wien, 1060 Vienna, Austria;* orcid.org/0000-0002-5868-229X

**Marcella Frauscher** − *AC2T research GmbH, 2700 Wiener Neustadt, Austria;* orcid.org/0000-0001-7939-9656

Complete contact information is available at: https://pubs.acs.org/10.1021/acsomega.4c00513


### Author Contributions

Conceptualization: J.P., M.F., M.M.-D.; investigation and methodology: J.P., M.M.-D., M.F.; data curation and formal analyses: J.P.; validation: J.P., M.M.-D., C.F., B.D., A.O., M.F.; writing—original draft: J.P.; writing—review and editing: J.P., M.M.-D., C.F., B.D., A.O., M.F.; and supervision: M.M.-D., M.F.


### Funding

This work was funded by the "Austrian COMET-Program" (project InTribology, no. 872176) via the Austrian Research Promotion Agency (FFG) and the Province of Niederösterreich and Vorarlberg. It was carried out within the 'Excellence Centre of Tribology' (AC2T research GmbH). We thank Shimadzu Austria for supporting this research by granting access to the Shimadzu GC2010 instrumentation and their constant service support.


### Notes

The authors declare no competing financial interest.

## ACKNOWLEDGMENTS


Special thanks to Bernhard Dewitz, Alexander Orfaniotis, Clemens Freydell, Andjelka Ristic, Michael Schandl, Andreas Wöhrer, Márton Reitter, and Victoria Dorrer for additional support.


## REFERENCES


(1) Bondioli, P.; Bella, L. D.; Rivolta, G. Evaluation of total and saturated monoglyceride content in biodiesel at low concentration. *Eur. J. Lipid Sci. Technol.* **2013**, *115*, 576−582.

(2) DIN Deutsches Institut für Normung e. V.; *Automotive fuels—Diesel—Requirements and test methods; German version EN 590:2022*; Beuth Verlag GmbH: Berlin, 2022. Doi: DOI: 10.31030/3337114.

(3) Masudi, A.; Muraza, O.; Jusoh, N. W. C.; Ubaidillah, U. Improvements in the stability of biodiesel fuels: recent progress and challenges. *Environmental Science and Pollution Research* **2023**, *30*, 14104−14125. December

(4) Neupane, D. Biofuels from Renewable Sources, a Potential Option for Biodiesel Production. *Bioengineering* **2023**, *10*, 29. December
(5) Singh, S. P.; Singh, D. Biodiesel production through the use of different sources and characterization of oils and their esters as the substitute of diesel: A review. *Renewable and Sustainable Energy Reviews* **2010**, *14*, 200−216. January
(6) van Grinsven, A.; van den Toorn, E.; van der Veen, R.; Kampman, B.; *Used Cooking Oil (UCO) as biofuel feedstock in the EU*, 2020, [Online]. Available: https://www.transportenvironment.org/wp-content/uploads/2021/07/CE_Delft__200247_UCO_as_biofuel_feedstock_in_EU_FINAL - v5_0.pdf. [Accessed 12 10 2023].
(7) U.S. Energy Information Administration; *Biofuels explained - Biodiesel, renewable diesel, and other biofuels*, 2022 [Online]. Available: https://www.eia.gov/energyexplained/biofuels/biodiesel-rd-other-basics.php [Accessed October 12, 2023].
(8) Alsultan, A. G.; Asikin-Mijan, N.; Ibrahim, Z.; Yunus, R.; Razali, S. Z.; Mansir, N.; Islam, A.; Seenivasagam, S.; Taufiq-Yap, Y. H. A Short Review on Catalyst, Feedstock, Modernised Process, Current State and Challenges on Biodiesel Production. *Catalysts* **2021**, *11*, 1261.
(9) Tang, H.; Guzman, R. C. D.; Salley, S. O.; Ng, K. Y. S. Formation of Insolubles in Palm Oil-, Yellow Grease-, and Soybean Oil-Based Biodiesel Blends After Cold Soaking at 4 °C. *J. Am. Oil Chem. Soc.* **2008**, *85*, 1173−1182.
(10) Ashley & Dumville Limited; *Why is fuel filter blocking still an issue?*, 2021 [Online]. Available: https://fueloilnews.co.uk/2021/05/why-is-fuel-filter-blocking-still-an-issue [Accessed October 12, 2023].
(11) British Broadcasting Corporation (BBC); *South Western Railway disruption after biofuel clogs engines*, 2023 [Online]. Available: https://www.bbc.com/news/uk-england-hampshire-65347331 [Accessed October 12, 2023].
(12) Hassan, T.; Rahman, M. M.; Rahman, M. A.; Nabi, M. N. Opportunities and challenges for the application of biodiesel as automotive fuel in the 21st century. *Biofuels, Bioprod. Bioref.* **2022**, *16*, 1353−1387.
(13) Santos, S. M.; Wolf-Maciel, M. R.; Fregolente, L. V. Cold flow properties: Applying exploratory analyses and assessing predictive methods for biodiesel and diesel-biodiesel blends. *Sustainable Energy Technologies and Assessments* **2023**, *57*, No. 103220.
(14) Wilson, M.; Herniman, J. M.; Barker, J.; Langley, G. J. Development of Simplified and Efficient Sample Preparation Methods for the Analysis of Problem Material within the Diesel Fuel Delivery System. *ACS Omega* **2023**, *8*, 36823−36834.
(15) Frauscher, M.; Pichler, J.; Agócs, A.; Dewitz, B.; Drexler, T.; Orfaniotis, A. Root causes for low-temperature filter blocking at petrol stations—A field study. *Fuel* **2024**, *366*, No. 131304.
(16) DIN Deutsches Institut für Normung e. V.; *Liquid petroleum products—Fatty acid methyl esters (FAME) for use in diesel engines and heating applications—Requirements and test methods; German version EN 14214:2012+A2:2019*, Beuth Verlag GmbH: Berlin, 2019. Doi: DOI: 10.31030/3005309.
(17) DIN Deutsches Institut für Normung e. V.; *Automotive fuels and fat and oil derivates—Determination of saturated monoglycerides content in Fatty Acid Methyl Esters (FAME)—Method by GC-FID; German version EN 17057:2018*, Beuth Verlag GmbH: Berlin, 2018. Doi: DOI: 10.31030/2811679.
(18) Cavalheiro, L. F.; Misutsu, M. Y.; Rial, R. C.; Viana, L. H.; Oliveira, L. C. S. Characterization of residues and evaluation of the physico chemical properties of soybean biodiesel and biodiesel: Diesel blends in different storage conditions. *Renewable Energy* **2020**, *151*, 454−462. May
(19) Chupka, G. M.; Yanowitz, J.; Chiu, G.; Alleman, T. L.; McCormick, R. L. Effect of Saturated Monoglyceride Polymorphism on Low-Temperature Performance of Biodiesel. *Energy Fuels* **2011**, *25*, 398−405. December
(20) DIN Deutsches Institut für Normung e. V.; *Fat and oil derivatives - Fatty Acid Methyl Esters (FAME)—Determination of free and total glycerol and mono-, di-, triglyceride contents; German version EN 14105:2020*, Beuth Verlag GmbH: Berlin, 2021. Doi: DOI: 10.31030/3181185.
(21) Alleman, T. L.; Christensen, E. D.; Moser, B. R. Improving biodiesel monoglyceride determination by ASTM method D6584−17. *Fuel* **2019**, *241*, 65−70. April
(22) DIN Deutsches Institut für Normung e. V.; *Petroleum products - Determination of water content using titration according to Karl Fischer*, Beuth Verlag GmbH: Berlin, 2020. Doi: DOI: 10.31030/3120598.
(23) DIN Deutsches Institut für Normung e. V.; *Protective gloves against dangerous chemicals and micro-organisms - Part 1: Terminology and performance requirements for chemical risks (ISO 374−1:2016 + Amd. 1:2018); German version EN ISO 374−1:2016 + A1:2018*, Beuth Verlag GmbH: Berlin, 2018. doi: DOI: 10.31030/2880843.
(24) U.S. Environmental Protection Agency; *Fact Sheet: Methylene Chloride or Dichloromethane (DCM)*, 2017 [Online]. Available: https://www.epa.gov/sites/default/files/2017-04/documents/fact_sheet_methylene_choride_or_dichloromethane_dcm.pdf [Accessed August 28, 2023].
(25) Frauscher, M.; Pichler, J.; Agócs, A.; Dewitz, B.; Drexler, T.; Orfaniotis, A. Elucidation of non-microbial filter blocking by a comprehensive techniques approach *Fuel* 2023.




https://doi.org/10.1021/acsomega.4c00513
*ACS Omega* 2024, 9, 23476−23484